NASA TECHNICAL REPORT

NASA TR R-403

NASA TR R-403

A QUALITATIVE STUDY OF THE COMPLETE SET OF SOLUTIONS OF THE DIFFERENTIAL EQUATION OF MOTION OF A TEST PARTICLE IN THE EQUATORIAL PLANE OF THE KERR GRAVITATIONAL FIELD

by Harry E. Montgomery and F. K. Chan

Goddard Space Flight Center
Greenbelt, Md. 20771

NATIONAL AERONAUTICS AND SPACE ADMINISTRATION • WASHINGTON, D. C. • MARCH 1973

1. Report No. NASA TR R-403	2. Government Accession No.	3. Recipient's Catalog No.
4. Title and Subtitle A Qualitative Study of the Complete Set of Solutions of the Differential Equation of Motion of a Test Particle in the Equatorial Plane of the Kerr Gravitational Field		5. Report Date March 1973 6. Performing Organization Code
7. Author(s) Harry E. Montgomery and F. K. Chan		8. Performing Organization Report No. G-1071
9. Performing Organization Name and Address Goddard Space Flight Center Greenbelt, Maryland 20771		10. Work Unit No. 11. Contract or Grant No. 13. Type of Report and Period Covered Technical Report
12. Sponsoring Agency Name and Address National Aeronautics and Space Administration Washington, D.C. 20546		14. Sponsoring Agency Code
15. Supplementary Notes		

16. Abstract

A study is made of the mathematical solution of the differential equation of motion of a test particle in the equatorial plane of the Kerr gravitational field, using S (Schwarzschild-like) coordinates. The equation studied is

$$\left(\frac{du}{d\phi}\right)^2 = B(u)\frac{D^2(u)}{E^2(u)}$$

where

$$B(u) = \beta(h + ea)^2u^3 - [h^2 + (1 - e^2)a^2]\,u^2 + \beta u - (1 - e^2),$$
$$D(u) = a^2u^2 - \beta u + 1,$$
$$E(u) = -\beta(h + ea)u + h,$$

and $u = 1/r$ is the inverse radius, $\frac{1}{2}\beta$ is the mass of central body, a is the negative of the specific angular momentum of the central body, h is the specific angular momentum of the test particle, and e is related to the "energy" of the test particle. A qualitative solution of this equation leads to the conclusion that there can only be 25 different types of orbits. For each value of a, the results are presented in a master diagram for which h and e are the parameters. A master diagram divides the h, e parameter space into regions such that at each point within one of these regions the types of admissible orbits are qualitatively the same. A pictorial representation of the "physical" orbits in the r, ϕ plane is also given.

17. Key Words (Selected by Author(s))	18. Distribution Statement
Kerr gravitational field Equation of motion Schwarzschild metric Orbital mechanics	Unclassified–Unlimited

19. Security Classif. (of this report)	20. Security Classif. (of this page)	21. No. of Pages	22. Price*
Unclassified	Unclassified	193	$3.00

*For sale by the National Technical Information Service, Springfield, Virginia 22151.

PREFACE

The major part of this work is taken from a doctoral dissertation submitted by Harry E. Montgomery, and directed by F. K. Chan, to the Department of Space Science and Applied Physics, Catholic University of America, Washington, D.C. The remaining part, Appendix A, is taken from the course "Advanced Celestial Mechanics" taught by the second author during the academic year 1968-69.

CONTENTS

CONTENTS (concluded)

Page

NOTATION

a	negative of angular momentum per unit mass of the rotating central body
$A(u)$	linear function of u defined by Equation 48
$A^*(u^*)$	linear function of u^* defined by Equation 19
$B(u)$	cubic function of u defined by Equation 45
$B^*(u^*)$	cubic function of u^* defined by Equation 20
$C^*(u^*)$	fifth degree polynomial in u^* defined by Equation 21
$D(u)$	second degree polynomial in u defined by Equation 46
$D^*(u^*)$	second degree polynomial in u^* defined by Equation 27
e	constant of the motion related to the energy of the particle, given by Equation 38 for equatorial orbits and by Equation 89 in general
e^*	constant of the motion related to the energy of the particle, given by Equation 24 for equatorial orbits and by Equation 122 in general
$E(u)$	linear function of u defined by Equation 47
$E^*(u^*)$	linear function of u^* defined by Equation 28
$f(u)$	function defined by Equation 165
$\mathbf{g}_{\mu\nu}$	the metric tensor
h	constant of the motion related to the angular momentum of the particle, given by Equation 37 for equatorial orbits and by Equation 88 in general
h^*	constant of the motion related to the angular momentum of the particle, given by Equation 23 for equatorial orbits and Equation 121 in general
H	quantity defined by Equation 156
m	mass of the rotating central body
r	radial coordinate in S form defined by Equation 15
r^*	radial coordinate in E form defined by Equation 8
s	proper time

t	a time coordinate in S form defined by Equation 15
t^*	a time coordinate in E form defined by Equation 8
u	inverse radius, $1/r$
u^*	inverse radius, $1/r^*$
$u_{B1,B2,B3}$	roots of the cubic $B(u) = 0$, which are also denoted by $u_{\mathrm{I,II,III}}$ in the figures
$u'_{B1,B2}$	roots of the quadratic $B'(u) = 0$, which are also denoted by $u'_{\mathrm{I,II}}$ in the figures
u''_B	root of $B''(u) = 0$ (also denoted by u_s), which is the point of symmetry of the cubic $B(u)$
u_c	repeated root of $f(u) = 0$
$u_{D1,D2}$	roots of the quadratic $D(u) = 0$, given by Equation 197
u_E	root of the linear equation $E(u) = 0$, given by Equation 206
u_f	root of $f(u) = 0$
u_s	see u''_B
$u_{\mathrm{I,II,III}}$	see $u_{B1,B2,B3}$
$u'_{\mathrm{I,II}}$	see $u'_{B1,B2}$
V	quantity defined by Equation 141
W	a measure of the energy of the particle, given by Equation 153
x, y, z	spacelike coordinates in M form defined by Equation 1
β	quantity equal to $2m$
Δ	quantity defined by Equation 14
Δ^*	quantity defined by Equation 69
θ, ϕ	angular coordinates in S form defined by Equation 15
θ^*, ϕ^*	angular coordinates in E form defined by Equation 8

A QUALITATIVE STUDY OF THE COMPLETE SET OF SOLUTIONS OF THE DIFFERENTIAL EQUATION OF MOTION OF A TEST PARTICLE IN THE EQUATORIAL PLANE OF THE KERR GRAVITATIONAL FIELD

by
Harry E. Montgomery
Goddard Space Flight Center
and
F. K. Chan*
Catholic University of America

INTRODUCTION

In 1963, Kerr (Reference 1) presented an exact solution of Einstein's empty-space field equations that might be the exterior field of a rotating body. He presented his metric in two sets of coordinates which were later labeled as the E and the M coordinates. He also stated that the two parameters in his solution are the Schwarzschild mass and the specific angular momentum of the central body.

In 1964, Boyer and Price (Reference 2) used Kerr's metric in E coordinates and obtained the equation of motion of a particle in the equatorial plane and then studied the precession of the pericenter of the orbit. By comparing this result with the motion of the pericenter as determined by Lense and Thirring (Reference 3), who had obtained in 1918 the perturbations of the elements of planetary orbits in an approximate gravitational field of a uniformly rotating sphere of constant density, Boyer and Price identified the two parameters m and $-a$ in the Kerr metric as the mass of the sphere and the specific angular momentum of the sphere, thus confirming Kerr's assertion.

In 1966, Carter (Reference 4) studied the motion of a particle along the symmetry axis of the Kerr gravitational field using E coordinates.

In 1967, Boyer and Lindquist (Reference 5) discussed some coordinate systems useful in the study of the Kerr metric which they called the Minkowski-like M, Eddington-like E, and Schwarzschild-like S coordinates. Certain properties of the Kerr metric, including the behavior of geodesics lying in the equatorial plane, were examined in some detail.

In 1968, DeFelice (Reference 6) investigated the geodesic motion in the equatorial plane of the gravitational field of a rotating source using E coordinates. The differential equations of the geodesics were studied to obtain the shape of the loci of turning points of test particles without introducing numerical values of the parameters involved. Figures were given that show the behavior of geodesics for different ranges of these parameters.

*F. K. Chan is presently with Computer Sciences Corp., Silver Spring, Md. 20910.

In 1968, Carter (Reference 7) demonstrated that the Hamilton-Jacobi equation for a test particle using E coordinates can be separated.

The present work deals with the motion of a particle in a Kerr gravitational field. It begins with a brief review of the Kerr metric in the three coordinate systems and also a derivation of the equations of motion of a test particle. These equations are derived in the E and the S coordinate systems.

Next, a step-by-step procedure is presented for the qualitative analysis of the complete set of orbits of a test particle in the equatorial plane, using S coordinates. The results for each value of a are represented in a master diagram that gives the complete topological genera of the orbits for various ranges of the two parameters: the angular momentum per unit mass of the test particle h and the "energy" per unit mass of the test particle e. In addition, the physical orbits corresponding to the master diagram are given.

A discussion is then given of the determination of the direction of orbital motion, the scaling of solutions for $\beta \neq 2$, conversion of results of the present S coordinates to E coordinates, and, finally, the pseudosingularity at $u = u_D$.

The method of solution used in the analysis relies heavily upon Chan's qualitative solution of the motion of a particle in the Schwarzschild gravitational field. Because this work is unpublished, it is presented in Appendix A. The algebraic details that were omitted in the text are included as Appendix B.

EQUATIONS OF MOTION OF A TEST PARTICLE IN THE KERR GRAVITATIONAL FIELD

Various Forms of the Kerr Metric

For a rotating body, the exterior gravitational field is described by the metric originally given by Kerr (Reference 1) in the form (henceforth referred to as the Minkowski-like M form)

$$ds^2 = -dx^2 - dy^2 - dz^2 + dt^{*2} - \frac{2mr^{*3}k^2}{r^{*4} + a^2z^2} , \tag{1}$$

where k is given by

$$(r^{*2} + a^2)r^*k = r^{*2}(x\,dx + y\,dy) + ar^*(x\,dy - y\,dx) + (r^{*2} + a^2)(z\,dz + r^*\,dt^*) . \tag{2}$$

The coordinate r^* is defined by

$$r^{*4} - (R^2 - a^2)r^{*2} - a^2z^2 = 0 , \tag{3}$$

where

$$R^2 = x^2 + y^2 + z^2 . \tag{4}$$

In these equations m can be interpreted as the Schwarzschild mass and $-a$ the angular momentum per unit mass about the z axis. However, in this form of the line element, it is difficult to understand truly the physical nature of the "radial" coordinate r^* because of the presence of too many off-diagonal terms in the metric tensor $\mathbf{g}_{\mu\nu}$. Moreover, setting the parameter a equal to zero does not simply yield the well-known Schwarzschild metric. In his work, Kerr also introduced the following transformation,

$$x = (r^{*2} + a^2)^{1/2} \sin\theta^* \cos\left(\phi^* - \tan^{-1}\frac{a}{r^*}\right), \tag{5}$$

$$y = (r^{*2} + a^2)^{1/2} \sin\theta^* \sin\left(\phi^* - \tan^{-1}\frac{a}{r^*}\right) , \tag{6}$$

$$z = r^* \cos\theta^* , \tag{7}$$

to obtain the line element in the form (henceforth referred to as the Eddington-like E form)

$$ds^2 = -dr^{*2} - 2a \sin^2\theta^* dr^* d\phi^* - (r^{*2} + a^2) \sin^2\theta^* d\phi^{*2} - P^* d\theta^{*2} + dt^{*2} - \frac{2mr^*}{P^*}(dr^* + a \sin^2\theta^* d\phi^* + dt^*)^2 , \tag{8}$$

where P^* is defined by

$$P^* \equiv r^{*2} + a^2 \cos^2\theta^* . \tag{9}$$

Even now with the elimination of some off-diagonal terms in $\mathfrak{g}_{\mu\nu}$, it is still difficult to interpret the radial coordinate r^* or to obtain the Schwarzschild metric directly by setting $a = 0$.

However, Boyer and Lindquist (Reference 5) later introduced the following transformation:

$$r = r^* , \tag{10}$$

$$\theta = \theta^* , \tag{11}$$

$$d\phi = d\phi^* + \frac{a\, dr^*}{\Delta} , \tag{12}$$

$$dt = dt^* - \frac{\beta r^*\, dr^*}{\Delta} , \tag{13}$$

where

$$\Delta \equiv r^2 - \beta r + a^2 , \tag{14}$$

which then reduces Equation 8 to the form (henceforth referred to as the Schwarzschild-like S form)

$$ds^2 = -P\left(\frac{dr^2}{\Delta} + d\theta^2\right) - (r^2 + a^2) \sin^2\theta\, d\phi^2 + dt^2 - \frac{\beta r}{P}(a \sin^2\theta\, d\phi + dt)^2 , \tag{15}$$

where

$$P \equiv r^2 + a^2 \cos^2\theta . \tag{16}$$

The outstanding feature of this equation is that it has only one off-diagonal component $\mathfrak{g}_{\phi t}$ and reduces nicely to the standard Schwarzschild metric when $a = 0$.

The transformation given by Equations 10 to 14 reveals that there is a mathematical pseudo-singularity introduced when $\Delta = 0$. Even though in this respect the E coordinates appear to be better for analysis of the Kerr metric, it turns out that the S coordinates are preferable in terms of physical significance in that they determine the location of horizons or stationary null hypersurfaces when $\Delta = 0$. (For a more detailed discussion, see Boyer and Lindquist (Reference 5).)

Equations of Motion for a Test Particle in the Equatorial Plane

Boyer and Price (Reference 2) used the E form of the Kerr metric in their study on the interpretation of the parameter $-a$ as the angular momentum per unit mass of the central spinning body. For test particles with orbits in the equatorial plane they obtained the following equation of motion:

$$A^*(u^*)\left(\frac{du^*}{d\phi^*}\right)^2 + 2aB^*(u^*)\frac{du^*}{d\phi^*} - C^*(u^*) = 0\,, \tag{17}$$

where

$$u^* = \frac{1}{r^*}\,, \tag{18}$$

$$A^*(u^*) = -\beta(h^* + e^*a)^2u^* + h^{*2} + (1 - e^{*2})a^2\,, \tag{19}$$

$$B^*(u^*) = \beta(h^* + e^*a)^2u^{*3} - [h^{*2} + (1 - e^{*2})a^2]u^{*2} + \beta u^* - (1 - e^{*2})\,, \tag{20}$$

$$\begin{aligned} C^*(u^*) = {} & \beta a^2(h^* + e^*a)^2u^{*5} - \left\{\beta^2(h^* + e^*a)^2 + a^2[h^{*2} + (1 - e^{*2})a^2]\right\}u^{*4} \\ & + 2\beta[h^*(h^* + e^*a) + a^2]u^{*3} - [h^{*2} + \beta^2 + 2(1 - e^{*2})a^2]u^{*2} \\ & + \beta(2 - e^{*2})u^* - (1 - e^{*2})\,, \end{aligned} \tag{21}$$

$$\beta = 2m\,, \tag{22}$$

$$h^* = a\left(1 + \frac{\beta}{r^*}\right)\dot{r}^* + \left(r^{*2} + a^2 + \frac{\beta a^2}{r^*}\right)\dot{\phi}^* + \frac{\beta a}{r^*}\,\dot{t}^*\,, \tag{23}$$

$$e^* = -\frac{\beta}{r^*}\,\dot{r}^* - \frac{\beta a}{r^*}\,\dot{\phi}^* + \left(1 - \frac{\beta}{r^*}\right)\dot{t}^*\,. \tag{24}$$

It can be shown that

$$C^* \equiv B^*D^* \tag{25}$$

$$A^*D^* + a^2B^* \equiv E^{*2}\,, \tag{26}$$

where

$$D^*(u^*) = a^2u^{*2} - \beta u^* + 1 \tag{27}$$

$$E^*(u^*) = -\beta(h^* + e^*a)u + h^*\,. \tag{28}$$

Next, the equation of motion in the S form will be derived from first principles. (It may also be obtained from Equation 17, which is for the E coordinates, and Equations 10 and 12, which are the equations of transformation from (r^*, ϕ^*) to (r, ϕ). A method of finding equations of motion corresponding to a general metric $\mathbf{g}_{\mu\nu}$ is given by Synge (Reference 8). If the line element is denoted as

$$ds^2 = \mathbf{g}_{\mu\nu}\,dx^\mu\,dx^\nu \qquad \mu, \nu = 1, 2, 3, 4 \tag{29}$$

and the Lagrangian $F(x, \dot{x})$ is defined by

$$F(x, \dot{x}) = \mathbf{g}_{\mu\nu}\,\dot{x}^\mu\,\dot{x}^\nu\,, \tag{30}$$

then the equations of motion are given by

$$\frac{d}{ds}\frac{\partial F}{\partial \dot{x}^\mu} - \frac{\partial F}{\partial x^\mu} = 0 \qquad \text{for } \mu = 1, 2, 3, 4 , \tag{31}$$

where

$$\dot{x}^\mu \equiv \frac{dx^\mu}{ds} . \tag{32}$$

Now, for the case of equatorial orbits we have $\theta = \pi/2$, so that from Equation 15 the Lagrangian becomes

$$F = -\frac{r^2 \dot{r}^2}{\Delta} - (r^2 + a^2)\,\dot{\phi}^2 + \dot{t}^2 - \frac{\beta}{r}(a\,\dot{\phi} + \dot{t})^2 . \tag{33}$$

Hence, the following three equations corresponding to r, ϕ, and t result:

$$\frac{d}{ds}\frac{\partial F}{\partial \dot{r}} - \frac{\partial F}{\partial r} = 0 , \tag{34}$$

$$\frac{d}{ds}\frac{\partial F}{\partial \dot{\phi}} - \frac{\partial F}{\partial \phi} = 0 , \tag{35}$$

$$\frac{d}{ds}\frac{\partial F}{\partial \dot{t}} - \frac{\partial F}{\partial t} = 0 . \tag{36}$$

These three equations and the line-element equation (Equation 15) constitute a set of equations of which only three are independent. It is simplest to use Equations 15, 35, and 36 to obtain the equation of motion in the equatorial plane.

Because F, which is given by Equation 33, is not a function of ϕ, Equation 35 implies that $\partial F/\partial \dot{\phi}$ is equal to a constant $-2h$; therefore,

$$\frac{\partial F}{\partial \dot{\phi}} = -2(r^2 + a^2)\,\dot{\phi} - \frac{2\beta a}{r}(a\,\dot{\phi} + \dot{t}) = -2h . \tag{37}$$

Similarly, because F is not a function of t, $\partial F/\partial \dot{t}$ is equal to a constant $2e$; thus

$$\frac{\partial F}{\partial \dot{t}} = 2\,\dot{t} - \frac{2\beta}{r}(a\,\dot{\phi} + \dot{t}) = 2e . \tag{38}$$

From Equations 37 and 38 for $\dot{\phi}$ and $\dot{t}$, it follows that

$$\dot{\phi} = \frac{1}{r\Delta}\,[h(r - \beta) - \beta a e] , \tag{39}$$

$$\dot{t} = \frac{1}{r\Delta}\,[e(r^3 + a^2 r + \beta a^2) + \beta a h] . \tag{40}$$

If $u = 1/r$, then

$$\dot{r}^2 = \frac{\dot{\phi}^2}{u^4}\left(\frac{du}{d\phi}\right)^2 . \tag{41}$$

Equations 39 and 40 then become

$$\dot{\phi} = \frac{1}{\Delta}\,[-\beta(h + ea)u + h] , \tag{42}$$

$$\dot{t} = \frac{1}{u^2 \Delta} \left[e(1 + a^2 u^2 + \beta a^2 u^3) + \beta a h u^3 \right] . \tag{43}$$

Substitution of these equations into the line element given by Equation 15 yields

$$\left(\frac{du}{d\phi} \right)^2 = B(u) \frac{D^2(u)}{E^2(u)} , \tag{44}$$

where

$$B(u) = \beta(h + ea)^2 u^3 - [h^2 + (1 - e^2)a^2] u^2 + \beta u - (1 - e^2) , \tag{45}$$

$$D(u) = a^2 u^2 - \beta u + 1 , \tag{46}$$

$$E(u) = -\beta(h + ea)u + h . \tag{47}$$

In addition, $A(u)$ is defined by

$$A(u) = -\beta(h + ea)^2 u + h^2 + (1 - e^2)a^2 . \tag{48}$$

It follows from Equation 26 that the following identity holds:

$$AD + a^2 B \equiv E^2 . \tag{49}$$

Equation 44 is studied extensively in the next section and was chosen in preference to Equation 17 because it is simpler and its metric reduces to the standard Schwarzschild metric when $a = 0$.

With the S coordinates the equation of equatorial orbital motion has been obtained in a simpler form as given by Equation 44. The E form obtained by Boyer and Price as given by Equation 17 may also be reduced to a simpler form, as follows: Completing the square in Equation 17 results in

$$\left(\frac{du^*}{d\phi^*} + \frac{aB^*}{A^*} \right)^2 - \frac{B^*}{A^{*2}} (A^* D^* + a^2 B^*) = 0 . \tag{50}$$

By using the identity in Equation 26, Equation 50 takes the form

$$\left(\frac{du^*}{d\phi^*} + \frac{aB^*}{A^*} \right)^2 - \frac{B^* E^{*2}}{A^{*2}} = 0 . \tag{51}$$

Letting

$$\frac{du^+}{d\phi^+} \equiv \frac{du^*}{d\phi^*} + \frac{aB^*}{A^*} \tag{52}$$

$$u^+ = u^* , \tag{53}$$

then

$$\left(\frac{du^+}{d\phi^+} \right)^2 = \frac{B^* E^{*2}}{A^{*2}} . \tag{54}$$

When $a = 0$, this equation also reduces to the equation of motion in Appendix A except for a factor of

h^{*2}. Because $u^+ = u^*$, Equation 52 yields

$$d\phi^+ = \frac{A^*\, d\phi^*\, dr^*}{A^*\, dr^* - aB^* r^{*2}\, d\phi^*} , \tag{55}$$

or

$$d\phi^* = \frac{A^*\, d\phi^+\, dr^*}{A^*\, dr^* + aB^* r^{*2}\, d\phi^+} . \tag{56}$$

Hence, Equations 53 and 55 give the transformation from (r^*, ϕ^*) to (r^+, ϕ^+). However, one drawback of this transformation is that Equation 55 involves the constants of motion h^* and e^* of the test particle because of the presence of B^* in the equation. This is to be contrasted with the transformation from (r^*, ϕ^*) to (r, ϕ) given by Equations 10 and 12 for which no such weakness occurs.

Equations of Motion of a Test Particle Not Restricted to the Equatorial Plane

The differential equations for general orbits using the E form of the Kerr metric have been derived in this study. Because the method of derivation is the same as that used to obtain Equations 102 to 105 in the S form, the resulting equations are presented, without derivation, for future reference. Using the following definitions,

$$x_1^* = r^* , \tag{57}$$

$$x_2^* = \theta^* , \tag{58}$$

$$x_3^* = \phi^* , \tag{59}$$

$$x_4^* = t^* , \tag{60}$$

$$x_5^* = \dot{r}^* , \tag{61}$$

$$x_6^* = \dot{\theta}^* , \tag{62}$$

and letting the dot denote d/ds, the differential equations of motion are

$$\dot{x}_1^* = x_5^* , \tag{63}$$

$$\dot{x}_2^* = x_6^* , \tag{64}$$

$$\dot{x}_3^* = \frac{-1}{P^*\Delta^* \sin^2 x_2^*} (\beta a e^* x_1^* \sin^2 x_2^* + \beta h^* x_1^* - h^* P^* + a P^* x_5^* \sin^2 x_2^*) , \tag{65}$$

$$\dot{x}_4^* = \frac{1}{P^*\Delta^*} [\beta a h^* x_1^* + e^* P^* (x_1^{*2} + a^2) + e^* \beta a^2 x_1^* \sin^2 x_2^* + \beta x_1^* P^* x_5^*] , \tag{66}$$

$$\dot{x}_5^* = \frac{b_2^*}{a_{21}^*} \tag{67}$$

$$\dot{x}_6^* = \frac{a_{21}^* b_1^* - a_{11}^* b_2^*}{a_{12}^* a_{21}^*} , \tag{68}$$

where

$$\Delta^* \equiv x_1^{*2} - \beta x_1^* + a^2 , \tag{69}$$

$$a_{11}^* = 2x_5^* + 2ax_5^*\Phi_2 \sin^2 x_2^* + 2a\,\dot{\phi}^* \sin^2 x_2^* + 2(x_1^{*2} + a^2)\,\dot{\phi}^*\Phi_2 \sin^2 x_2^* - 2\,\dot{t}^* T_2 + \frac{2P^*(\dot{t}^* - e^*)T_2}{\beta x_1^*} , \tag{70}$$

$$a_{12}^* = 2P^* x_6^* , \tag{71}$$

$$a_{21}^* = 2 + 2a\Phi_2 \sin^2 x_2^* + 2T_2 , \tag{72}$$

$$b_1^* = -2ax_5^*\Phi_1 \sin^2 x_2^* - 4ax_5^* x_6^*\,\dot{\phi}^* \sin x_2^* \cos x_2^* - 2x_1^* x_5^*\,\dot{\phi}^{*2} \sin^2 x_2^* - 2(x_1^{*2} + a^2)x_6^*\,\dot{\phi}^{*2} \sin x_2^* \cos x_2^* - 2(x_1^{*2} + a^2)\Phi_1\,\dot{\phi}^* \sin^2 x_2^* - \dot{P}^* x_6^{*2} + 2\,\dot{t}^* T_1 - \frac{\dot{P}^*(\dot{t}^* - e^*)}{\beta x_1^*} - \frac{2P^*(\dot{t}^* - e^*)T_1}{\beta x_1^*} + \frac{P^* x_5^*(\dot{t}^* - e^*)^2}{\beta x_1^{*2}} , \tag{73}$$

$$b_2^* = -2a\Phi_1 \sin^2 x_2^* - 4a\,\dot{\phi}^* x_6^* \sin x_2^* \cos x_2^* - 2T_1 + 2x_1^*\,\dot{\phi}^{*2} \sin^2 x_2^* + 2x_1^* x_6^{*2} + \frac{\beta Q^{*2}}{P^*} - \frac{2\beta x_1^{*2} Q^2}{P^{*2}} , \tag{74}$$

$$\dot{t}^* = \frac{1}{P^*\Delta^*}[\beta a h^* x_1^* + e^* P^*(x_1^{*2} + a^2) + e^*\beta a^2 x_1^* \sin^2 x_2^* + \beta x_1^* P^* x_5^*] , \tag{75}$$

$$\dot{\phi}^* = -\frac{1}{P^*\Delta^* \sin^2 x_2^*}(\beta a e^* x_1^* \sin^2 x_2^* + \beta h^* x_1^* - h^* P^* + aP^* x_5^* \sin^2 x_2^*) , \tag{76}$$

$$Q^* = \frac{P^*}{\beta x_1^*}(\dot{t}^* - e^*) , \tag{77}$$

$$\dot{P}^* = 2x_1^* x_5^* - 2a^2 x_6^* \cos x_2^* \sin x_2^* , \tag{78}$$

$$T_1 = \frac{1}{P^*\Delta^*}[\beta a h^* x_5^* + e^*\,\dot{P}^*(x_1^{*2} + a^2) + 2e^* P^* x_1^* x_5^* + e^*\beta a^2 x_5^* \sin^2 x_2^* + 2e^*\beta a^2 x_1^* x_6^* \sin x_2^* \cos x_2^* + \beta P^* x_5^{*2} + \beta x_1^*\,\dot{P}^* x_5^*] - \frac{\dot{t}^*}{P^*\Delta^*}[\Delta^*\,\dot{P}^* + P(2x_1^* x_5^* - \beta x_5^*)] , \tag{79}$$

$$T_2 = \frac{\beta x_1^*}{\Delta^*} , \tag{80}$$

$$\Phi_1 = \frac{1}{P^*\Delta^* \sin^2 x_2^*} \left\{ -\beta a e^* x_5^* \sin^2 x_2^* - 2\beta a e^* x_1^* x_6^* \sin x_2^* \cos x_2^* \right.$$
$$- \beta h^* x_5^* + h^* \dot{P}^* - a \dot{P}^* x_5^* \sin^2 x_2^* - 2aP^* x_5^* x_6^* \sin x_2^* \cos x_2^*$$
$$\left. - \dot{\phi}^* [(2x_1^* x_5^* - \beta x_5^*) P^* \sin^2 x_2^* + \dot{P}^* \Delta^* \sin^2 x_2^* + 2P^* \Delta^* x_6^* \sin x_2^* \cos x_2^*] \right\} , \tag{81}$$

$$\Phi_2 = -\frac{1}{\Delta^*} . \tag{82}$$

Equations 63 to 68 with appropriate initial conditions $x^*(s_0) = x_{i_0}^*$ can be solved by numerical integration. Only five of the values of $x_{i_0}^*$ may be chosen independently and the remaining one must be chosen to satisfy Equation 8 at $s = s_0$.

Next, the general equations of motion in S form will be derived. From Equation 15, the Lagrangian is

$$F = -P \left(\frac{\dot{r}^2}{\Delta} + \dot{\theta}^2 \right) - (r^2 + a^2) \dot{\phi}^2 \sin^2 \theta + t^2 - \frac{\beta r}{P} (a \dot{\phi} \sin^2 \theta + \dot{t})^2 . \tag{83}$$

Then, from Equation 31, the following four equations corresponding to θ, ϕ, t, and r are obtained:

$$\frac{d}{ds} \frac{\partial F}{\partial \dot{\theta}} - \frac{\partial F}{\partial \theta} = 0 , \tag{84}$$

$$\frac{d}{ds} \frac{\partial F}{\partial \dot{\phi}} - \frac{\partial F}{\partial \phi} = 0 , \tag{85}$$

$$\frac{d}{ds} \frac{\partial F}{\partial \dot{t}} - \frac{\partial F}{\partial t} = 0 , \tag{86}$$

$$\frac{d}{ds} \frac{\partial F}{\partial \dot{r}} - \frac{\partial F}{\partial r} = 0 . \tag{87}$$

Equations 84 to 87 and the line-element equation (Equation 15) constitute a set of equations of which only four are independent. Equations 15 and 85 to 87 were chosen for this study. In Equation 83, F is not a function of ϕ or t. Hence, Equations 85 and 86 imply that $\partial F/\partial \dot{\phi}$ and $\partial F/\partial \dot{t}$ are equal to constants, denoted respectively as $-2h$ and $2e$. Therefore,

$$\frac{\partial F}{\partial \dot{\phi}} = -2(r^2 + a^2) \dot{\phi} \sin^2 \theta - \frac{2\beta r a \sin^2 \theta}{P} (a \dot{\phi} \sin^2 \theta + \dot{t}) = -2h , \tag{88}$$

$$\frac{\partial F}{\partial \dot{t}} = 2\dot{t} - \frac{2\beta r}{P} (a \dot{\phi} \sin^2 \theta + \dot{t}) = 2e . \tag{89}$$

These equations are linear in $\dot{\phi}$ and $\dot{t}$ and can be solved directly to obtain

$$\dot{\phi} = \frac{1}{P\Delta}\left[-\beta a e r + \frac{h}{\sin^2\theta}(P - \beta r)\right] \tag{90}$$

$$\dot{t} = \frac{1}{P\Delta}\left\{\beta a h r + e\left[P(r^2 + a^2) + \beta a^2 r \sin^2\theta\right]\right\}, \tag{91}$$

From Equation 87, the following Euler equation is obtained corresponding to the r coordinate:

$$\frac{2P}{\Delta}\ddot{r} + \frac{2\dot{r}}{\Delta^2}(\Delta\dot{P} - P\dot{\Delta}) - \frac{\dot{r}^2}{\Delta^2}[2r\Delta - P(2r - \beta)] - 2r\dot{\theta}^2 - 2r\dot{\phi}^2\sin^2\theta - \frac{\beta Q^2}{P} + \frac{2\beta r^2}{P^2}Q^2 = 0. \tag{92}$$

Finally, Equation 15 differentiated with respect to s becomes

$$\frac{2P}{\Delta}\dot{r}\ddot{r} + \frac{\dot{r}^2}{\Delta^2}(\Delta\dot{P} - P\dot{\Delta}) + \dot{P}\dot{\theta}^2 + 2P\dot{\theta}\ddot{\theta}$$

$$+ 2r\dot{r}\dot{\phi}^2\sin^2\theta + 2(r^2 + a^2)\dot{\theta}\dot{\phi}^2\sin\theta\cos\theta + 2(r^2 + a^2)\dot{\phi}\ddot{\phi}\sin^2\theta$$

$$- 2\dot{t}\ddot{t} + \frac{2P}{\beta r}(\dot{t} - e)\ddot{t} + \frac{\dot{P}(\dot{t} - e)^2}{\beta r} - \frac{P}{\beta r^2}(\dot{t} - e)^2\dot{r} = 0. \tag{93}$$

Equations 90 to 93 can be put into a form that is convenient for numerical integration by letting

$$x_1 = r, \tag{94}$$

$$x_2 = \theta, \tag{95}$$

$$x_3 = \phi, \tag{96}$$

$$x_4 = t, \tag{97}$$

$$x_5 = \dot{r}, \tag{98}$$

$$x_6 = \dot{\theta}. \tag{99}$$

By definition, we obtain

$$\dot{x}_1 = x_5, \tag{100}$$

$$\dot{x}_2 = x_6. \tag{101}$$

Then, Equations 90 and 91 become

$$\dot{x}_3 = \frac{1}{P\Delta}\left[-\beta a e x_1 + \frac{h}{\sin^2 x_2}(P - \beta x_1)\right] \tag{102}$$

$$\dot{x}_4 = \frac{1}{P\Delta}\left\{\beta a h x_1 + e[P(x_1^2 + a^2) + \beta a^2 x_1 \sin^2 x_2]\right\} \quad . \tag{103}$$

Solving Equations 92 and 93 for $\ddot{r}$ and $\ddot{\theta}$ and using Equations 94 to 99, it follows that

$$\dot{x}_5 = \frac{b_2}{a_{21}} \tag{104}$$

$$\dot{x}_6 = \frac{a_{21}b_1 - a_{11}b_2}{a_{12}a_{21}} \tag{105}$$

where

$$P = x_1^2 + a^2 \cos^2 x_2 \ , \tag{106}$$

$$\Delta = x_1^2 - \beta x_1 + a^2 \ , \tag{107}$$

$$b_1 = -\frac{x_5^2}{\Delta^2}(\Delta \dot{P} - P\dot{\Delta}) - \dot{P}x_6^2 - 2x_1x_5\dot{\phi}^2 \sin^2 x_2 - 2(x_1^2 + a^2)x_6\dot{\phi}^2 \sin x_2 \cos x_2$$
$$- 2(x_1^2 + a^2)\dot{\phi}\ddot{\phi}\sin^2 x_2 + 2\dot{t}\ddot{t} - \frac{2P}{\beta x_1}(\dot{t} - e)\ddot{t} - \frac{\dot{P}}{\beta x_1}(\dot{t} - e)^2 + \frac{P}{\beta x_1^2}(\dot{t} - e)^2 x_5 \ , \tag{108}$$

$$b_2 = -\frac{2x_5}{\Delta^2}(\dot{P}\Delta - P\dot{\Delta}) + \frac{x_5^2}{\Delta^2}[2x_1\Delta - P(2x_1 - \beta)] + 2x_1x_6^2 + 2x_1\dot{\phi}^2 \sin^2 x_2 + \frac{\beta}{P}Q^2 - \frac{2\beta x_1^2}{P^2}Q^2 \ ,$$

(109)

$$a_{11} = \frac{2Px_5}{\Delta} \ , \tag{110}$$

$$a_{12} = 2Px_6 \ , \tag{111}$$

$$a_{21} = \frac{2P}{\Delta} \ , \tag{112}$$

$$\dot{P} = 2x_1x_5 - 2a^2x_6 \cos x_2 \sin x_2 \ , \tag{113}$$

$$\dot{\Delta} = 2x_1x_5 - \beta x_5 \ , \tag{114}$$

$$Q = \frac{P}{\beta x_1}(\dot{t} - e) \ , \tag{115}$$

$$\dot{t} = \frac{1}{P\Delta}\left\{\beta a h x_1 + e[P(x_1^2 + a^2) + \beta a^2 x_1 \sin^2 x_2]\right\} , \tag{116}$$

$$\dot{\phi} = \frac{1}{P\Delta}\left[-e\beta a x_1 + \frac{h}{\sin^2 x_2}(P - \beta x_1)\right] , \tag{117}$$

$$\ddot{t} = \frac{1}{P\Delta}\left\{\beta a h x_5 + e[\dot{P}(x_1^2 + a^2) + 2x_1 x_5 P + \beta a^2 x_5 \sin^2 x_2 + 2\beta a^2 x_1 x_6 \sin x_2 \cos x_2]\right\} - \frac{\dot{t}}{P\Delta}(\Delta \dot{P} + P \dot{\Delta}) , \tag{118}$$

$$\ddot{\phi} = \frac{1}{P\Delta}\left[-e\beta a x_5 + \frac{h}{\sin^2 x_2}(\dot{P} - \beta x_5) - \frac{2h x_6 \cos x_2}{\sin^3 x_3}(P - \beta x_1)\right] - \frac{\dot{\phi}}{P\Delta}(\dot{P}\Delta + P\dot{\Delta}) . \tag{119}$$

Equivalence of the Constants of Motion in the *S* and *E* Forms

In Equation 17 for equatorial motion in the *E* form, there appear the two constants e^* and h^*, which are given by Equations 23 and 24. In the corresponding equation in the *S* form (Equation 44), there appear the constants e and h, which are given by Equations 37 and 38. It is obvious that these two sets of constants are not independent of each other. It will be shown that they are indeed identical. Moreover, this identity holds not only for the case of motion in the equatorial plane but for all motion.

From the *E* form of the Kerr metric given by Equation 8, the Lagrangian $F^*(r^*, \theta^*, \dot{r}^*, \dot{\theta}^*, \dot{t}^*, \dot{\phi}^*)$ is

$$F^* = -\dot{r}^{*2} - 2a\,\dot{r}^*\,\dot{\phi}^* \sin^2\theta^* - (r^{*2} + a^2)\,\dot{\phi}^{*2} \sin^2\theta^* - P^*\,\dot{\theta}^{*2} + \dot{t}^{*2} - \frac{\beta r^*}{P^*}(\dot{r}^* + a\,\dot{\phi}^* \sin^2\theta^* + \dot{t}^*)^2 . \tag{120}$$

Because F^* is not a function of ϕ^*, it follows that $\partial F^*/\partial\dot{\phi}^*$ may be set equal to a constant $-2h^*$; thus

$$h^* = a \sin^2\theta^*\left(1 + \frac{\beta r^*}{P^*}\right)\dot{r}^* + \sin^2\theta^*\left(r^{*2} + a^2 + \frac{\beta r^* a^2 \sin^2\theta^*}{P^*}\right)\dot{\phi}^* + \frac{\beta a r^*}{P^*}\,\dot{t}^* \sin^2\theta^* . \tag{121}$$

Similarly, because F^* is not a function of t^*, $\partial F^*/\partial t^*$ may be set equal to a constant $2e^*$ to obtain

$$e^* = -\frac{\beta r^*}{P^*}\,\dot{r}^* - \frac{\beta a r^* \sin^2\theta^*}{P^*}\,\dot{\phi}^* + \left(1 - \frac{\beta r^*}{P^*}\right)\dot{t}^* . \tag{122}$$

Solution of Equations 88 and 89 for motion in *S* coordinates for h and e yields

$$h = \left(r^2 + a^2 + \frac{\beta r a^2 \sin^2\theta}{P}\right)\dot{\phi} \sin^2\theta + \frac{\beta r a \sin^2\theta}{P}\,\dot{t} , \tag{123}$$

$$e = -\frac{\beta r a}{P}\,\dot{\phi}\,\sin^2\theta + \left(1 - \frac{\beta r}{P}\right)\dot{t}\,. \tag{124}$$

Next, from Equations 10 to 13, it follows that

$$\dot{r} = \dot{r}^*\,, \tag{125}$$

$$\dot{\theta} = \dot{\theta}^*\,, \tag{126}$$

$$\dot{\phi} = \dot{\phi}^* + \frac{a\,\dot{r}^*}{\Delta}\,, \tag{127}$$

$$\dot{t} = \dot{t}^* - \frac{\beta r^*\,\dot{r}^*}{\Delta^*}\,. \tag{128}$$

Substitution for r, θ, $\dot{\phi}$, and $\dot{t}$ from Equations 10, 11, 127, and 128 into Equation 123 leads to

$$h = \left(r^{*2} + a^2 + \frac{\beta r^* a^2\,\sin^2\theta^*}{P^*}\right)\sin^2\theta^*\left(\dot{\phi}^* + \frac{a\,\dot{r}^*}{\Delta^*}\right) + \frac{\beta r^* a\,\sin^2\theta^*}{P^*}\left(\dot{t}^* - \frac{\beta r^*\,\dot{r}^*}{\Delta^*}\right). \tag{129}$$

Rearrangement of terms and substitution from Equation 14 yield

$$h = \frac{a\,\dot{r}^*\,\sin^2\theta^*}{\Delta^*}\left(\Delta^* + \frac{\Delta^*\beta r}{P^*}\right) + \sin^2\theta^*\,\dot{\phi}^*\left(r^{*2} + a^2 + \frac{\beta r^* a^2\,\sin^2\theta^*}{P^*}\right) + \frac{\beta r^* a\,\sin^2\theta^*}{P^*}\,\dot{t}^*\,, \tag{130}$$

or

$$h = a\,\dot{r}^*\,\sin^2\theta^*\left(1 + \frac{\beta r^*}{P^*}\right) + \sin^2\theta^*\,\dot{\phi}^*\left(r^{*2} + a^2 + \frac{\beta r^* a^2\,\sin^2\theta^*}{P^*}\right) + \frac{\beta r^* a\,\sin^2\theta^*}{P^*}\,\dot{t}^*\,,$$

which is precisely Equation 121; hence,

$$h \equiv h^*\,. \tag{131}$$

Similarly, substitution for r, θ, $\dot{\phi}$, and $\dot{t}$ from Equations 10, 11, 127, and 128 into Equation 124 leads to

$$e = -\frac{\beta r^* a}{P^*}\,\sin^2\theta^*\left(\dot{\phi}^* + \frac{a\,\dot{r}^*}{\Delta^*}\right) + \left(1 - \frac{\beta r^*}{P^*}\right)\left(\dot{t}^* - \frac{\beta r^*\,\dot{r}^*}{\Delta^*}\right). \tag{132}$$

Again, rearrangement of terms and substitution from Equations 14 yield

$$e = -\frac{\beta r^*\,\dot{r}^*}{P^*} - \frac{\beta r^* a\,\sin^2\theta^*}{P^*}\,\dot{\phi}^* + \left(1 - \frac{\beta r^*}{P^*}\right)\dot{t}^* \tag{133}$$

or

$$e = -\frac{\beta r^*}{P^*}\,\dot{r}^* - \frac{\beta a r^*\,\sin^2\theta^*}{P^*}\,\dot{\phi}^* + \left(1 - \frac{\beta r^*}{P^*}\right)\dot{t}^*\,,$$

which is precisely Equation 122; therefore,

$$e \equiv e^*\,. \tag{134}$$

ANALYSIS OF EQUATORIAL ORBITS

Approach

A geometric-topological approach is used in the following analysis because there is no known direct analytical approach that provides exact solutions. Moreover, even if one exists, it is expected that it would be rather long and cumbersome. For instance, in the case of the Schwarzschild gravitational field, a complete analytical solution of orbits as given by Hagihara (Reference 9) required 110 pages in final journal form and was heavily dependent on elliptic functions.

As in Appendix A, the results for each value of a are represented in a master diagram that gives the complete topological genera of the orbits for various ranges of the two parameters h and e. In particular, in the Newtonian limit, the quantity $W \equiv e^2 - 1$ is the analog of $2E$, where E is the energy per unit mass of the test particle.

Summary of the Equation To Be Studied

The equation of motion in the S form of a test particle in the equatorial plane of the Kerr gravitational field has been derived:

$$\left(\frac{du}{d\phi}\right)^2 = B(u)\frac{D^2(u)}{E^2(u)}\,, \tag{44}$$

where

$$B(u) = \beta(h + ea)^2u^3 - [h^2 + (1 - e^2)a^2]u^2 + \beta u - (1 - e^2)\,, \tag{45}$$

$$D(u) = a^2u^2 - \beta u + 1\,, \tag{46}$$

$$E(u) = -\beta(h + ea)u + h\,. \tag{47}$$

The constants of motion h and e are given by

$$h = \left(r^2 + a^2 + \frac{\beta a^2}{r}\right)\frac{d\phi}{ds} + \frac{\beta a}{r}\frac{dt}{ds} \tag{135}$$

$$e = -\frac{\beta a}{r}\frac{d\phi}{ds} + \left(1 - \frac{\beta}{r}\right)\frac{dt}{ds}\,. \tag{136}$$

Without loss of generality, $a \geqslant 0$ is taken for the sake of simplicity of discussion. The quantities u, ϕ, h, and e have in Newtonian orbits the counterparts inverse radius, true anomaly, angular momentum per unit mass of test particle, and energy per unit mass of test particle, respectively.

Investigation of the Cubic $B(u)$

The cubic $B(u)$ appearing in Equation 44 degenerates into $h^2f(u)$ for $a = 0$, where $f(u)$ in this case is the one for the Schwarzschild gravitational field and h is a constant. Chan has made a complete study of $f(u)$ for $a = 0$ and his results are now extended for values of $a \neq 0$. In view of this, it is

desirable to study the cubic curve $B(u)$. For $h + ea \neq 0$, $B(u) = 0$ can have only zero, one, two, or three positive roots. A general approach in this direction would require the algebraic knowledge of roots of the cubic equation, and this is available, but the analysis becomes very cumbersome algebraically. In addition, it becomes more involved, for instance, in the case of one real positive root, whether the remaining two roots are real but negative or are complex conjugates. Alternatively, the following approach can be taken: On successively differentiating

$$B(u) = \beta(h + ea)^2 u^3 - [h^2 + (1 - e^2)a^2]u^2 + \beta u + e^2 - 1 , \qquad (45)$$

it follows that

$$B'(u) = \frac{dB}{du} = 3\beta(h + ea)^2 u^2 - 2[h^2 + (1 - e^2)a^2]u + \beta \qquad (137)$$

$$B''(u) = \frac{d^2B}{du^2} = 6\beta(h + ea)^2 u - 2[h^2 + (1 - e^2)a^2] . \qquad (138)$$

Hence, $B''(u)$ is a straight line intersecting the u axis at

$$u''_B \equiv u_s = \frac{h^2 + (1 - e^2)a^2}{3\beta(h + ea)^2} , \qquad (139)$$

where u_s is the point of symmetry of the cubic $B(u)$.

The intercepts, u'_{B1} and u'_{B2} if they exist, of the parabola $B'(u)$ with the u axis are given by

$$u'_{B1,B2} = \frac{h^2 + (1 - e^2)a^2}{3\beta(h + ea)^2}\left(1 \pm \sqrt{V}\right) \qquad (140)$$

where

$$V \equiv 1 - \frac{3\beta^2(h + ea)^2}{[h^2 + (1 - e^2)a^2]^2} . \qquad (141)$$

Now, in view of equation 139, Equation 140 can also be written in the form

$$u'_{B1,B2} = u_s\left(1 \pm \sqrt{V}\right) \qquad (142)$$

where for $u_s > 0$, the minus sign is associated with u'_{B1} and the plus sign with u'_{B2} and for $u_s < 0$ the plus sign is associated with u'_{B1} and the minus sign with u'_{B2}.

From the coefficients of the parabola $B'(u)$, noting that $\beta > 0$ in Equation 137, it follows that $B'(u)$ can be classified into seven categories, as shown in Figure 1:

(a) No real root, $u_s > 0$

(b) One real positive double root

(c) Two distinct real positive roots

(d) No real root, $u_s = 0$

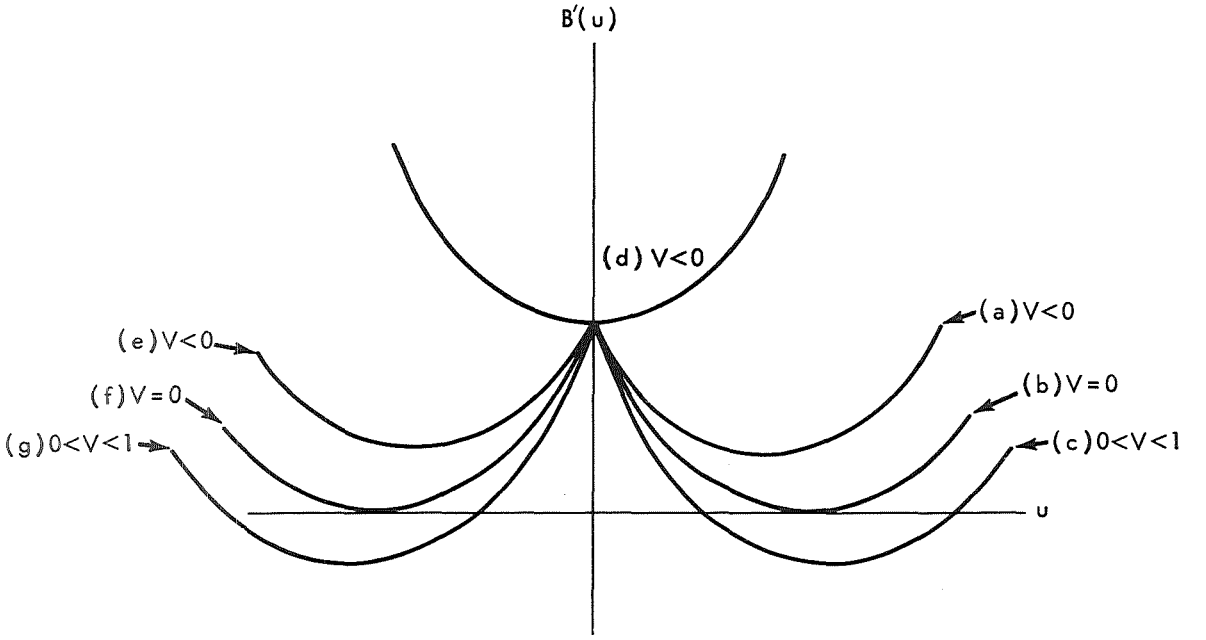

Figure 1—Criterion for the seven classes of trace cubic curves.

(e) No real root, $u_s < 0$

(f) One real negative double root

(g) Two distinct real negative roots

Equations 141 and 142 indicate that

(1) $V < 0$ for cases (a), (d), and (e).

(2) $V = 0$ for cases (b) and (f).

(3) $0 < V < 1$ for cases (c) and (g).

Corresponding to these, the cubic $B(u)$ can be classified into seven categories as shown in Figure 2; for each case, all conceivable curves are qualitatively illustrated and are not obtained by simple vertical translation from one another as can be verified by Equation 45. As a concrete example for discussion, the cubic-curve category c was chosen because it contains many features shared by the other types. The cubic $B(u)$ is shown in Figure 3 with the three roots $u_{B1,B2,B3}$ (indicated by $u_{I,II,III}$ in the figure) of $B(u) = 0$. In general, any real root of $B(u) = 0$ is denoted by u_B.

For a double root,

$$B(u_B) = 0 \tag{143}$$

$$B'(u_B) = 0\,. \tag{144}$$

Hence, double roots of two types occur:

(1) $$u_{B1} = u_{B2} = u'_{B1}\,. \tag{145}$$

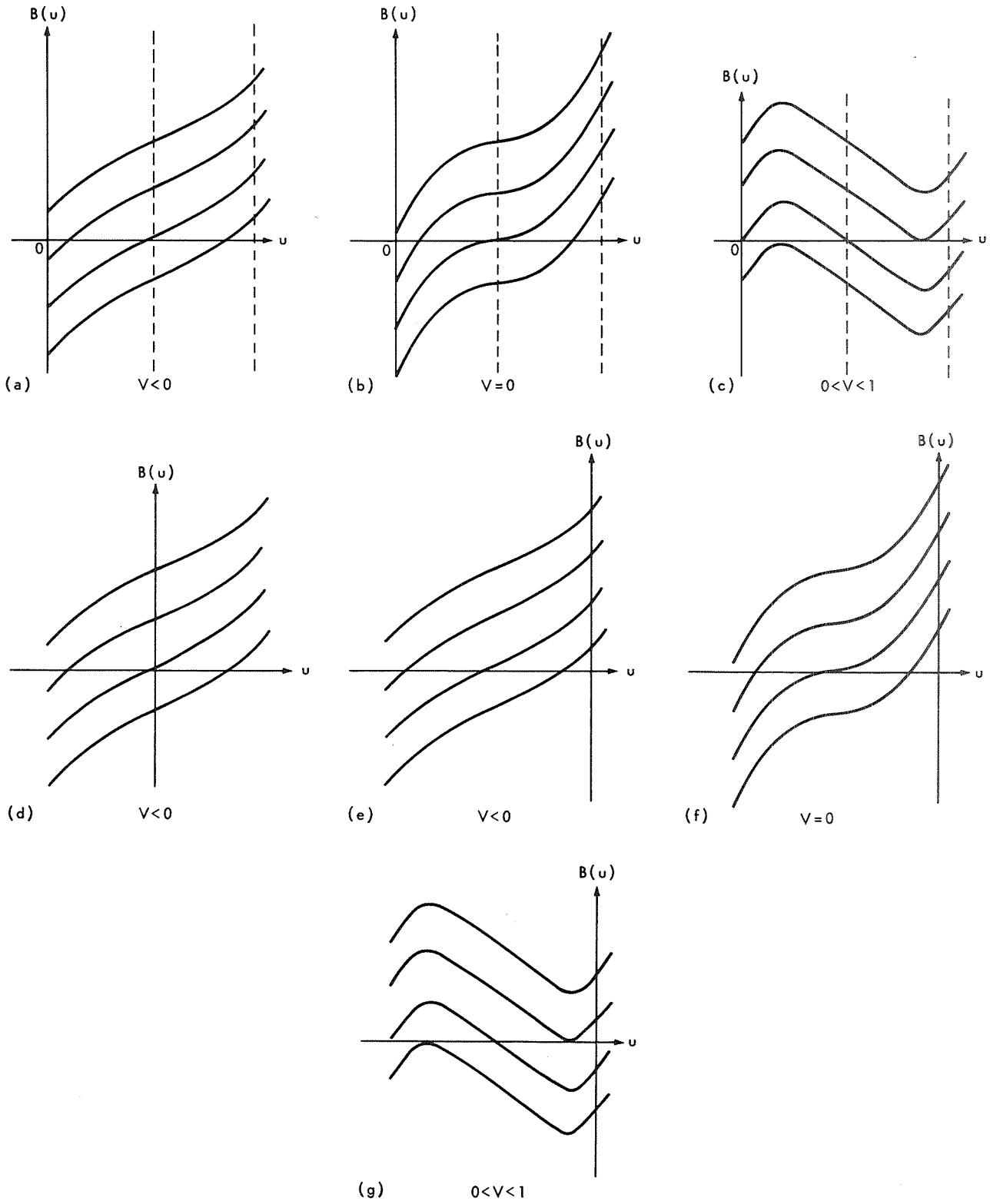

Figure 2—Curves for each of the seven classes of trace cubic.

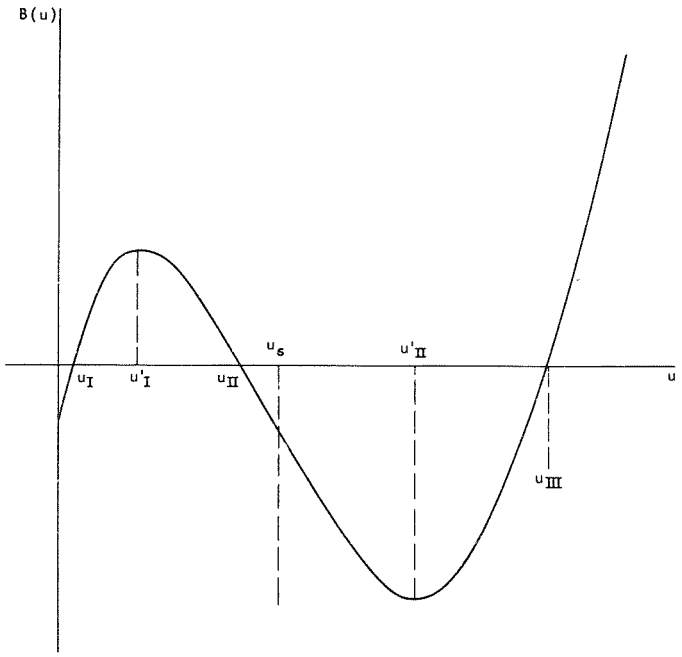

Figure 3—Cubic curve of category c with $W < 0$.

(2) $$u_{B2} = u_{B3} = u'_{B2} \ . \tag{146}$$

For double roots of type 1, $u_{B1} = u_{B2}$ and Equation 143 becomes $B(u'_{B1}) = 0$. Substituting u'_{B1} from Equation 142,

$$-\sqrt{V}\left[\frac{2}{3}\beta u_s - 2\beta(h+ea)^2 u_s^3\right] = (1-e^2) - \beta u_s + 2\beta(h+ea)^2 u_s^3 \ , \tag{147}$$

the square of which is

$$V\left[\frac{2}{3}\beta u_s - 2\beta(h+ea)^2 u_s^3\right]^2 = [(1-e^2) - \beta u_s + 2\beta(h+ea)^2 u_s^3]^2 \ . \tag{148}$$

Similarly, for double roots of type 2, $u_{B2} = u'_{B2}$, and Equation 143 becomes $B(u'_{B2}) = 0$. Substituting u'_{B2} from Equation 142 and then squaring the resultant equation yields again Equation 148. That is, Equation 148 gives solutions of both type 1 and type 2 double roots of $B(u) = 0$.

Substituting for u_s and V from Equations 139 and 141 into Equation 148, the following equation is obtained after much tedious algebraic work:

$$A_6 h^6 + A_5 h^5 + A_4 h^4 + A_3 h^3 + A_2 h^2 + A_1 h + A_0 = 0 \ , \tag{149}$$

where the coefficients $A_i(e, a, \beta)$ are given by

$$A_0 = a^2[4(1-e^2)^4 a^4 + \beta^2 a^2(27e^8 - 72e^6 + 62e^4 - 16e^2 - 1) + 4\beta^4 e^2] \ , \tag{150a}$$

$$A_1 = \beta^2 ea[a^2(108e^6 - 252e^4 + 180e^2 - 36) + 8\beta^2] \ , \tag{150b}$$

$$A_2 = 12(1 - e^2)^3 a^4 + \beta^2 a^2 (162e^6 - 324e^4 + 182e^2 - 20) + 4\beta^4 \,, \tag{150c}$$

$$A_3 = \beta^2 ea(108e^4 - 180e^2 + 72) \,, \tag{150d}$$

$$A_4 = 12(1 - e^2)^2 a^2 + \beta^2 (8 - 36e^2 + 27e^4) \,, \tag{150e}$$

$$A_5 = 0 \,, \tag{150f}$$

$$A_6 = 4(1 - e^2) \,. \tag{150g}$$

Now, in principle, h can be solved as a function of e with a and β as parameters. However, this cannot be done in general because Equation 149 is of the sixth order. Instead, a relation between h and e with a and β as parameters may be found by numerical methods. That is, for a given set (a, β) a value of e is fixed and then values of h that satisfy Equation 149 are computed. This is then done for another value of e to obtain the corresponding values of h. Some typical results are presented in Figures 4 to 7; these figures are for $\beta = 2$ and $a = 0$, 0.7, 1, and 1.4, respectively. The symbols S and U designate, respectively, the loci for which double roots of $B(u) = 0$ of types 1 and 2 occur. That is, the S line is given by eliminating u'_{B1} between

$$\left.\begin{aligned} B(u'_{B1}; h, e, a, \beta) &= 0 \\ \text{and} \qquad B'(u'_{B1}; h, e, a, \beta) &= 0 \,, \end{aligned}\right\} \tag{151}$$

whereas the U line is given by eliminating u'_{B2} between

$$\left.\begin{aligned} B(u'_{B2}; h, e, a, \beta) &= 0 \\ \text{and} \qquad B'(u'_{B2}; h, e, a, \beta) &= 0 \,. \end{aligned}\right\} \tag{152}$$

It follows from Equations 142, 145, and 146 that there are no double roots of $B(u) = 0$ for $V < 0$. Because of this, the curves for which $V = 0$, known as V lines, are also plotted in Figures 4 to 7. From Equation 45 it can be seen that the intercept of the cubic $B(u)$ with the $B(u)$ axis is given by

$$B(0) = e^2 - 1 = W \,, \tag{153}$$

so that

$$\left.\begin{aligned} B(0) < 0 \qquad & \text{for } W < 0 \\ B(0) > 0 \qquad & \text{for } W > 0 \,. \end{aligned}\right\} \tag{154}$$

In these figures, the W lines are defined by $W(e) = 0$, where $W(e)$ is given by Equation 153.

Next, the cubic $B(u)$ is classified according to regions of the h, e space for a given set of (a, β). For $a = 0$, $B(u)$ degenerates to $h^2 f(u)$ where $f(u)$ is the cubic studied by Chan in Appendix A. In Figure A15 and Table A2, he has already classified the cubic into seven essentially different regions of the h, W space labeled 1, 2, 3, 4, 4*, 5, and 5*. Table 1 gives the properties of the cubic $B(u)$ in these regions and two other regions 6 and 6* which exist because of the additional cases of the quadratic $B'(u)$ corresponding to $u_s < 0$.

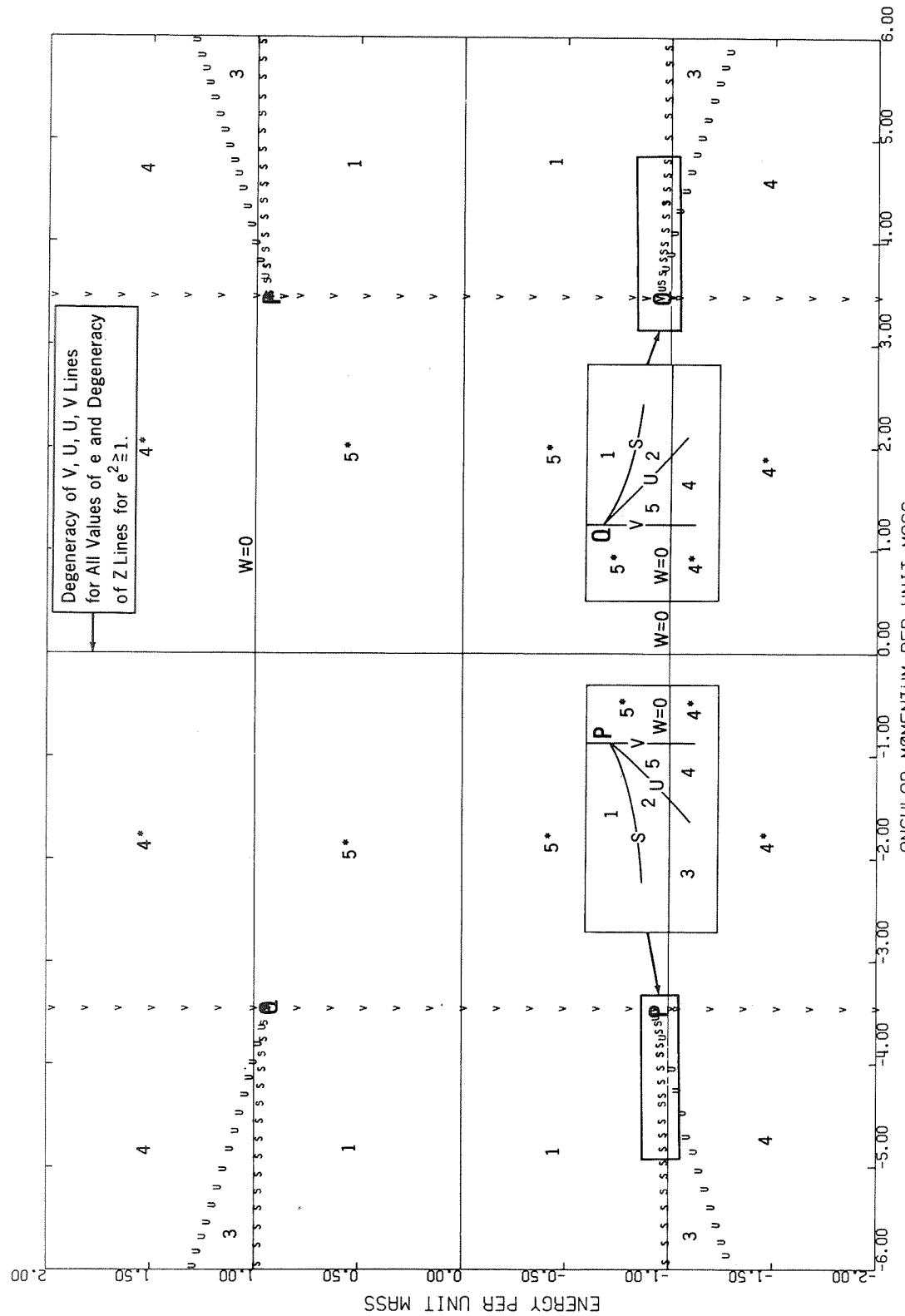

Figure 4—Classification of h, e space according to characteristics of $B(u)$ curve for $a = 0.0$.

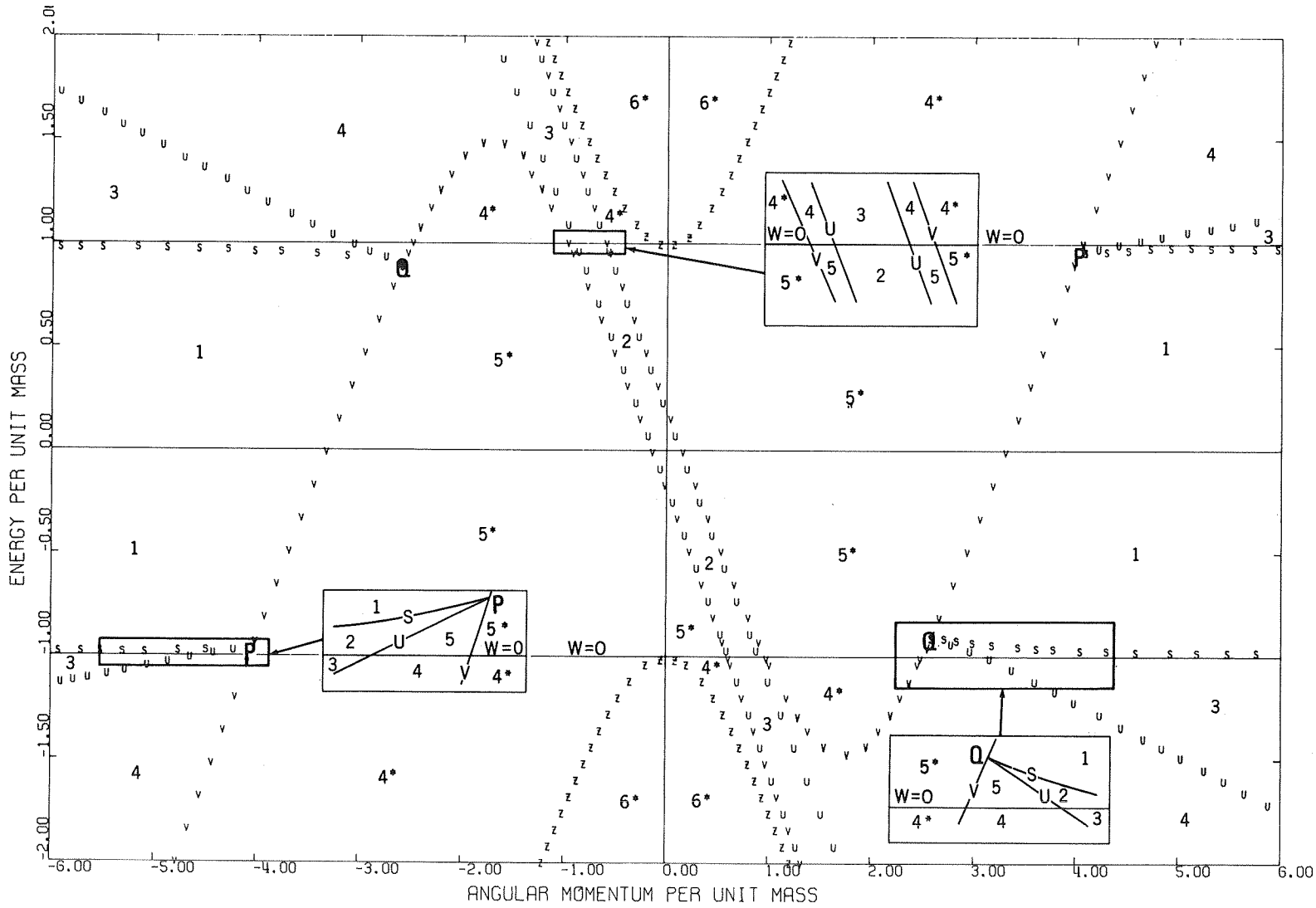

Figure 5—Typical classification of h, e space according to characteristics of $B(u)$ curve for $0 < a < 1$ (shown here for $a = 0.7$).

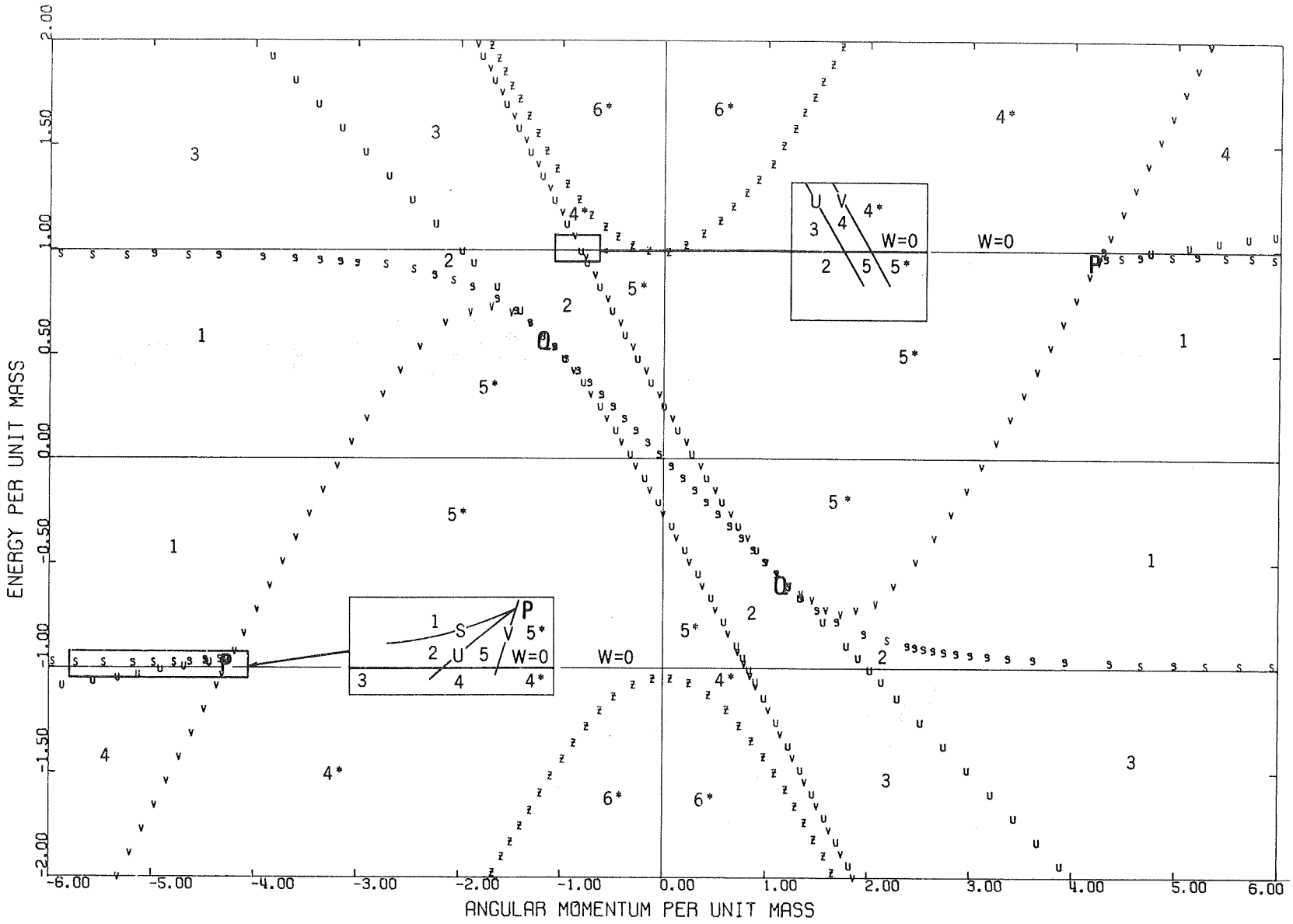

Figure 6—Classification of h, e space according to characteristics of $B(u)$ curve for a = 1.0.

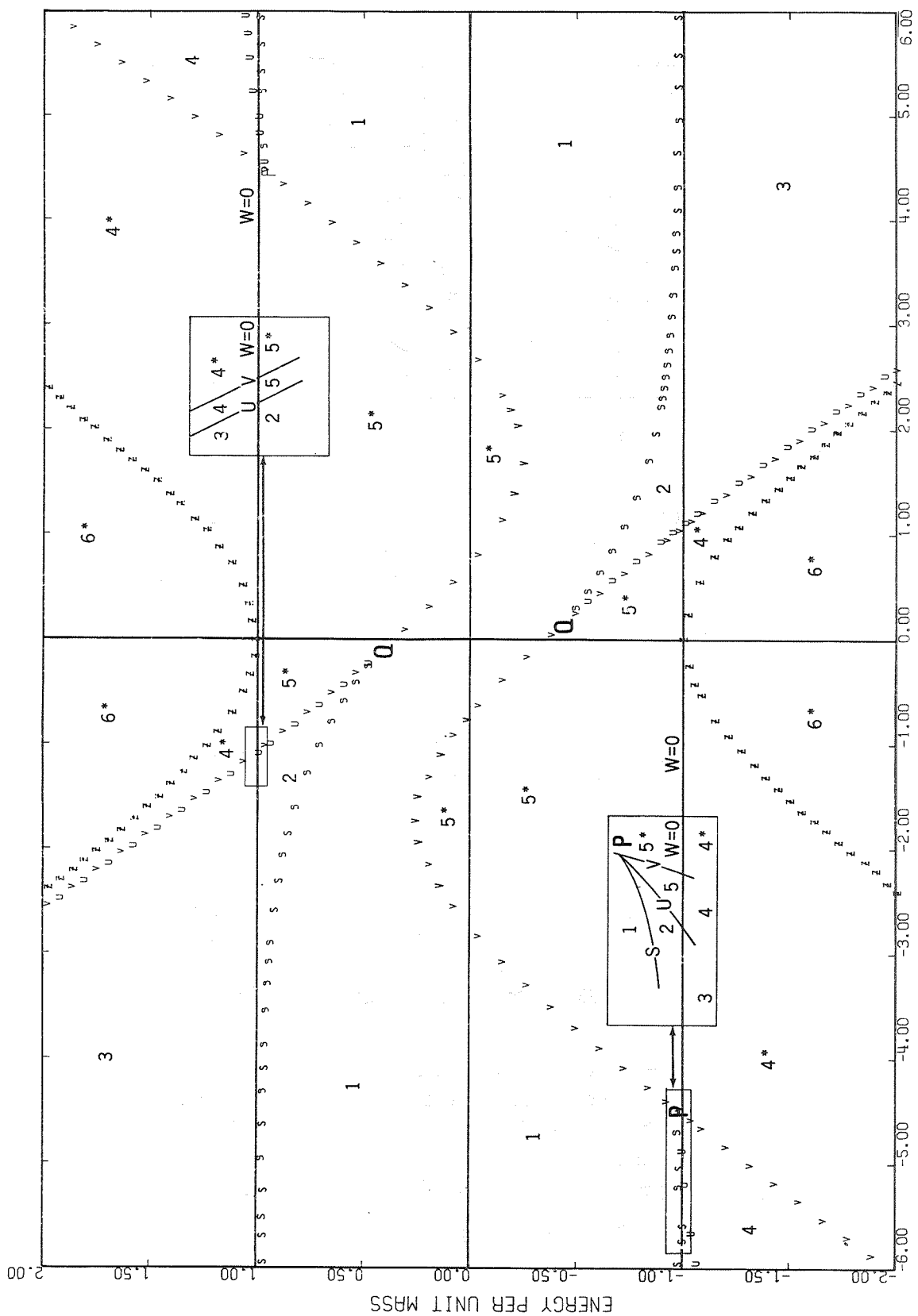

Figure 7—Typical classification of h, e space according to characteristics of $B(u)$ curve for $a > 1.0$ (shown here for $a = 1.4$).

Table 1—Characteristics of the cubic $B(u)$ for various regions of the master diagram.

Region	$B(u'_{\mathrm{I}})$	$B(u'_{\mathrm{II}})$	V	W	u_s
1	<0	<0	>0	<0	>0
2	>0	<0	>0	<0	>0
3	>0	<0	>0	>0	>0
4	>0	>0	>0	>0	>0
4*	([a])	([a])	<0	>0	>0
5	>0	>0	>0	<0	>0
5*	([a])	([a])	<0	<0	>0
6	>0	>0	>0	>0	<0
6*	([a])	([a])	<0	>0	<0

[a] u'_{B1} and u'_{B2} do not exist for $V < 0$.

These cubics are shown in Figure 8. Using a one-to-one correspondence between Figures 4 and A15, the regions in Figure 4 are labeled. A little consideration reveals that the regions in Figures 5 to 7 can be labeled as shown. Figure 4 is a master diagram for $a = 0$; however, Figures 5 to 7 are not yet master diagrams because $f(u) = B(u)D^2(u)/E^2(u)$ and not just $B(u)/h^2$ must be considered for $a \neq 0$.

For convenience, Z and H are defined as

$$Z \equiv h^2 + (1 - e^2)a^2 \tag{155}$$

$$H \equiv h + ea\,. \tag{156}$$

For $Z > 0$ and $H \neq 0$, the cubic $B(u)$ of Equation 45 is similar to the one studied by Chan, which is

$$f(u) = 2mu^3 - u^2 + \frac{2m}{h^2}u + \frac{W}{h^2} \tag{157}$$

and hence the labeling of regions 1, 2, 3, 4, 4*, 5, and 5* of Figures 5 to 7 follow from Chan's work (Appendix A). The characteristics of the cubic $B(u)$ corresponding to these regions are shown in Figure 8, which is equivalent to Table 1. We have already noted that for all seven of these regions the point of symmetry u_s given by Equation 139 and the roots u'_{B1} and u'_{B2} of $B'(u) = 0$ given by Equation 140 are greater than zero.

In addition, two new regions previously mentioned occur for $Z < 0$ and $H \neq 0$. In these two regions the point of symmetry of the $B(u)$ curve and the roots of $B'(u) = 0$ are both less than zero. In region 6*, since $V < 0$, it is obvious that $B(u) = 0$ has only a single root, which is negative. In region 6, it can be proved that $B(u'_{B1}) > 0$ and $B(u'_{B2}) > 0$ so that there can only be one negative root of $B(u) = 0$. The details are given in Appendix B. Because of these additional regions, the lines for which

$$Z \equiv h^2 + (1 - e^2)a^2 = 0\,, \tag{158}$$

known as the Z lines, are plotted in Figures 5 to 7.

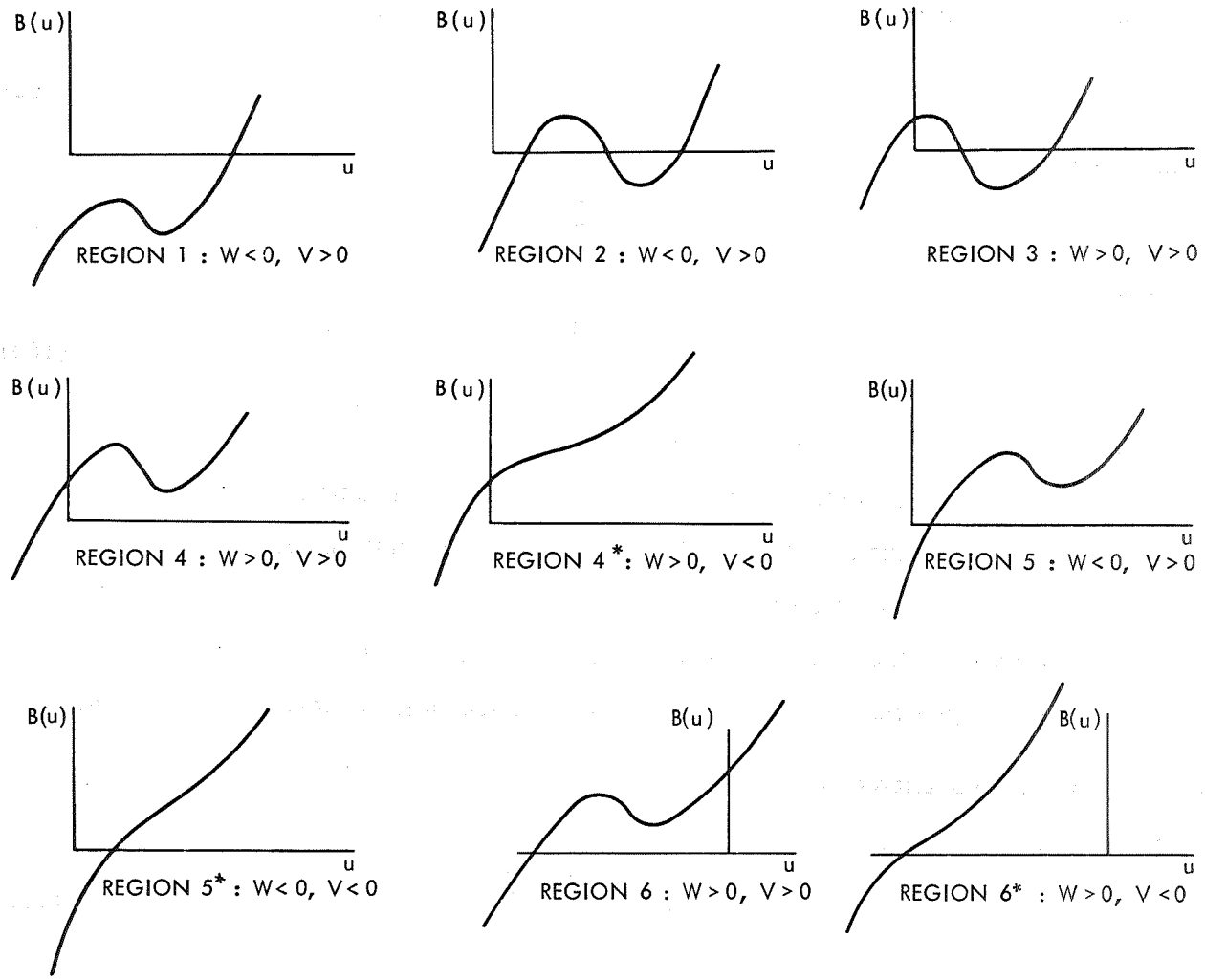

Figure 8—Characteristics of the $B(u)$ curve in various regions.

Finally, it remains to discuss the special case in which $H = 0$. For this, it is convenient to define the H line by

$$H \equiv h + ea = 0 \,, \tag{159}$$

which is always a straight line. From Equations 45 and 159 it is seen that on an H line, $B(u)$ becomes the quadratic

$$B(u) = -a^2u^2 + \beta u + e^2 - 1 \,. \tag{160}$$

The roots of this equation are

$$u_{B1,B2} = \frac{\beta \pm \sqrt{\beta^2 - 4a^2(1 - e^2)}}{2a^2} \,. \tag{161}$$

From Equation 161, it is noted that Equation 160 has distinct roots for

$$e^2 > 1 - \frac{\beta^2}{4a^2}, \tag{162}$$

a double root at

$$e^2 = 1 - \frac{\beta^2}{4a^2}, \tag{163}$$

and no real roots for

$$e^2 < 1 - \frac{\beta^2}{4a^2}. \tag{164}$$

As a summary, in the h, e plane for a given set (a, β)—

(1) The S and U lines give the condition for double roots of the cubic $B(u) = 0$.

(2) The V lines give the condition for double roots of the quadratic $B'(u) = 0$.

(3) The W lines give the condition for $B(0) = 0$.

(4) The Z lines give the condition for which the point of symmetry $u_s = 0$.

(5) The H lines give the condition for which $B(u)$ is a quadratic; otherwise, $B(u)$ is a cubic.

Investigation of the Function $f(u)$

Now consider the equation

$$f(u) = B(u)\frac{D^2(u)}{E^2(u)} \tag{165}$$

where $B(u)$, $D(u)$, and $E(u)$ (defined in Equations 45 to 47) are cubic, quadratic, and linear in u, respectively. Let u_f be any root of the equation

$$f(u) = 0. \tag{166}$$

For a double root,

$$f(u_f) = 0 \tag{167}$$

$$f'(u_f) = 0. \tag{168}$$

Specifically, let u_c be any value for which these two equations hold. It can be shown that Equations 167 and 168 are the necessary and sufficient condition for a circular orbit to exist. (See Appendix A discussion of Equations A7 to A10 and A19.)

Table 2 presents all of the conceivable combinations of the zeros of $B(u)$, $D(u)$, and $E(u)$ for which Equation 166 could possibly have a degenerate root u_c. That most of these cases are impossible can be shown as follows: Let u_B, u_D, and u_E be any real root of $B(u) = 0$, $D(u) = 0$, and $E(u) = 0$,

Table 2—Ways in which $f(u) = 0$ could have a degenerate root u_c.

Case	Number of Roots of $B(u) = 0$ Equal to u_c	Number of Roots of $D(u) = 0$ Equal to u_c	Number of Roots of $E(u) = 0$ Equal to u_c
1[a]	0	1	0
2[a]	0	2	0
3	0	2	1
4	1	1	0
5	1	2	0
6	1	2	1
7[a]	2	0	0
8	2	1	0
9	2	1	1
10	2	2	0
11[a]	2	2	1
12[a]	3	0	0
13	3	1	0
14	3	1	1
15	3	2	0
16[a]	3	2	1

[a]These cases are actually possible.

respectively. That is, by definition

$$\left.\begin{aligned} B(u_B) &\equiv 0\,, \\ D(u_D) &\equiv 0\,, \\ E(u_E) &\equiv 0\,. \end{aligned}\right\} \tag{169}$$

The condition

$$\left.\begin{aligned} B(u_D) &= 0 \\ u_B &= u_D \end{aligned}\right\} \tag{170}$$

is examined first. From Equation 49, which is

$$AD + a^2 B \equiv E^2\,, \tag{49}$$

and the definition $D(u_D) \equiv 0$,

$$a^2 B(u_D) = E^2(u_D)\,. \tag{171}$$

It follows that

$$B(u_D) = 0 \Longleftrightarrow E(u_D) = 0\,. \tag{172}$$

Hence, cases 3, 4, 5, 8, 10, 13, and 15 of Table 2 are impossible.

Next, the condition

$$\left.\begin{aligned} \mathrm{D}'(u_D) &= 0 \\ B(u_D) &= 0 \end{aligned}\right\} \tag{173}$$

is considered. Differentiation of Equation 49 results in

$$A'D + A\,D' + a^2\,B' = 2E\,E' \,. \tag{174}$$

From Equations 49, 174, and the definition $D(u_D) \equiv 0$, it follows that

$$A(u_D)\,D'(u_D) + a^2\,B'(u_D) = 2E(u_D)\,E'(u_D) \,. \tag{175}$$

Hence, from Equations 171, 173, and 175,

$$\left.\begin{aligned} D'(u_D) &= 0 \\ B(u_D) &= 0 \end{aligned}\right\} \Rightarrow B'(u_D) = 0 \,. \tag{176}$$

Therefore, case 6 of Table 2 is impossible.

The condition

$$\left.\begin{aligned} B(u_E) &= 0 \\ B'(u_E) &= 0 \end{aligned}\right\} \tag{177}$$

is examined next. From Equations 49 and 174 and the definition $E(u_E) \equiv 0$, the following are obtained:

$$A(u_E)D(u_E) + a^2 B(u_E) = 0 \tag{178}$$

$$A'(u_E)D(u_E) + A(u_E)\,D'(u_E) + a^2\,B'(u_E) = 0 \,. \tag{179}$$

From Equations 177 to 179, therefore,

$$A(u_E)D(u_E) = 0 \tag{180}$$

$$A'(u_E)D(u_E) + A(u_E)\,D'(u_E) = 0 \,. \tag{181}$$

For Equation 180, there are three cases: (a) $A(u_E) = 0$ and $D(u_E) = 0$, (b) $A(u_E) = 0$ and $D(u_E) \neq 0$, and (c) $A(u_E) \neq 0$ and $D(u_E) = 0$. It is shown in Appendix B that $A(u_E) = 0$ and $D(u_E) = 0$ cannot be satisfied simultaneously and hence case a is impossible. From Equation 181, it is seen that

$$A'(u_E)D(u_E) = 0 \,, \tag{182}$$

so that

$$A'(u_E) = 0 \,. \tag{183}$$

It is shown in Appendix B that $A'(u_E) \neq 0$ for any finite u_E, and hence case b is impossible. Finally, from Equation 181,

$$A(u_E)\,D'(u_E) = 0 \,, \tag{184}$$

so that

$$D'(u_E) = 0 \,. \tag{185}$$

It follows from this discussion that

$$\left.\begin{aligned} B(u_E) &= 0 \\ B'(u_E) &= 0 \end{aligned}\right\} \Rightarrow \left\{\begin{aligned} D(u_E) &= 0 \\ D'(u_E) &= 0 \end{aligned}\right. \,. \tag{186}$$

From the identity

$$D(u_E) = 0 \Longleftrightarrow u_D = u_E \Longleftrightarrow E(u_D) = 0\,, \tag{187}$$

Equation 186 becomes

$$\left.\begin{aligned} B(u_E) &= 0 \\ B'(u_E) &= 0 \end{aligned}\right\} \Rightarrow \left\{\begin{aligned} E(u_D) &= 0 \\ D'(u_D) &= 0 \end{aligned}\right. . \tag{188}$$

Hence, cases 9 and 14 of Table 2 are impossible.

From Equations 45 to 47, we see that $B(u; h, e, a, \beta) = 0$, $D(u; a, \beta) = 0$, and $E(u; h, e, a, \beta) = 0$ do not contain any common factors for all values of (h, e, a, β). It follows that there exist values of (h, e, a, β) for which cases 1, 2, 7, and 12 are possible.

From Equations 172 and 176, the following is obtained:

$$\left.\begin{aligned} D(u_D) &= 0 \\ D'(u_D) &= 0 \\ E(u_D) &= 0 \end{aligned}\right\} \Rightarrow \left\{\begin{aligned} B(u_D) &= 0 \\ B'(u_D) &= 0 \end{aligned}\right. . \tag{189}$$

Because it is obvious from Equations 46 and 47 that the left-hand side of Equation 189 can be satisfied, case 11 is possible.

Finally, for case 16, consider only the equations

$$\left.\begin{aligned} D(u_D) &= 0\,, \\ D'(u_D) &= 0\,, \\ E(u_D) &= 0\,, \\ B''(u_D) &= 0\,. \end{aligned}\right\} \tag{190}$$

The remaining two equations, $B(u_D) = 0$ and $B'(u_D) = 0$, are automatically satisfied in view of Equation 189. It is shown in Appendix B that this set of equations has the solution given by the following equations:

$$e = \pm\frac{1}{\sqrt{3}}\,, \tag{191a}$$

$$h = \mp\frac{2}{\sqrt{3}}a\,, \tag{191b}$$

$$\beta = \pm 2a\,, \tag{191c}$$

$$u_D = \pm\frac{1}{a}\,. \tag{191d}$$

Hence, case 16 is possible.

In summary, all the possible cases for which $f(u) = 0$ can have a degenerate root at u_c are 1, 2, 7, 11, 12, and 16, as indicated in Table 2.

Next, the properties of the cubic $B(u)$ at the values u_D and u_E will be investigated. From Equation 171 it follows that

$$\begin{aligned} B(u_D) &= \frac{1}{a^2} E^2(u_D) \\ &= \frac{1}{a^2} [h - \beta(h + ea)u_D]^2 \\ &= \frac{1}{a^2} (h - h\beta u_D - a\beta e u_D)^2 , \end{aligned} \tag{192}$$

which, in view of the definition $D(u_D) = 0$ or

$$D(u_D) = a^2 u_D^2 - \beta u_D + 1 = 0 , \tag{193}$$

becomes

$$\begin{aligned} B(u_D) &= \frac{1}{a^2} [h - h(a^2 u_D^2 + 1) - a\beta e u_D]^2 \\ &= u_D^2 (ahu_D + \beta e)^2 . \end{aligned} \tag{194}$$

It is obvious that

$$\left.\begin{aligned} B(u_D) = 0 &\Longleftrightarrow h = -\frac{e\beta}{au_D} \\ B(u_D) &> 0 \qquad \text{otherwise} , \end{aligned}\right\} \tag{195}$$

where u_D is either of the two real roots u_{D1} and u_{D2}.

In view of this, the D_1 line and D_2 line in the h, e space for a given set (a, β) are defined by the respective equations:

$$\left.\begin{aligned} D_1 &\equiv h + \frac{e\beta}{au_{D1}} = 0 \\ D_2 &\equiv h + \frac{e\beta}{au_{D2}} = 0 , \end{aligned}\right\} \tag{196}$$

where u_{D1} and u_{D2} are the two roots of $D(u) = 0$; i.e.,

$$u_{D1,D2} = \frac{\beta \pm \sqrt{\beta^2 - 4a^2}}{2a^2} . \tag{197}$$

In general, a D line refers to either one of these and thus may be defined by eliminating u between the equations

$$\left.\begin{aligned} B(u;h,e,a,\beta) &= 0 \\ D(u;a,\beta) &= 0\,. \end{aligned}\right\} \tag{198}$$

It is shown in Appendix B that $B(u_E)$ has the following two equivalent forms:

$$B(u_E) = \frac{ae^2}{\beta^2(h+e)^2}(eh - a + ae^2)\left[\left(\frac{h}{e}\right)^2 + \frac{\beta^2}{a}\,\frac{h}{e} + \beta^2\right] \tag{199}$$

$$B(u_E) = \frac{a}{\beta^2(h+ae)^2}(eh - a + ae^2)\left(h + \frac{e\beta}{au_{D1}}\right)\left(h + \frac{e\beta}{au_{D2}}\right). \tag{200}$$

For convenience, the E_1 line in the h, e space for a given value of a is defined as

$$E_1 = eh - a + ae^2 = 0\,. \tag{201}$$

For the case $\beta^2 - 4a^2 \geqslant 0$, so that by Equation 197 the roots of $D(u) = 0$ are real, it is preferable to use Equation 200 from which results

$$\left.\begin{aligned} B(u_E) = 0 \Longleftrightarrow & \left\{\begin{array}{l} h, e \text{ on } D \text{ line} \\ \text{or } h, e \text{ on } E_1 \text{ line} \end{array}\right\} \\ B(u_E) \gtrless 0 \qquad & \text{otherwise.} \end{aligned}\right\} \tag{202}$$

In this case, the sign of $B(u_E)$ is determined by the combination of the D and E_1 lines. Typical results are presented in Figures 9 and 10 for $\beta = 2$ and $a = 0.7$ and $a = 1$, respectively. In Figure 10 the regions between the D lines disappear for $a = 1$.

For the case $\beta^2 - 4a^2 < 0$, so that the roots of $D(u) = 0$ are not real, it is preferable to use Equation 199 from which can be seen that

$$B(u_E) = 0 \Longleftrightarrow h, e \text{ on } E_1 \text{ line} \tag{203}$$

in view of

$$\left(\frac{h}{e}\right)^2 + \frac{\beta^2}{a}\,\frac{h}{e} + \beta^2 \neq 0$$

because the discriminant $(\beta^2/a^2)(\beta^2 - 4a^2) < 0$. Moreover,

$$\left(\frac{h}{e}\right)^2 + \frac{\beta^2}{a}\,\frac{h}{e} + \beta^2 > 0\,. \tag{204}$$

Hence, in this case the sign of $B(u_E)$ is determined by the E_1 line only. Typical results are presented in Figure 11 for $\beta = 2$ and $a = 1.4$.

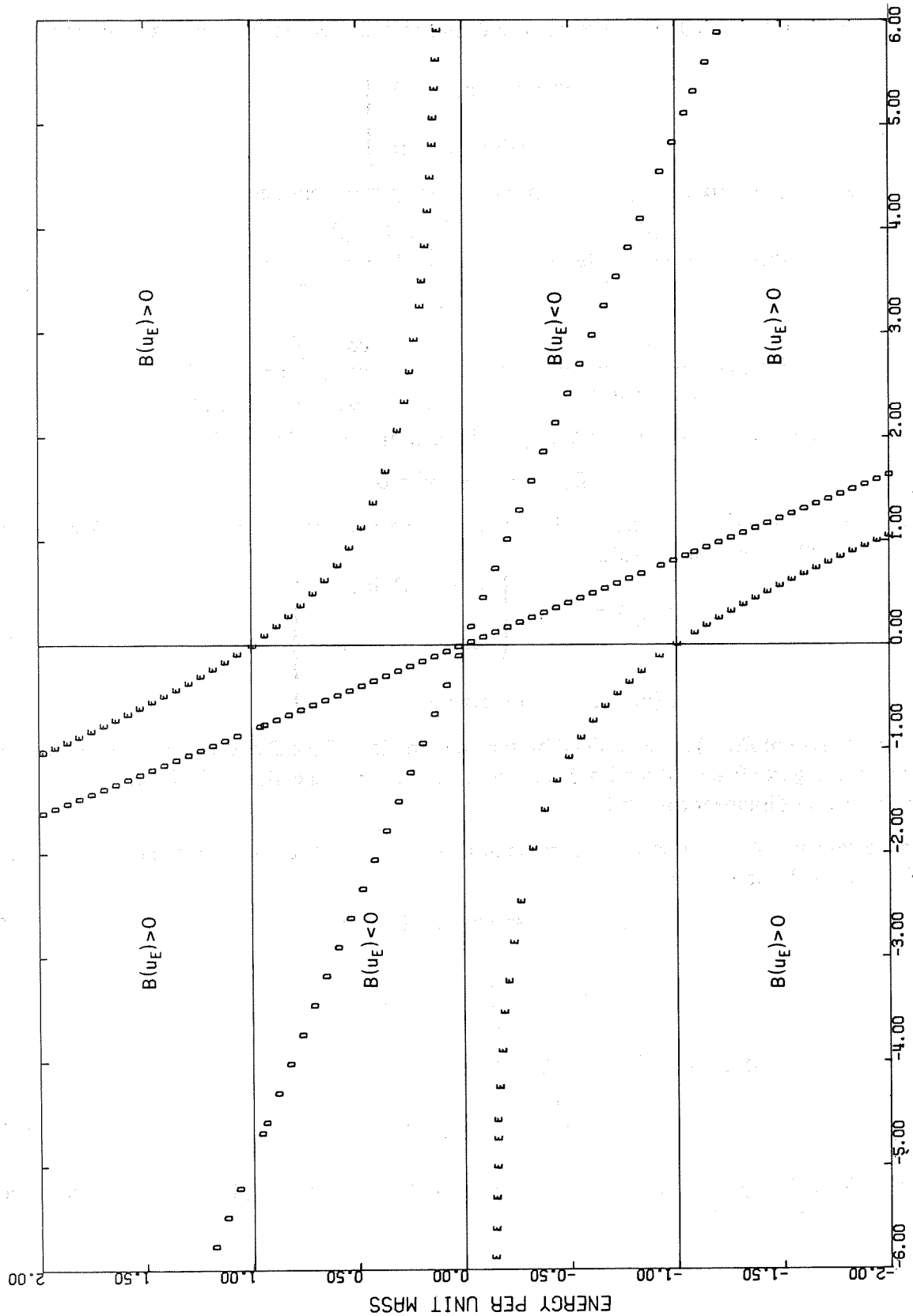

Figure 9—Typical classification of h, e space according to the sign of $B(u_E)$ for $0.0 < a < 1.0$ (shown here for $a = 0.7$).

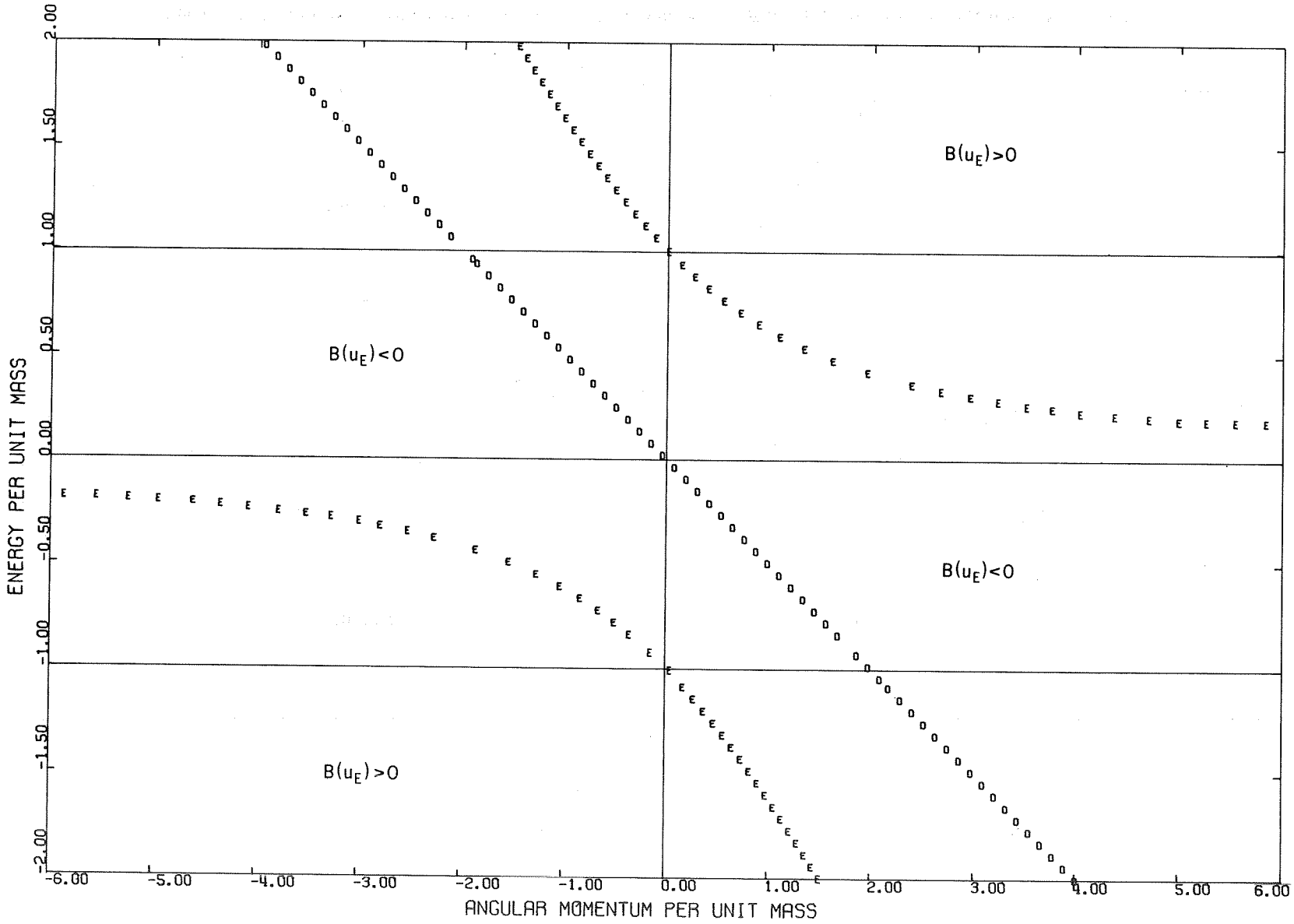

Figure 10—Classification of h, e space according to the sign of $B(u_E)$ for $a = 1.0$.

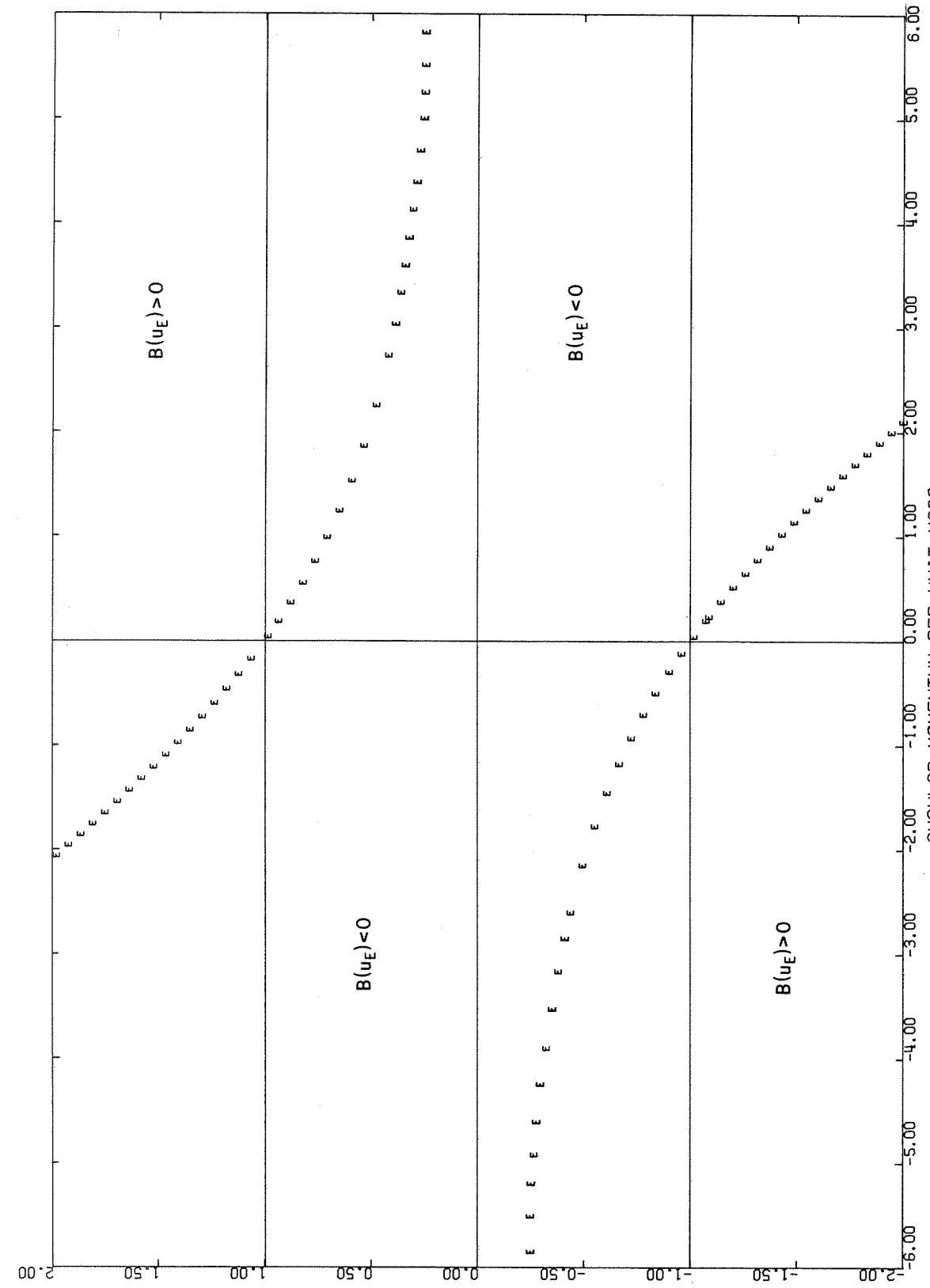

Figure 11—Typical classification of *h*, *e* space according to the sign of $B(u_E)$ for $1.0 < a < \infty$ (shown here for $a = 1.4$).

It follows that the E_1 line is defined by eliminating u between

$$\left.\begin{aligned} B(u;h,e,a,\beta) &= 0 \\ E(u;h,e,a,\beta) &= 0\ ; \\ D(u;a,\beta) &\neq 0\ . \end{aligned}\right\} \tag{205}$$

and

but

Now that the sign of $B(u_D)$ and $B(u_E)$ can be determined in various regions of the h, e space, the conditions that determine the relation between the order of u_E, u_{D1}, and u_{D2} must be found as follows:

From the definition of u_E which yields

$$u_E = \frac{h}{\beta(h+ea)}\ , \tag{206}$$

it is noted that the difference δ defined by

$$\delta \equiv u_D - u_E \tag{207}$$

can also be written as

$$\delta = \frac{1}{\beta(h+ea)}\left[\beta u_D ea + h(\beta u_D - 1)\right]\ , \tag{208}$$

where u_D is defined by

$$a^2u_D^2 - \beta u_D + 1 = 0\ . \tag{209}$$

From Equations 208 and 209, it follows that

$$\delta = \frac{a^2u_D^2}{\beta(h+ea)}\left(h + \frac{\beta e}{au_D}\right)\ , \tag{210}$$

or

$$\left.\begin{aligned} \delta_1 \equiv u_{D1} - u_E &= \frac{a^2u_{D1}^2}{\beta(h+ea)}\left(h + \frac{e\beta}{au_{D1}}\right) \\ \delta_2 \equiv u_{D2} - u_E &= \frac{a^2u_{D2}^2}{\beta(h+ea)}\left(h + \frac{e\beta}{au_{D2}}\right) \end{aligned}\right\} \tag{211}$$

Thus, the ordering of u_E, u_{D1}, and u_{D2} is determined by the H and D lines.

Moreover, from Equation 209 and the relation

$$u_{D1}u_{D2} = \frac{1}{a^2} \tag{212}$$

derived from it, Equation 196 for the two D lines may also be written as

$$\left.\begin{aligned} D_1 &\equiv h + ea(1 + a^2u_{D2}^2) = 0 \\ D_2 &\equiv h + ea(1 + a^2u_{D1}^2) = 0\ . \end{aligned}\right\} \tag{213}$$

Hence, the H line does not lie between the two D lines. Also, the D_1 line has a less-negative slope than the D_2 line. Typical results are presented in Figures 12 to 14 for $\beta = 2$ and $a = 0.7$, 1, and 1.4, respectively.

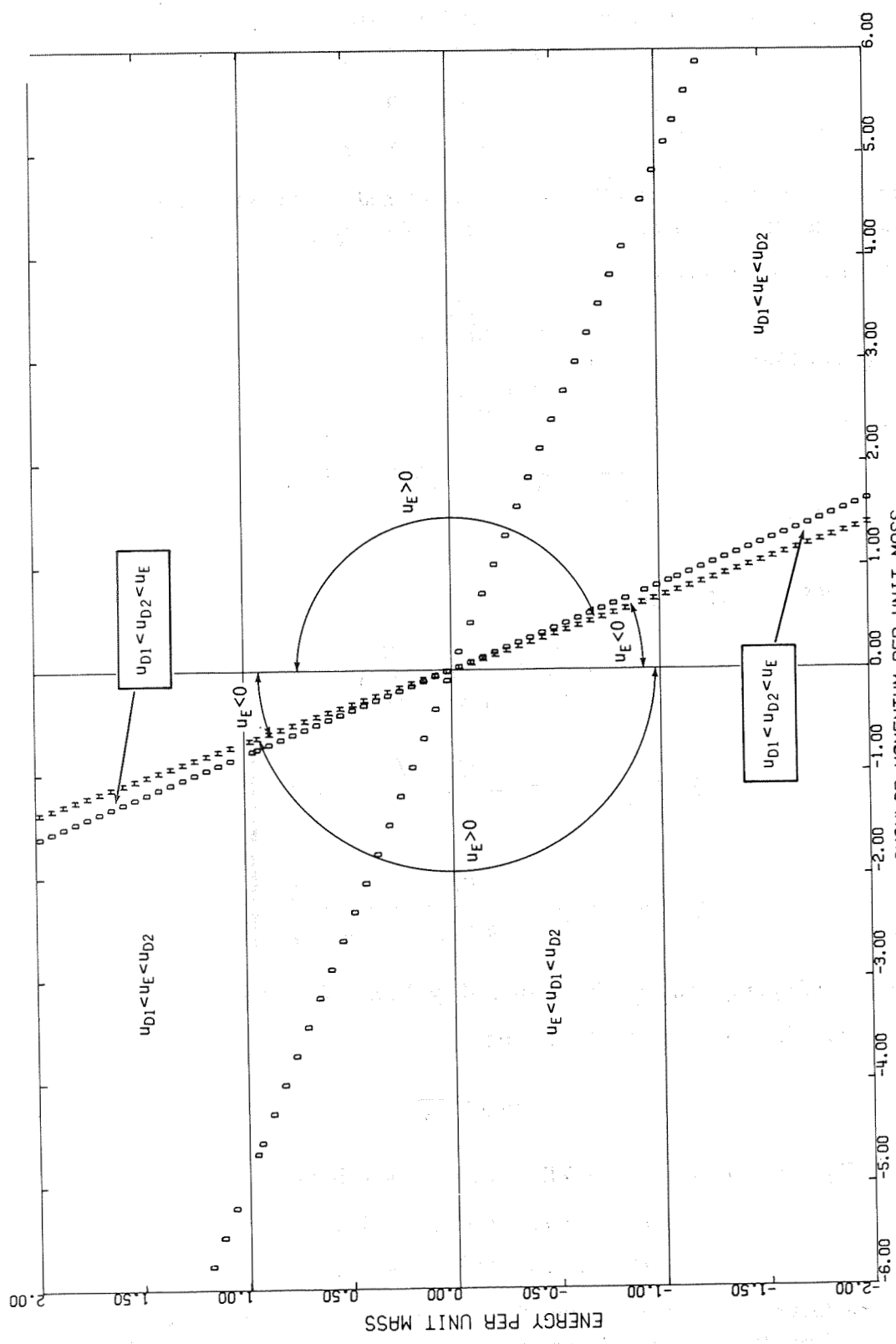

Figure 12—Typical classification of h, e space according to the ordering of u_E, u_{D1}, and u_{D2} and sign of u_E for $0 < a < 1.0$ (shown here for $a = 0.7$).

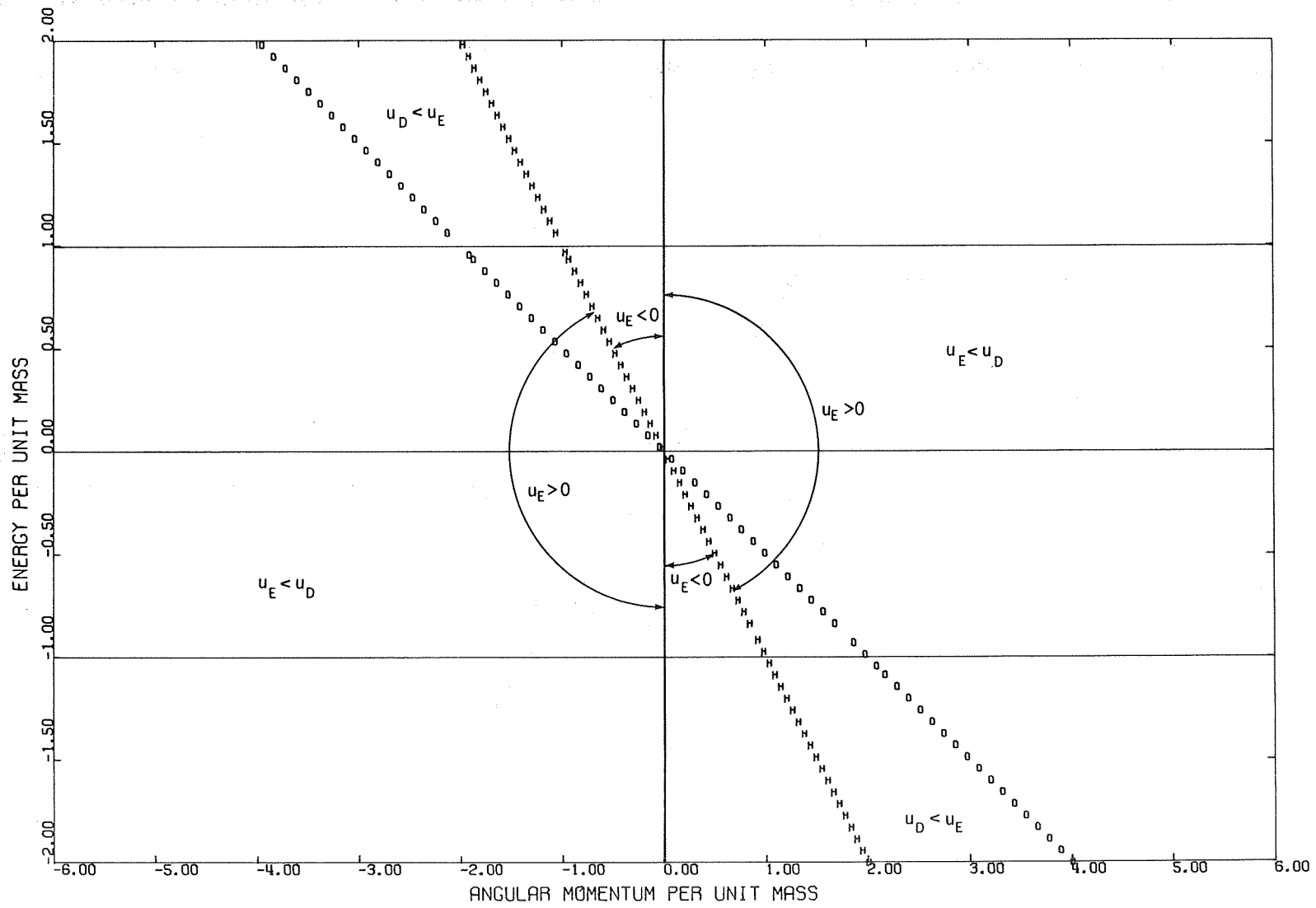

Figure 13—Classification of h, e space according to the ordering of u_E, u_{D1}, and u_{D2} and sign of u_E for a = 1.0; in this case, $u_{D1} = u_{D2}$.

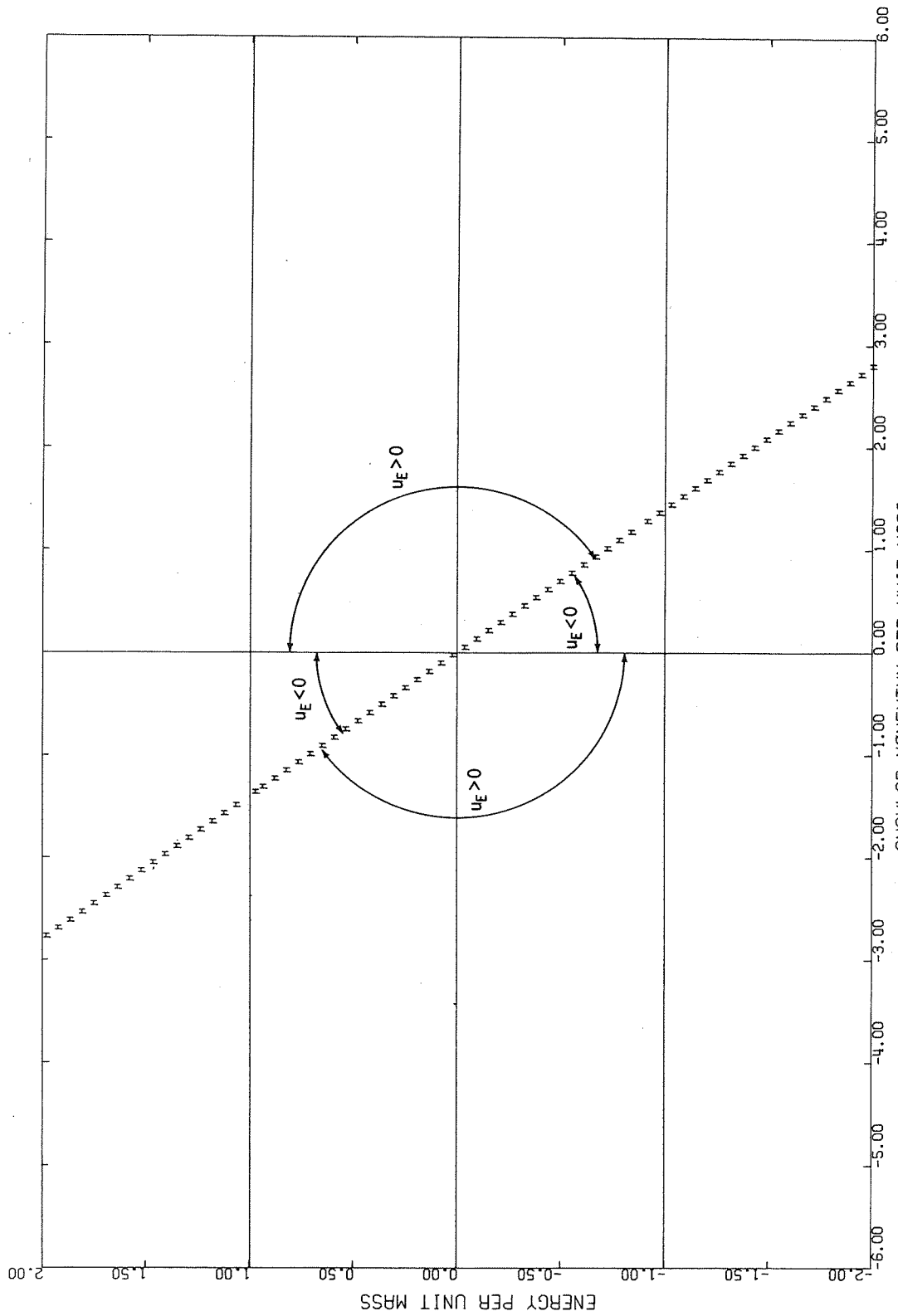

Figure 14—Typical classification of h, e space according to the ordering of u_E, u_{D1}, and u_{D2} and sign of u_E for $1 < a < \infty$ (shown here for $a = 1.4$); in the case $1.0 < a < \infty$, no roots u_{D1} and u_{D2} can exist for $D(u) = 0$.

(In these diagrams, subscripts 1 and 2 in the two D lines and subscript 1 from the E_1 line have been omitted for the sake of simplicity. This use of notation should not result in the erroneous interpretation of these lines as the $D(u) = 0$ and $E(u) = 0$ lines, as defined in Equations 46 and 47. Rather, any line in the h, e space can denote at most only a relation $F(h, e; a, \beta) = 0$, where a and β are parameters, and cannot involve u.)

Finally, from Equations 197 and 206 it can be seen that

$$u_{D1,D2} > 0, \tag{214}$$

$$\left.\begin{array}{lll} u_E > 0 & \text{for} & \dfrac{h}{h+ea} > 0, \\ < 0 & \text{for} & \dfrac{h}{h+ea} < 0, \\ = 0 & \text{for} & h = 0, \\ = \pm\infty & \text{for} & h + ea = 0. \end{array}\right\} \tag{215}$$

As a summary of this investigation of the function $f(u)$, the following points are given concerning the h, e space for a given set (a, β):

(1) The positive definiteness of $B(u_D)$ is determined by the D lines.

(2) The sign of $B(u_E)$ is determined by the combination of the D and E_1 lines.

(3) The ordering of u_E, u_{D1}, and u_{D2} is determined by the combination of the D and H lines.

(4) u_{D1} and u_{D2} depend only on (a, β); $u_{D1} > 0$ and $u_{D2} > 0$.

(5) The sign of u_E is determined by the combination of the e axis, $h = 0$, and the H line, $h + ea = 0$.

(6) There are two D lines for $\beta^2 - 4a^2 > 0$, one degenerate D line for $\beta^2 - 4a^2 = 0$, and none for $\beta^2 - 4a^2 < 0$.

Construction of the Master Diagram

In this section, the results of the two preceding sections will be used to construct the master diagram for each a such that it will give all admissible orbits corresponding to a given set h, e and $\beta = 2$ in Equation 44.

For concreteness, first consider the case of $a = 0.7$, which illustrates all the features of $0 < a < 1$. Superposition of Figures 5, 9, and 12 produces Figure 15. It is now necessary to divide the regions 1, 2, 3, 4, 4*, 5, 5*, 6, and 6* into subregions which we will label with a letter as a suffix (Table 3). With the information in Figure 8 and Table 3, it is quite easy to determine the ordering of the roots of $B(u) = 0$, $D(u) = 0$, and $E(u) = 0$ in the subregions of 1, 4, 4*, 5, 5*, 6, and 6*. However, this determination is more difficult in the subregions of 2 and 3 because it appears that the values of all these roots must be known explicitly to effect their ordering. The roots of $D(u) = 0$ and $E(u) = 0$ are given

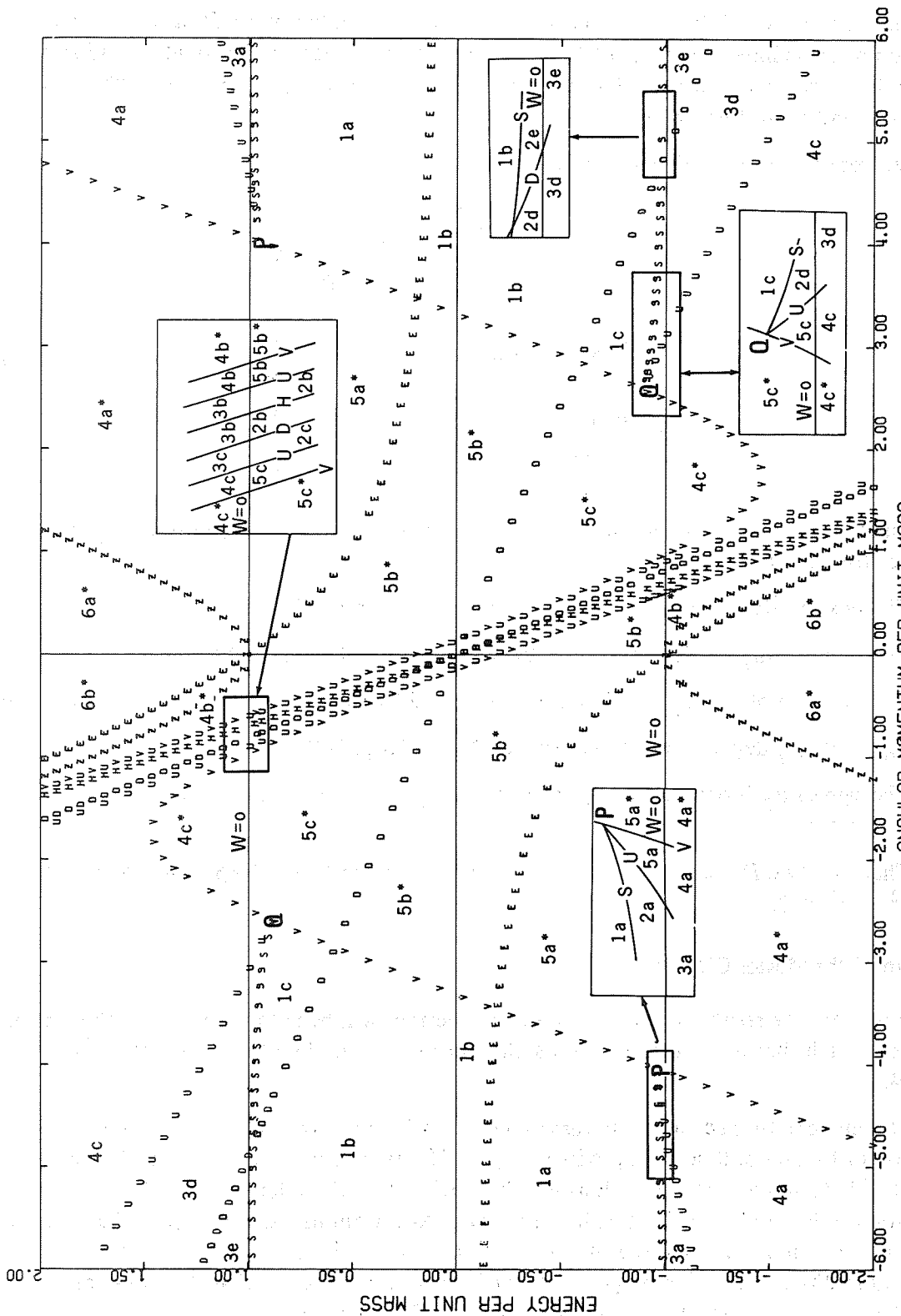

Figure 15–Typical master diagram for classification of orbits for $0.0 < a < 1.0$ (shown here for $a = 0.7$); obtained from superposition of Figures 5, 9, and 12.

Table 3—Characteristics of the cubic $B(u)$ for various subregions of h, e space for $0 < a < 1$.

Region	u_E	Ordering of u_{D1}, u_{D2}, u_E	$B(u_E)$	$B(u'_{\mathrm{I}})$	$B(u'_{\mathrm{II}})$	V	W	u_s
1a	>0	$u_E < u_{D1} < u_{D2}$	>0					
1b	>0	$u_E < u_{D1} < u_{D2}$	<0	<0	<0	>0	<0	>0
1c	>0	$u_{D1} < u_E < u_{D2}$	>0					
2a	>0	$u_E < u_{D1} < u_{D2}$	>0					
2b	>0	$u_{D1} < u_{D2} < u_E$	<0					
2b′	<0	$u_E < u_{D1} < u_{D2}$	<0	>0	<0	>0	<0	>0
2c	>0	$u_{D1} < u_E < u_{D2}$	>0					
2d	>0	$u_{D1} < u_E < u_{D2}$	>0					
2e	>0	$u_E < u_{D1} < u_{D2}$	<0					
3a	>0	$u_E < u_{D1} < u_{D2}$	>0					
3b	>0	$u_{D1} < u_{D2} < u_E$	<0					
3b′	<0	$u_E < u_{D1} < u_{D2}$	<0	>0	<0	>0	>0	>0
3c	>0	$u_{D1} < u_E < u_{D2}$	>0					
3d	>0	$u_{D1} < u_E < u_{D2}$	>0					
3e	>0	$u_E < u_{D1} < u_{D2}$	<0					
4a	>0	$u_E < u_{D1} < u_{D2}$	>0					
4b	<0	$u_E < u_{D1} < u_{D2}$	<0	>0	>0	>0	>0	>0
4c	>0	$u_{D1} < u_E < u_{D2}$	>0					
4a*	>0	$u_E < u_{D1} < u_{D2}$	>0					
4b*	<0	$u_E < u_{D1} < u_{D2}$	<0	[a]	[a]	<0	>0	>0
4c*	>0	$u_{D1} < u_E < u_{D2}$	>0					
5a	>0	$u_E < u_{D1} < u_{D2}$	>0					
5b	<0	$u_E < u_{D1} < u_{D2}$	<0	>0	>0	>0	<0	>0
5c	>0	$u_E < u_{D1} < u_{D2}$	>0					
5a*	>0	$u_E < u_{D1} < u_{D2}$	>0					
5b*	>0	$u_E < u_{D1} < u_{D2}$	<0	[a]	[a]	<0	<0	>0
5b*′	<0	$u_E < u_{D1} < u_{D2}$	<0					
5c*	>0	$u_{D1} < u_E < u_{D2}$	>0					
6a	>0	$u_E < u_{D1} < u_{D2}$	>0	>0	>0	>0	>0	<0
6b	<0	$u_E < u_{D1} < u_{D2}$	$\gtrless 0$					
6a*	>0	$u_E < u_{D1} < u_{D2}$	>0	[a]	[a]	<0	>0	<0
6b*	<0	$u_E < u_{D1} < u_{D2}$	$\gtrless 0$					

[a]Because $V < 0$ in these regions, u'_{I} and u'_{II} do not exist.

Note: Because in subregions 2b, 2b′, 3b, 3b′, 5b*, and 5b*′ $B(u_E) < 0$ and $(du/d\phi)^2 \equiv f(u_E) = B(u_E)[D^2(u_E)/E^2(u_E)]$, it is unnecessary to distinguish between the primed and unprimed subregions in the master diagram.

explicitly by equations 197 and 206. The roots of the cubic $B(u) = 0$ are available from the algebraic theory of cubic equations but, as already mentioned, this leads to very cumbersome algebraic expressions. Alternately, the same objective may be achieved by going continuously along some desirable

curve in the h, e space from a subregion with known ordering to one whose ordering has to be determined.

For instance, consider the boxed region P in the third quadrant of Figure 15. If we begin with (a) any point in subregion 1a, then we know from Figure 8 and Table 3 that the ordering of the roots is as shown in Figure 16a. Let us now take any continuous curve that goes from this starting point to (b) any point on the boundary given by the S line, then to (c) any point in region 2a, next to (d) any point on the boundary given by the W line, and finally to (e) any point in subregion 3a. Then, the ordering of the roots is obtained as shown in Figure 16.

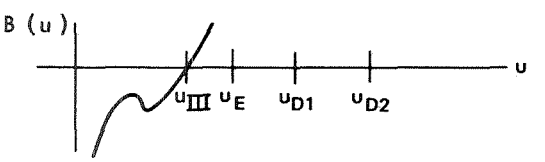

(a) SUBREGION 1a

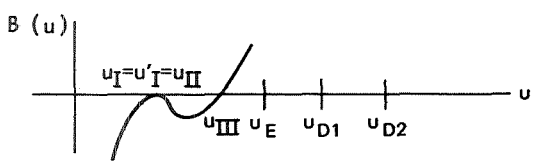

(b) S-LINE BETWEEN SUBREGIONS 1a AND 2a

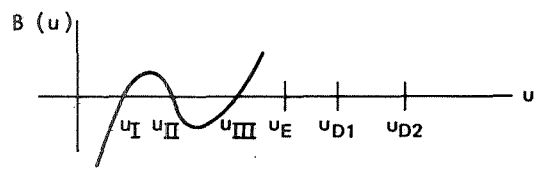

(c) SUBREGION 2a

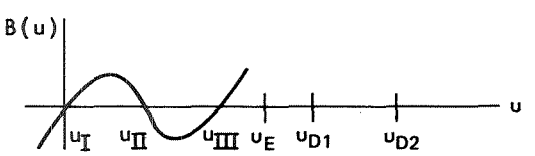

(d) W-LINE BETWEEN SUBREGIONS 2a AND 3a

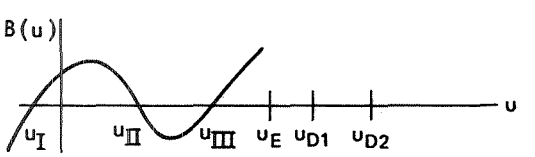

(e) SUBREGION 3a

Figure 16—Ordering of u_E, u_{D1}, and u_{D2} in some illustrative subregions of the third quadrant in the master diagram of Figure 15.

In the same way, we obtain the ordering in subregions 2d, 2e, 3d, and 3e in the fourth quadrant of Figure 15 by starting from any point in subregion 1c as shown in Figure 17.

Next, to determine the ordering of the roots in subregions 2b and 2c in the second quadrant of Figure 15, it is simplest to consider first any point on the H line in subregion 2b. The $B(u)$ curve is now the degenerate quadratic given by Equation 160. From Equation 195, $B(u_D) > 0$ because the point under consideration is not on a D line. From Equation 215, it follows that $u_E = \pm\infty$. Consequently, the ordering of the roots is as shown in Figure 18a. As described for Figure 16, the ordering of the roots is obtained as shown in Figure 18.

Finally, the ordering of the roots in subregions 3b and 3c can be obtained from Figure 18; the ordering is the same except that now $u_{B1} < 0$ because $B(0) > 0$ in region 3.

From a knowledge of the ordering of the roots of $B(u) = 0$, $D(u) = 0$, and $E(u) = 0$ and from the fact that

$$f(u) = B(u)\frac{D^2(u)}{E^2(u)}, \qquad (165)$$

a complete characterization can be made of the $f(u)$ curve in various subregions of the h, e space for a given set (a, β). For the present case of $0 < a < 1$, this characterization is given in Figure 19. For this reason, Figure 15 is known as a "master diagram." It is specifically for $a = 0.7$, but qualitatively valid for $0 < a < 1$.

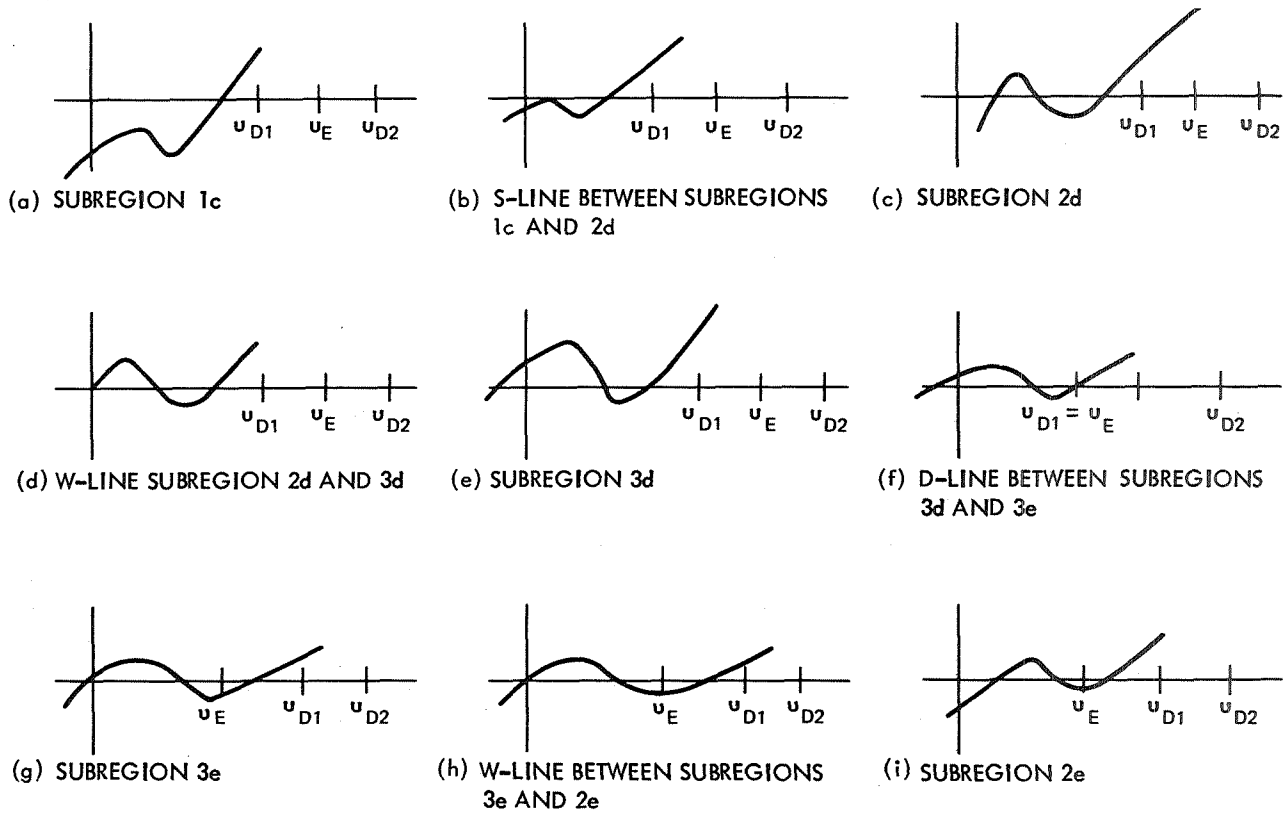

Figure 17—Ordering of u_E, u_{D1}, and u_{D2} in some illustrative subregions of the fourth quadrant in the master diagram of Figure 15.

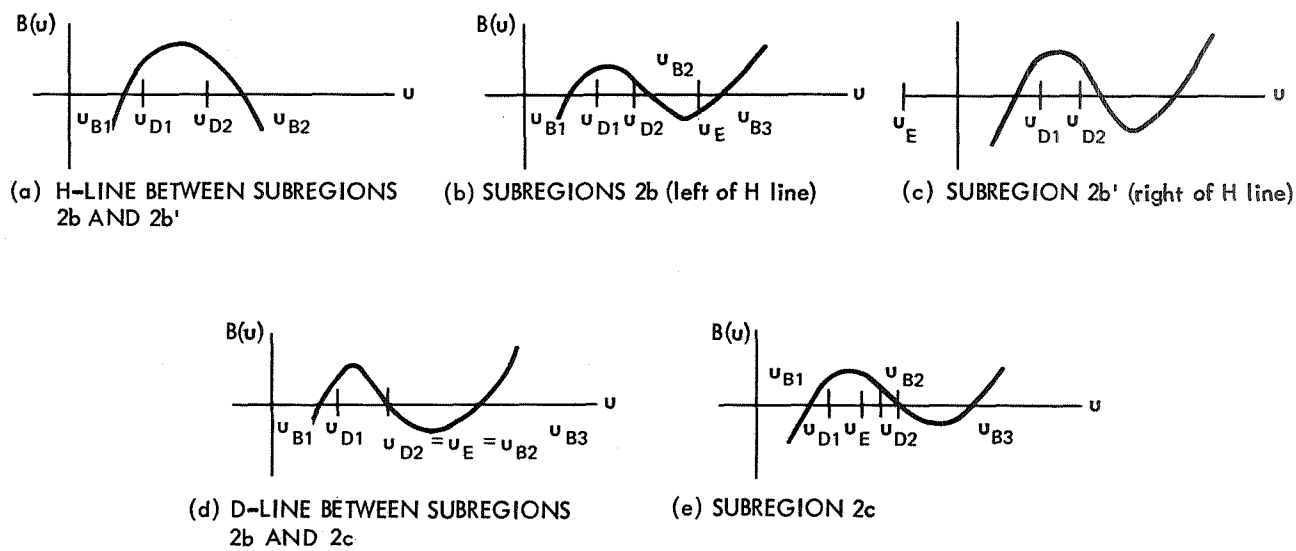

Figure 18—Ordering of u_E, u_{D1}, and u_{D2} in some illustrative subregions of the second quadrant in the master diagram of Figure 15.

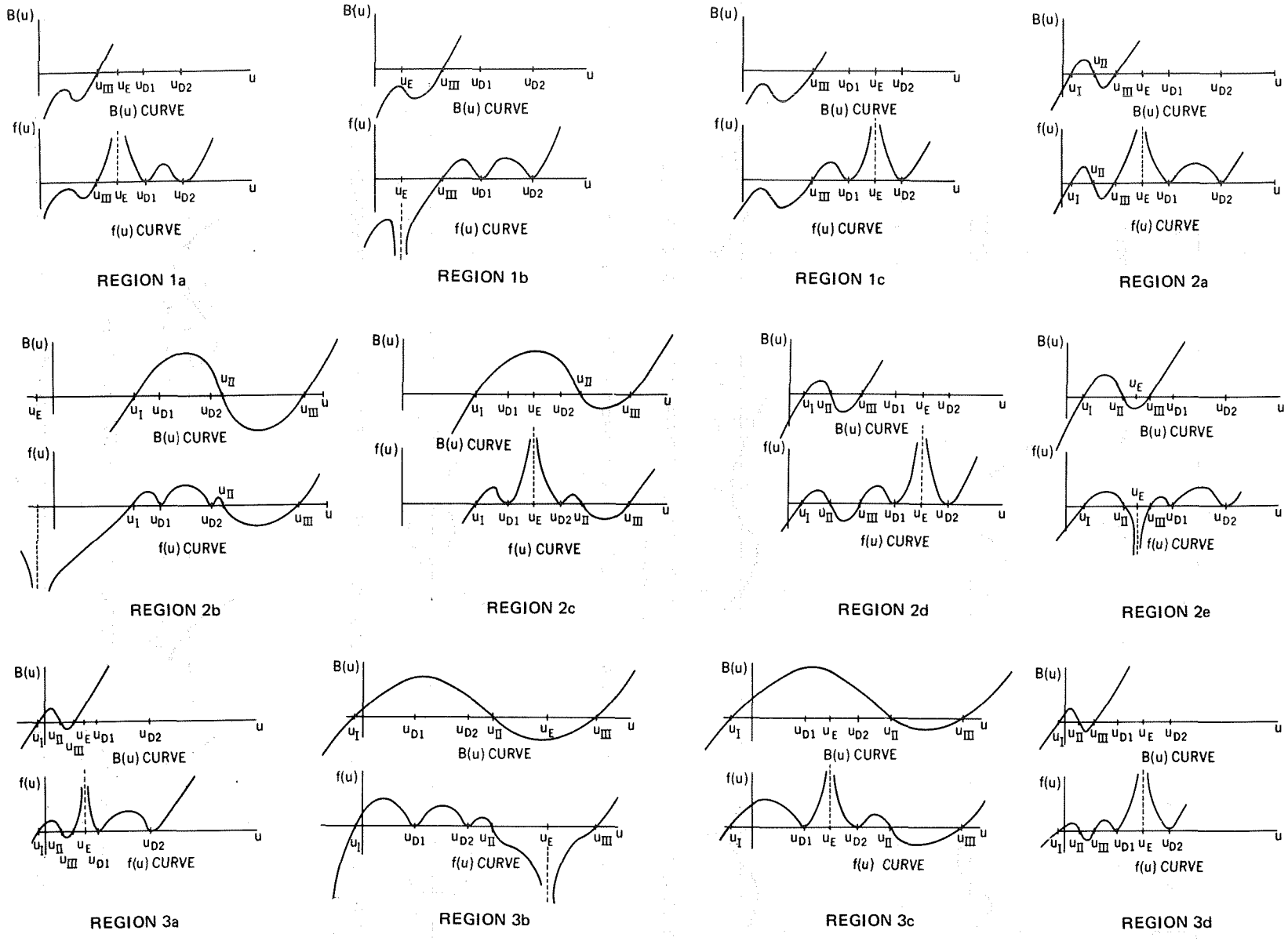

Figure 19—Characteristics of the $f(u)$ curve in various subregions for $0 < a < 1$.

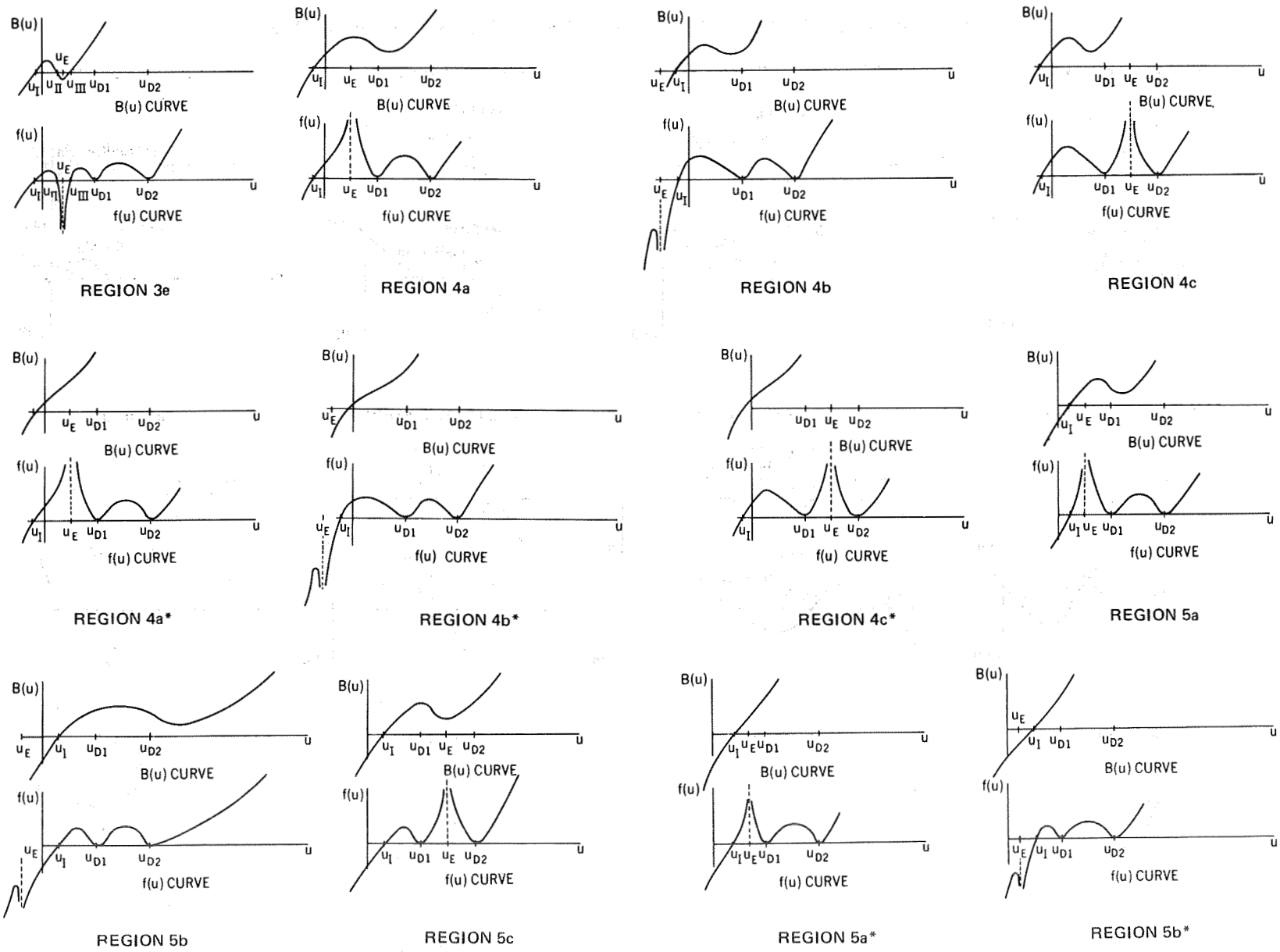

Figure 19 (continued)—Characteristics of the $f(u)$ curve in various subregions for $0 < a < 1$.

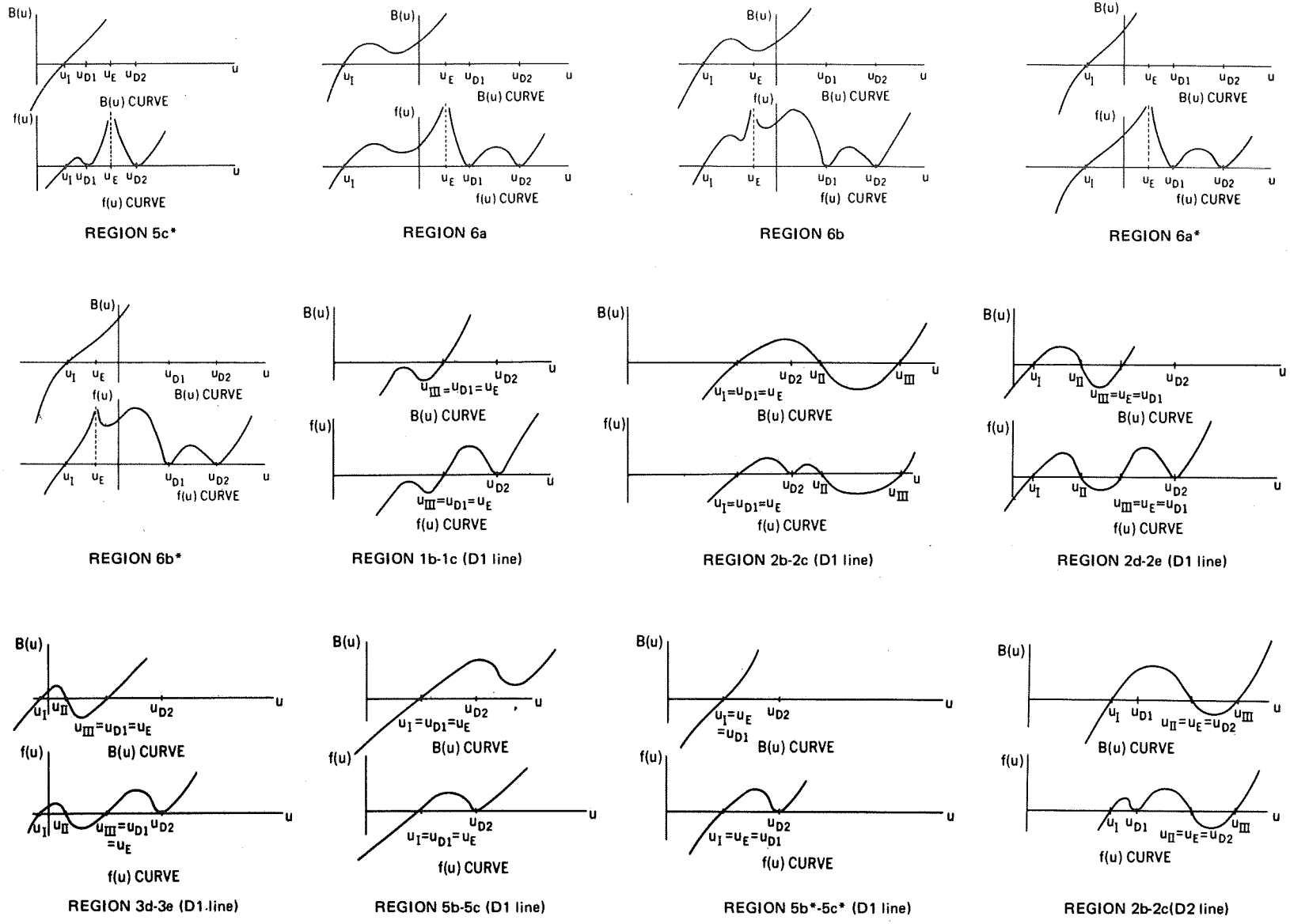

Figure 19 (continued)—Characteristics of the $f(u)$ curve in various subregions for $0 < a < 1$.

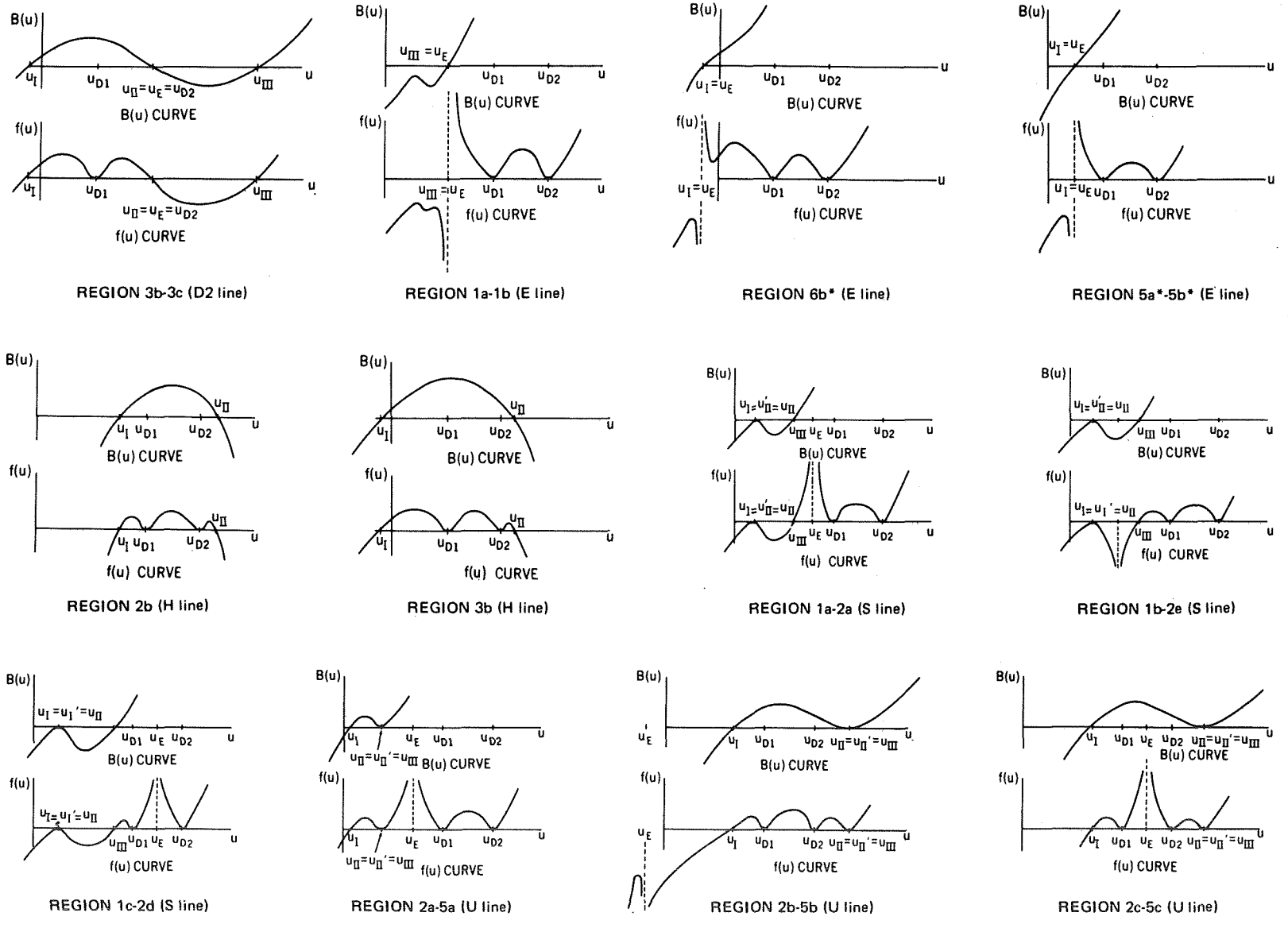

Figure 19 (continued)—Characteristics of the $f(u)$ curve in various subregions for $0 < a < 1$.

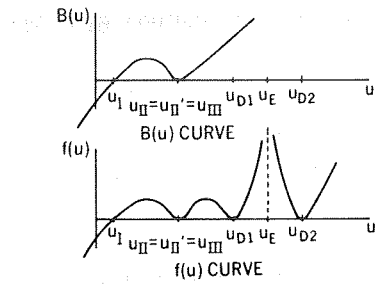

REGION 2d-5c (U line)

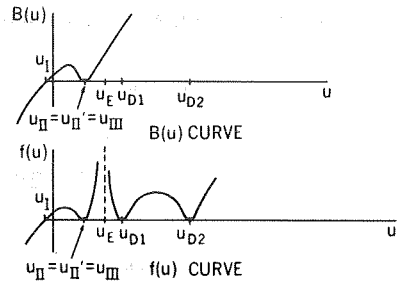

REGION 3a-4a (U line)

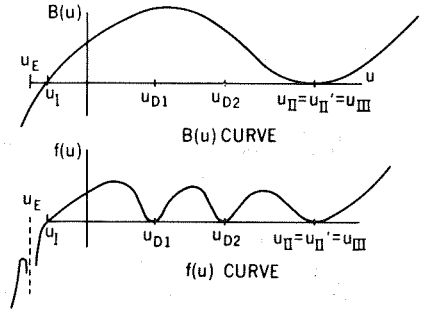

REGION 3b-4b (U line)

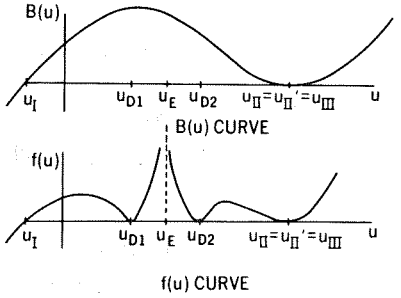

REGION 3c-4c (U line)

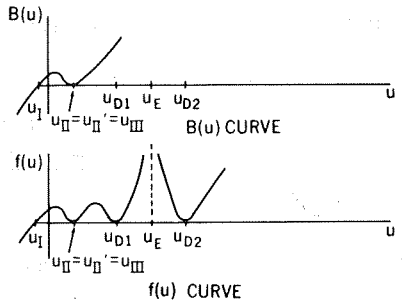

REGION 3d-4c (U line)

Figure 19 (concluded)—Characteristics of the $f(u)$ curve in various subregions for $0 < a < 1$.

In the same way, the characterization for the case of $a = 1$ is given in Figures 20 and 21 and Table 4, and for the case $a = 1.4$, which is qualitatively valid for $1 < a < \infty$, the characterization is given in Figures 22 and 23 and Table 5.

Master diagrams for $\beta = 2$ and for values of a ranging from $a = 0$ to $a = 100$ are presented in Appendix C. Figures C1 to C10 are for $a = 0$, 0.1, 0.2, 0.3, 0.4, 0.5, 0.6, 0.7, 0.8, and 0.9; Figure C11 is for $a = 1$; and Figures C12 to C38 are for $a = 1.1$, 1.2, 1.3, 1.4, 1.5, 1.6, 1.7, 1.8, 1.9, 2, 3, 4, 5, 6, 7, 8, 9, 10, 20, 30, 40, 50, 60, 70, 80, 90, and 100.

The method of obtaining the mathematical solutions $u(\phi)$ from the differential equation, Equation 44, is discussed next. The equation

$$\left(\frac{du}{d\phi}\right)^2 = f(u) = B(u)\frac{D^2(u)}{E^2(u)} \tag{216}$$

is autonomous; therefore, the whole one-parameter family of solutions is given by

$$F(\phi + c, u) = 0\,, \tag{217}$$

where c is an arbitrary constant. That is, if any one solution in the family is known, the others in the family are obtained by a translation. However, from the theory of nonlinear first-order ordinary differential equations it is possible that there are singular solutions of Equation 216 that are not included in Equation 217. These singular solutions are of various types, among which are the "isolated" solution, the envelope, and the "asymptotic" envelope as discussed in Appendix A. Hence, because the $f(u)$ curve is already classified in Figures 19, 21, and 23 for $0 < a < 1$, $a = 1$, and $1 < a < \infty$, respectively, it is quite easy to sketch qualitatively the solutions $u(\phi)$ in the various subregions of the three kinds of master diagrams typified by Figures 15, 20, and 22.

The special case in which there is a subregion with $f(u_E) = +\infty$; i.e., $B(u_E) > 0$, $D(u_E) \neq 0$, and $E(u_E) = 0$, gives quite unexpected results because it leads to

$$\left(\frac{du}{d\phi}\right)_{u=u_E} = \pm\infty\,, \tag{218}$$

and, at first sight, it is uncertain which of the two branches should be taken to continue the solution $u(\phi)$ at u_E. The governing principle is that the solution is to be continued in such a way that the proper time s always increases. From Equations 14, 42, 46, and 47, the following is obtained:

$$\frac{d\phi}{ds} = \frac{u^2 E(u)}{D(u)}\,. \tag{219}$$

From this equation and the condition given by Equation 218, it follows that an orbit must be chosen with a reversal in ϕ at u_E.

The qualitative solutions for each subregion of the master diagram are presented in Appendix D for $0 < a < 1$ (Figures D1 to D15), $a = 1$ (Figures D16 to D29), and $1 < a < \infty$ (Figures D30 to D42). In addition, the "physical orbits", i.e., orbits in the r, ϕ plane, are sketched.

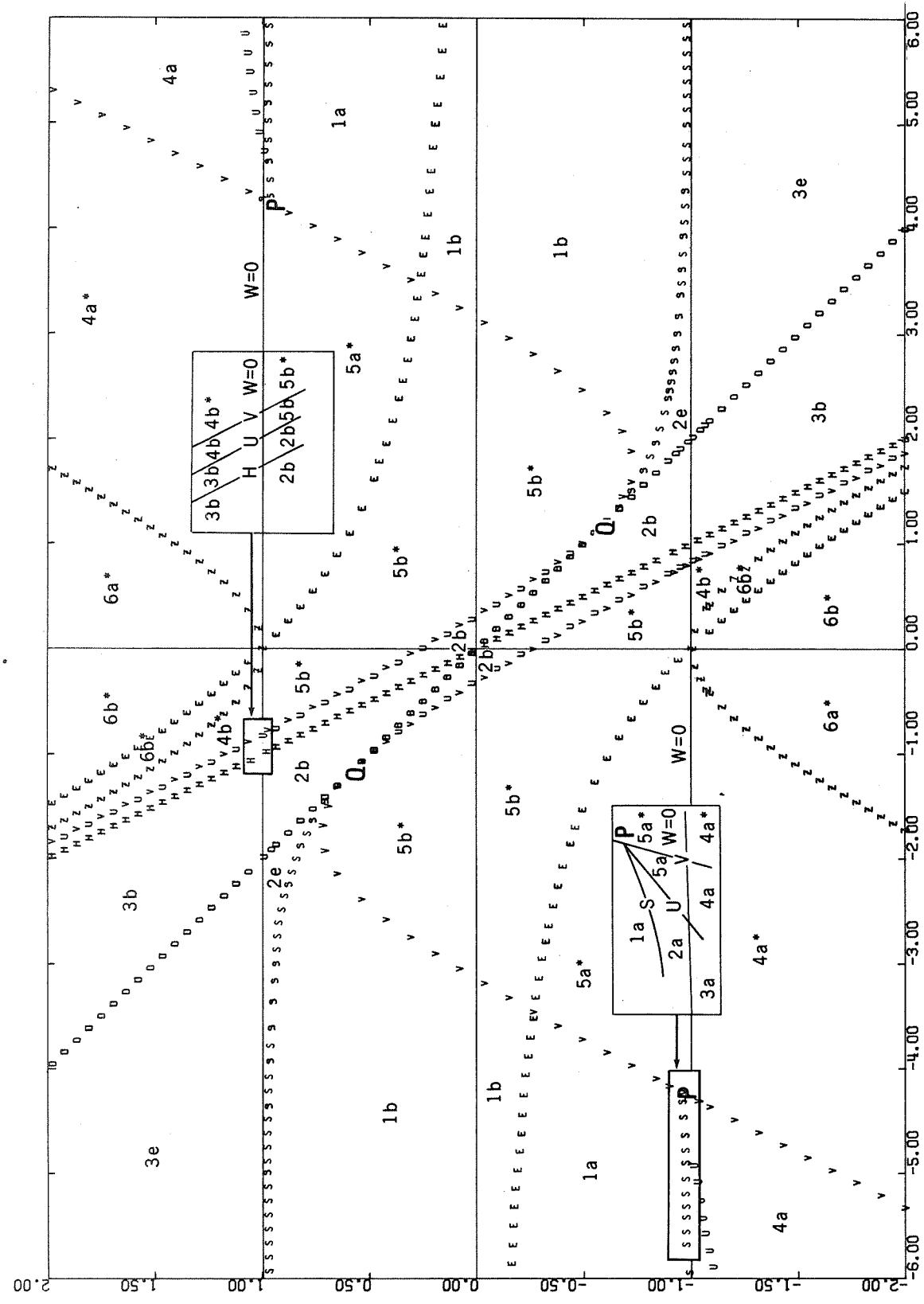

Figure 20—Master diagram for classification of orbits for $a = 1.0$, obtained from superposition of Figures 6, 10, and 13.

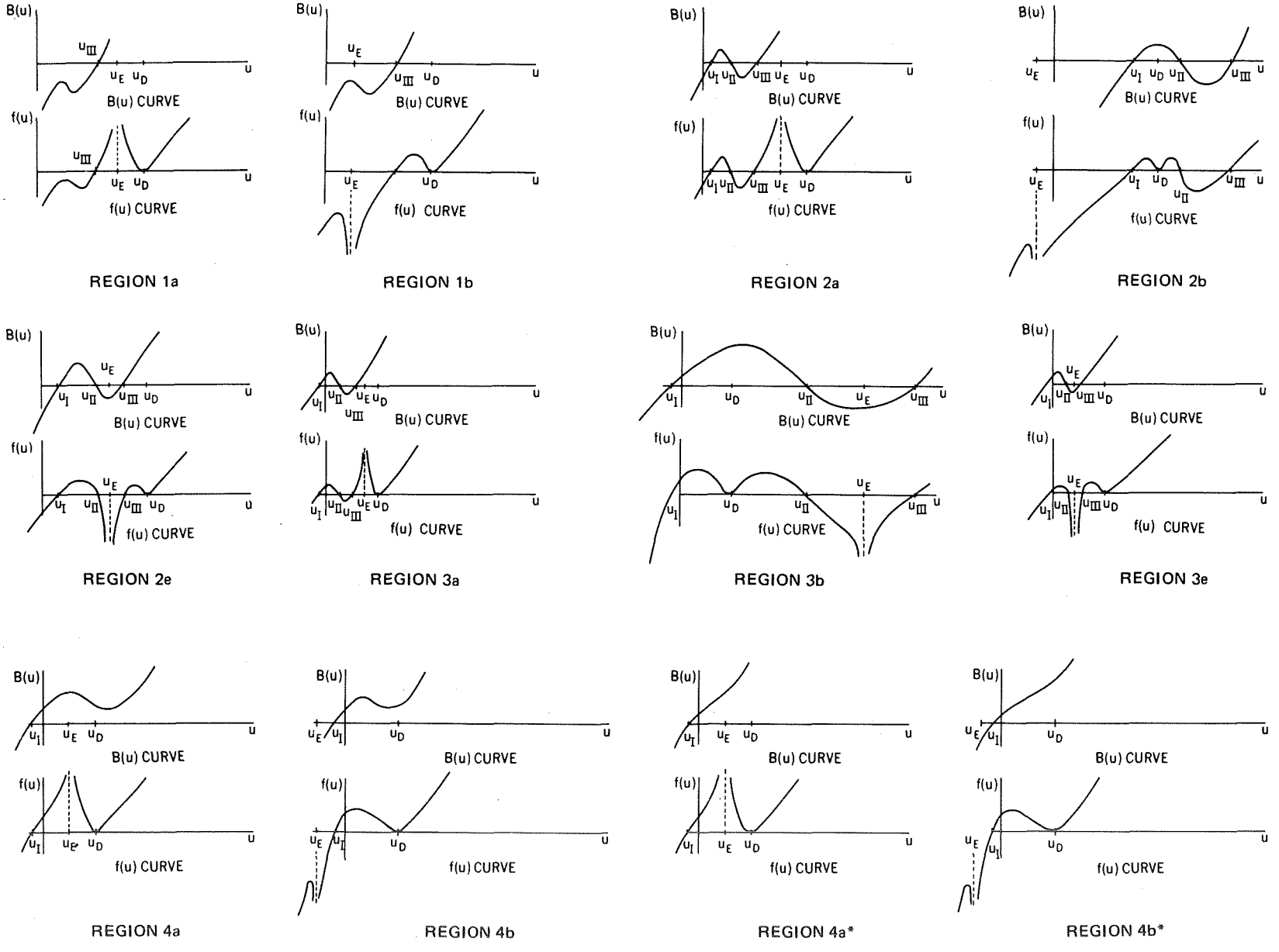

Figure 21—Characteristics of the $f(u)$ curve in various subregions for $a = 1$.

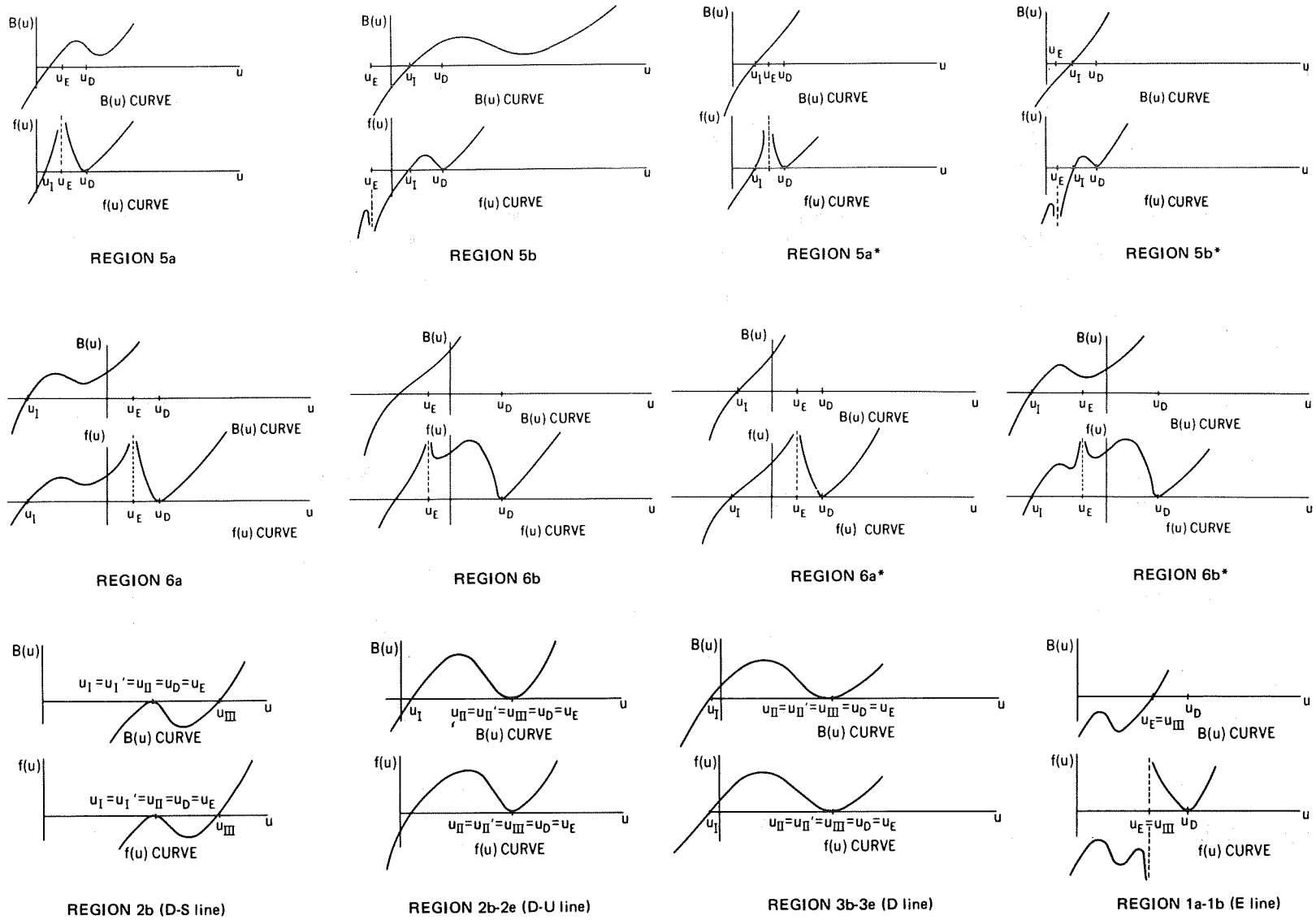

Figure 21 (continued)—Characteristics of the $f(u)$ curve in various subregions for $a = 1$.

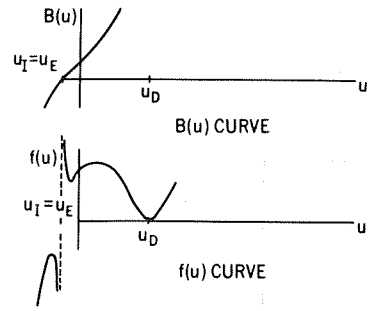

REGION 6b* (E line)

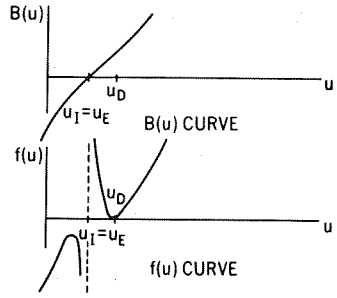

REGION 5a*-5b* (E line)

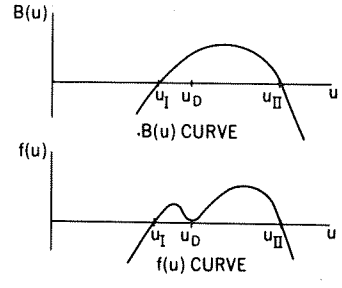

REGION 2b (H line)

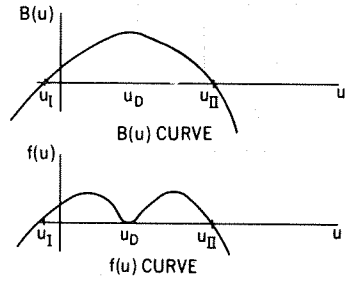

REGION 3b (H line)

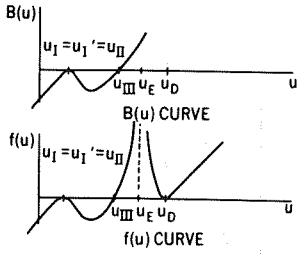

REGION 1a-2a (S line)

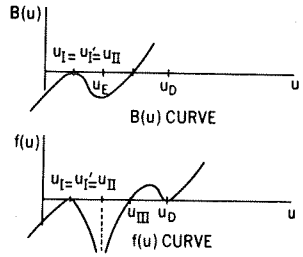

REGION 1b-2e (S line)

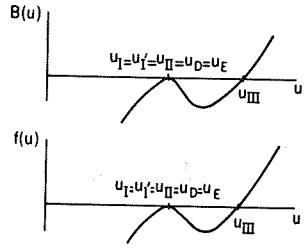

REGION 2b (S-D line)

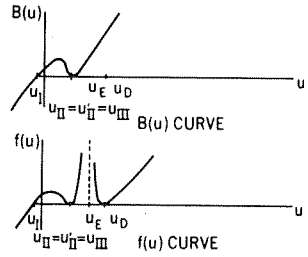

REGION 2a-5a (U line)

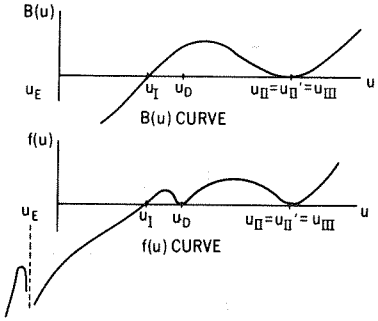

REGION 2b-5b (U line)

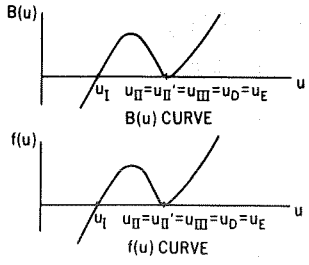

REGION 2b-2e (U-D line)

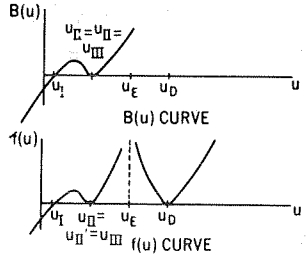

REGION 3a-4a (U line)

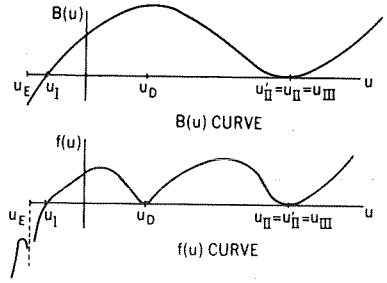

REGION 3b-4b (U line)

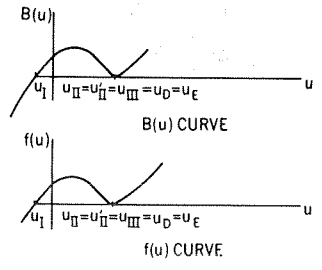

REGION 3b-3e (U-D line)

Figure 21 (concluded)—Characteristics of the $f(u)$ curve in various subregions for $a = 1$.

Table 4–Characteristics of the cubic $B(u)$ for various subregions of h, e space for $a = 1$.

Region	u_E	Ordering of $u_D = u_{D1} = u_{D2}$ and u_E	$B(u_E)$	$B(u'_{\mathrm{I}})$	$B(u'_{\mathrm{II}})$	V	W	u_s
1a	>0	$u_E < u_D$	>0					
1b	>0	$u_E < u_D$	<0	<0	<0	>0	<0	>0
1c								
2a	>0	$u_E < u_D$	>0					
2b	>0	$u_D < u_E$						
2b′	<0	$u_E < u_D$	<0	>0	<0	>0	<0	>0
2c								
2d								
2e	>0	$u_E < u_D$						
3a	>0	$u_E < u_D$	>0					
3b	>0	$u_D < u_E$						
3b′	<0	$u_E < u_D$	<0	>0	<0	>0	>0	>0
3c								
3d								
3e	>0	$u_E < u_D$	<0					
4a	>0	$u_E < u_D$	>0					
4b	<0	$u_E < u_D$	<0	>0	>0	>0	>0	>0
4c								
4a*	>0	$u_E < u_D$	>0					
4b*	<0	$u_E < u_D$	<0	[a]	[a]	<0	>0	>0
4c*								
5a	>0	$u_E < u_D$	>0					
5b	<0	$u_E < u_D$		>0	>0	>0	<0	>0
5c			<0					
5a*	>0	$u_E < u_D$	>0					
5b*	>0	$u_E < u_D$	<0					
5b*′	<0	$u_D < u_E$		[a]	[a]	<0	<0	>0
5c*								
6a	>0	$u_E < u_D$	>0	>0	>0	>0	>0	<0
6b	<0	$u_E < u_D$	$\gtrless 0$					
6a*	>0	$u_E < u_D$	>0	[a]	[a]	<0	>0	<0
6b*	<0	$u_E < u_D$	$\gtrless 0$					

[a]Because $V < 0$ in these regions, u'_{I} and u'_{II} do not exist.

Note: Because in subregions 2b, 2b′, 3b, 3b′, 5b*, and 5b*′ $B(u_E) < 0$ and $(du/d\phi)^2 \equiv f(u_E) = B(u_E)[D^2(u_E)/E^2(u_E)]$, it is unnecessary to distinguish between the primed and unprimed subregions in the master diagram.

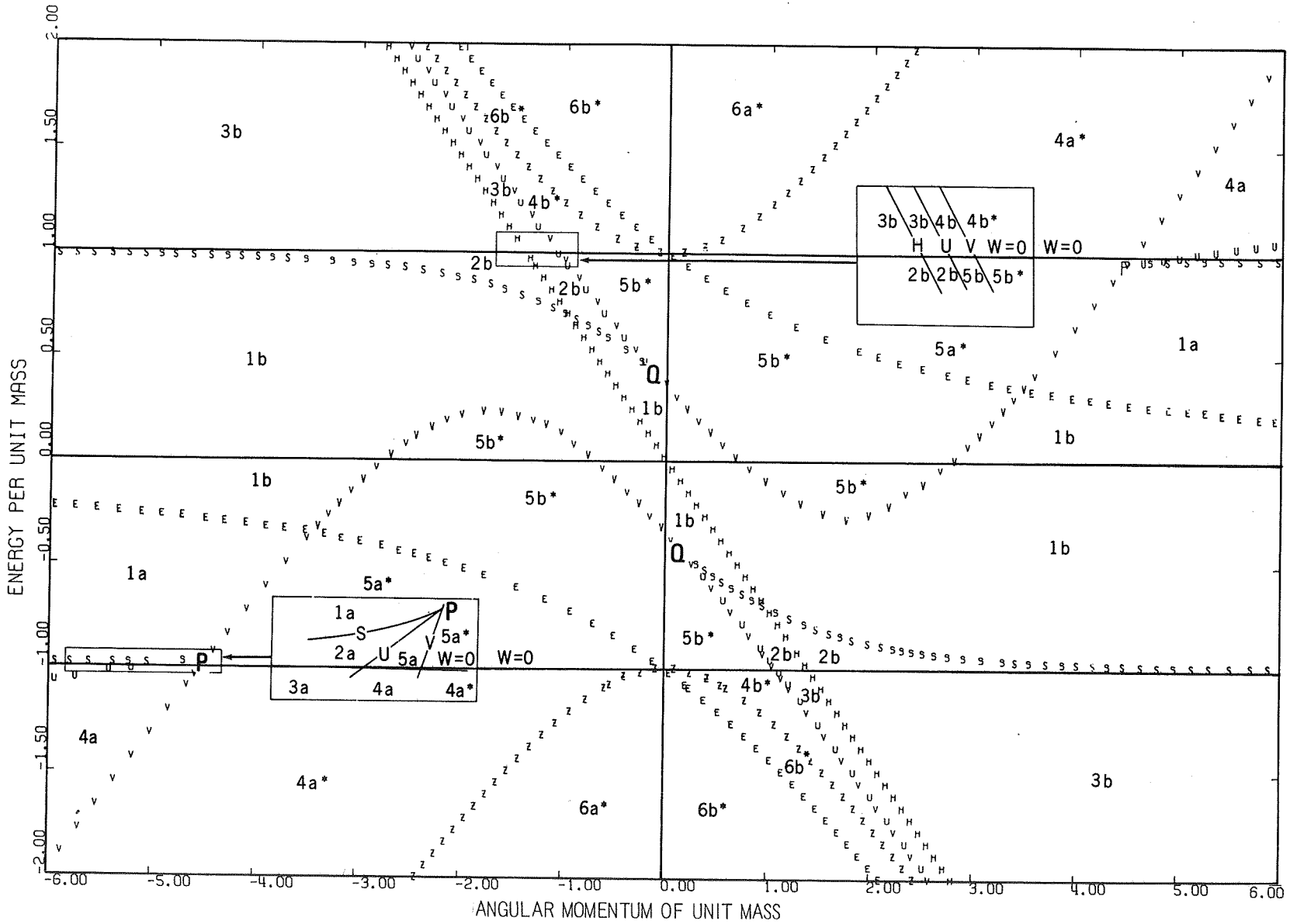

Figure 22—Typical master diagram for classification of orbits for $1.0 < a < \infty$ (shown here for $a = 1.4$), obtained from superposition of Figures 7, 11, and 14.

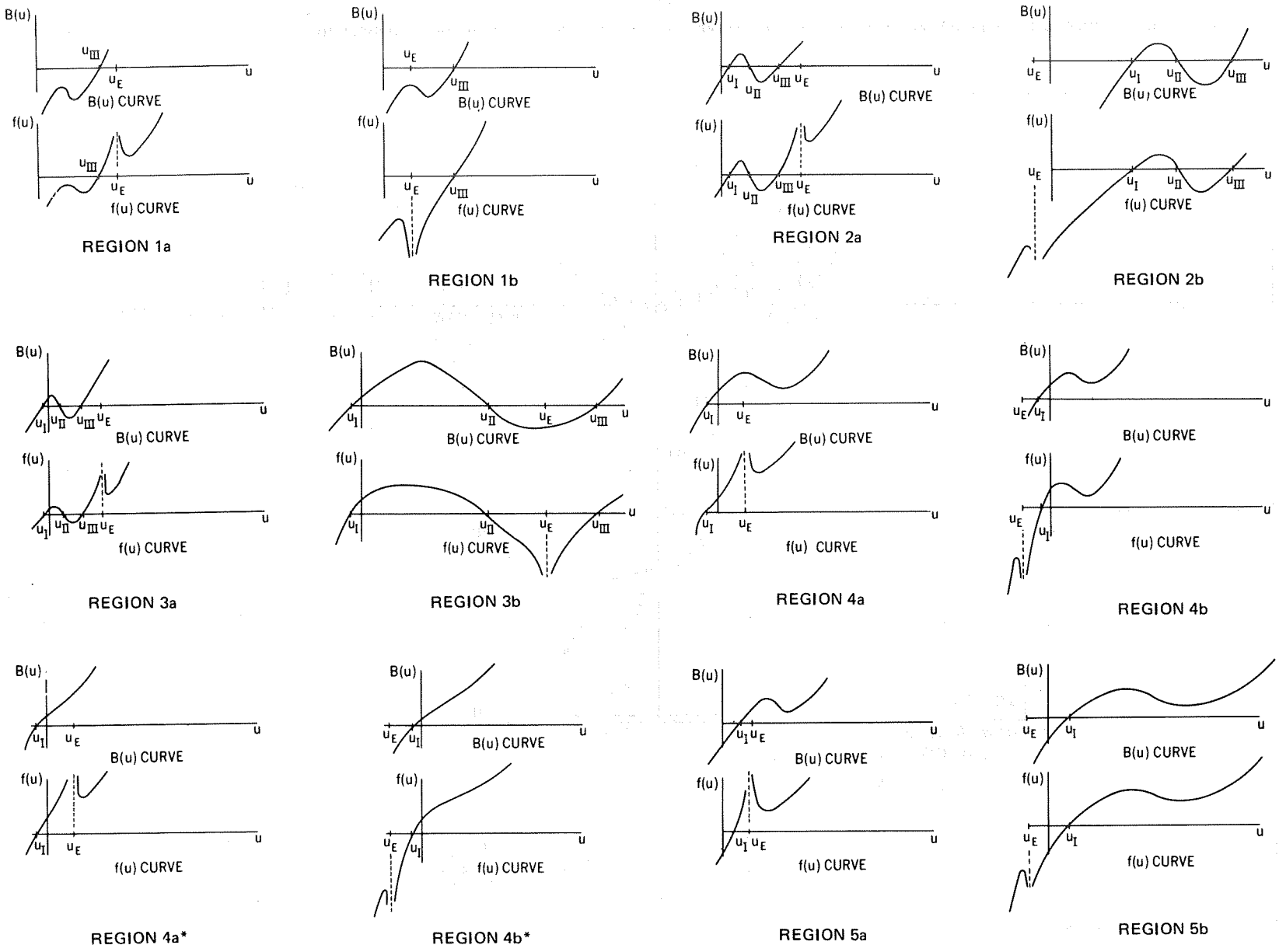

Figure 23—Characteristics of the $f(u)$ curve in various subregions for $1 < a < \infty$.

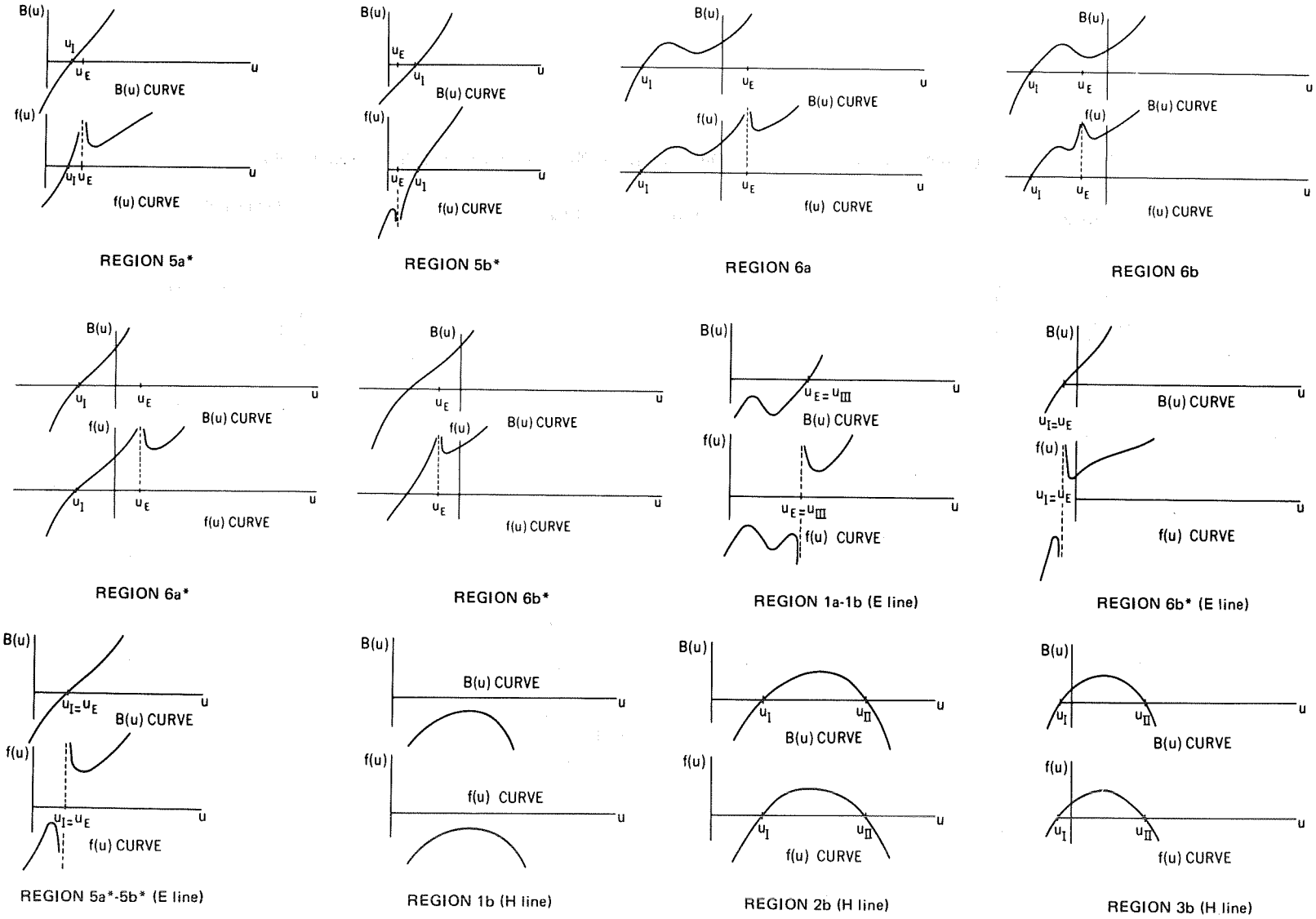

Figure 23 (continued)—Characteristics of the $f(u)$ curve in various subregions for $1 < a < \infty$.

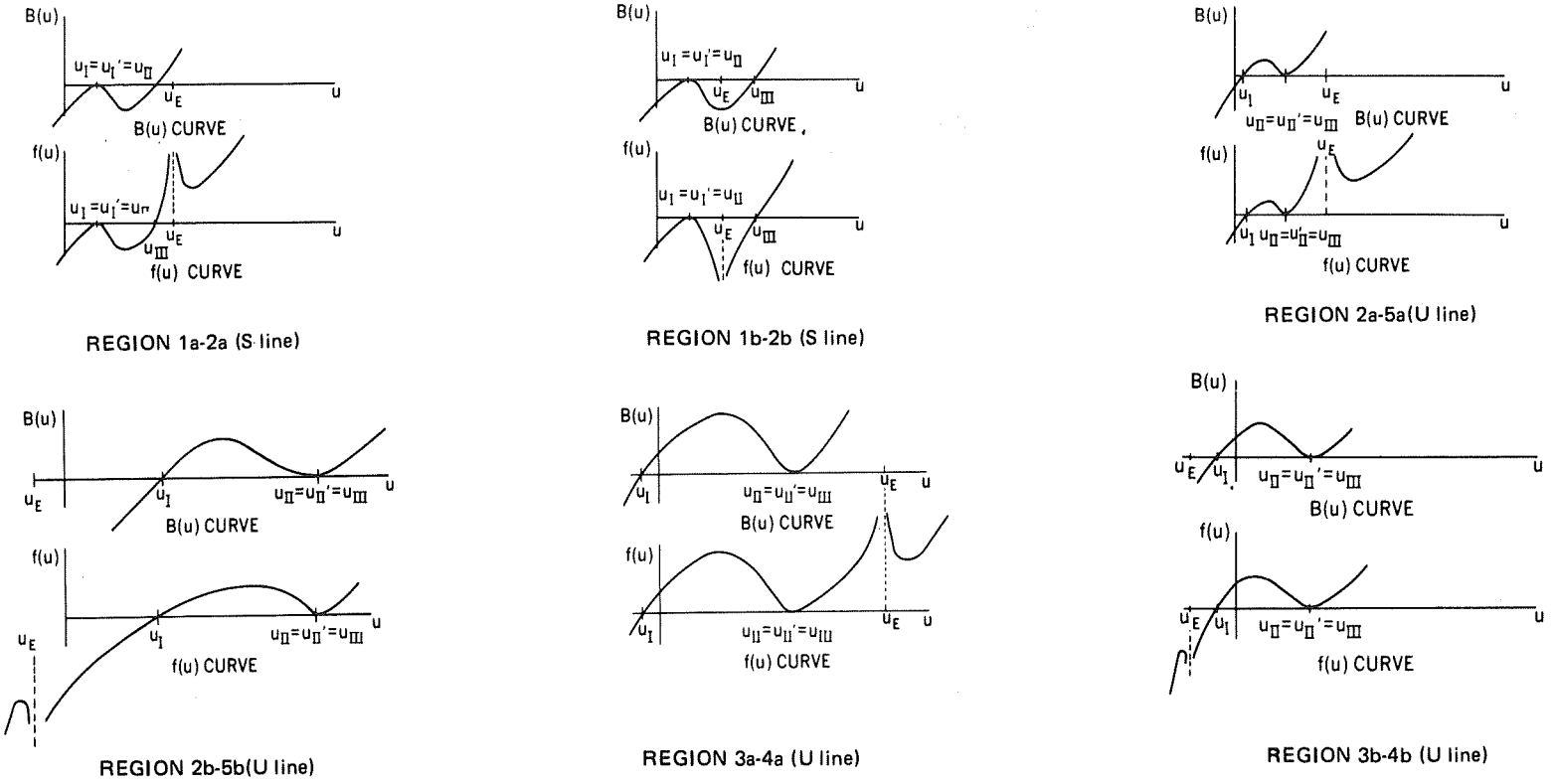

Figure 23 (concluded)—Characteristics of the $f(u)$ curve in various subregions for $1 < a < \infty$.

Table 5—Characteristics of the cubic $B(u)$ for various subregions of h, e space for $a > 1$.[a]

Region	u_E	$B(u_E)$	$B(u_I')$	$B(u_{II}')$	V	W	u_s
1a	>0	>0					
1b	>0	<0	<0	<0	>0	<0	>0
1c							
2a	>0	>0					
2b	>0	<0					
2b′	<0	<0	>0	<0	>0	<0	>0
2c							
2d							
2e							
3a	>0	>0					
3b	>0	<0					
3b′	<0	<0	>0	>0	>0	>0	>0
3c							
3d							
3e							
4a	>0	>0					
4b	<0	<0	>0	>0	>0	>0	>0
4c							
4a*	>0	>0					
4b*	<0	<0	([b])	([b])	<0	>0	>0
4c*							
5a	>0	>0					
5b	<0	<0	>0	>0	>0	<0	>0
5c							
5a*	>0	>0					
5b*	>0	<0	([b])	([b])	<0	<0	>0
5b*′	<0	<0					
5c*							
6a	>0	>0	>0	>0	>0	>0	<0
6b	<0	$\gtrless 0$					
6a*	>0	>0	([b])	([b])	<0	>0	<0
6b*	<0	$\gtrless 0$					

[a]Because $a > 1$ and $\beta = 2$, u_{D1} and u_{D2} do not exist.

[b]Because $V < 0$ in these regions, u_I' and u_{II}' do not exist.

Note: Because in subregions 2b, 2b′, 3b, 3b′, 5b*, and 5b*′ $B(u_E) < 0$ and $(du/d\phi)^2 = f(u_E) = B(u_E)[D^2(u_E)/E^2(u_E)]$, it is unnecessary to distinguish between the primed and unprimed subregions in the master diagram.

From these diagrams, a collection of all the various types of orbits is obtained (Figure 24); there are 25 essentially different ones. In this diagram, the name given to describe each orbit attempts to illustrate its properties at r_{max} and r_{min}. For example, for orbit of type 6, the outer part of the orbit is like that of a parabola whereas the inner part is that of a limit circle.

All the results of the solutions given in Appendix D and Figure 24 are tabulated in Table 6, which shows all admissible orbits in each subregion of a master diagram for $0 < a < 1$, $a = 1$, and $1 < a < \infty$.

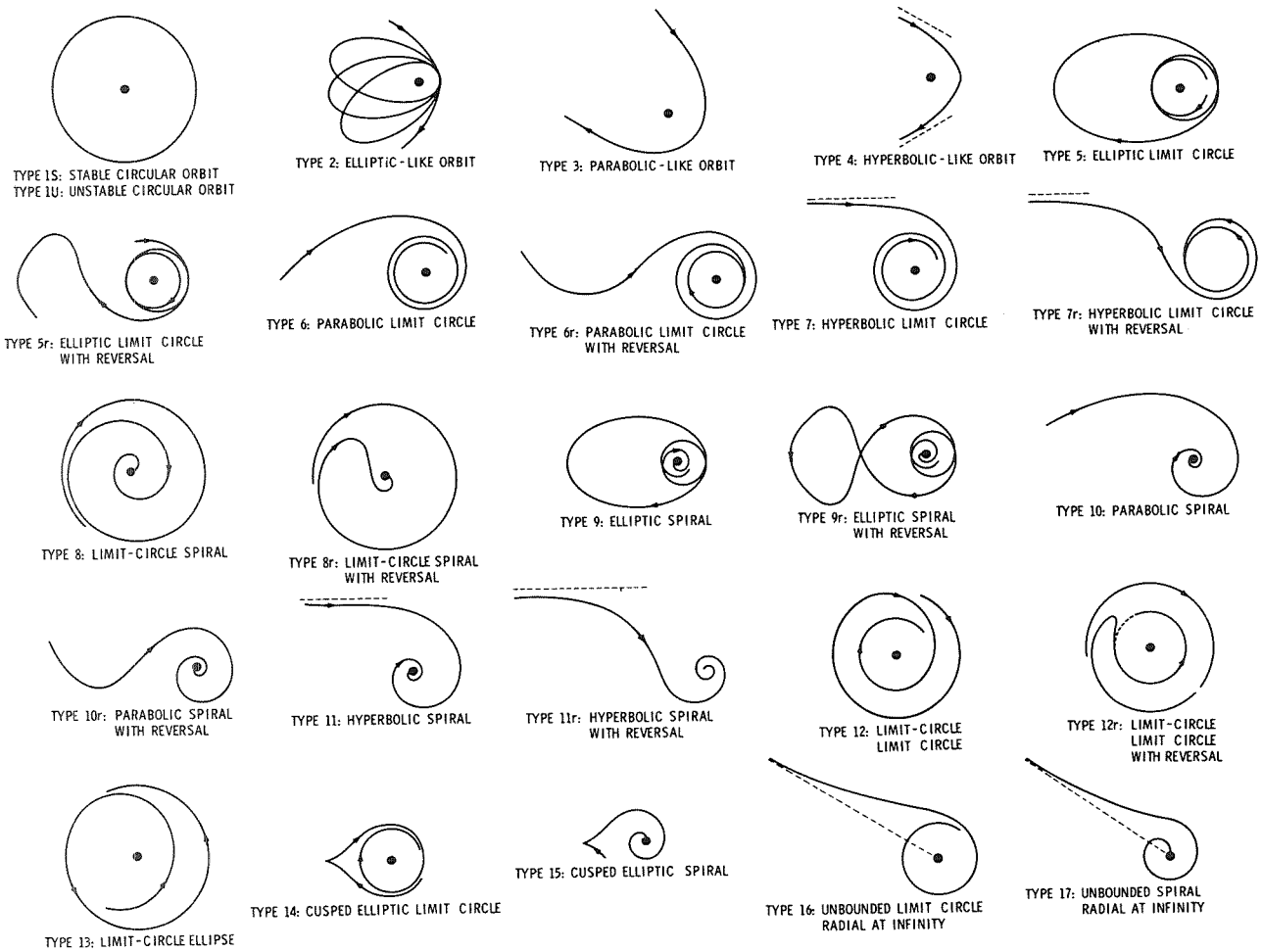

Figure 24—Types of orbits that exist in the equatorial plane of the Kerr gravitational field.

Table 6—Complete classification of the orbits of a test particle in the equatorial plane of the Kerr gravitational field by region and subregion of the master diagrams.

Schwarzschild Metric $a = 0$		Kerr Metric					
		$0 < a < 1$		$a = 1$		$1 < a < \infty$	
Region[a]	Admissible Orbits	Subregion[a]	Admissible Orbits	Subregion[a]	Admissible Orbits	Subregion[a]	Admissible Orbits
1	9	1a	1*U*, 5r, 8, 12	1a	1*U*, 5r, 8	1a	9r
		1b	1*U*, 5, 8, 12	1b	1*U*, 5, 8	1b	9
		1c	1*U*, 5, 8, 12r				
2	2, 9	2a	1*U*, 2, 5r, 8, 12	2a	1*U*, 2, 5r, 8	2a	2, 9r
		2b	1*U*, 5, 9, 12, 13	2b	1*U*, 5, 9, 13	2b	2, 9
		2c	1*U*, 5, 9, 12r, 13				
		2d	1*U*, 2, 5, 8, 12r				
		2e	1*U*, 2, 5, 8, 12	2e	1*U*, 2, 5, 8		
3	4, 9	3a	1*U*, 4, 5r, 8, 12	3a	1*U*, 4, 5r, 8	3a	4, 9r
		3b	1*U*, 7, 9, 12, 13	3b	1*U*, 7, 9, 13	3b	4, 9
		3c	1*U*, 7, 9, 12r, 13				
		3d	1*U*, 4, 5, 12r, 8				
		3e	1*U*, 4, 5, 8, 12	3e	1*U*, 4, 5, 8		
4	11	4a	1*U*, 7r, 8, 12	4a	1*U*, 7r, 8	4a	11r
		4b	1*U*, 7, 8, 12	4b	1*U*, 7, 8	4b	11
		4c	1*U*, 7, 8, 12r				
4*	11	4a*	1*U*, 7r, 8, 12	4a*	1*U*, 7r, 8	4a*	11r
		4b*	1*U*, 7, 8, 12	4b*	1*U*, 7, 8	4b*	11
		4c*	1*U*, 7, 8, 12r				
5	9	5a	1*U*, 5r, 8, 12	5a	1*U*, 5r, 8	5a	9r
		5b	1*U*, 5, 8, 12	5b	1*U*, 5, 8	5b	9
		5c	1*U*, 5, 8, 12r				
5*	9	5a*	1*U*, 5r, 8, 12	5a*	1*U*, 5r, 8	5a*	9r
		5b*	1*U*, 5, 8, 12	5b*	1*U*, 5, 8	5b*	9
		5c*	1*U*, 5, 8, 12r				

Table 6—Complete classification of the orbits of a test particle in the equatorial plane of the Kerr gravitational field by region and subregion of the master diagrams—concluded.

Schwarzschild Metric $a = 0$		Kerr Metric					
		$0 < a < 1$		$a = 1$		$1 < a < \infty$	
Region[a]	Admissible Orbits	Subregion[a]	Admissible Orbits	Subregion[a]	Admissible Orbits	Subregion[a]	Admissible Orbits
		6a	1*U*, 7r, 8, 12	6a	1*U*, 7r, 8	6a	11r
		6b	1*U*, 7, 8, 12	6b	1*U*, 7, 8	6b	11
		6a*	1*U*, 7r, 8, 12	6a*	1*U*, 7r, 8	6a*	11r
		6b*	1*U*, 7, 8, 12	6b*	1*U*, 7, 8	6b*	11
1-2 (*S* line)	1*S*, 9	1a-2a (*S* line)	1*S*, 1*U*, 5r, 8, 12	1a-2a (*S* line)	1*S*, 1*U*, 5r, 8	1a-2a (*S* line)	1*S*, 9r
		1b-2e (*S* line)	1*S*, 1*U*, 5, 8, 12	1b-2e (*S* line)	1*S*, 1*U*, 5, 8	1b-2b (*S* line)	1*S*, 9
		1c-2d (*S* line)	1*S*, 1*U*, 5, 8, 12r	2b (*S-D* line)	1*S*, 9		
2-5 (*U* line)	1*U*, 5, 8	2a-5a (*U* line)	1*U*, 5, 8, 12, 12r	2a-5a (*U* line)	1*U*, 5, 8, 12r	2a-5a (*U* line)	1*U*, 5, 8r
		2b-5b (*U* line)	1*U*, 5, 8, 12	2b-5b (*U* line)	1*U*, 5, 8, 12	2b-5b (*U* line)	1*U*, 5, 8
		2c-5c (*U* line)	1*U*, 5, 8, 12, 12r	2b-2e (*U-D* line)	1*U*, 5, 8		
		2d-5c (*U* line)	1*U*, 5, 8, 12, 12r				
3-4 (*U* line)	1*U*, 7, 8	3a-4a (*U* line)	1*U*, 7, 8, 12, 12r	3a-4a (*U* line)	1*U*, 7, 8, 12r	3a-4a (*U* line)	1*U*, 7, 8r
		3b-4b (*U* line)	1*U*, 7, 8, 12	3b-4b (*U* line)	1*U*, 7, 8, 12	3b-4b (*U* line)	1*U*, 7, 8
		3c-4c (*U* line)	1*U*, 7, 8, 12, 12r	3b-3e (*U-D* line)	1*U*, 7, 8		
		3d-4c (*U* line)	1*U*, 7, 8, 12, 12r				
2-3 ($W = 0$ line)	3, 9	2a-3a ($W = 0$ line)	1*U*, 3, 5r, 8, 12	2a-3a ($W = 0$ line)	1*U*, 3, 5r, 8	2a-3a ($W = 0$ line)	3, 9r
		2b-3b ($W = 0$ line)	1*U*, 6, 9, 12, 13	2b-3b ($W = 0$ line)	1*U*, 6, 9, 13	2b-3b ($W = 0$ line)	3, 9
		2c-3c ($W = 0$ line)	1*U*, 6, 9, 12r, 13				
		2d-3d ($W = 0$ line)	1*U*, 3, 5, 8, 12r				
		2e-3e ($W = 0$ line)	1*U*, 3, 5, 8, 12	2e-3e ($W = 0$ line)	1*U*, 3, 5, 8		
4-5 ($W = 0$ line)	10	4a-5a ($W = 0$ line)	1*U*, 6r, 8, 12	4a-5a ($W = 0$ line)	1*U*, 6r, 8	4a-5a ($W = 0$ line)	10r
		4b-5b ($W = 0$ line)	1*U*, 6, 8, 12	4b-5b ($W = 0$ line)	1*U*, 6, 8	4b-5b ($W = 0$ line)	10
		4c-5c ($W = 0$ line)	1*U*, 6, 8, 12r				

4*-5* (*W* = 0 line)	10	4a*-5a* (*W* = 0 line)	1*U*, 6r, 8, 12	4a*-5a* (*W* = 0 line)	1*U*, 6r, 8	4a*-5a* (*W* = 0 line)	10r
		4b*-5b* (*W* = 0 line)	1*U*, 6, 8, 12	4b*-5b* (*W* = 0 line)	1*U*, 6, 8	4b*-5b* (*W* = 0 line)	10
		4c*-5c* (*W* = 0 line)	1*U*, 6, 8, 12r				
		∩(2a, 3a, 4a, 5a)	1*U*, 6, 8, 12, 12r	∩(2a, 3a, 4a, 5a)	1*U*, 6, 8, 12r	∩(2a, 3a, 4a, 5a)	1*U*, 6, 8r
		∩(2b, 3b, 4b, 5b)	1*U*, 6, 8, 12	∩(2b, 3b, 4b, 5b)	1*U*, 6, 8, 12	∩(2b, 3b, 4b, 5b)	1*U*, 6, 8
		∩(2c, 3c, 4c, 5c)	1*U*, 6, 8, 12, 12r	∩(2b, 3b, 3e, 2e)	1*U*, 6, 8		
		∩(2d, 3d, 4c, 5c)	1*U*, 6, 8, 12, 12r				
		1a-1b (*E* line)	1*U*, 8, 12, 14	1a-1b (*E* line)	1*U*, 8, 14	1a-1b (*E* line)	15
		6b* (*E* line)	1*U*, 7, 8, 12	6b* (*E* line)	1*U*, 7, 8	6b* (*E* line)	11
		5a*-5b* (*E* line)	1*U*, 8, 12, 14	5a*-5b* (*E* line)	1*U*, 8, 14	5a*-5b* (*E* line)	15
∩(2, 3, 4, 5)	6, 8	∩(*E* line, *W* = 0 line)	8, 12, 16	∩(*E* line, *W* = 0 line)	8, 16	∩(*E* line, *W* = 0 line)	17
		2b (*H* line)	1*U*, 5, 12, 13	2b (*H* line)	1*U*, 5, 13	1b (*H* line)	None
		3b (*H* line)	1*U*, 7, 12, 13	3b (*H* line)	1*U*, 7, 13	2b (*H* line)	2
						3b (*H* line)	4
		1b-1c (*D*1 line)	1*U*, 5, 8	2b (*D*-*S* line)	1*S*, 9		
		2b-2c (*D*1 line)	1*U*, 5, 9, 13	2b-2e (*D*-*U* line)	1*U*, 5, 8		
		2d-2e (*D*1 line)	1*U*, 2, 5, 8	3b-3e (*D* line)	1*U*, 7, 8		
		3d-3e (*D*1 line)	1*U*, 4, 5, 8				
		5b-5c (*D*1 line)	1*U*, 5, 8				
		5b*-5c* (*D*1 line)	1*U*, 5, 8				
		2b-2c (*D*2 line)	1*U*, 5, 9, 13				
		3b-3c (*D*2 line)	1*U*, 7, 9, 13				
		∩(2b, 2c, 3b, 3c)	1*U*, 6, 9, 13	∩(2b, 2e, 3b, 3e)	1*U*, 6, 8		
		∩(2d, 2e, 3d, 3e)	1*U*, 3, 5, 8				

[a]Regions or subregions separated by a hyphen denote the boundary common to the regions or subregions. The symbol ∩ denotes the boundary point common to the subregions that follow it.

DISCUSSION

In this section, four topics will be discussed: (1) the determination of direction of orbital motion for a given set of constants of motion (h, e) for the test particle in the Kerr field of a central body with mass $m = 1$ and a given specific angular momentum $-a$, (2) the scaling of master diagrams and solutions from the case in which $\beta \equiv 2m = 2$ to one in which $\beta \neq 2$, (3) the conversion of the results obtained in the S coordinates to those in the E coordinates, and (4) the behavior of solutions in the neighborhood of the pseudosingularity at $u = u_D$.

Direction of Orbital Motion

From Appendix D, which illustrates the admissible types of orbits in each subregion of a master diagram for the cases of $0 < a < 1$, $a = 1$, and $1 < a < \infty$, it is observed that the mathematical solution $u(\phi)$ of Equation 44 has two branches at every point in the ϕ, u plane in which the one-parameter family of solutions $F(\phi + c, u) = 0$ is defined. One would expect that the branch to be taken is determined by the specific angular momentum h of the test particle. Such is the case in the Schwarzschild gravitational field. For the present case there is the more general condition given by Equation 219,

$$\frac{d\phi}{ds} = \frac{u^2 E(u)}{D(u)} = \frac{u^2 [-\beta(h + ea)u + h]}{a^2 u^2 - \beta u + 1}, \tag{220}$$

in which the proper time s is taken to be always increasing. This equation thus determines the direction of orbital motion.

For an illustrative case, consider a central body with $\beta = 2$ and $a = 0.7$ and a test particle with $h < 0$ and $e < 0$ such that (h, e) lies in region 1a in the third quadrant of the master diagram given by Figure 15. (There is also a subregion 1a in the first quadrant for which $h > 0$ and $e > 0$.) Table 6 indicates that there are four kinds of orbits for this subregion: $1U$, 5r, 8, and 12, which are then obtained from Figure 24. In subregion 1a of Figure 15, $h + ea < 0$; and Figure D1 shows that $0 < u_E < u_{D1} < u_{D2}$. With this information, Figure 25 was constructed, which indicates that ϕ decreases for $u_{B3} \leqslant u < u_E$ and $u_{D1} < u < u_{D2}$ and ϕ increases for $u_E < u < u_{D1}$ and $u_{D2} < u$. Consequently, the orbits have direction of motion as shown in Figure 26.

Scaling of Master Diagrams and Solutions

In this work, the value $\beta = 2$ was arbitrarily set by taking the central body to have mass $m = 1$. The results of this study can easily be applied to the case $\beta \neq 2$: Suppose that for a given set (h, e, a, β) there is the solution

$$u = u(\phi; h, e, a, \beta) \tag{221}$$

of the differential equation

$$\left(\frac{du}{d\phi}\right)^2 = B(u)\frac{D^2(u)}{E^2(u)}. \tag{44}$$

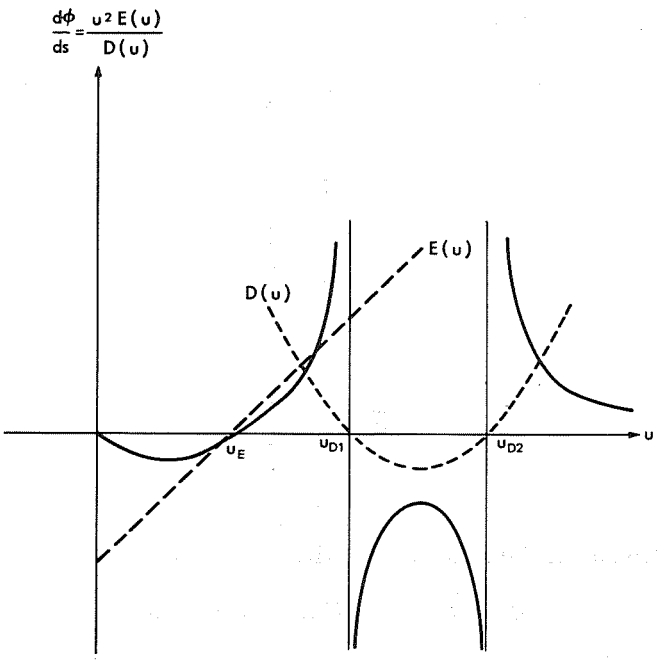

Figure 25—Illustrative case of determination of sign of $d\phi/ds$.

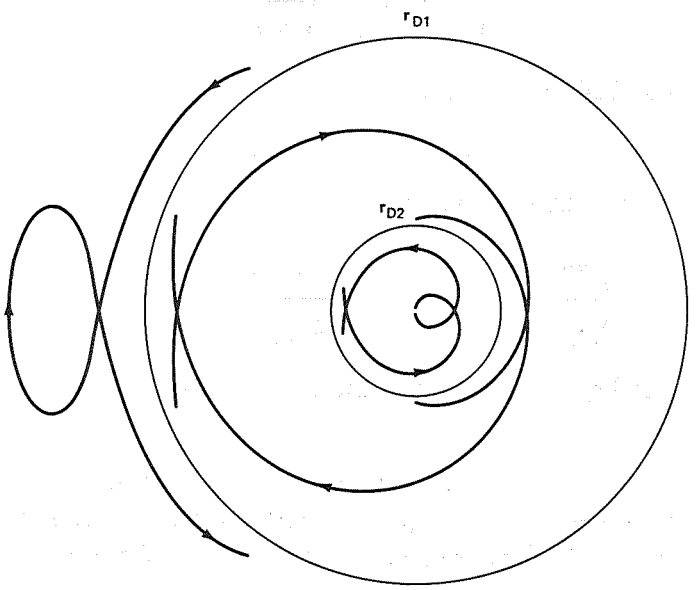

Figure 26—Illustrative case of determination of direction of motion.

Next, let a set of new variables $(\bar{\phi}, \bar{u}, \bar{h}, \bar{e}, \bar{a}, \bar{\beta})$ be defined by

$$\left.\begin{aligned} \bar{\phi} &= \phi \\ \bar{u} &= \frac{u}{\lambda} \\ \bar{h} &= \lambda h \\ \bar{e} &= e \\ \bar{a} &= \lambda a \\ \bar{\beta} &= \lambda \beta \end{aligned}\right\} \tag{222}$$

where λ is an arbitrary constant not equal to zero; then, it is obvious from Equations 45 to 47 that

$$\left.\begin{aligned} B(\bar{u}; \bar{h}, \bar{e}, \bar{a}, \bar{\beta}) &\equiv B(u; h, e, a, \beta) \\ D(\bar{u}; \bar{a}, \bar{\beta}) &\equiv D(u; a, \beta) \\ E(\bar{u}; \bar{h}, \bar{e}, \bar{a}, \bar{\beta}) &\equiv \lambda E(u; h, e, a, \beta) \end{aligned}\right\} \tag{223}$$

and that

$$\left(\frac{d\bar{u}}{d\bar{\phi}}\right)^2 \equiv \frac{1}{\lambda^2}\left(\frac{du}{d\phi}\right)^2 . \tag{224}$$

From Equations 44, 223, and 224, it follows that

$$\bar{u} = \bar{u}(\bar{\phi}; \bar{h}, \bar{e}, \bar{a}, \bar{\beta}) \tag{225}$$

is automatically a solution of the differential equation

$$\left(\frac{d\bar{u}}{d\bar{\phi}}\right)^2 = \frac{B(\bar{u}; \bar{h}, \bar{e}, \bar{a}, \bar{\beta}) D^2(\bar{u}; a, \beta)}{E^2(\bar{u}; \bar{h}, \bar{e}, \bar{a}, \bar{\beta})} . \tag{226}$$

Hence, the transformations in Equation 222 yield the desired scaling of the master diagram and the solution.

As a concrete example, consider the case of a central body with mass $m = 5$ (i.e., $\bar{\beta} = 10$) and specific angular momentum $-\bar{a} = -3$ and a test particle with constants of motion $\bar{h} = 7$ and $\bar{e} = 11$. Because the master diagrams in this work are constructed for $\beta = 2$, from Equation 222 it follows that

$$\lambda = \frac{\bar{\beta}}{\beta} = 5 . \tag{227}$$

the master diagram for which

$$a = \frac{\bar{a}}{\lambda} = \frac{3}{5} = 0.6 \tag{228}$$

and the subregion containing the point

$$\left.\begin{aligned} h &= \frac{\bar{h}}{\lambda} = \frac{7}{5} = 1.4 \\ e &= \bar{e} = 11 \end{aligned}\right\} \tag{229}$$

are then used to obtain the various types of admissible orbits and the direction of motion. From these orbits in the r, ϕ plane, the orbits in the $\bar{r}, \bar{\phi}$ plane are obtained from the relations $\bar{r} = \lambda r = 5r$ and $\bar{\phi} = \phi$. That is, the desired admissible orbits are stretched by a factor of 5.

Conversion of Results From S to E Form

The present qualitative solutions are obtained by considering the differential equation that is in the S form, Equation 44. However, to obtain the solutions in the E form for which the differential equation is

$$A^* \left(\frac{du^*}{d\phi^*}\right)^2 + 2aB^* \frac{du^*}{d\phi^*} - C^* = 0 , \tag{230}$$

where A^*, B^*, and C^* are given by Equations 19 to 21, it is not necessary to solve this more complicated equation. Instead, Equations 10, 12, 14, and 46 are used to obtain

$$\begin{aligned} \frac{du^*}{d\phi^*} &= \frac{du}{d\phi^*} \\ &= \frac{du}{d\phi}\frac{d\phi}{d\phi^*} \\ &= \frac{du}{d\phi}\left(1 + \frac{a}{\Delta}\frac{dr^*}{d\phi^*}\right) \\ &= \frac{du}{d\phi}\left(1 - \frac{a}{u^2\Delta}\frac{du}{d\phi^*}\right) \\ &= \frac{du}{d\phi}\left(1 - \frac{a}{D}\frac{du}{d\phi^*}\right) , \end{aligned} \tag{231}$$

where $D \neq 0$. Therefore,

$$\frac{du}{d\phi^*} = \frac{D\, du/d\phi}{D + a\, du/d\phi} . \tag{232}$$

In view of the fact that $(h^*, e^*) \equiv (h, e)$ as proved earlier, Equation 232 gives the solution $u(\phi^*; h^*, e^*, a, \beta)$ in the E form from a knowledge of the solution $u(\phi; h, e, a, \beta)$ in the S form when $D \neq 0$.

Because $du/d\phi \to \pm\infty$ as $u \to u_E$, it is concluded from Equation 232 that

$$\lim_{du/d\phi \to \pm\infty} \frac{du}{d\phi^*} = \frac{D(u_E)}{a} . \tag{233}$$

Equation 231 indicates that if $D \neq 0$, then

$$\frac{du}{d\phi} = 0 \Longleftrightarrow \frac{du}{d\phi^*} = 0 , \tag{234}$$

which holds at $u = u_B$, as can be easily seen from Equation 44.

For the case in which $du/d\phi \neq 0$ or $du/d\phi \neq \pm\infty$, Equation 231 may also be used to study the qualitative nature of the conversion of $du/d\phi$ to $du/d\phi^*$ as follows: For simplicity, let $a > 0$. Then, there are two cases: $D > 0$ and $D < 0$.

For $D > 0$, there are four subcases. Subcase 1 has the conditions

$$\frac{du}{d\phi} > 0$$

$$\frac{du}{d\phi^*} > 0 ,$$

so that

$$0 < \frac{du/d\phi^*}{du/d\phi} = 1 - \frac{a}{D}\frac{du}{d\phi^*} < 1$$

or

$$\frac{du}{d\phi^*} < \frac{du}{d\phi} . \tag{235}$$

In subcase 2,

$$\frac{du}{d\phi} > 0$$

$$\frac{du}{d\phi^*} < 0 ,$$

so that

$$0 > \frac{du/d\phi^*}{du/d\phi} = 1 - \frac{a}{D}\frac{du}{d\phi^*} > 0 ,$$

which is a contradiction; hence, this case is impossible. For subcase 3,

$$\frac{du}{d\phi} < 0$$

$$\frac{du}{d\phi^*} < 0 ,$$

so that

$$0 < \frac{du/d\phi^*}{du/d\phi} = 1 - \frac{a}{D}\frac{du}{d\phi^*} > 1$$

or

$$\frac{du}{d\phi^*} < \frac{du}{d\phi} . \tag{236}$$

Subcase 4 has the conditions

$$\frac{du}{d\phi} < 0$$

$$\frac{du}{d\phi^*} > 0 ,$$

so that

$$0 > \frac{du/d\phi^*}{du/d\phi} = 1 - \frac{a}{D}\frac{du}{d\phi^*}$$

which is a possibility and for this

$$\frac{du}{d\phi^*} > \frac{du}{d\phi} . \tag{237}$$

Similarly, the corresponding four subcases for $D < 0$ are the following:

(1)

$$\frac{du}{d\phi} > 0$$

$$\frac{du}{d\phi^*} > 0 ;$$

$$\frac{du}{d\phi^*} > \frac{du}{d\phi} . \tag{238}$$

(2)

$$\frac{du}{d\phi} > 0$$

$$\frac{du}{d\phi^*} < 0 ;$$

$$\frac{du}{d\phi^*} < \frac{du}{d\phi} . \tag{239}$$

(3)

$$\frac{du}{d\phi} < 0$$

$$\frac{du}{d\phi^*} < 0 ;$$

$$\frac{du}{d\phi^*} > \frac{du}{d\phi} \,. \tag{240}$$

(4)

$$\frac{du}{d\phi} < 0$$

$$\frac{du}{d\phi^*} > 0 \,,$$

which is impossible.

Thus, Equations 233 to 240 are sufficient to provide all the pertinent information for conversion of any solution in the ϕ, u plane to one in the ϕ^*, u plane, provided that $D \neq 0$ anywhere in the solution. Because Equation 230 is also autonomous, the one-parameter family of solutions is given by

$$G(\phi^* + c, u) = 0 \tag{241}$$

so that all the remaining members in the family can be obtained from any one member by a simple translation. Figures 27 and 28 illustrate, respectively, the transformation of $u(\phi)$ to $u(\phi^*)$ in the neighborhood of a turning point and of a reversal point.

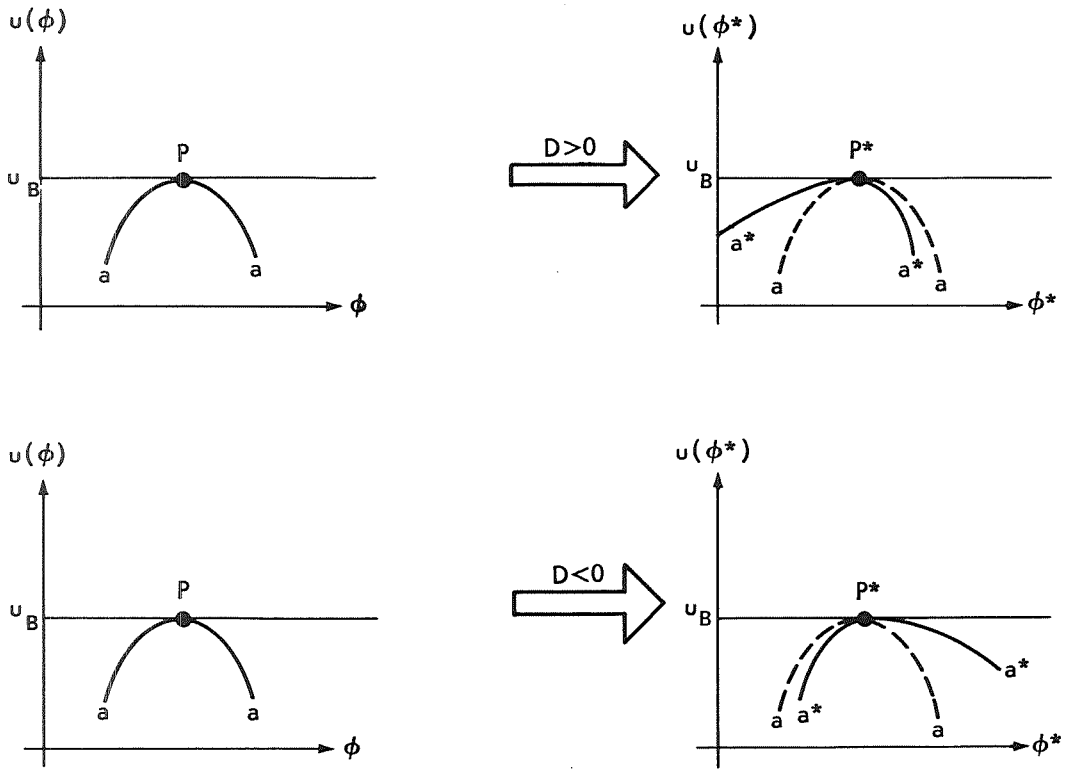

Figure 27—Conversion of *S* form to *E* form in the neighborhood of a turning point *P*.

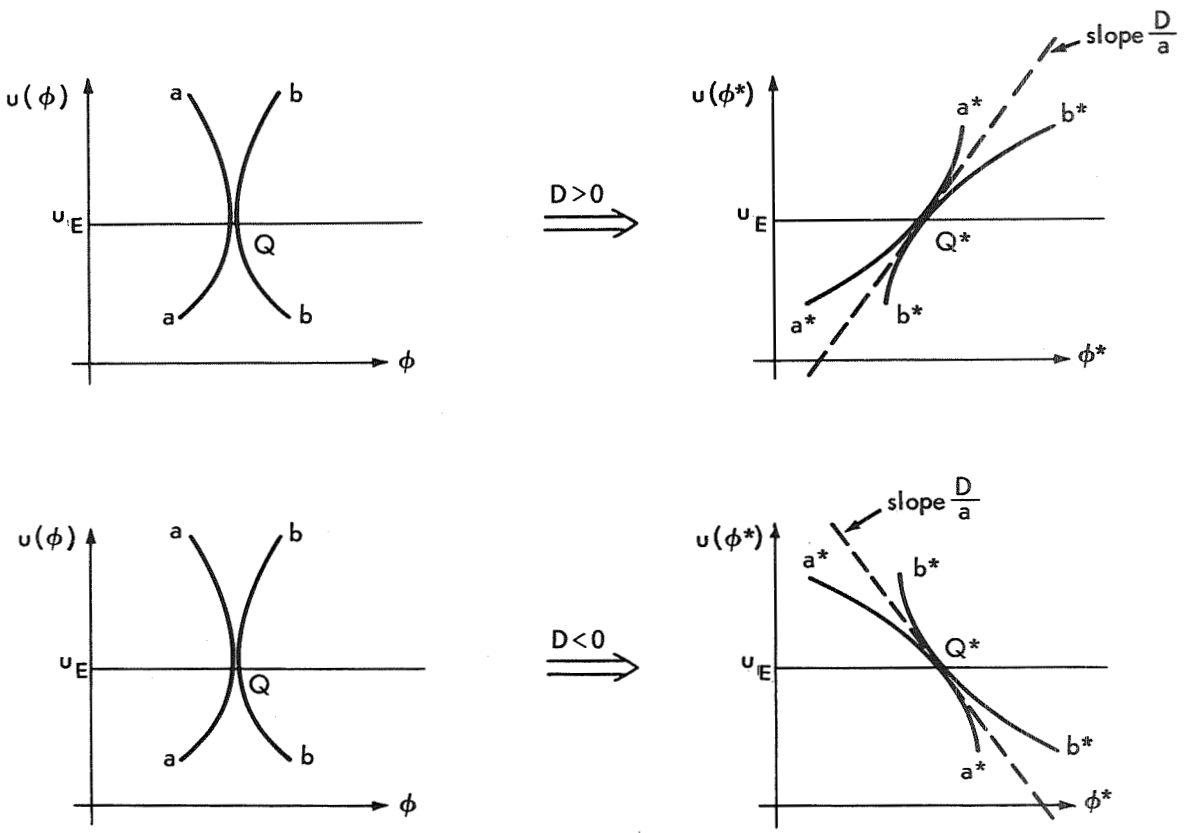

Figure 28—Conversion of S form to E form in the neighborhood of reversal point Q.

Pseudosingularity at $u = u_D$

In the transformation from E to S coordinates given by Equations 10 to 13, a pseudosingularity is introduced when $\Delta = 0$; i.e., $D(u) = 0$. This means that the transformation of the qualitative results back from S to E coordinates holds only if $D \neq 0$; i.e., $u \neq u_D$.

It remains now to study the behavior of solutions $u(\phi^*)$ in the neighborhood of $u = u_D$. For this, we must go directly to the equation of motion in E form (Equation 17) which, in view of $u \equiv u^*$, $e \equiv e^*$, and $h \equiv h^*$, may be written simply as

$$A(u)\left(\frac{du}{d\phi^*}\right)^2 + 2aB(u)\frac{du}{d\phi^*} - B(u)D(u) = 0 \tag{242}$$

or

$$\frac{du}{d\phi^*} = \frac{-aB \pm \sqrt{B(a^2B + AD)}}{A}. \tag{243}$$

Hence, if $D(u) = 0$, then

$$\left(\frac{du}{d\phi^*}\right)_{u=u_D} = 0 \tag{244a}$$

or

$$\left(\frac{du}{d\phi^*}\right)_{u=u_D} = -\frac{2aB(u_D)}{A(u_D)} . \tag{244b}$$

Now from Equation 172 which is

$$u_D = u_E \iff B(u_D) = 0 \tag{245}$$

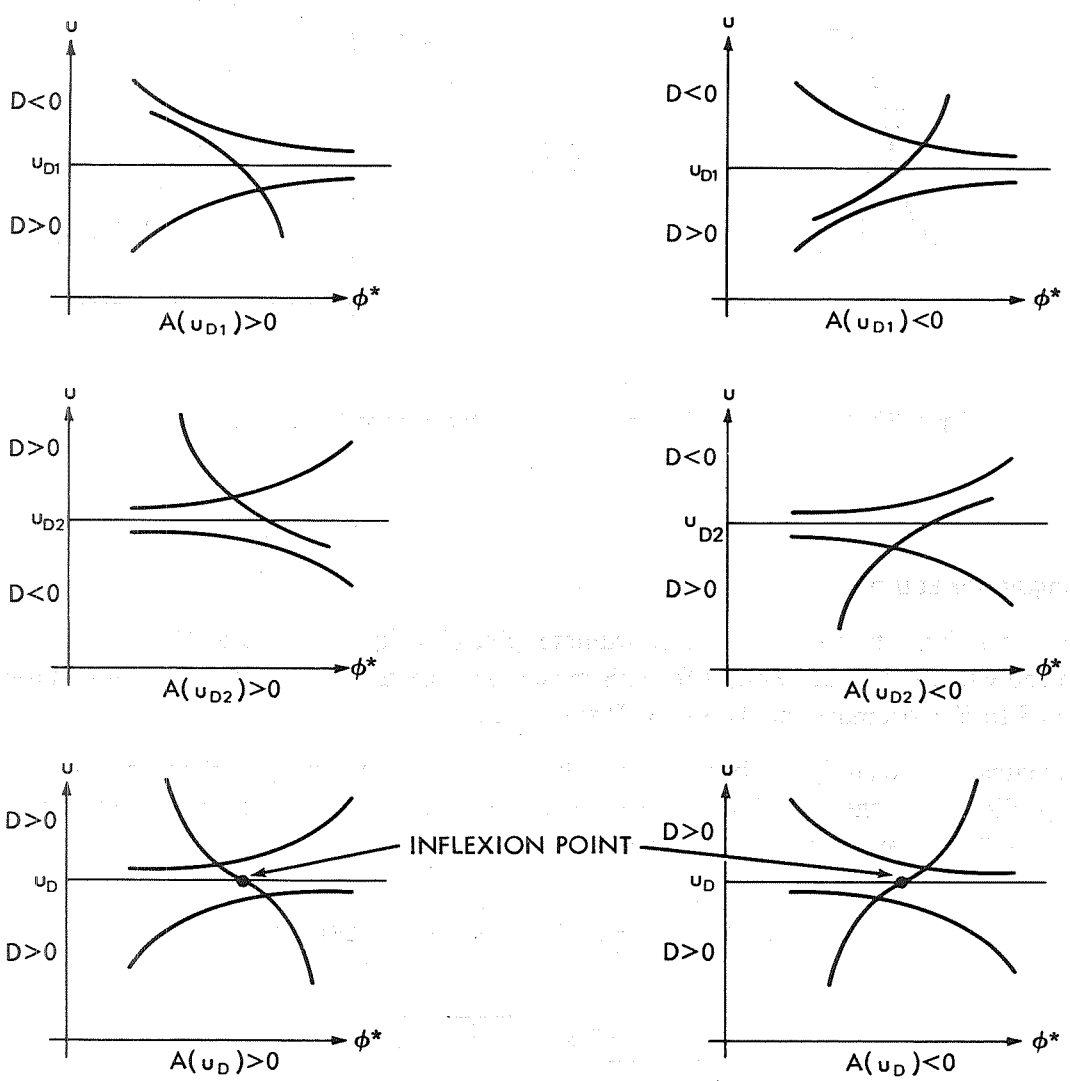

Figure 29—Behavior of solution $u(\phi^*)$ in the neighborhood of $u = u_D \neq u_E$.

and Equation 244, it follows that only the neighborhood of $u = u_D \neq u_E$ need be studied because otherwise the only possibility is

$$\left(\frac{du}{d\phi^*}\right)_{u=u_D=u_E} = 0 . \tag{246}$$

This equation and the results of the conversion from S to E form suffice to determine the qualitative nature of the solution $u(\phi^*)$ in the neighborhood of $u = u_D = u_E$.

Remembering that by Equation 195 $B(u_D) > 0$ under these conditions and using Equations 236 to 241 and 244, the six cases for the solution $u(\phi^*)$ in the neighborhood of $u = u_D \neq u_E$ are determined as illustrated in Figure 29.

Finally, Equation 243 indicates that, at a reversal point in the solution $u(\phi^*)$, $A(u) = 0$ must hold. In other words,

$$\frac{du}{d\phi^*} = \pm\infty \Rightarrow u = u_A , \tag{247}$$

where

$$u_A = \frac{h^2 + (1 - e^2)a^2}{\beta(h + ea)^2} , \tag{248}$$

which is obtained from Equations 19, 131, and 134.

CONCLUSIONS

The main results are summarized as follows:

(1) For equatorial orbital motion, the differential equation in the S coordinates is used because of its simple form.

(2) For $\beta = 2$ and $0 < a < \infty$, several master diagrams are obtained for the h, e space of parameters.

(3) These master diagrams are of three types corresponding to the ranges $0 < a < 1$, $a = 1$, and $1 < a < \infty$.

(4) Each master diagram is divided into subregions such that each has the same types of admissible orbits.

(5) There are 25 essentially different types of orbits for $a \neq 0$ (Kerr metric) as compared to 11 for $a = 0$ (Schwarzschild metric).

(6) Among the most interesting results are orbits with reversal points or cusps.

(7) A method is given for scaling master diagrams and solutions for the case of $\beta \neq 2$.

Goddard Space Flight Center
National Aeronautics and Space Administration
Greenbelt, Maryland, January 27, 1972
630-22-01-01-51

REFERENCES

1. Kerr, R. P.: "Gravitational Field of a Spinning Mass as an Example of Algebraically Special Metric." *Phys. Rev. Lett.* 11(5): 237, 1963.

2. Boyer, R. H.; and Price, T. G.: "An Interpretation of the Kerr Metric in General Relativity." *Proc. Cambridge Phil. Soc.* 61: 531, 1964.

3. Lense, J.; and Thirring, H.: "Über den Einfluss der Eigenrotation zer Zentralkörper auf die Bewegung der Planeten und Monde nach der Einsteinschen Gravitationstheorie." *Phys. Z.* 19: 156, 1918.

4. Carter, B.: "Complete Analytic Extension of the Symmetry Axis of Kerr's Solution." *Phys. Rev.* 141(4): 1242, 1966.

5. Boyer, R. H.; and Lindquist, R. W.: "Maximal Analytic Extension of the Kerr Metric." *J. Math. Phys.* 8(2): 265, 1967.

6. DeFelice, F.: "Equatorial Motion in the Gravitational Field of Rotating Source." *Nuovo Cimento B* 57(2): 351, 1968.

7. Carter, B.: "Global Structure of the Kerr Family of Gravitational Fields." *Phys. Rev.* 174(5): 1559, 1968.

8. Synge, J. L.: *Relativity: The General Theory.* North-Holland Pub. Co., 1964.

9. Hagihara, Y.: "Theory of the Relativistic Trajectories in a Gravitational Field of Schwarzschild." *Japan J. Astron. Geophys.* 8: 67, 1931.

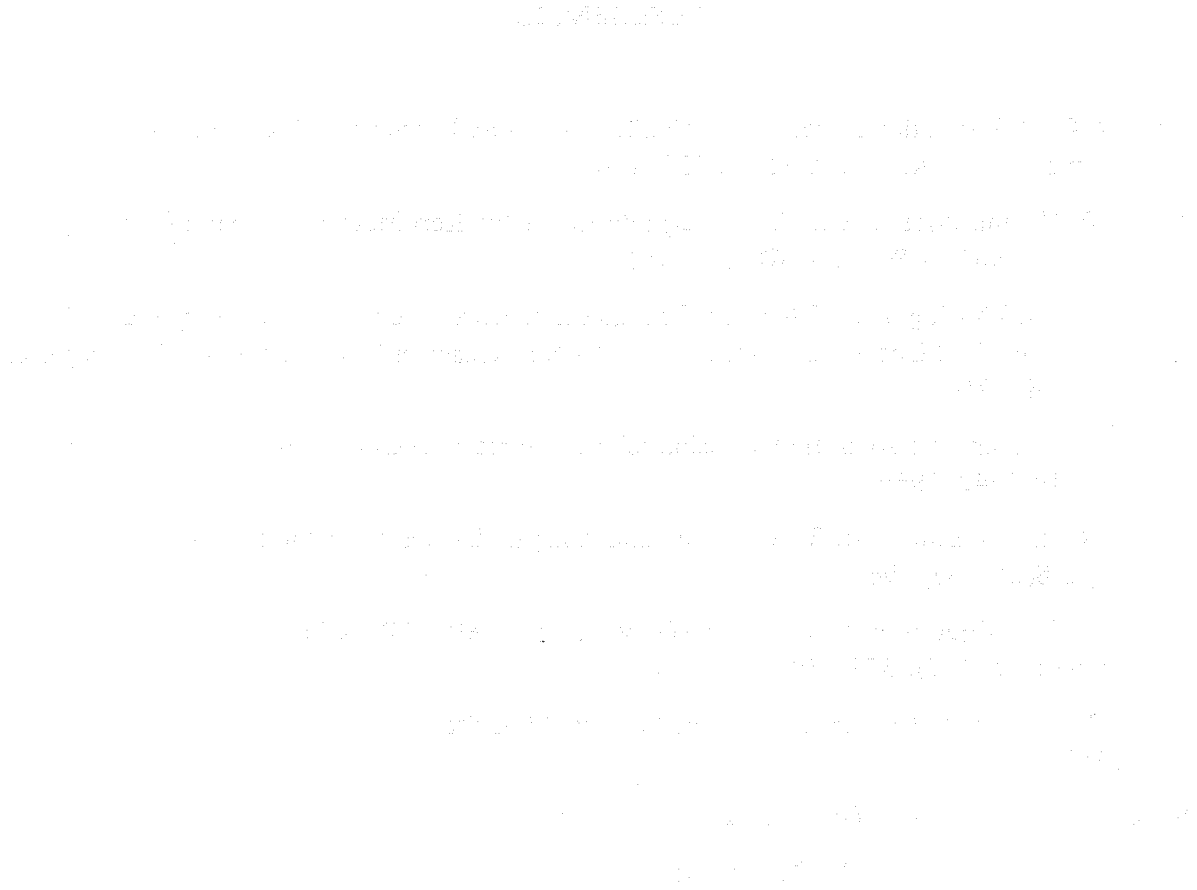

Appendix A

A QUALITATIVE STUDY OF THE COMPLETE SET OF SOLUTIONS OF THE DIFFERENTIAL EQUATION OF MOTION OF A TEST PARTICLE IN THE EXTERIOR SCHWARZSCHILD GRAVITATIONAL FIELD

F. K. Chan
Department of Space Science and Applied Physics
Catholic University of America
Washington, D.C.

INTRODUCTION

The relativistic orbits of a test particle around a centrally attracting mass have been studied time and again since Einstein (References A1 and A2) first studied the quasi-elliptic orbits in connection with his analysis of the precession of the orbit of Mercury around the Sun. Later work on this type of orbit has been contributed by several authors among whom are Droste (References A3 and A4), de Sitter (References A5 and A6), Greenhill (Reference A7), and Forsyth (Reference A8). Although Droste and Morton (Reference A9) have also considered various other types of orbits, their works are not really complete because they do not give an exhaustive account of all possible types of orbits. It was not until the work of Hagihara (Reference A10) that a truly complete and exhaustive analytical treatment of the whole problem was first published. Work following this includes that of Kaplan (Reference A11) who studied only the circular orbits, Darwin (References A12 and A13) who obtained a fairly detailed but not totally complete account of the various types of orbits, Metzner (Reference A14) who essentially completed the studies of Darwin, and Galkin (Reference A15) who made some study, though not elaborately revealed, on certain aspects of relativistic orbits. A fairly complete account is also given by Arzeliès (Reference A16). However, the works of Hagihara, Darwin, and Arzeliès, to mention the most authoritative sources on the subject, are rather involved and rely heavily on the use of elliptic functions. A different and apparently much simpler approach to the analysis of these orbits, involving a qualitative study of the solutions of the governing differential equation of motion of the test particle, was obtained by the present author in 1965 with only a knowledge, at that time, of the first paper of Darwin. The analysis given here is essentially taken from his unpublished work on certain aspects of nonlinear ordinary differential equations in which he studied, as an example, the relativistic differential equation of motion of a test particle in an exterior Schwarzschild gravitational field.

ANALYSIS

The motion of a test particle in the exterior Schwarzschild gravitational field produced by a spherical body of mass m is given by the well-known equation

$$\left(\frac{du}{d\phi}\right)^2 = 2mu^3 - u^2 + \frac{2m}{h^2}u + \frac{W}{h^2}, \tag{A1}$$

where h and W are constants of the motion dependent only on the initial conditions of the test particle. The quantity h may be interpreted as the angular momentum per unit rest mass of the particle, except now, as contrasted with the Newtonian analog, it is defined in terms of the rate of change of the angle ϕ with respect to the proper time s of the particle, i.e.,

$$r^2 \frac{d\phi}{ds} = h . \tag{A2}$$

The quantity W may be interpreted as a measure of the "energy" of the particle and in the Newtonian limit it reduces to $2E$, where E is the total energy per unit mass of the particle.

Topological properties of the solutions satisfying Equation A1 will be studied by considering the geometric-topological nature of the surface $\Phi(\phi, u, v) = 0$, where for convenience $(du/d\phi)^2$ is denoted by v. In Equation A1, ϕ does not appear explicitly; consequently, in the ϕ, u, v space, the surface $\Phi(\phi, u, v) = 0$ is a cylinder with a cubic curve as the trace in the u, v plane. Because the radius r is defined to be nonnegative, the region to be studied is in the ϕ, u plane for which $u \geqslant 0$. Furthermore, it is necessary that $v \geqslant 0$; therefore, the region to be considered in the ϕ, u plane is that for which $u \geqslant 0$ and $v \geqslant 0$. Consequently, conditions are sought for which there are zero, one, two, or three positive roots of the trace cubic curve. A general approach in this direction would require the algebraic knowledge of roots of the cubic equation and this is available; but the analysis becomes very cumbersome algebraically. In addition, it becomes more involved, for instance, in the case of one real positive root whether the remaining two roots are real but negative or are complex conjugates.

However, in the following analysis the surface $\Phi(\phi, u, v) = 0$ will be studied without having to consider these difficulties. In this process, a geometric meaning will be given to the angular momentum h and the energy W. Also, because the surface is cylindrical, only the trace in the u, v plane will be considered.

For convenience, the expression on the right-hand side of Equation A1 is denoted by $f(u)$, so that

$$\left(\frac{du}{d\phi}\right)^2 = v^2 = f(u) = 2mu^3 - u^2 + \frac{2m}{h^2}u + \frac{W}{h^2}, \tag{A3}$$

$$f'(u) = 6mu^2 - 2u + \frac{2m}{h^2}, \tag{A4}$$

$$f''(u) = 12mu - 2 . \tag{A5}$$

It is seen that $f''(u)$ does not involve h or W and is therefore independent of the initial conditions of the test particle. In other words, the curve $f''(u)$ is the same for all orbits in the field of a gravitational mass m; it is a straight line intersecting the u axis at $u = 1/6m$ or $r = 6m$.

The first integral of $f''(u)$, i.e., $f'(u)$, is a parabola with the axis of symmetry at $u_s = 1/6m$. From Equation A4, it is seen that the angular momentum appears in the constant of integration. If they exist, the intercepts u'_{f1} and u'_{f2} of this parabola $f'(u)$ with the u axis are given by

$$u'_{f1,f2} = \frac{1}{6m}\left(1 \pm \sqrt{1 - \frac{12m^2}{h^2}}\right), \tag{A6}$$

which indicates that $0 \leqslant u'_{f1} \leqslant 1/6m$ and $1/6m \leqslant u'_{f2} \leqslant 1/3m$. A sketch of this family of parabolas, with h^2 as the parameter, is shown in Figure A1.

The second integral of $f''(u)$, i.e., $f(u)$, is a cubic curve and involves a second arbitrary constant given by W/h^2. That is, the quantity W which is a measure of the energy of the particle appears only in the second integral of $f''(u)$, whereas the angular momentum h makes its first appearance in the first integral of $f'(u)$. A sketch of this family of cubic curves, with W as the parameter, corresponding to the four cases of the parabolas given in Figure A1, is shown in Figure A2.

The two intercepts, if they exist, of the parabola $f'(u)$ determine the maximum and the minimum of the cubic curve $f(u)$ and are in turn determined by the angular momentum. Consequently, the role of the angular momentum h is to determine the distance of separation between the points of maximum and minimum in the $f(u)$ curve, whereas the quantity W or rather W/h^2 determines its vertical displacement.

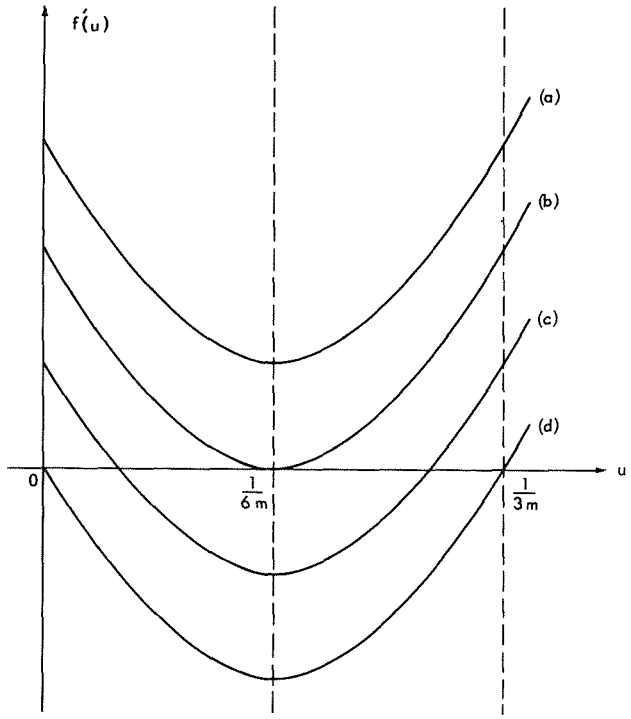

Figure A1—Criterion for the four classes of trace cubic curves.

The region in the ϕ, u plane for which $u \geqslant 0$ and $v \geqslant 0$ is a simply connected one for the case in which $0 < h \leqslant 12m^2$, as seen in Figure A2. However, for $h^2 > 12m^2$, it is possible for this region to consist of two simply connected regions that are disjoint from each other (see Figures A2c and A2d); this situation corresponds to the case in which the cubic curve $f(u)$ has two or three real positive roots.

Attention will be focused on the trace cubic curve as shown in Figure A2c because it contains features that are shared by the other three types. For example, consider the surface $\Phi(\phi, u, v) = 0$ with trace on the u, v plane as shown in Figure A3. The quantities u'_{f1} and u'_{f2} (u'_{I} and u'_{II} in the figure) correspond to the two roots of the parabola $f'(u) = 0$ and are given by Equation A6, whereas the quantities u_{f1}, u_{f2},

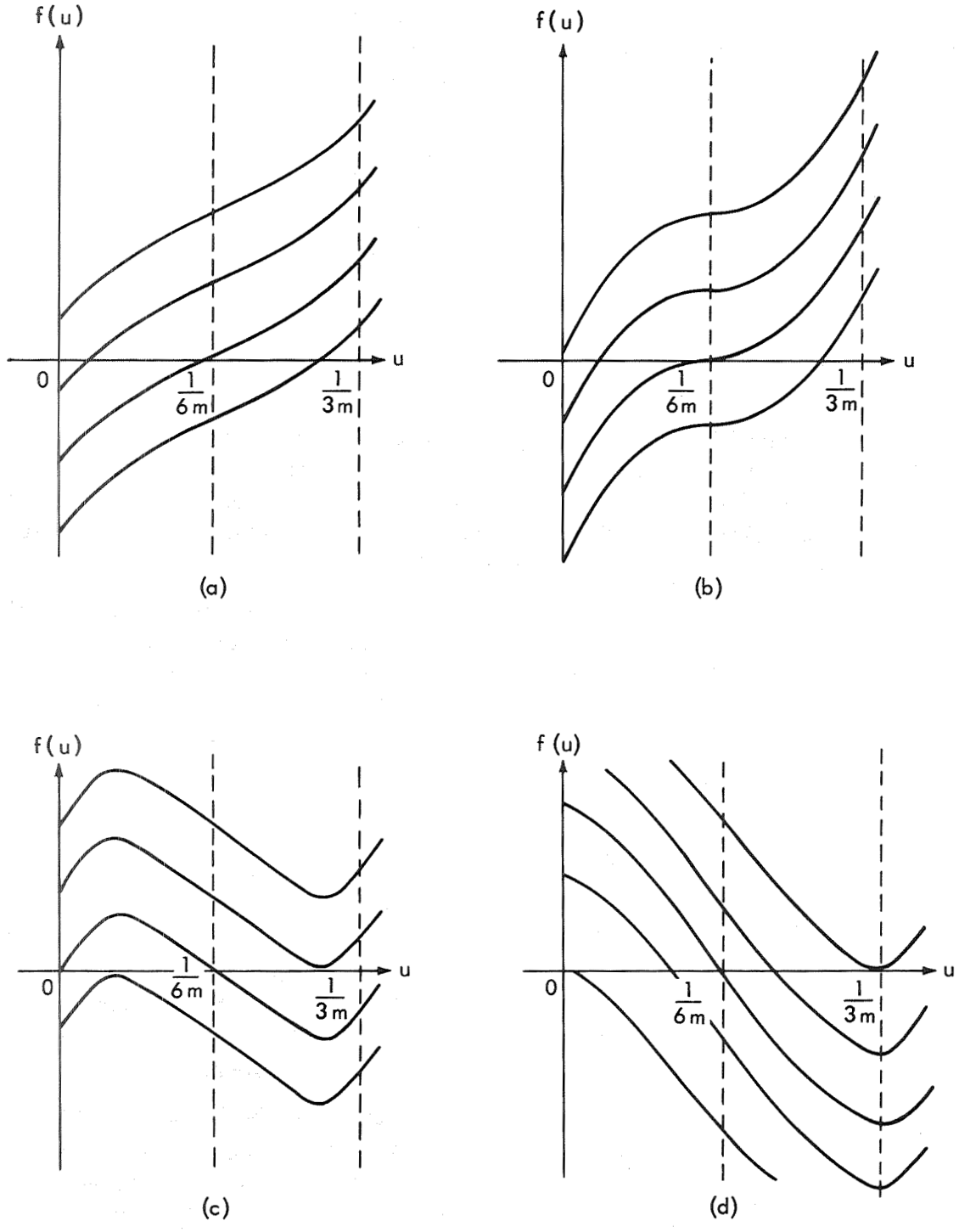

Figure A2—The four classes of trace cubic curves.

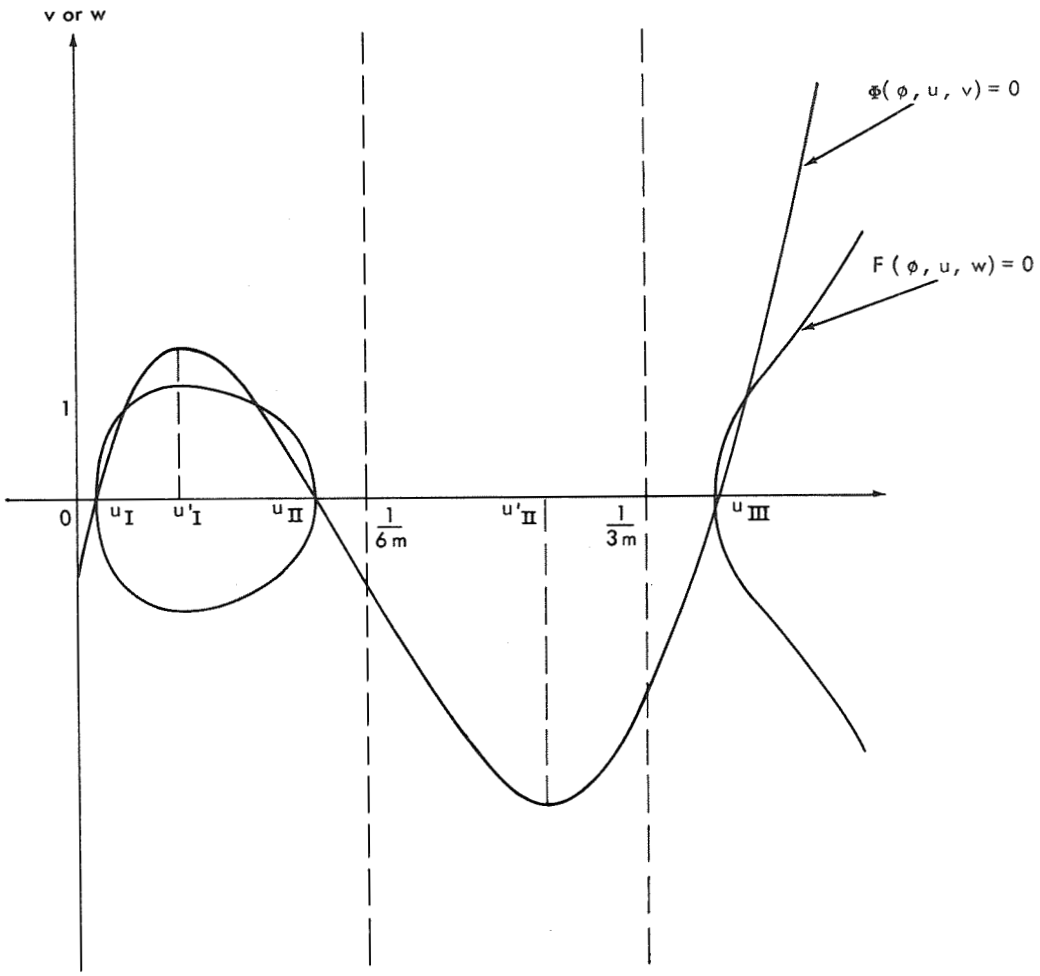

Figure A3—Trace cubic curve of class c with $W < 0$ and $1/4m < u'_{II} < 1/3m$.

and u_{f3} (u_I, u_{II}, u_{III}) correspond to the three roots of the cubic curve $f(u) = 0$. From this, the surface $F(\phi, u, w) = 0$ is obtained (Figure A3) where $w = du/d\phi$; this surface corresponds to Equation A1 in the ϕ, u, w space.

From $F(\phi, u, w) = 0$, it is easily seen that in the ϕ, u plane the three lines $u = u_{f1}$, u_{f2}, and u_{f3} correspond to envelopes or singular solutions; this result follows from the sufficient conditions (see Reference 17):

$$F(\phi, u, w) = 0 , \tag{A7}$$

$$\frac{\partial F}{\partial w} = 0 , \tag{A8}$$

$$\frac{\partial F}{\partial \phi} + w \frac{\partial F}{\partial u} = 0 , \tag{A9}$$

$$\frac{\partial F}{\partial u} \neq 0 . \tag{A10}$$

From the trace of the surface $F(\phi, u, v) = 0$ as shown in Figure A3, the family of solutions $u = u(\phi)$ as shown in Figure A4 is obtained.

The solutions $u_{f1} \leqslant u(\phi) \leqslant u_{f2}$ are periodic and almost sinusoidal. In fact, they correspond to the elliptic orbits of the Newtonian theory for which the trace in the u, v plane is a parabola so that the corresponding trace in the u, w plane is a circle. As contrasted with the Newtonian theory, the relativistic theory gives an additional region $u(\phi) \geqslant u_{f3}$, where solutions exist.

Let us now study the effects of shifting vertically the surface $\Phi(\phi, u, v) = 0$ or, equivalently, the trace in the u, v plane. This corresponds to the parameter W assuming various values.

If this cubic curve is lowered, the $u(\phi)$ solutions as shown in Figure A4 retain their topological properties until the situation is reached where the roots u_{f1} and u_{f2} coincide, given a double root $u = u_{f1} = u_{f2} = u'_{f1}$. Here the whole family of solutions $u_{f1} \leqslant u(\phi) \leqslant u_{f2}$ has degenerated into a single line $u = u'_{f1}$ which is now an "isolated solution" and corresponds to the case of circular orbits. (Per-

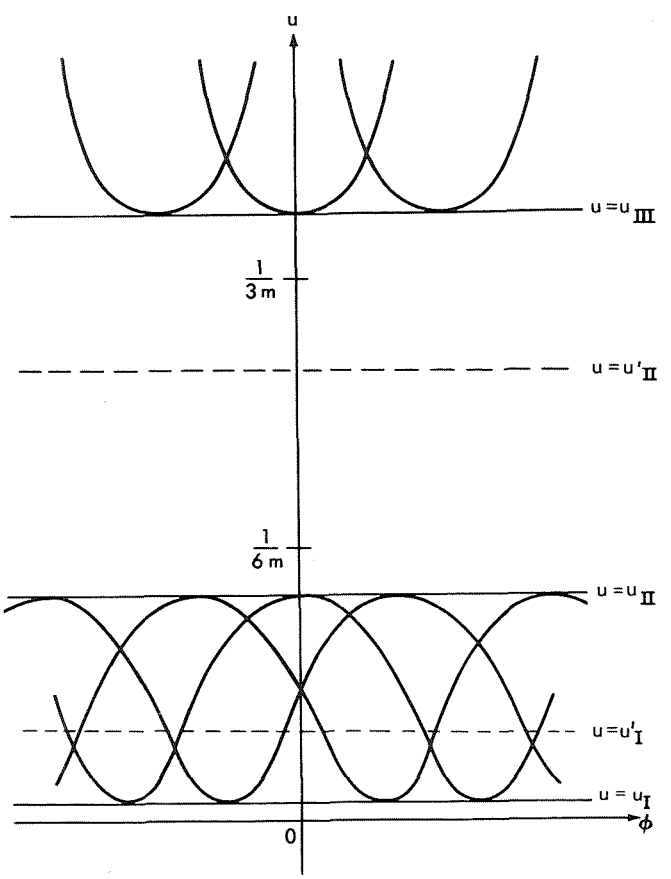

Figure A4—Solutions $u(\phi)$ corresponding to differential equation given by trace cubic curve of Figure A3.

haps it should be pointed out here that the three singular solutions $u = u_{f1}$, u_{f2}, and u_{f3} as shown in Figure A4 are not physically admissible as real orbits because they are three circles of different radii but with the same angular momentum h and also the same "energy" measure W. However, they are mathematically admissible because they are also solutions of the differential equation of motion.) On shifting the trace curve lower, we see that only the region $u(\phi) \geqslant u_{f3}$ continues to persist and nothing essentially different happens thereafter.

Now if the trace curve as shown in Figure A3 is raised, again there are no topological changes in the solutions $u(\phi)$ until either one of two situations occurs: Either the cubic curve at $u = 0$ becomes positive before the minimum point at $u = u'_{f2}$ does or vice versa; i.e., either $f(0) > f(u'_{f2})$ or vice versa. As shown later in this analysis, the criteria for these two cases are $1/4m < u'_{f2} \leqslant 1/3m$ and $1/6m \leqslant u'_{f2} < 1/4m$, respectively. However, for the present discussion, it does not matter which happens first, and only the former case will be considered in detail. When this situation is reached, there is no change in the mathematical properties of the solutions $u(\phi)$; they are still oscillatory in nature except that now they assume at various points the value $u(\phi) = 0$. Physically, however, it means that the particle starting at some initial radius greater than $1/u$ either begins to move inward, corresponding to one family of solutions, to some smaller radius and then flies off to infinity or, on the other hand, it begins to move outward to infinity, corresponding to the other family of solutions. In either case, the particle "barely" makes it to infinity.

Now, for the sake of convenience, an orbit is classified as elliptic-, parabolic-, or hyperbolic-like according to whether W is less than, equal to, or greater than zero. This criterion reduces to that for Newtonian orbits except that now the orbits are not true ellipses, parabolas, or hyperbolas. Also, the orbits shown in the upper region of Figure A4 will be referred to as "captured" orbits because they are bounded and eventually fall into the central attracting mass because $u(\phi) \to \infty$ as $\phi \to \pm\infty$.

If we continue to raise the trace cubic curve higher, no essential changes occur in the orbits except that they become hyperbolic-like. Eventually the situation is reached in which the roots u_{f2} and u_{f3} coincide, thus giving a double root $u = u_{f2} = u_{f3} = u'_{f2}$. The traces on the u, v plane and the u, w plane now appear as shown in Figure A5.

If the variable η is defined as

$$\eta = u - u'_{f2} , \tag{A11}$$

then it may be verified that Equation A1 can also be written as

$$\left(\frac{du}{d\phi}\right)^2 = a_2\eta^2 + a_3\eta^3 , \tag{A12}$$

where

$$a_2 = 12mu'_{f2} - 2 \tag{A13}$$

$$a_3 = 12m . \tag{A14}$$

Because $h^2 > 12m^2$ for the type of trace cubic curve being considered (see Figure A2c), from Equations A6 and A13 it follows that we have $a_2 > 0$.

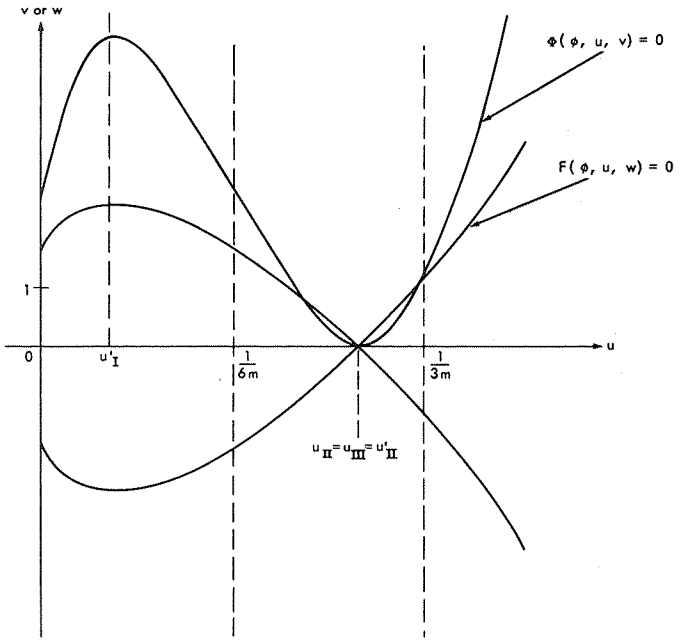

Figure A5—Trace cubic curve of class c with $W > 0$ and $1/4m < u'_{II} < 1/3m$.

In a small neighborhood of the line $u = u'_{f2}$ in the ϕ, u plane,

$$\left(\frac{du}{d\phi}\right)^2 = a_2\eta^2 \tag{A15a}$$

or

$$\left(\frac{d\eta}{d\phi}\right)^2 = a_2\eta^2 \tag{A15b}$$

from which the whole family of solutions is given by

$$\eta = C\exp\left(\pm\sqrt{a_2}\phi\right) \tag{A16a}$$

or

$$u = u'_{f2} + C\exp\left(\pm\sqrt{a_2}\phi\right). \tag{A16b}$$

In other words, instead of having the regular type of envelope at $u = u'_{f2}$, there is an "asymptotic" envelope and the family of solutions $u(\phi)$ is shown as sketched in Figure A6. For completeness of discussion, if $h^2 = 12m^2$, then $a_2 = 0$ and Equation A12 becomes

$$\left(\frac{du}{d\phi}\right)^2 = a_3\eta^3\ , \tag{A17}$$

from which is obtained

$$u = u'_{f2} + 4\left(C \pm \sqrt{a_3}\ \phi\right)^{-2}\ , \tag{A18}$$

thus giving solutions that are essentially the same in nature as those sketched in Figure A6.

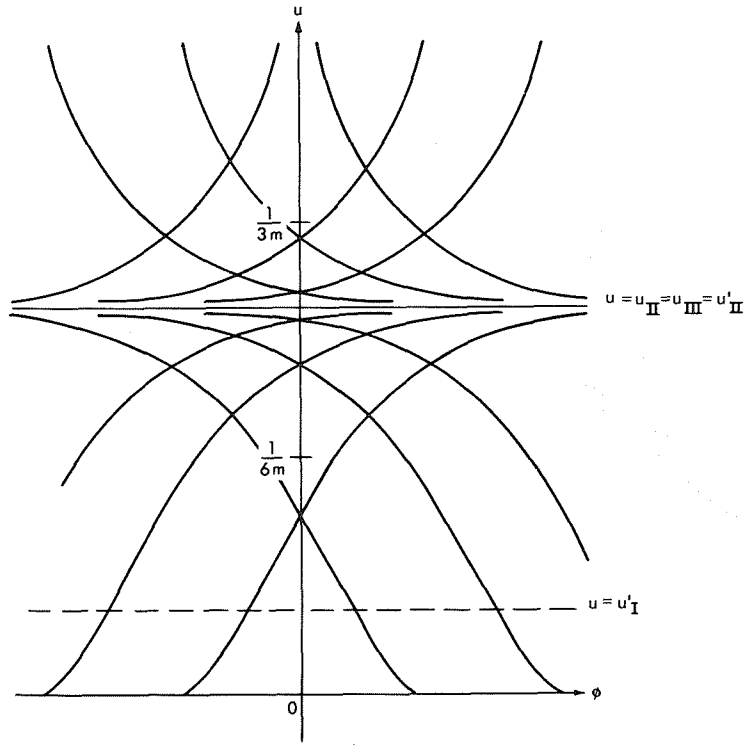

Figure A6—Solutions $u(\phi)$ corresponding to differential equation given by trace cubic curve of Figure A5.

Corresponding to the two solutions passing through a given point in the ϕ, u plane, from Figure A6 is seen that a test particle, starting at some initial radius greater than $1/u'_{f2}$, would either spiral in toward a circle of radius $1/u'_{f2}$ or would fly off to infinity. Similarly, if it is initially inside that circle it would either spiral out toward it or would fall into the center of the attracting mass m. The circle of radius $1/u'_{f2}$ in this case is a physically admissible orbit and any particle starting to move on it will continue to do so. However, this circular orbit is unstable with regard to any small perturbation in the sense that any outward disturbance would send the particle off to infinity whereas any inward one would send it into the center of the attracting mass. In contrast, the circular orbits previously discussed with radius $1/u'_{f1}$ are stable because any perturbation, inward or outward, would result in an elliptic-like orbit close to the unperturbed circular one.

Considering now the case in which the minimum point of the trace cubic curve becomes positive before the point at $u = 0$ does (i.e., $f(u'_{f2}) > f(0)$), it is seen that there are essentially no differences from the previous case as illustrated in Figures A5 and A6 except that now the orbits are bounded instead of unbounded, as shown in Figures A7 and A8.

Summarizing the more important results obtained up to this point, the conditions $0 \leqslant u'_{f1} \leqslant 1/6m$ and $1/6m \leqslant u'_{f2} \leqslant 1/3m$ have been established and, from the nature of the solutions illustrated in Figures A4, A6, and A8, it is seen that circular orbits with radius $6m < r < \infty$ are always stable whereas those with radius $3m \leqslant r \leqslant 6m$ are always unstable with regard to perturbations. Moreover, for $4m < r \leqslant 6m$ the outward perturbed orbits are bounded whereas for $3m \leqslant r \leqslant 4m$ they are unbounded;

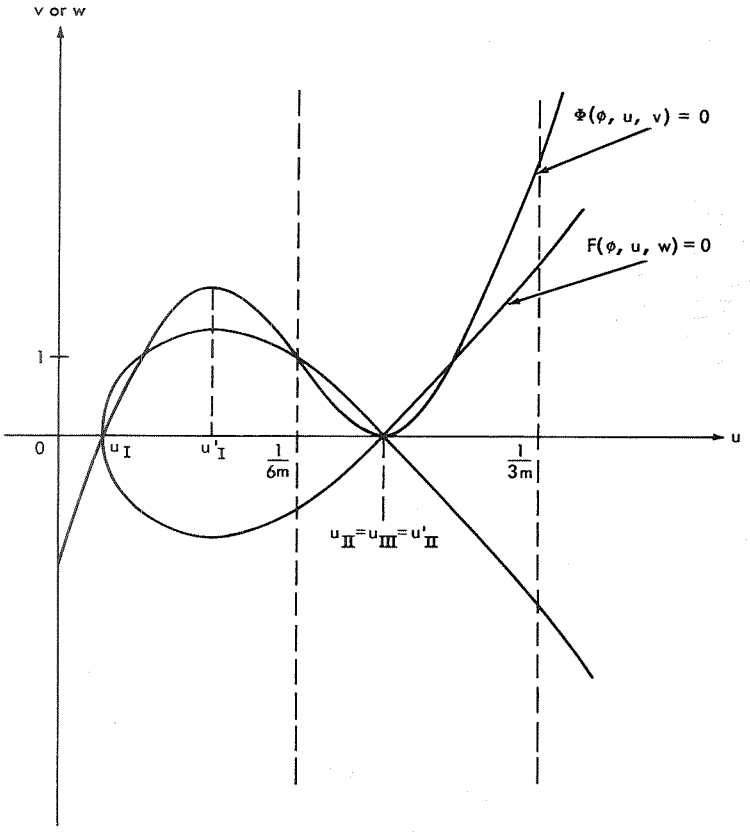

Figure A7—Trace cubic curve of class c with $W < 0$ and $1/6m < u'_{II} < 1/4m$.

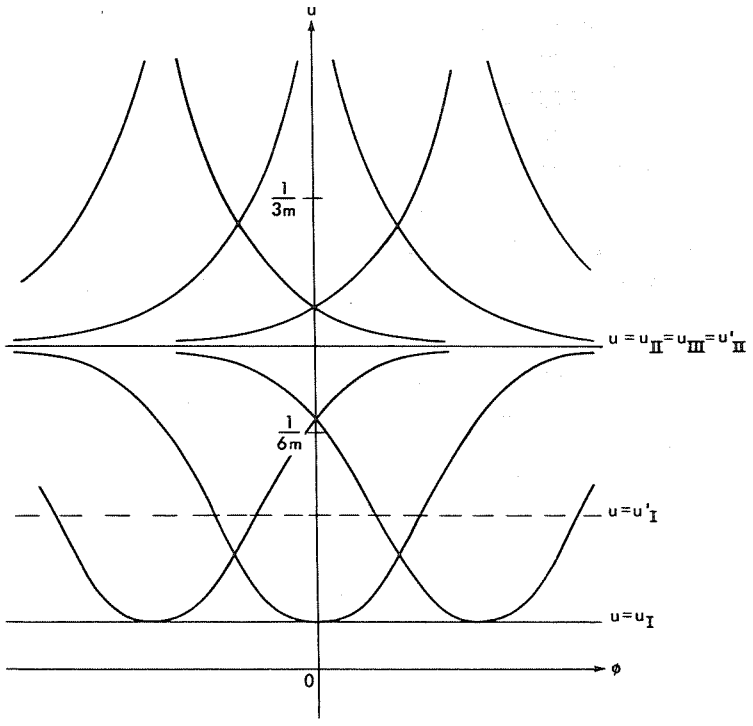

Figure A8—Solutions $u(\phi)$ corresponding to differential equation given by trace cubic curve of Figure A7.

in both cases the inward perturbed orbits eventually fall into the central attracting mass m. The main result is that no circular orbit can exist with a radius $r < 3m$. It has also been established that, because $1/6m \leqslant u'_{f2} < 1/4m$ corresponds to the case of $f(0) < f(u'_{f2})$, all the elliptic-like orbits must have a perihelion not less than $4m$. (See Figure A7.) Similarly, because $1/4m < u'_{f2} \leqslant 1/3m$ corresponds to the case of $f(0) > f(u'_{f2})$, therefore all hyperbolic-like orbits must have a perihelion not less than $3m$. (See Figure A5.) Also, the minimum perihelion for a parabolic-like orbit is $4m$.

If both the trace cubic curves as shown in Figures A5 and A7 are raised, then the two corresponding families of solutions $u(\phi)$ are obtained as shown in Figures A9 and A10. On further raising the trace cubic curve in Figure A7 so that it is everywhere positive for $u \geqslant 0$, then the family of solutions in Figure A10 will look essentially like that in Figure A9. No further changes occur in either of these two cases on continued vertical displacement of this trace curve.

The orbits in the lower region of Figure A6 ($W > 0$) are referred to as "hyperbolic limit circles" and the corresponding ones in Figure A8 ($W < 0$) as "elliptic limit circles." The orbits in the upper region in these two diagrams are called "limit-circle spirals." For the case of $W = 0$ in Figure A6 or A8, orbits occur in the lower region which are referred to as "parabolic limit circles." Finally, those in Figures A9 and A10 are called "hyperbolic spirals" and "elliptic spirals," respectively. As contrasted with the mathematical representation of these various types of orbits in the ϕ, u plane, Figure A11 illustrates the physical appearance of these orbits. In this diagram, the name given to describe each orbit attempts to illustrate its properties at r_{max} and r_{min}. Thus, elliptic spirals and captured orbits are classified as of the same type.

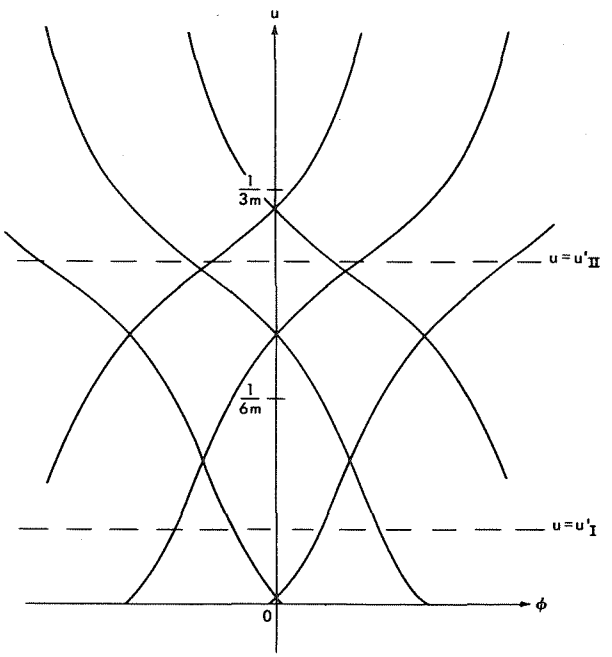

Figure A9—Solutions $u(\phi)$ corresponding to differential equation given by trace cubic curve of Figure A5 with a larger positive value of W.

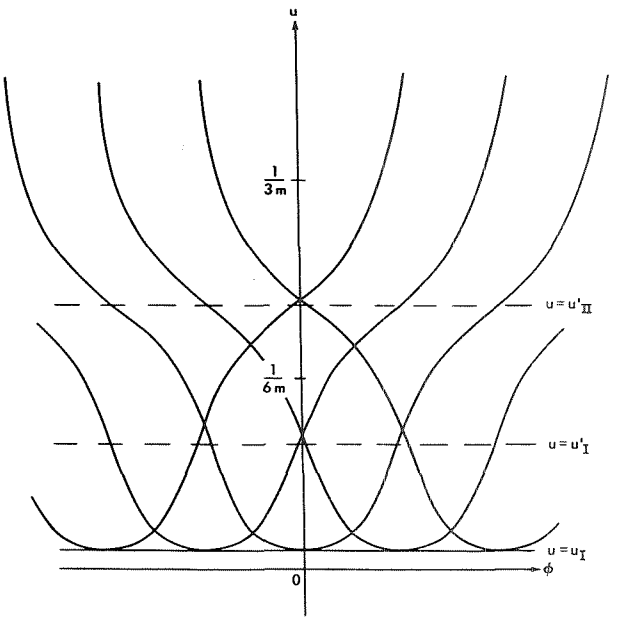

Figure A10—Solutions $u(\phi)$ corresponding to differential equation given by trace cubic curve of Figure A7 with a less-negative value of W.

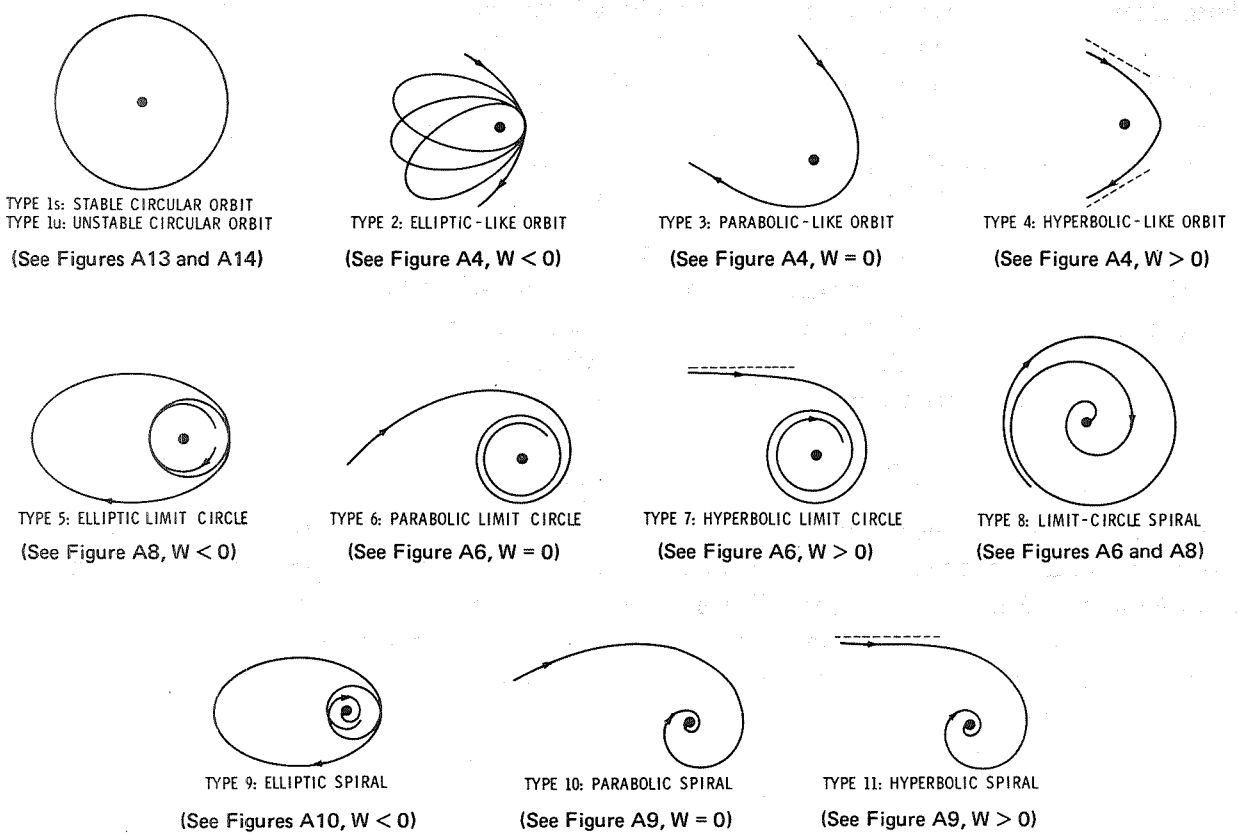

Figure A11—Physical appearance of various types of orbits.

Although the trace curve in the u, v plane as shown in Figure A2c has been discussed specifically, the cases as shown in Figures A2b and A2d in the limits of $u'_{f1} = u'_{f2} = 1/6m$ and $u'_{f2} = 1/3m$, respectively, have actually also been covered. The remaining case as shown in Figure A2a is virtually the same as that of Figure A2b as far as the family of solutions $u(\phi)$ in the ϕ, u plane is concerned.

The next step is to show that $u'_{f2} = 1/4m$ is the line of demarcation for the two cases described earlier; i.e., whether $f(0) > f(u'_{f2})$ or vice versa. To do this, consider the following theorem:

For a general cubic curve of the form

$$y = ax^3 + bx^2 + cx + d\ ,$$

let $x = \bar{x}$ be the axis of symmetry of the cubic curve, let x_0 be the value of x corresponding to either the local maximum or the minimum value of y, and let $\tilde{x}_0$ be the value of x such that

$$y(\tilde{x}_0) = y(x_0)$$

for $\tilde{x}_0 \neq x_0$. Then the following relationship is always true:

$$2(x_0 - \bar{x}) = \bar{x} - \tilde{x}_0\ .$$

Accepting this theorem and returning to the problem, it can be seen that because the trace cubic

curve always has $u = 1/6m$ as its axis of symmetry, the following relations result: if

$$u'_{f2} = \frac{1}{4m} ,$$

$$\frac{1}{4m} < u'_{f2} \leqslant \frac{1}{3m} ,$$

$$\frac{1}{6m} \leqslant u'_{f2} \leqslant \frac{1}{4m} ,$$

then, respectively,

$$f(0) = f(u'_{f2}) ,$$

$$f(0) > f(u'_{f2}) ,$$

$$f(0) < f(u'_{f2}) ,$$

as shown in Figure A12.

The relationship between the radius and the angular momentum (per unit mass) for circular orbits is determined next. From the preceding discussion it is noted that circular orbits, whether stable or unstable, correspond to the situation in which there is a double root in the trace cubic curve in the u, v plane; i.e., $f(u_f) = 0$ and $f'(u_f) = 0$. For a specific value of angular momentum, these double roots are given by Equation A6. Denoting the inverse radius of a circular orbit by u_c, the following relationship is obtained between the radius ($r_c = 1/u_c$) of a given circular orbit around a gravitating mass m and the angular momentum per unit mass h which the particle must have to remain at that radius:

$$u_c = \frac{1}{6m}\left(1 \pm \sqrt{1 - \frac{12m^2}{h^2}}\right) . \qquad \text{(A19)}$$

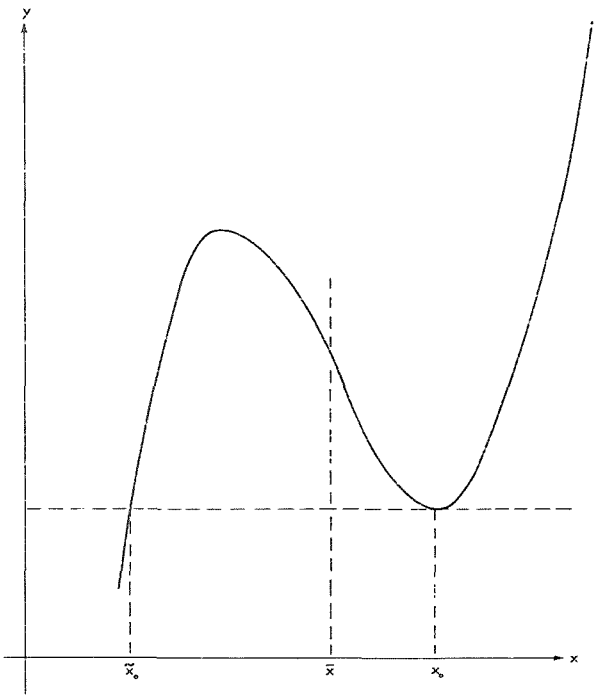

Figure A12—The general cubic curve illustrating the relation $\bar{x} - \bar{x}_0 = 2(x_0 - \bar{x})$.

It follows that for a given angular momentum, there exist two possible circular orbits; in Equation A19, the plus sign is associated with unstable circular orbits and the minus sign with stable circular orbits. In either case, it follows from this equation that circular orbits can only exist if the following inequality is satisfied:

$$V \equiv 1 - \frac{12m^2}{h^2} \geqslant 0 . \qquad \text{(A20)}$$

In Equation A19 the larger root corresponds to the family of unstable orbits as shown in Figure A13 whereas the small root corresponds to the family of stable orbits as shown in Figure A14.

Next, the relationship between the radius and the "energy" W_c for circular orbits is obtained from Equation A3:

$$W_c = -h^2 \left(2mu_c^3 - u_c^2 + \frac{2m}{h^2} u_c \right) . \tag{A21}$$

Substitution of u_c from Equation A19 yields

$$S \equiv W_{c1} = -\frac{1}{3}(1 - \alpha) + \frac{h^2}{108m^2}(\alpha^3 - 3\alpha + 2) \tag{A22}$$

for $0 \leqslant u_c \leqslant 1/6m$, and

$$U \equiv W_{c2} = -\frac{1}{3}(1 + \alpha) - \frac{h^2}{108m^2}(\alpha^3 - 3\alpha - 2) \tag{A23}$$

for $1/6m \leqslant u_c \leqslant 1/3m$, where

$$\alpha \equiv \sqrt{V} = \sqrt{1 - \frac{12m^2}{h^2}} \tag{A24}$$

From Equations A22 and A23 it is observed that the continuity result $S = U$ holds at $u_c = 1/6m$ (i.e., $\alpha = 0$) as expected.

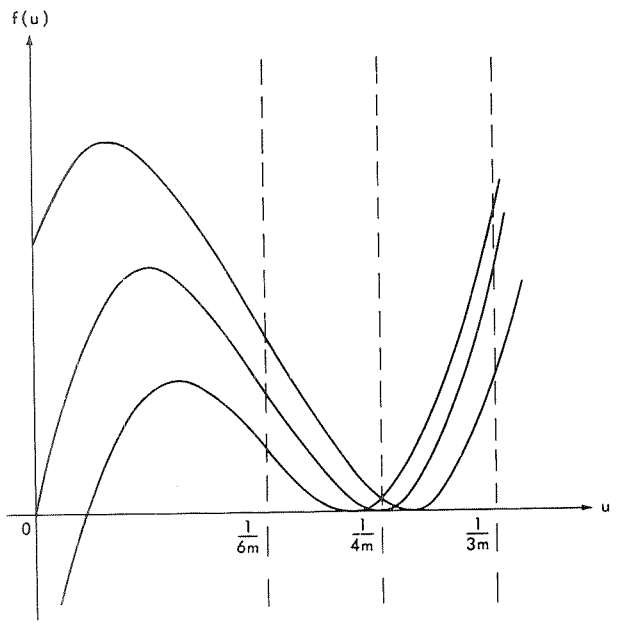

Figure A13—Criterion for unstable circular orbits, $3m \leqslant r \leqslant 6m$.

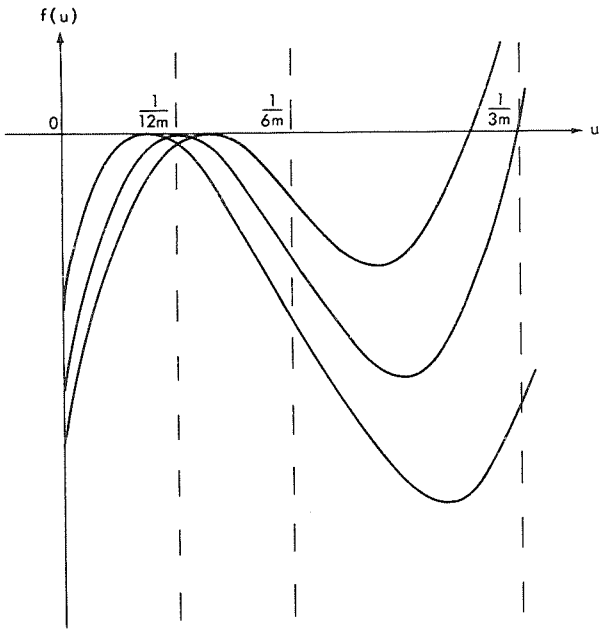

Figure A14—Criterion for stable circular orbits, $6m < r < \infty$.

Introducing, for convenience, the variable ξ defined by

$$\xi = \frac{h^2}{m^2} , \tag{A25}$$

the following asymptotic representations for S and U when $\xi \to \infty$ are obtained:

$$S = -\frac{1}{\xi} + 0\left(\frac{1}{\xi^2}\right) \tag{A26}$$

$$U = \frac{1}{27}\xi - \frac{2}{3} + 0\left(\frac{1}{\xi}\right) . \tag{A27}$$

The complete qualitative nature of the solutions of Equation A1 for all physically admissible ranges of the two parameters h and W has been studied. It is to be noted that the physically admissible ranges of h and W are $0 \leqslant h^2 < \infty$ and $-1 \leqslant W < \infty$, the latter condition resulting from the following equations:

$$\left(1 - \frac{2m}{r}\right)\frac{dt}{ds} = C \tag{A28}$$

$$W \equiv e^2 - 1 . \tag{A29}$$

All the results are represented in the master diagram shown in Figure A15, which gives the topological genera of the orbits corresponding to a given set of values of these two parameters. This diagram is to be used in conjunction with Table A1 and Figure A11 for determining the physical appearance of admissible orbits corresponding to a given set (h, W) in Equation A1.

Characteristics of the cubic curve $f(u)$ in various regions of the master diagram (Figure A15) are illustrated in Figure A16 and tabulated in Table A2.

From the Newtonian theory, the following relationships between the radius ($r_c = 1/u_c$) and the angular momentum per unit mass h and the energy per unit mass E hold for circular orbits:

$$h^2 = \frac{Gm}{u_c} \tag{A30}$$

$$2E_c = -\frac{G^2 m^2}{h^2} , \tag{A31}$$

so that the corresponding, but much less complicated, master diagram appears as in Figure A17. Because $W \to 2E$ in the Newtonian limit, the quantity $2E$ is used as the variable on the vertical axis. Also, the gravitational constant G, which is set to unity in the relativistic diagram, now makes its appearance in the variable on the horizontal axis.

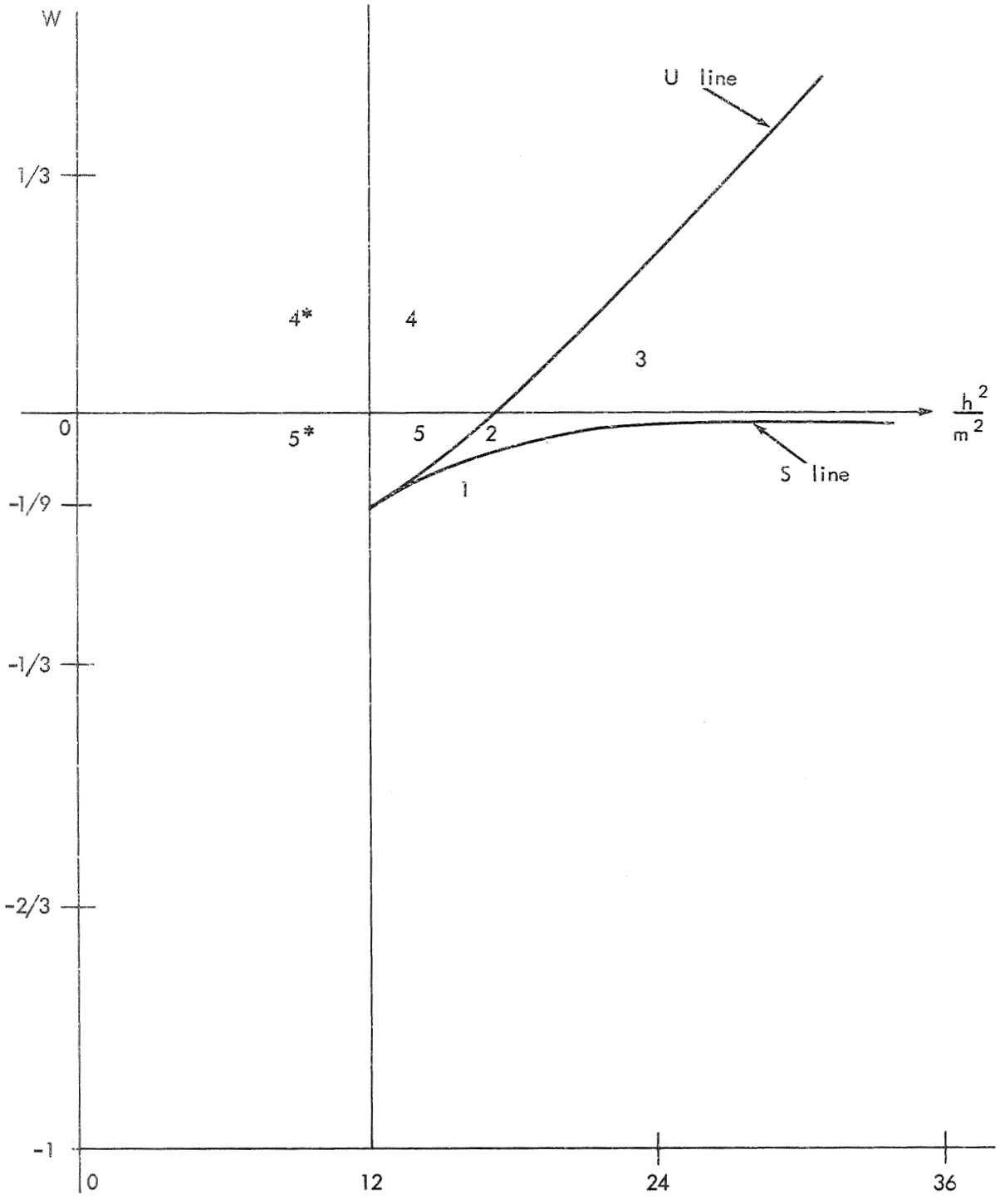

Figure A15—The master diagram for relativistic orbits in terms of W and h, both per unit rest mass of test particle.

Table A1—Complete classification of the orbits of a test particle in the equatorial plane of the Schwarzschild gravitational field.

Region of Master Diagram	Admissible Orbit Nos.
1	9
2	2, 9
3	4, 9
4	11
4*	11
5	9
5*	9
1-2 (S line)	1S, 9
2-5 (U line)	1U, 5, 8
3-4 (U line)	1U, 7, 8
2-3 ($W = 0$ line)	3, 9
4-5 ($W = 0$ line)	10
4*-5* ($W = 0$ line)	10
Intersection of 2, 3, 4, 5	6, 8

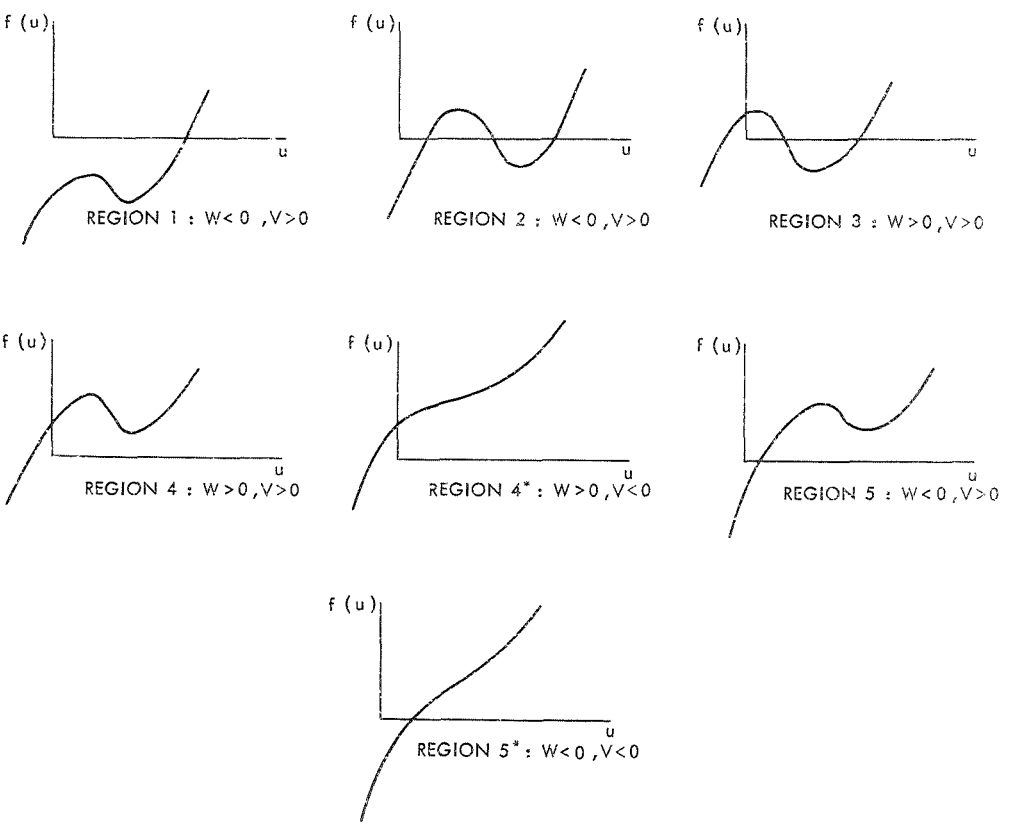

Figure A16—Characteristics of the $f(u)$ curve in various regions.

Table A2–Characteristics of the $f(u)$ curve for various regions of the master diagram.

Region	$f(u'_{f1})$	$f(u'_{f2})$	V	W	u_s
1	<0	<0	>0	<0	>0
2	>0	<0	>0	<0	>0
3	>0	<0	>0	>0	>0
4	>0	>0	>0	>0	>0
4*	([a])	([a])	<0	>0	>0
5	>0	>0	>0	<0	>0
5*	([a])	([a])	<0	<0	>0

[a] u'_{f1} and u'_{f2} do not exist for $V < 0$.

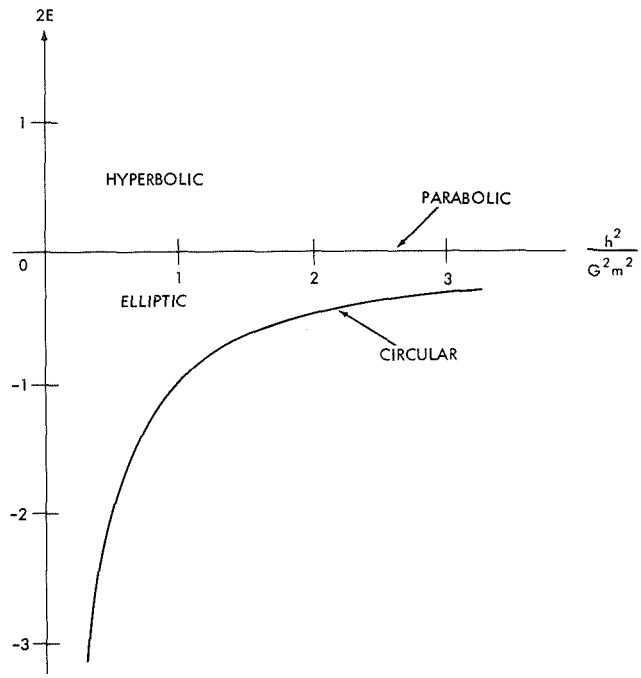

Figure A17–The master diagram for Newtonian orbits in terms of E and h, both per unit mass of test particle.

CONCLUSIONS

From a comparison of the results obtained from these two theories, it is concluded that–

(1) The S curve is identical with the $2E_c$ curve for large values of the variable h^2/m^2.

(2) There is no lower limit to the quantity $2E$ for the Newtonian orbits; but one does exist for for the energy measure W for the case of relativistic orbits.

(3) For a given set of $(h, 2E)$ there exists only one type of Newtonian orbit; for a given set of (h, W) there can exist one, two, or even three types of relativistic orbits.

(4) It is well known that the shape of Newtonian orbits is completely specified by only one parameter, the eccentricity ϵ, which is defined by the equation

$$\epsilon = \sqrt{1 + \frac{2Eh^2}{G^2 m^2}}$$

or

$$2E = (\epsilon^2 - 1)\frac{G^2 m^2}{h^2} .$$

However, in contrast, relativistic orbits of a given type cannot be specified by just one parameter.

(5) The relativistic orbits experience no singular behavior at $r = 2m$. This is an indirect proof of the lack of any intrinsic geometrical singularity at the Schwarzschild radius.

(6) In Newtonian theory, circular orbits are possible for all radii. However, in relativity theory, no circular orbit can exist with a radius $r < 3m$. Moreover, circular orbits are stable if $6m < r < \infty$ and unstable if $3m \leqslant r \leqslant 6m$. Finally, if $3m \leqslant r\ 4m$, the outward perturbed orbits are unbounded; whereas if $4m \leqslant r \leqslant 6m$, they are bounded. In both cases, the inward perturbed orbits eventually fall into the central attracting mass.

(7) In relativity theory, elliptic-like and parabolic-like orbits must have a perihelion not less than $4m$ whereas hyperbolic-like orbits must have a perihelion not less than $3m$. However, no such limits exist for their Newtonian analogs.

REFERENCES

A1. Einstein, A.: "Erklärung der Perihelbewegung des Mercur aus der Allegemeinen Relativistätsteorie." *Preuss. Akad. Wiss. Sitz.*, p. 831, 1915.

A2. Einstein, A.: "Näherungsweise Integration der Feldgleichungen der Gravitation." *Preuss. Akad. Wiss. Sitz.*, p. 688, 1916.

A3. Droste, J.: "On the Field of a Single Center in Einstein's Theory of Gravitation." *Proc. Kon. Ned. Acad. Wetensch. Amsterdam* 17: 998, 1915.

A4. Droste, J.: "The Field of a Single Centre in Einstein's Theory of Gravitation, and the Motion of a Particle in That Field." *Proc. Kon. Ned. Akad. Wetensch. Amsterdam* 19: 197, 1917.

A5. de Sitter, W.: "On Einstein's Theory of Gravitation and Its Astronomical Consequences." *Mon. Notic. Roy. Astron. Soc.* 76: 699, 1916.

A6. de Sitter, W.: "Planetary Motion and the Motion of the Moon According to Einstein's Theory." *Proc. Kon. Ned. Akad. Wetensch. Amsterdam* 19: 367, 1917.

A7. Greenhill, G.: "Newton-Einstein Planetary Orbit." *Phil. Mag.* 41: 143, 1921.

A8. Forsyth, A. R.: "Note on the Central Differential Equation in the Relativity Theory of Gravitation." *Proc. Roy. Soc. London Ser. A* 97: 145, 1920.

A9. Morton, W. B.: "The Forms of Planetary Orbits in the Theory of Relativity." *Phil. Mag.* 42: 511, 1921.

A10. Hagihara, Y.: "Theory of the Relativistic Trajectories in a Gravitational Field of Schwarzschild." *Jap. J. Astron. Geophys.* 8: 67, 1931.

A11. Kaplan, S. A.: "On Circular Orbits in Einstein's Theory of Gravitation." *Zh. Eksp. Teor. Fiz.* 19: 249, 1949.

A12. Darwin, C.: "The Gravity Field of a Particle." *Proc. Roy. Soc. Ser. A* 249: 180, 1959.

A13. Darwin, C.: "The Gravity Field of a Particle II." *Proc. Roy. Soc. Ser. A* 263: 39, 1962.

A14. Metzner, A. W.: "Observable Properties of Large Relativistic Masses." *J. Math. Phys.* 4: 1194, 1963.

A15. Galkin, S. L.: "The Motion of Particles in a Centrally-Symmetrical Static Field in the General Theory of Relativity." *Abstr. Sov. Gravita. Conf. 1st* (Moscow), 1961.

A16. Arzeliès, H.: "Trajectories Dans le Champ Exterieur de Schwarzschild (Cas de Particules)." Ch. 7 of *Relativité Généralisée Gravitation,* Gauthier-Villars & Cie. (Paris), 1961.

A17. Ince, E. J.: *Ordinary Differential Equations.* Dover Pub., Inc., 1956.

Appendix B

DETAILED DERIVATION OF RELATIONSHIPS USED IN ANALYSIS OF EQUATORIAL ORBITS

PROOF THAT $B(u'_B) > 0$ IN REGION 6

The expression for $B(u)$ is given by Equation 45, which is

$$B(u) = \beta(h + ea)^2 u^3 - [h^2 + (1 - e^2)a^2]u^2 + \beta u + e^2 - 1 , \tag{45}$$

and the roots of $B'(u) = 0$ are given by Equation 142:

$$u'_{B1,B2} = u_s \left(1 \pm \sqrt{V}\right) , \tag{142}$$

where

$$u_s = \frac{h^2 + (1 - e^2)a^2}{3\beta(h + ea)^2} \tag{B1}$$

$$V \equiv 1 - \frac{3\beta^2 (h + ea)^2}{[h^2 + (1 - e^2)a^2]^2} = 1 - \frac{1}{3u_s^2 (h + ea)^2} . \tag{B2}$$

In region 6,

$$u_s < 0 , \tag{B3}$$

$$0 < V < 1 , \tag{B4}$$

$$e^2 - 1 > 0 . \tag{B5}$$

Substitution of Equations 142, B1, and B2 into Equation 45 leads to

$$B(u'_B) = 2\beta \left(1 \pm \sqrt{V}\right) u_s \left[\frac{1}{3} - (h + ea)^2 u_s^2\right] + \frac{1}{3}\beta u_s + (e^2 - 1) . \tag{B6}$$

From Equations B2 and B4 it follows that

$$\frac{1}{3} - (h + ea)^2 u_s^2 < 0 . \tag{B7}$$

Hence, from Equations B3, B4, and B7, it is seen that

$$2\beta\left(1 \pm \sqrt{V}\right)u_s\left[\frac{1}{3} - (h + ea)^2 u_s^2\right] > 0 . \tag{B8}$$

Next, consider the remaining group of terms in Equation B6. For convenience, the following definition is made:

$$F(e, h) \equiv \frac{\beta u_s}{3} + e^2 - 1 . \tag{B9}$$

If Equation B1 is substituted into this equation, then

$$F(e, h) = \frac{1}{9(h + ea)^2}\left\{h^2[9(e^2 - 1) + 1] + 18ae(e^2 - 1)h + 9a^2e^2(e^2 - 1) + (1 - e^2)a^2\right\} , \tag{B10}$$

which is quadratic in h whose discriminant d is given by

$$\begin{aligned} d &= [18ae(e^2 - 1)]^2 - 4[9(e^2 - 1) + 1][9a^2e^2(e^2 - 1) + (1 - e^2)a^2] \\ &= -32a^2(e^2 - 1) . \end{aligned} \tag{B11}$$

Because $e^2 - 1 > 0$ by Equation B5, then

$$d < 0 \tag{B12}$$

and so

$$B(u_B') \neq 0 . \tag{B13}$$

Next it is noted that

$$F(e, 0) = e^2 - 1 + \frac{1 - e^2}{9e^2} > 0 , \tag{B14}$$

so that, in view of Equation B12, it follows that

$$F(e, h) = e^2 - 1 + \frac{\beta u_s}{3} > 0 . \tag{B15}$$

Hence, from Equations B8 and B15,

$$B(u_B') > 0 \tag{B16}$$

in region 6.

PROOF THAT $A(u_E) = 0$ AND $D(u_E) = 0$ SIMULTANEOUSLY ARE IMPOSSIBLE

From the equation

$$D(u) = a^2u^2 - \beta u + 1 \tag{46}$$

and the identity $E(u_E) = 0$ or, equivalently,

$$u_E = \frac{h}{\beta(h + ea)} , \tag{206}$$

the following is obtained:

$$D(u_E) = a^2 u_E^2 - \beta u_E + 1$$

$$= \frac{a^2 h^2}{\beta^2 (h + ea)^2} - \frac{\beta h}{\beta (h + ea)} + 1$$

$$= \frac{1}{\beta^2 (h + ea)^2} (a^2 h^2 + a\beta^2 eh + a^2 \beta^2 e^2) . \quad \text{(B17)}$$

The equation

$$A(u) = h^2 + (1 - e^2) a^2 - \beta (h + ea)^2 u \quad \text{(48)}$$

and Equation 206 yield

$$A(u_E) = h^2 + (1 - e^2) a^2 - h(h + ea)$$

$$= a^2 - a^2 e^2 - hea . \quad \text{(B18)}$$

Given the equations

$$A(u_E) = a^2 - a^2 e^2 - hea$$

$$= 0 \quad \text{(B19)}$$

$$D(u_E) = \frac{1}{\beta^2 (h + ea)^2} (a^2 h^2 + a\beta^2 eh + a^2 \beta^2 e^2)$$

$$= 0 , \quad \text{(B20)}$$

then substitution of *hea* from Equation B19 into Equation B20 leads to

$$\frac{1}{\beta^2 (h + ea)^2} (a^2 h^2 + \beta^2 a^2) = 0 , \quad \text{(B21)}$$

which is impossible because $\beta \neq 0$ and $a \neq 0$.

PROOF THAT $A'(u_E) = 0$ IS IMPOSSIBLE

From the equation

$$A(u) = h^2 + (1 - e^2) a^2 - \beta (h + ea)^2 u , \quad \text{(48)}$$

it follows that

$$A'(u) = -\beta (h + ea)^2 \quad \text{(B22)}$$

for all u. From this equation and

$$u_E = \frac{h}{\beta (h + ea)} , \quad \text{(206)}$$

it is seen that

$$A'(u_E) \neq 0 \quad \text{(B23)}$$

for any finite u_E.

SOLUTION OF $D(u_D) = 0$, $D'(u_D) = 0$, $E(u_D) = 0$, AND $B''(u_D) = 0$

From Equations 45 to 47 and 190, the following equations are obtained:

$$D(u_D) = a^2 u_D^2 - \beta u_D + 1 = 0 , \tag{193}$$

$$D'(u_D) = 2a^2 u_D - \beta = 0 , \tag{B24}$$

$$E(u_D) = -\beta(h + ea)u_D + h = 0 , \tag{B25}$$

$$B''(u_D) = 6\beta(h + ea)^2 u_D - 2[h^2 + (1 - e^2)a^2] = 0 . \tag{B26}$$

Equations 193 and B24 indicate that u_D is a double root of $D(u) = 0$, so that

$$u_D^2 = \frac{1}{a^2}$$

or

$$u_D = \pm\frac{1}{a} . \tag{191d}$$

Equations B24 and 191d yield

$$\beta = \pm 2a \tag{191c}$$

$$\beta u_D = 2 . \tag{B27}$$

Hence, substitution of u_D and β from Equations 191d and 191c into Equation B25 leads to

$$h = -2ea . \tag{B28}$$

Then, from Equations B26 to B28, the following are obtained:

$$3\beta e^2 a^2 u_D - (3e^2 a^2 + a^2) = 0 ,$$

$$6e^2 a^2 - 3e^2 a^2 - a^2 = 0 ,$$

$$3e^2 - 1 = 0 ,$$

$$e = \pm\frac{1}{\sqrt{3}} . \tag{191a}$$

Consequently, Equation B28 then gives

$$h = \mp\frac{2}{\sqrt{3}} a . \tag{191b}$$

FACTORIZATION OF $B(u_E)$

From Equations 178, B17, and B18, the following definitions result:

$$B(u_E) = -\frac{1}{a^2} A(u_E) D(u_E) , \tag{B29}$$

$$D(u_E) = \frac{a^2}{\beta^2 (h + ea)^2} \left(h^2 + \frac{\beta^2 eh}{a} + \beta^2 e^2 \right) , \tag{B30}$$

$$A(u_E) = -a(eh + ae^2 - a) . \tag{B31}$$

Equation B30 can be written in the form

$$D(u_E) = \frac{a^2}{\beta^2 (h + ea)^2} \left[h^2 + ha\beta e \left(\frac{\beta}{a^2} \right) + a^2 \beta^2 e^2 \left(\frac{1}{a^2} \right) \right] . \tag{B32}$$

From the definition

$$a^2 u_D^2 - \beta u_D + 1 = 0 , \tag{B33}$$

the sum $(u_{D1} + u_{D2})$ and product $u_{D1} u_{D2}$ of the roots are

$$\left.\begin{aligned} u_{D1} + u_{D2} &= \frac{\beta}{a^2} \\ u_{D1} u_{D2} &= \frac{1}{a^2} . \end{aligned}\right\} \tag{B34}$$

From this, Equation B32 can be written as

$$\begin{aligned} D(u_E) &= \frac{a^2}{\beta^2 (h + ea)^2} [h^2 + ha\beta e(u_{D1} + u_{D2}) + a^2 \beta^2 e^2 u_{D1} u_{D2}] \\ &= \frac{a^2}{\beta^2 (h + ea)^2} (h + a\beta e u_{D1})(h + a\beta e u_{D2}) \\ &= \frac{a^2}{\beta^2 (h + ea)^2} \left(h + \frac{\beta e}{a u_{D2}} \right) \left(h + \frac{\beta e}{a u_{D1}} \right) . \end{aligned} \tag{B35}$$

Hence, it follows from Equations B29, B31, and B32 that $B(u_E)$ can be written as

$$B(u_E) = \frac{a}{\beta^2 (h + ea)^2} (eh - a + ae^2) \left(h + \frac{e\beta}{a u_{D1}} \right) \left(h + \frac{e\beta}{a u_{D2}} \right) . \tag{200}$$

Similarly, from Equations B29 to B31,

$$B(u_E) = \frac{ae^2}{\beta^2 (h + e)^2} (eh - a + ae^2) \left[\left(\frac{h}{e} \right)^2 + \frac{\beta^2}{a} \frac{h}{e} + \beta^2 \right] . \tag{199}$$

Appendix C

MASTER DIAGRAMS FOR $\beta = 2$ AND VALUES OF a RANGING FROM $a = 0$ TO $a = 100$

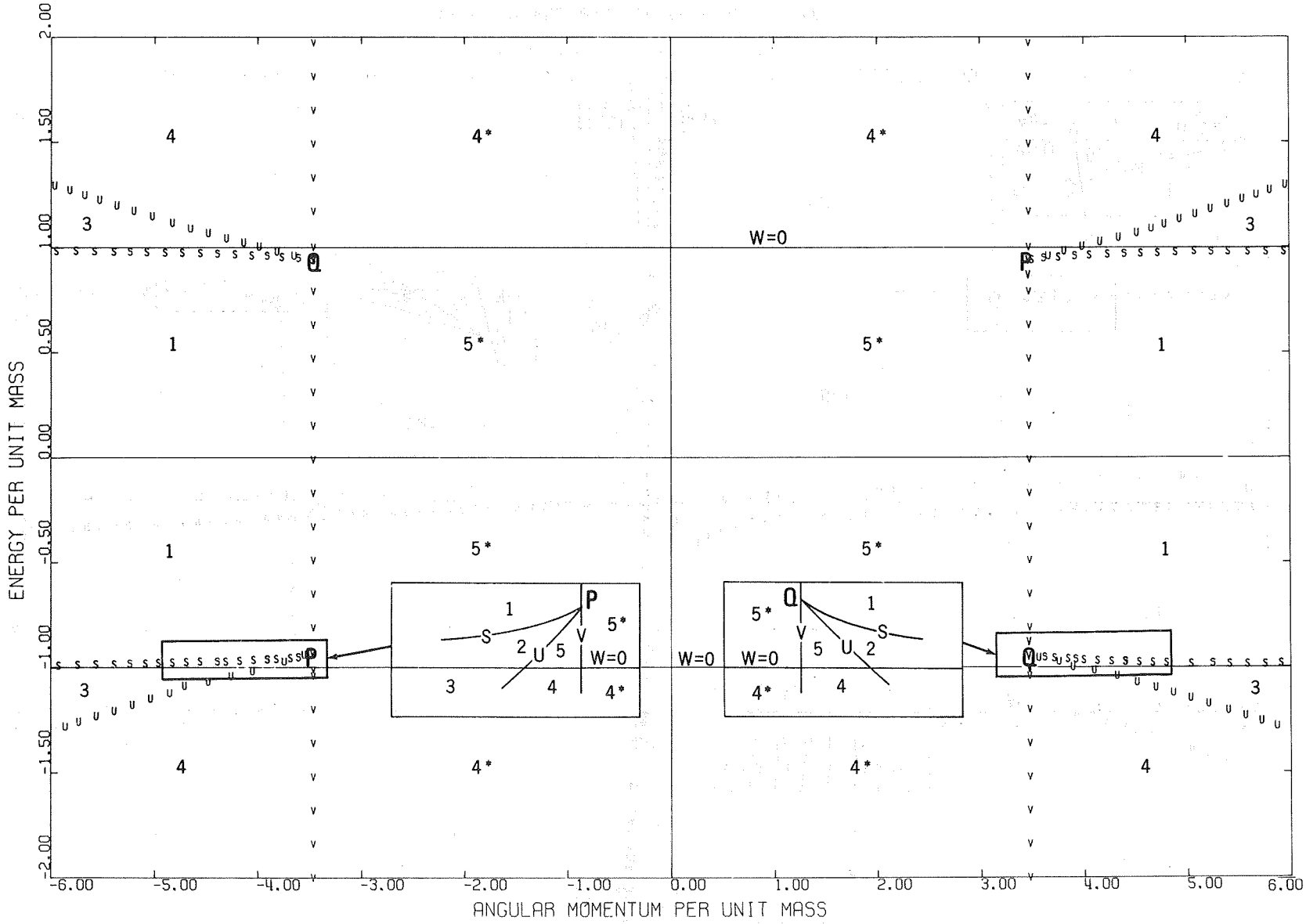

Figure C1—Master diagram for $a = 0.0$, $\beta = 2.0$.

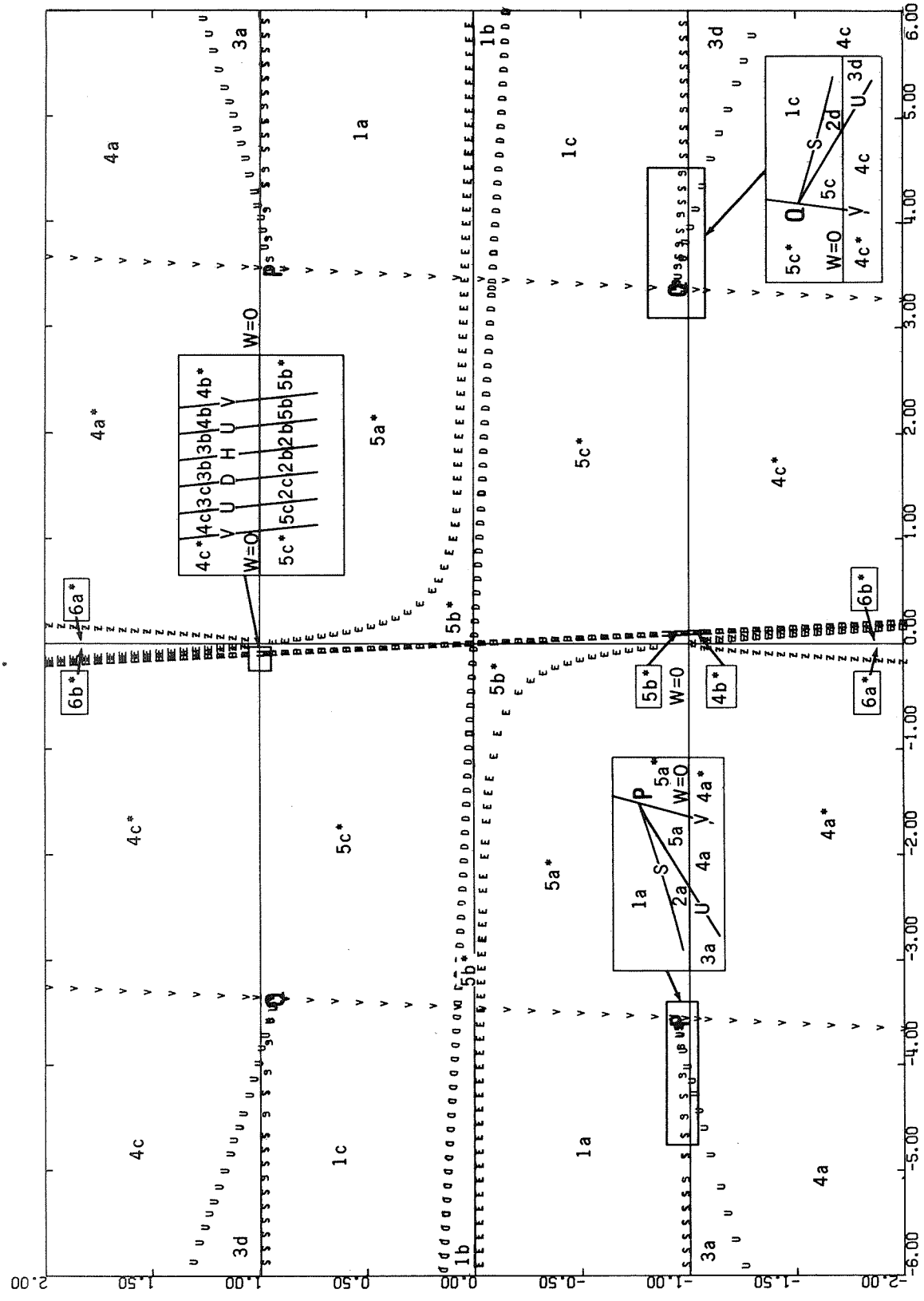

Figure C2—Master diagram for $a = 0.1, \beta = 2.0$.

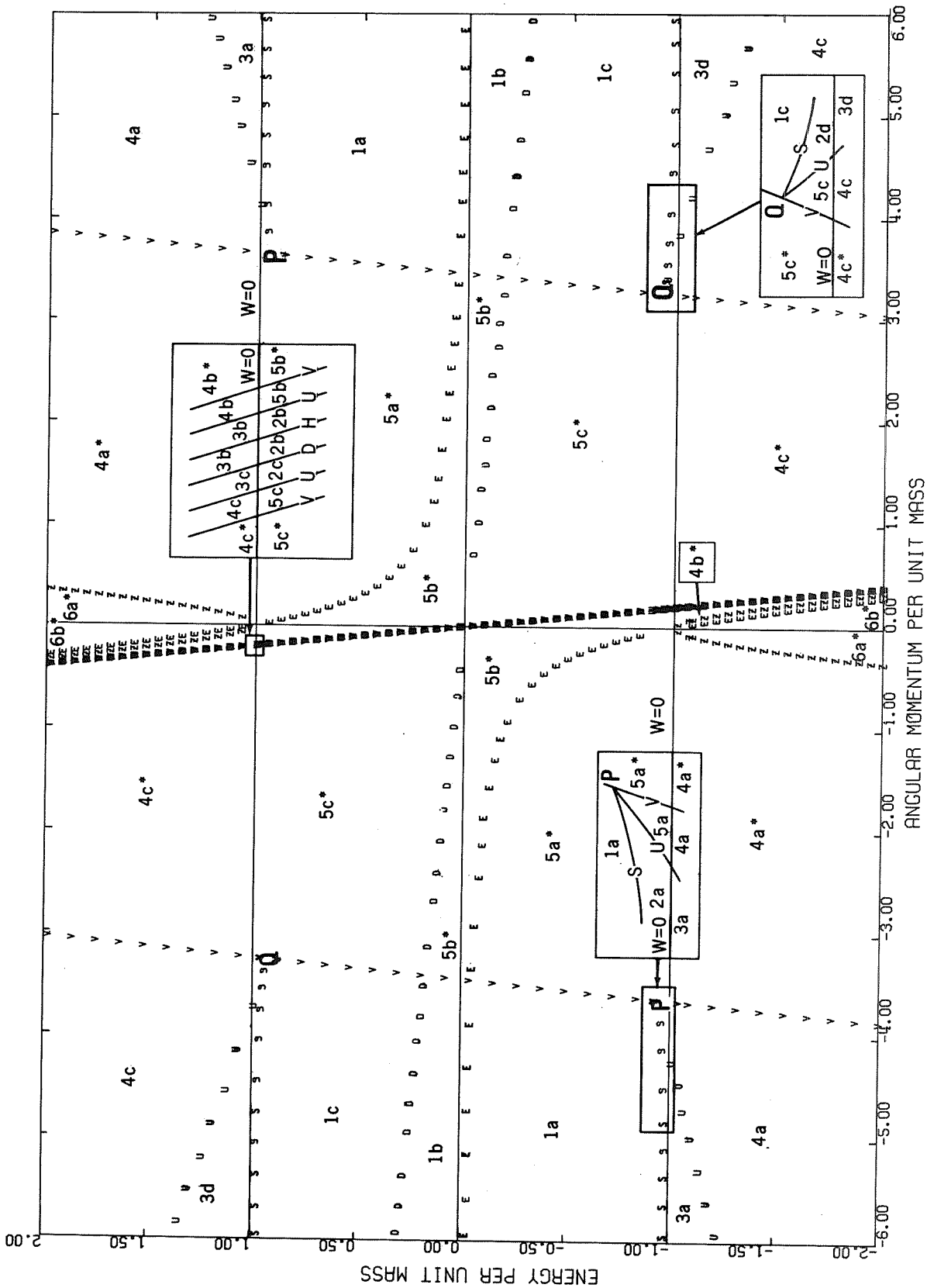

Figure C3—Master diagram for $a = 0.2$, $\beta = 2.0$.

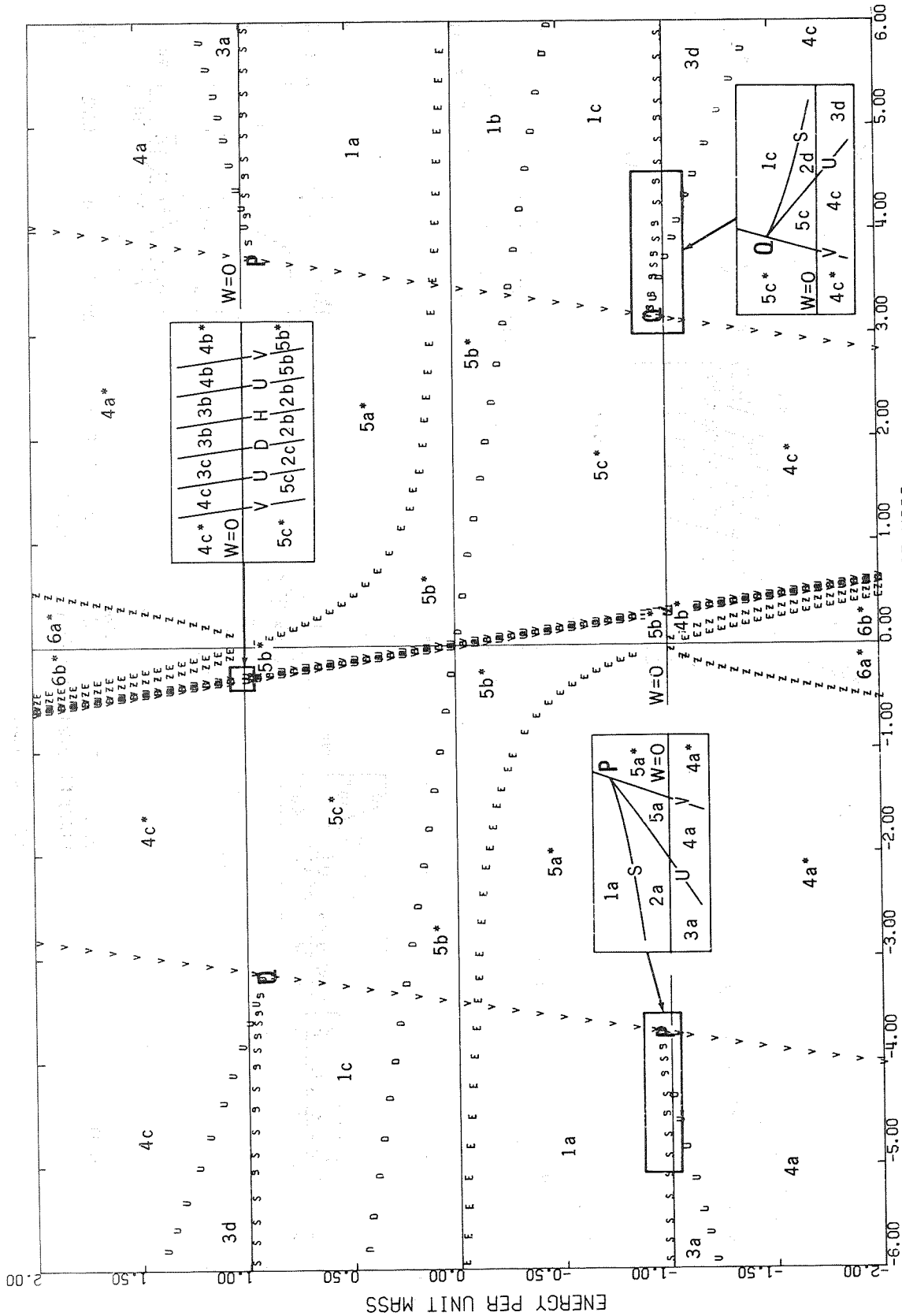

Figure C4--Master diagram for $a = 0.3, \beta = 2.0$.

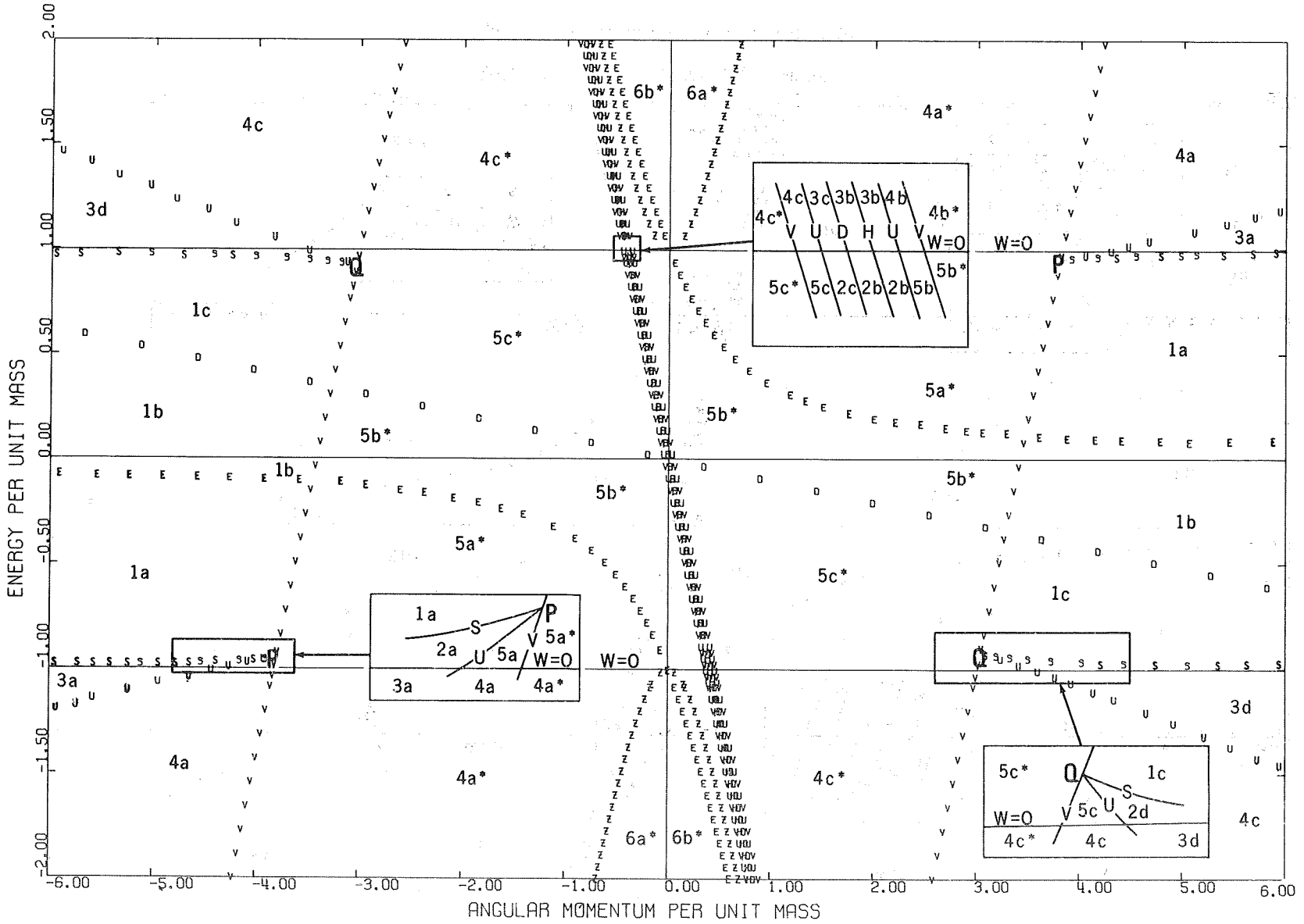

Figure C5—Master diagram for $a = 0.4$, $\beta = 2.0$.

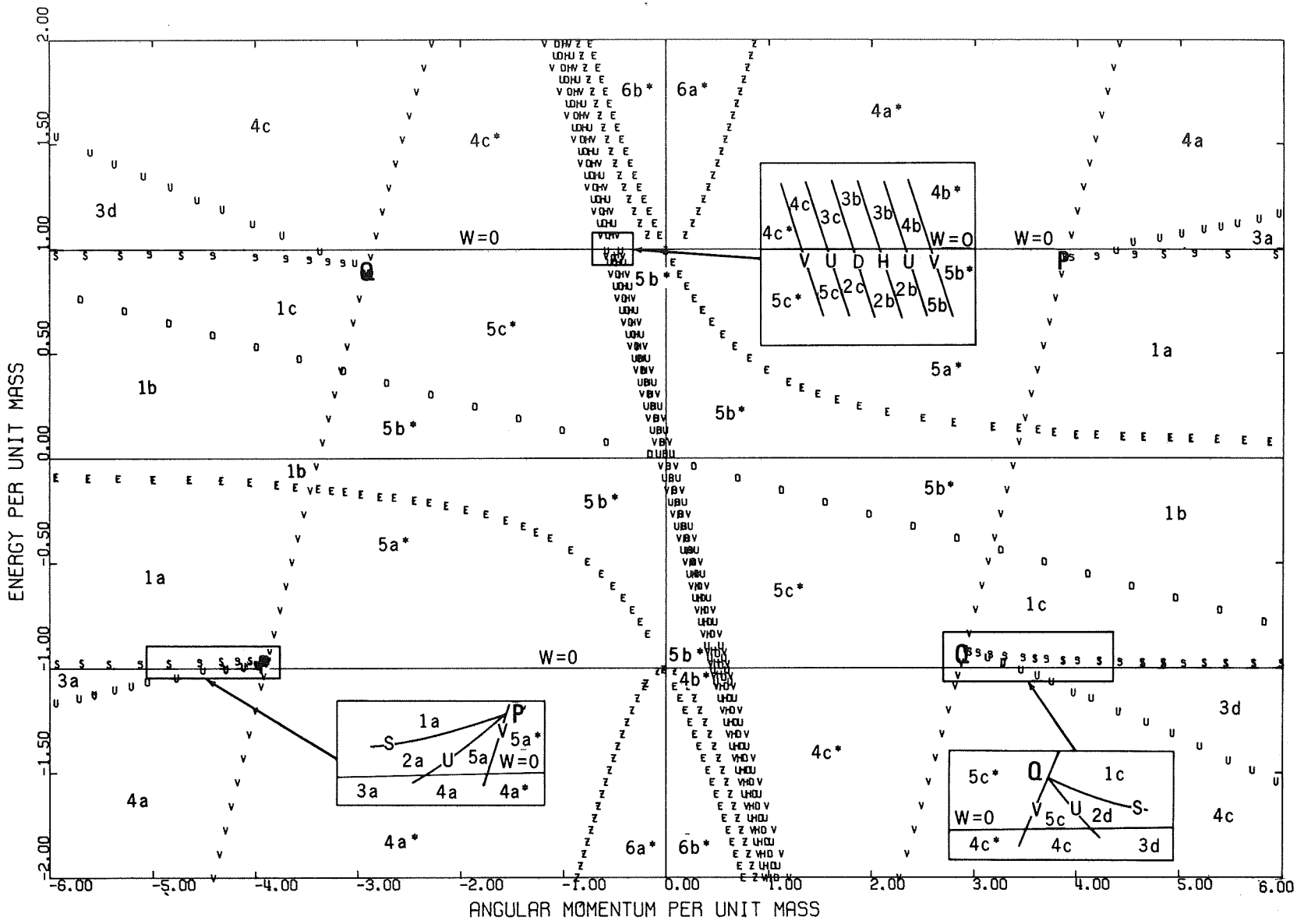

Figure C6—Master diagram for $a = 0.5$, $\beta = 2.0$.

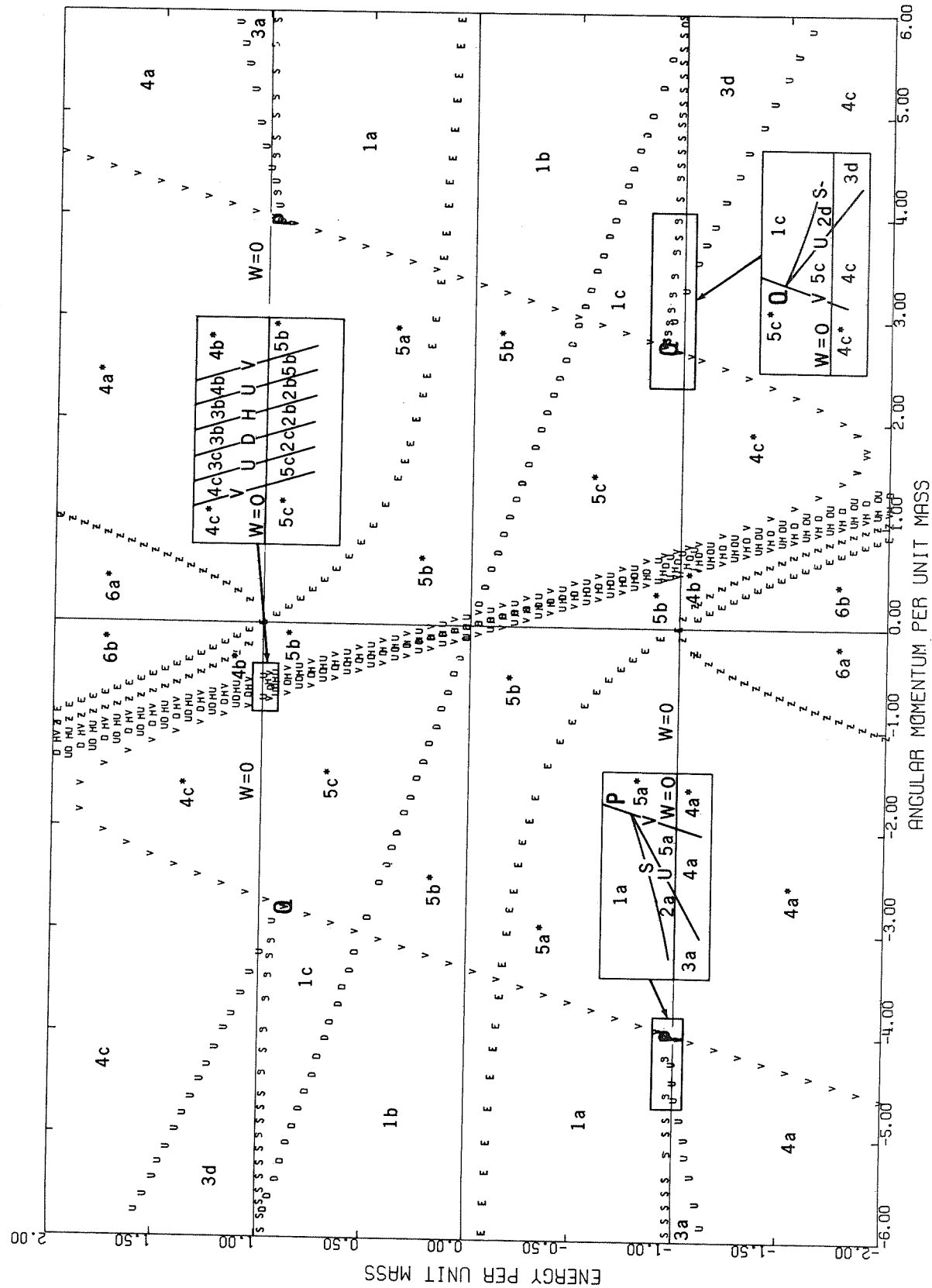

Figure C7—Master diagram for $a = 0.6, \beta = 2.0$.

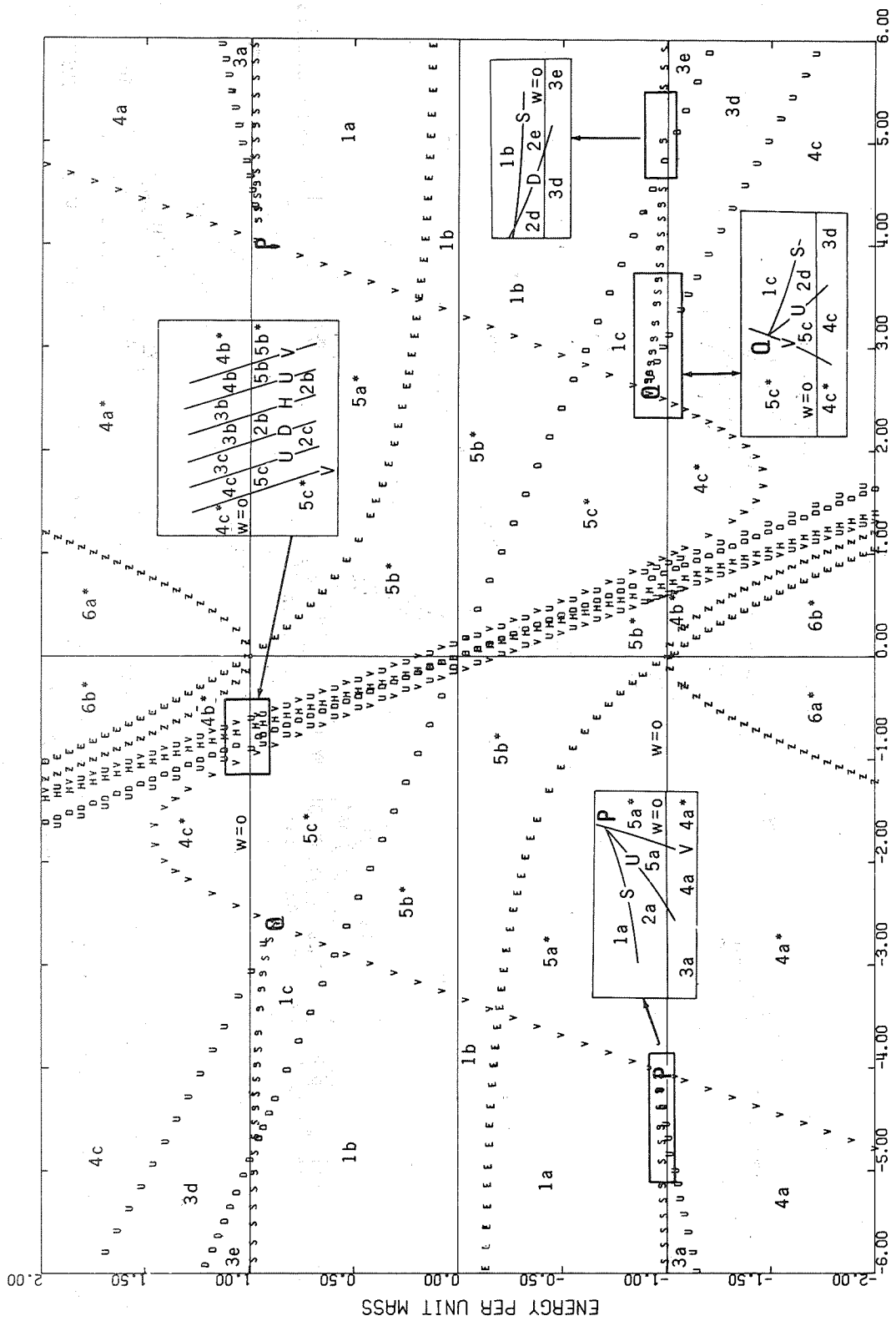

Figure C8–Master diagram for $a = 0.7$, $\beta = 2.0$.

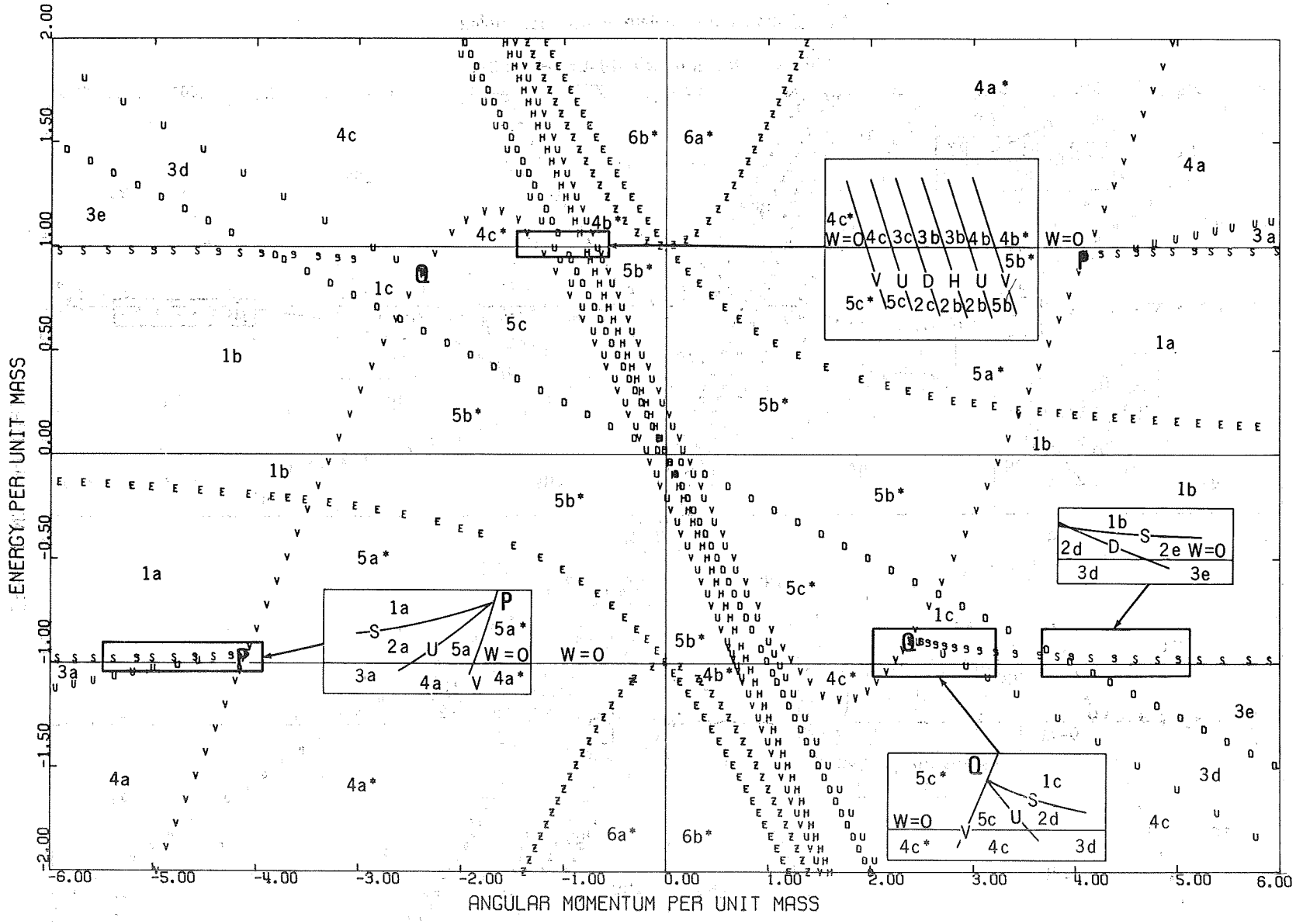

Figure C9—Master diagram for $a = 0.8$, $\beta = 2.0$.

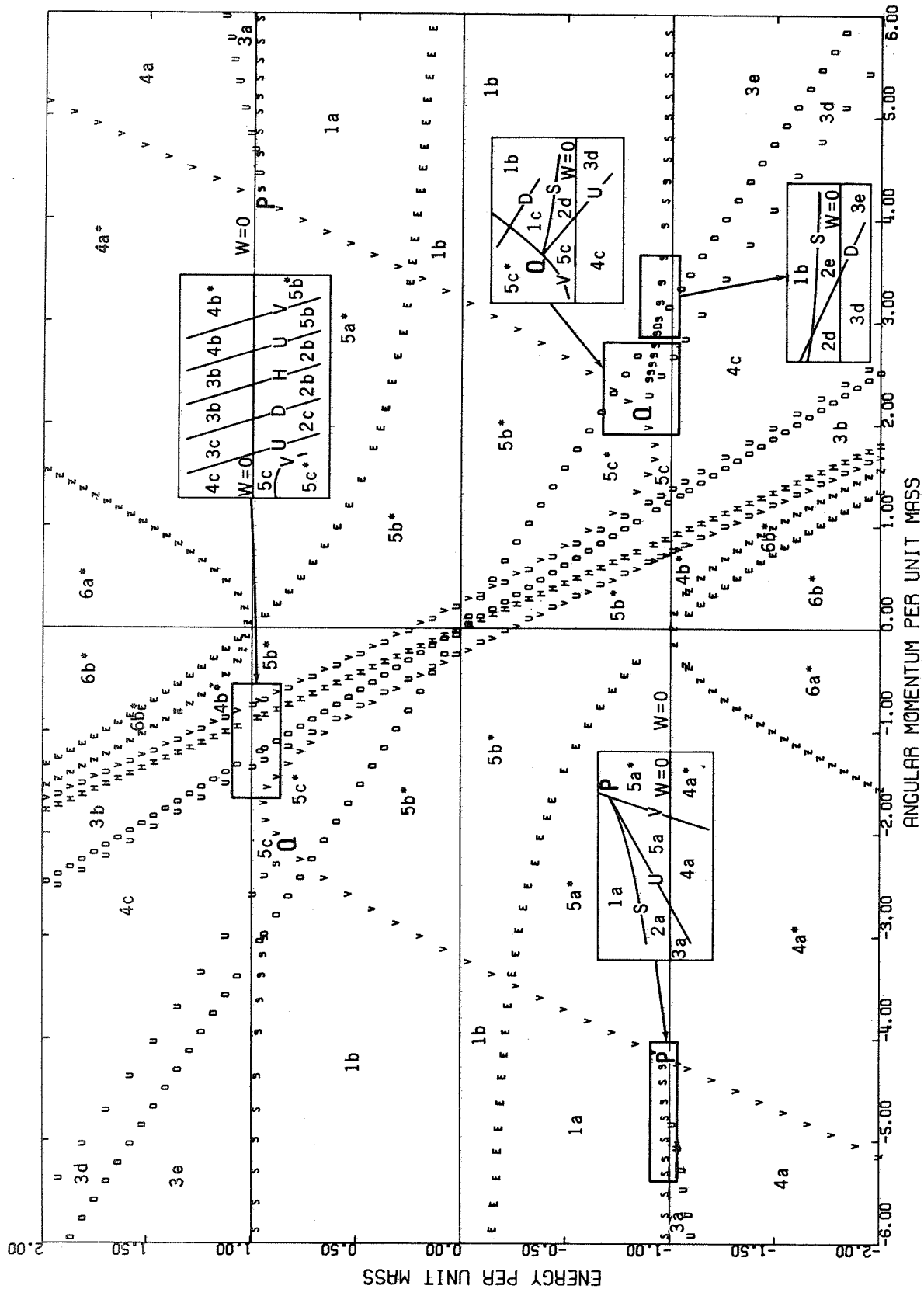

Figure C10—Master diagram for $a = 0.9, \beta = 2.0$.

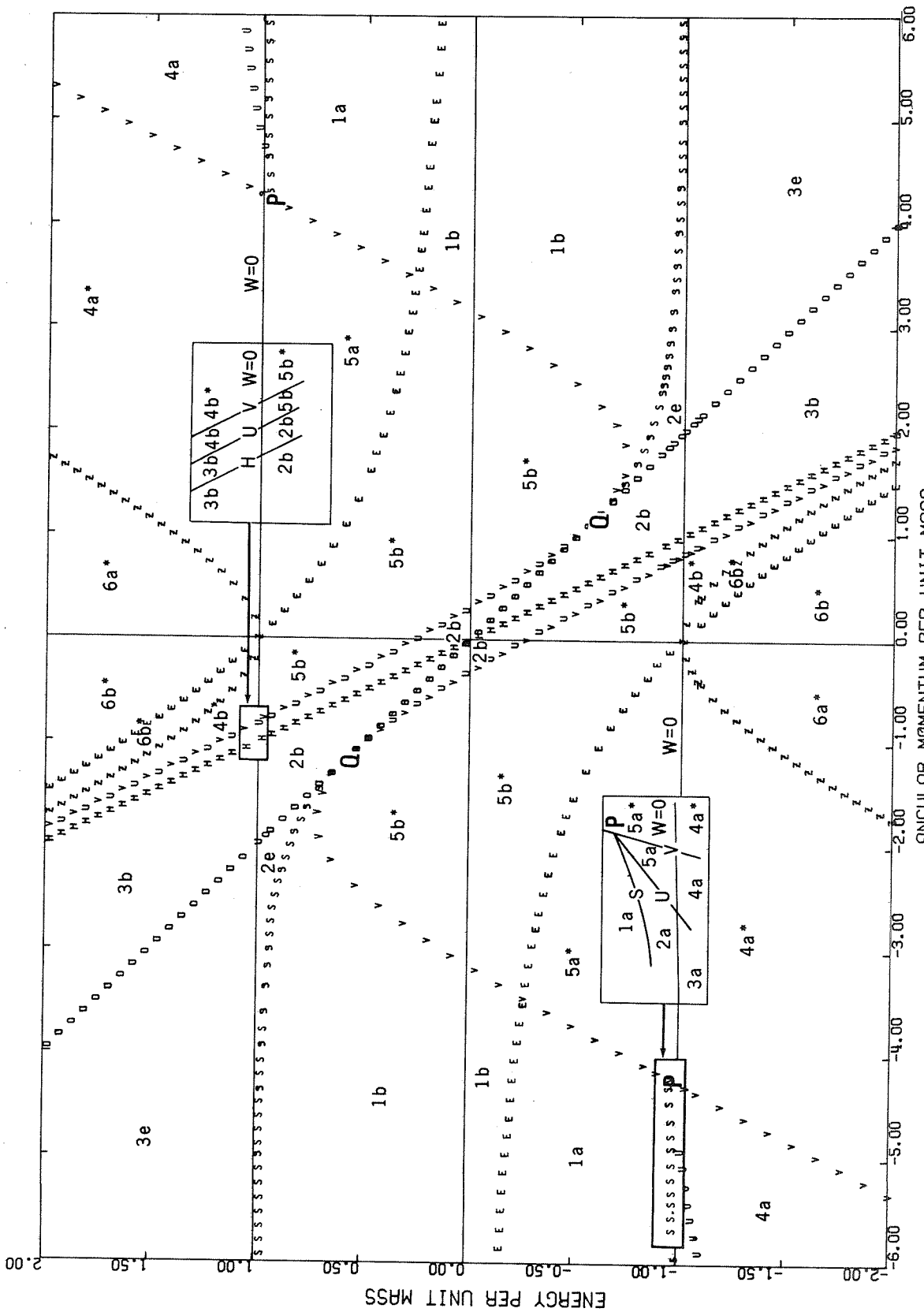

Figure C11—Master diagram for $a = 1.0, \beta = 2.0$.

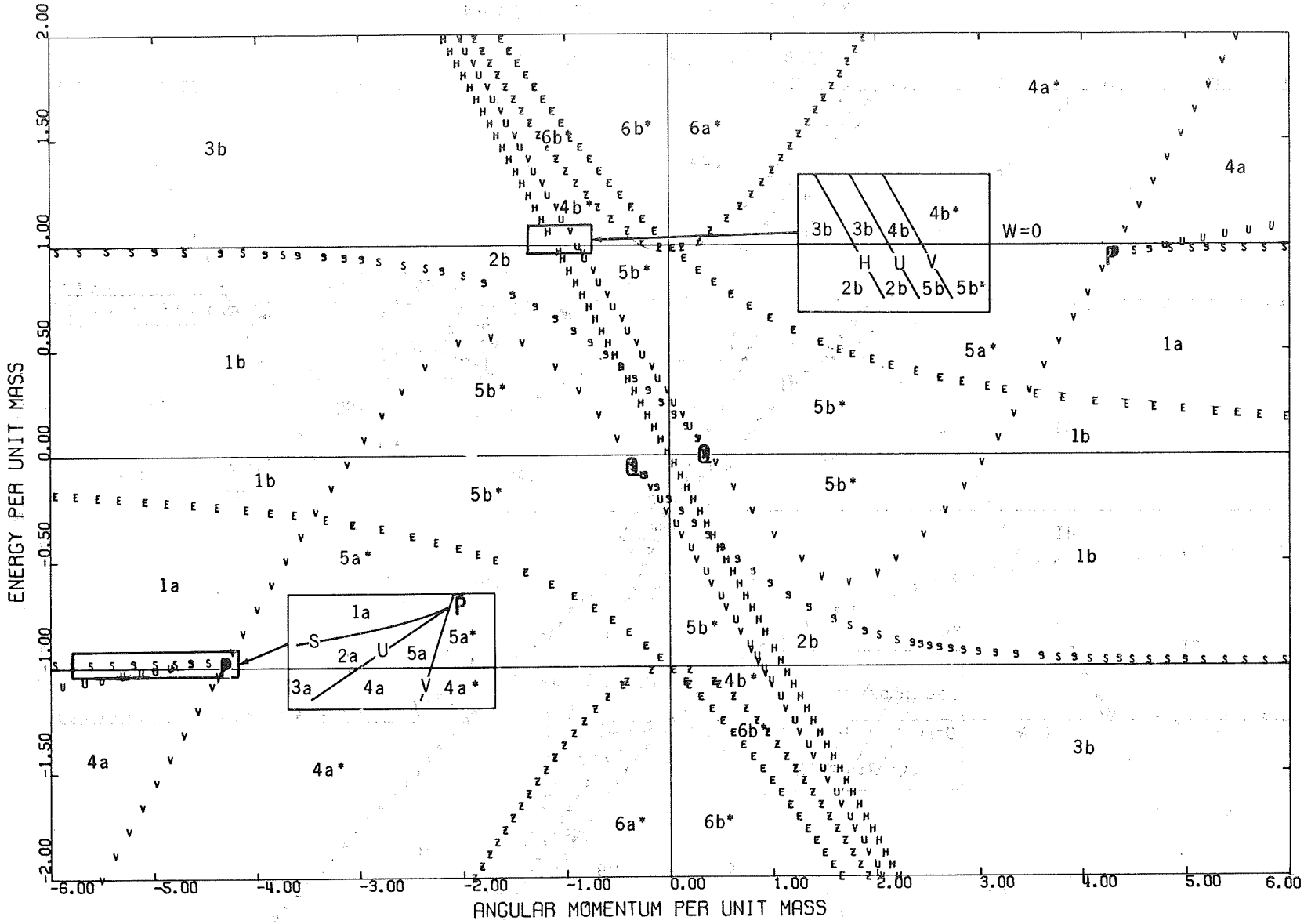

Figure C12—Master diagram for $a = 1.1$, $\beta = 2.0$.

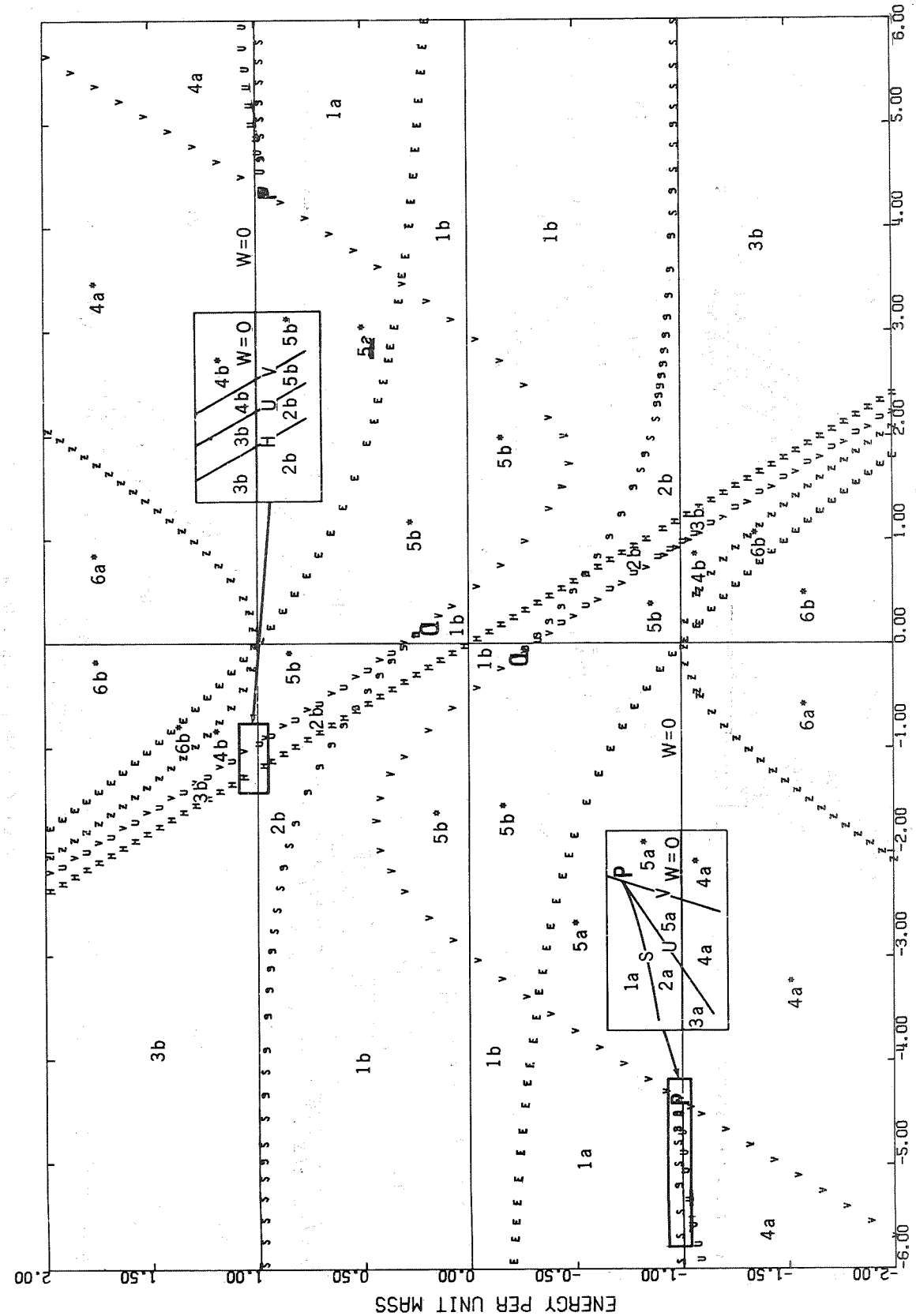

Figure C13—Master diagram for $a = 1.2, \beta = 2.0$.

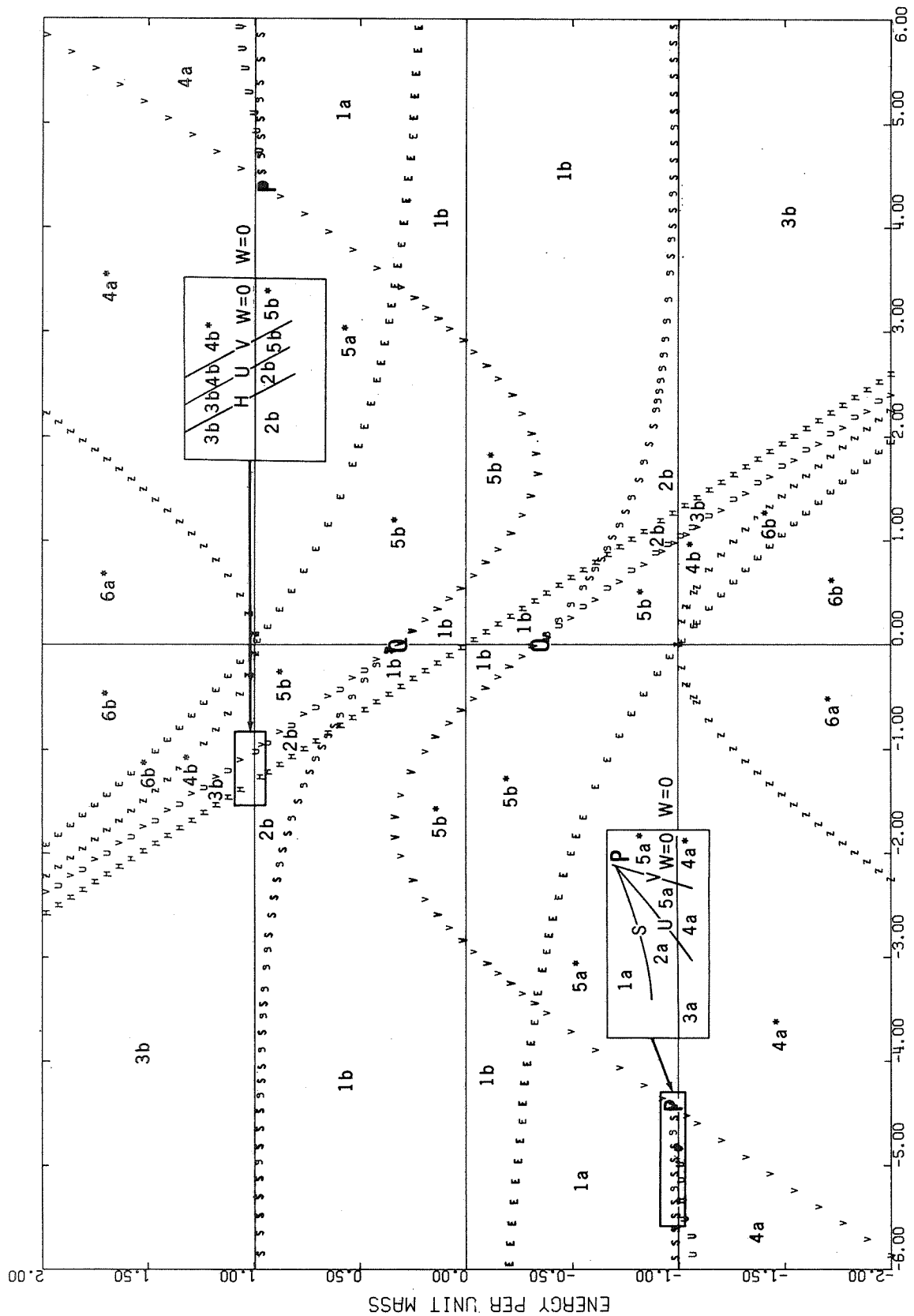

Figure C14–Master diagram for $a = 1.3, \beta = 2.0$.

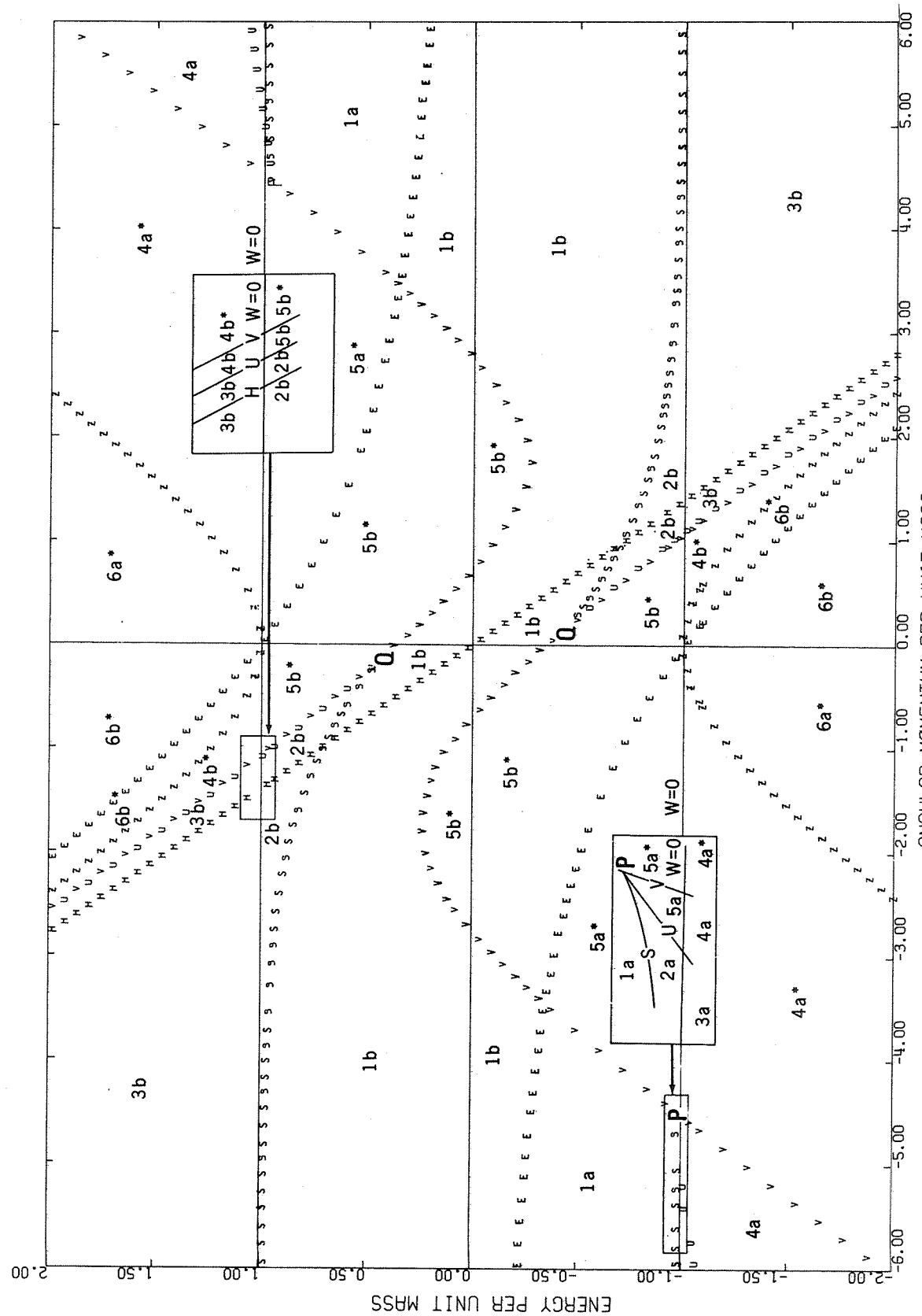

Figure C15—Master diagram for $a = 1.4, \beta = 2.0$.

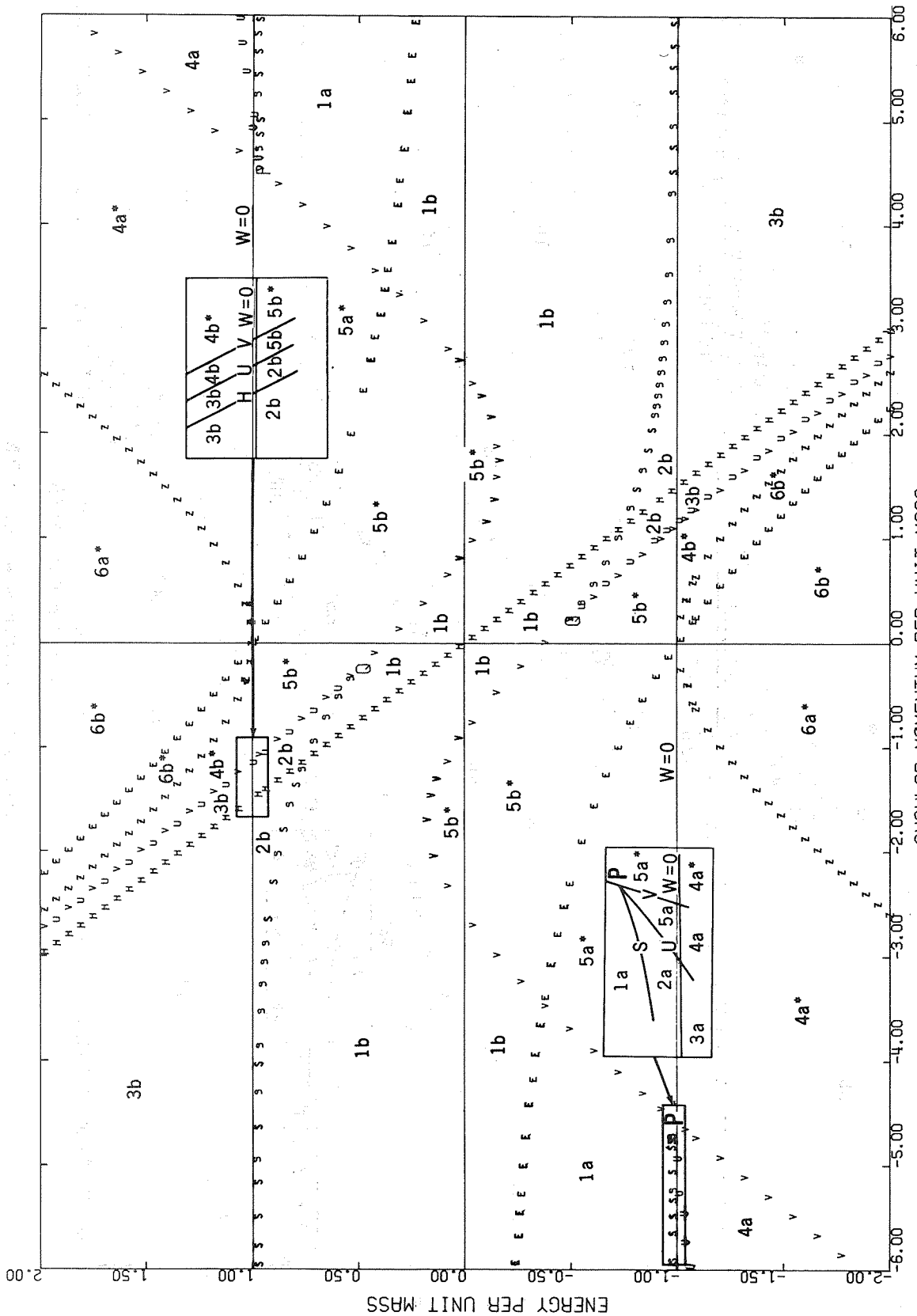

Figure C16–Master diagram for $a = 1.5, \beta = 2.0$.

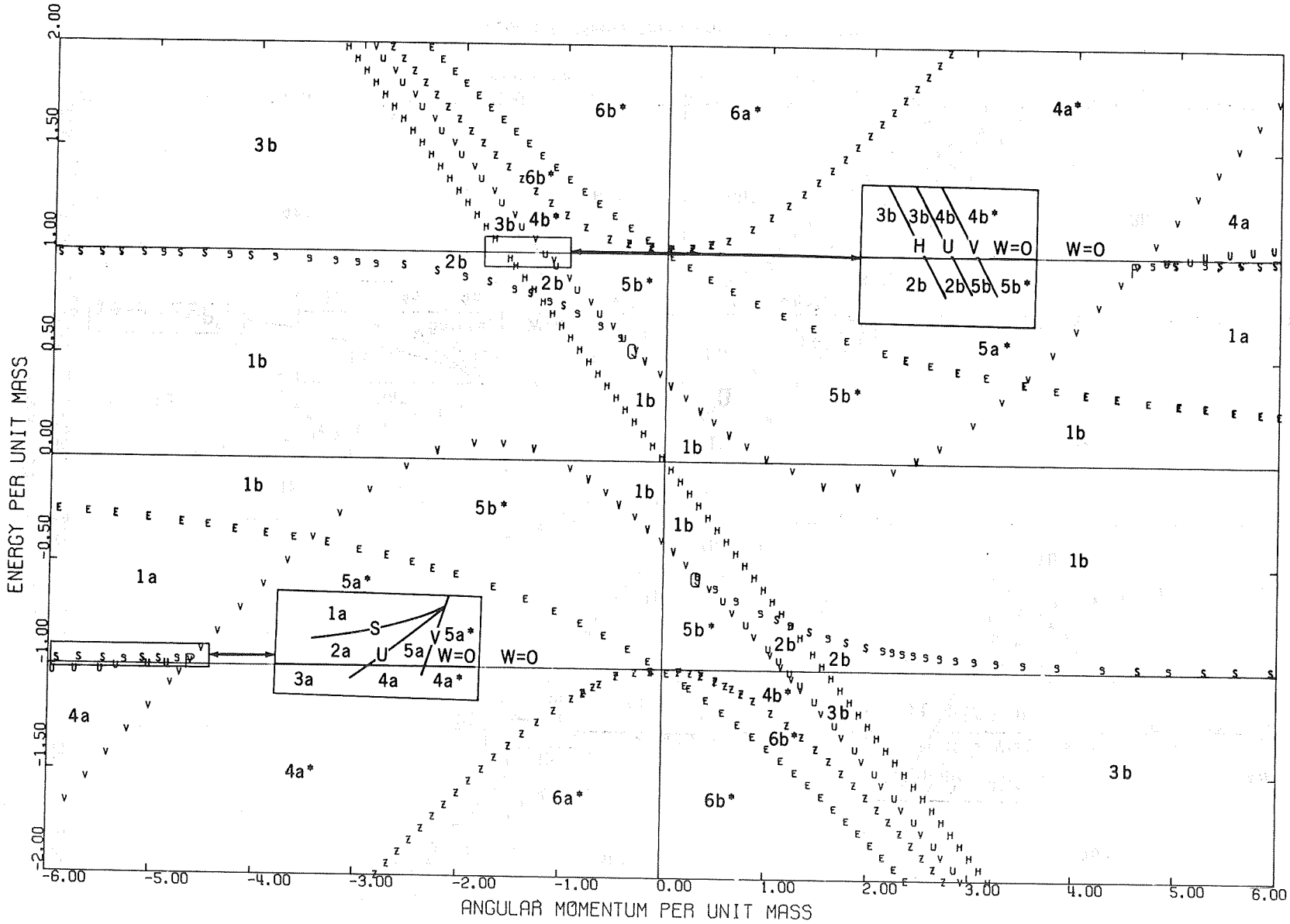

Figure C17—Master diagram for $a = 1.6$, $\beta = 2.0$.

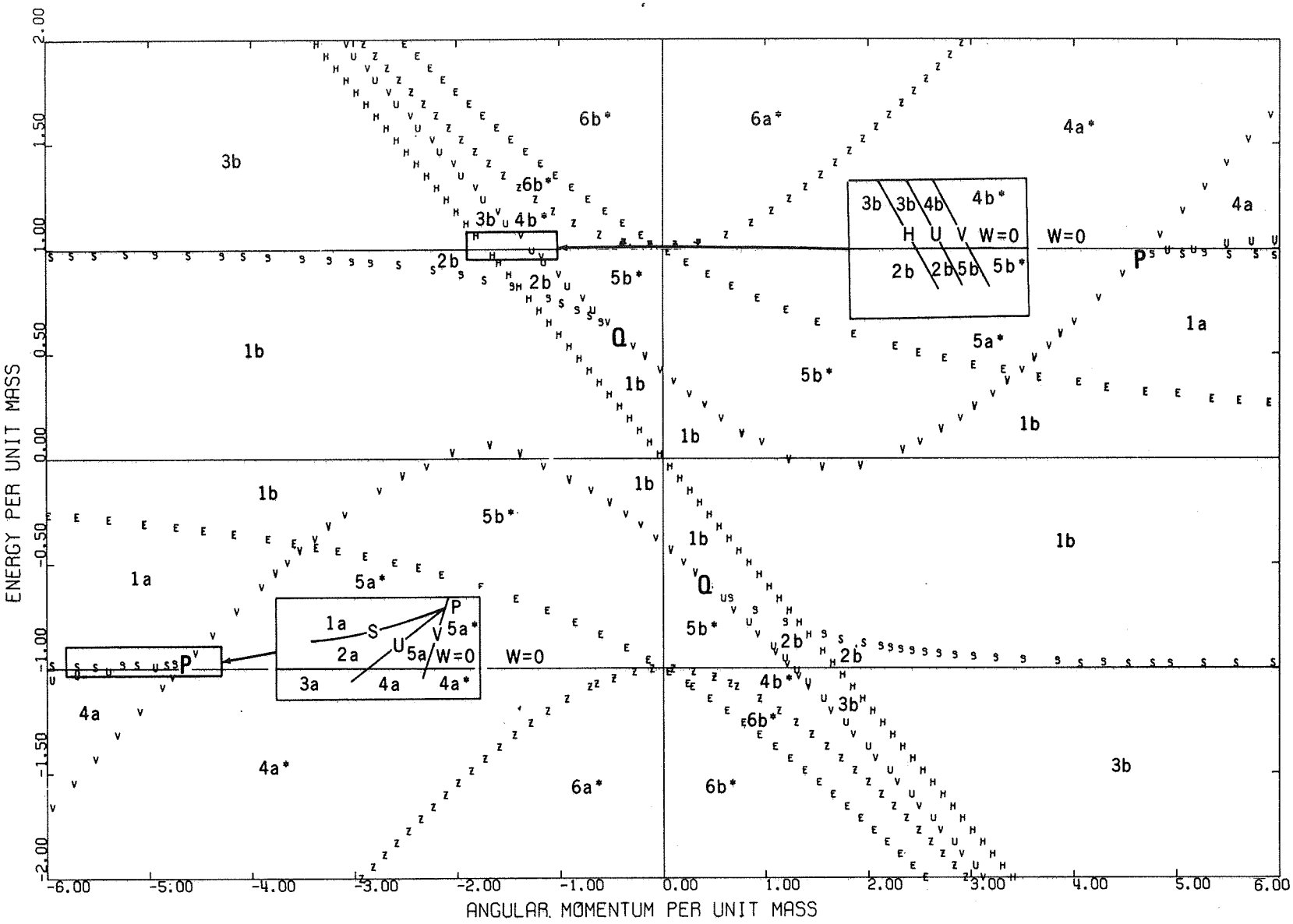

Figure C18—Master diagram for $a = 1.7$, $\beta = 2.0$.

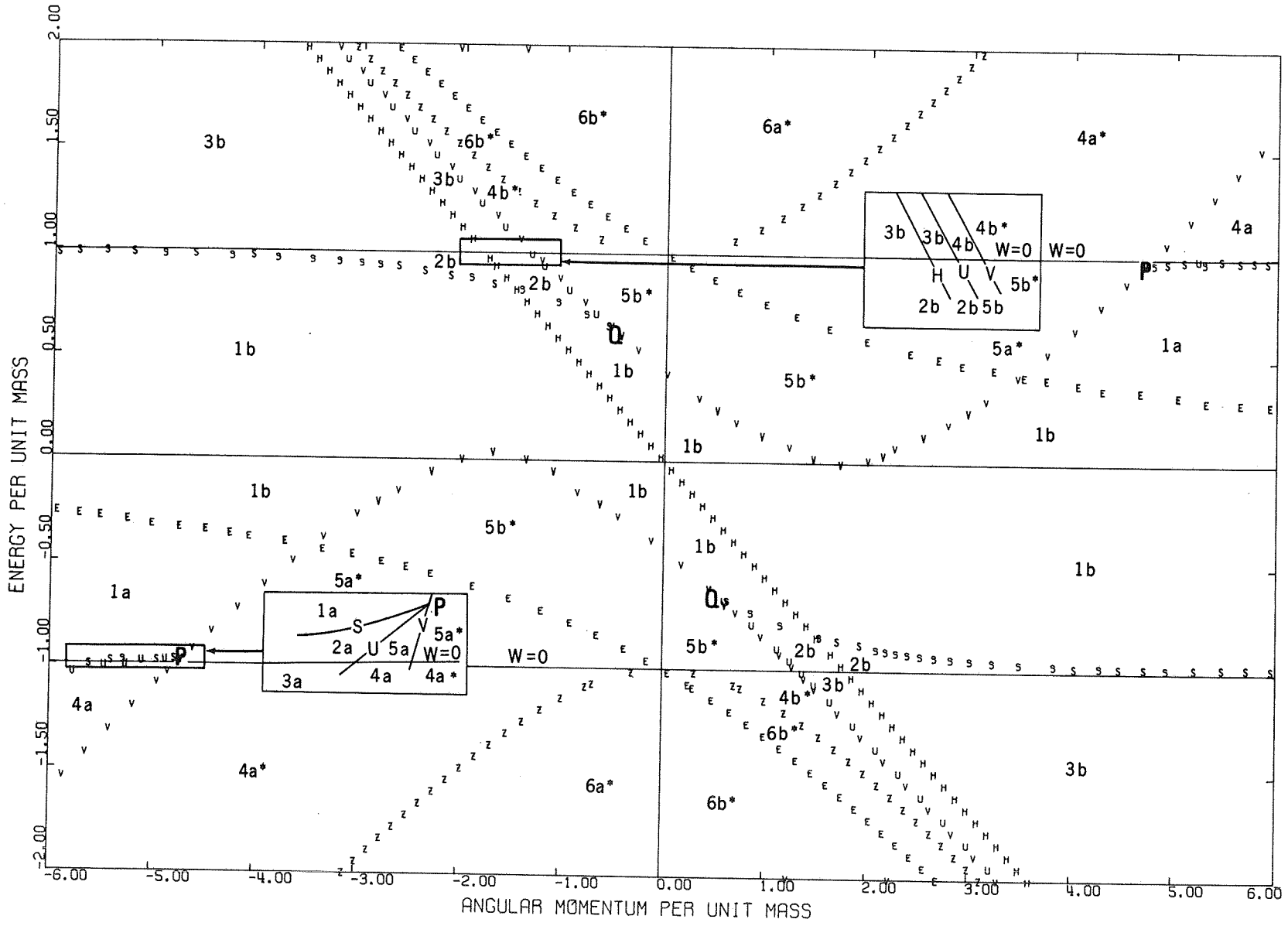

Figure C19—Master diagram for $a = 1.8$, $\beta = 2.0$.

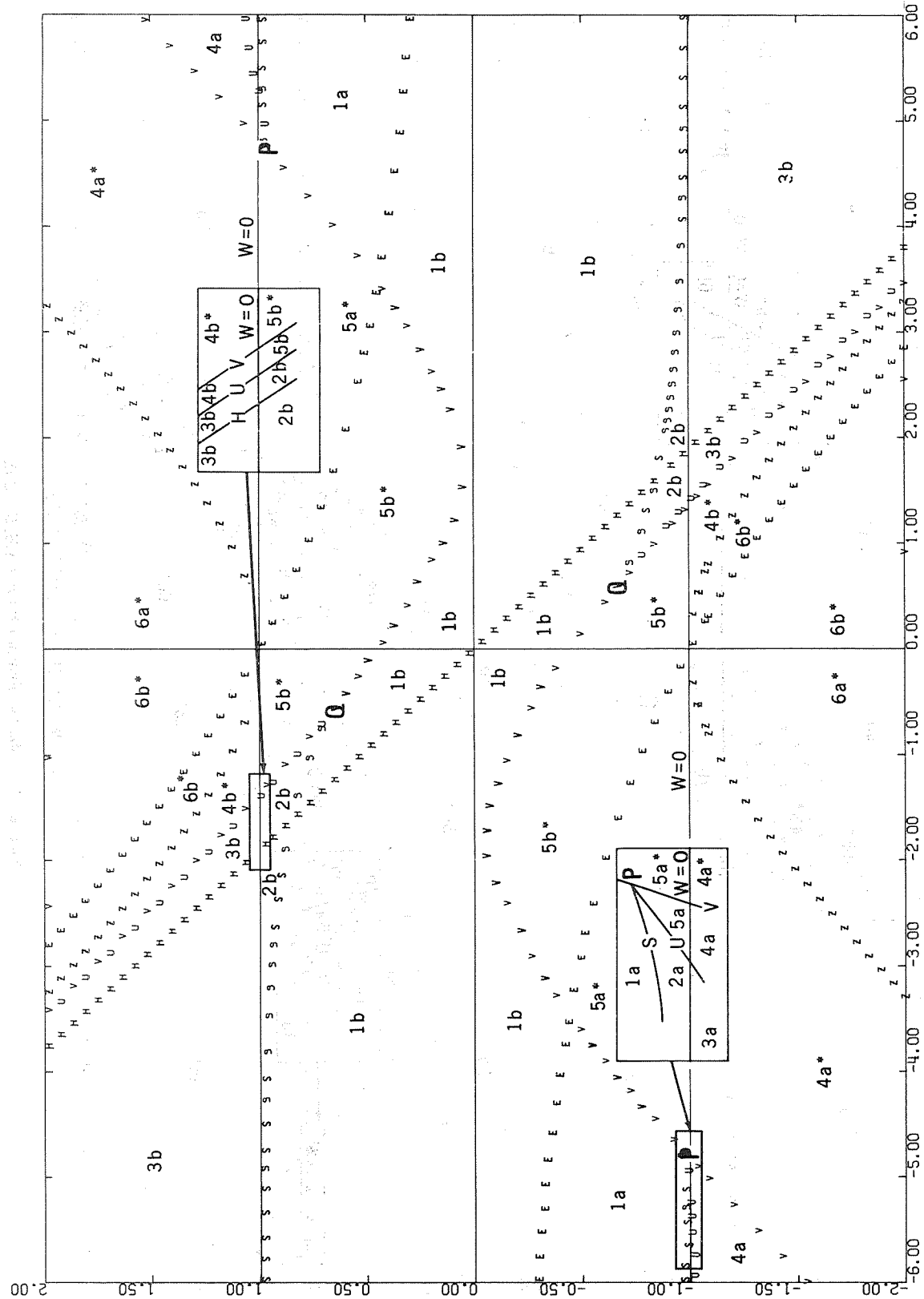

Figure C20–Master diagram for $a = 1.9$, $\beta = 2.0$.

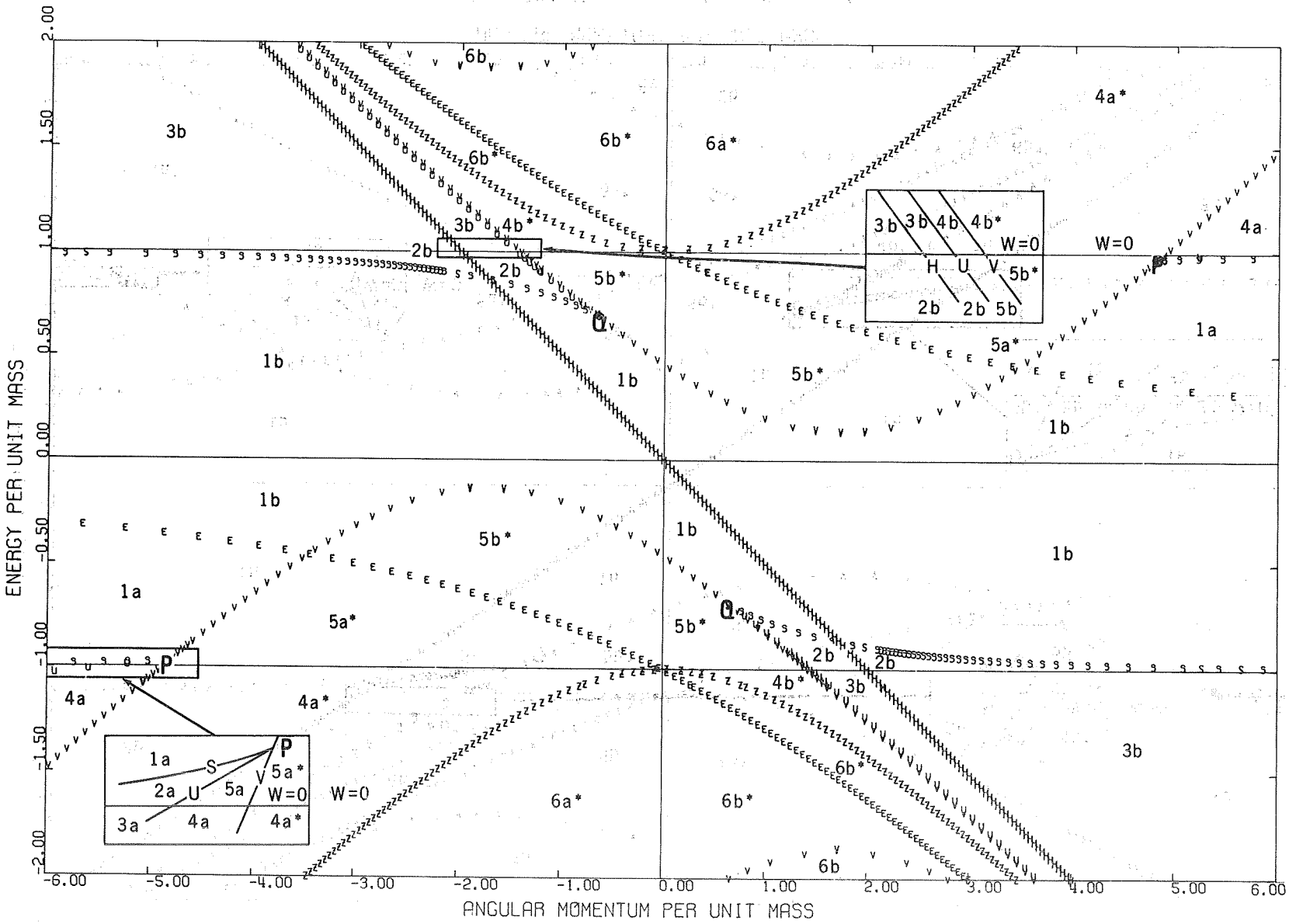

Figure C21—Master diagram for $a = 2.0$, $\beta = 2.0$.

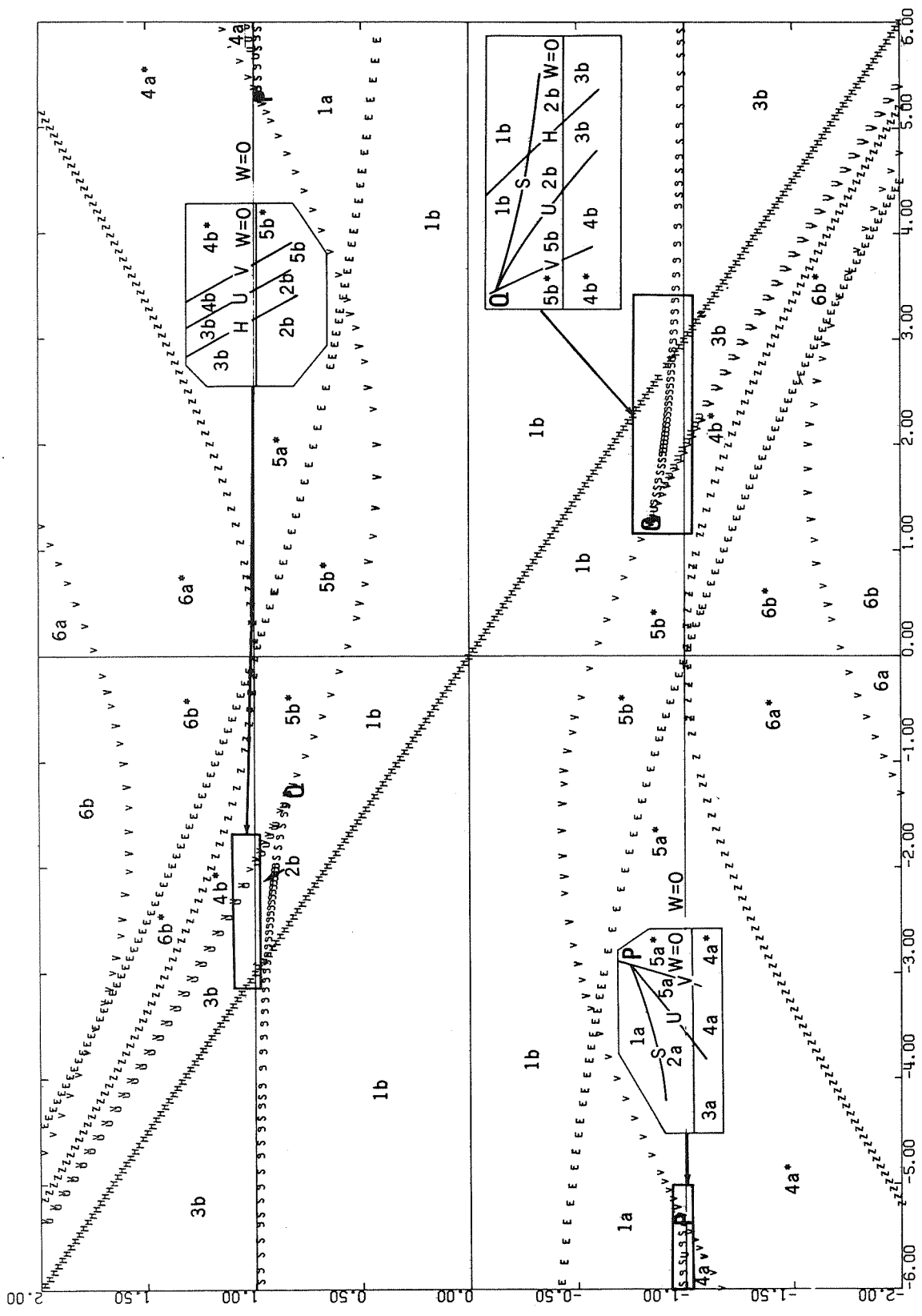

Figure C22—Master diagram for $a = 3.0, \beta = 2.0$.

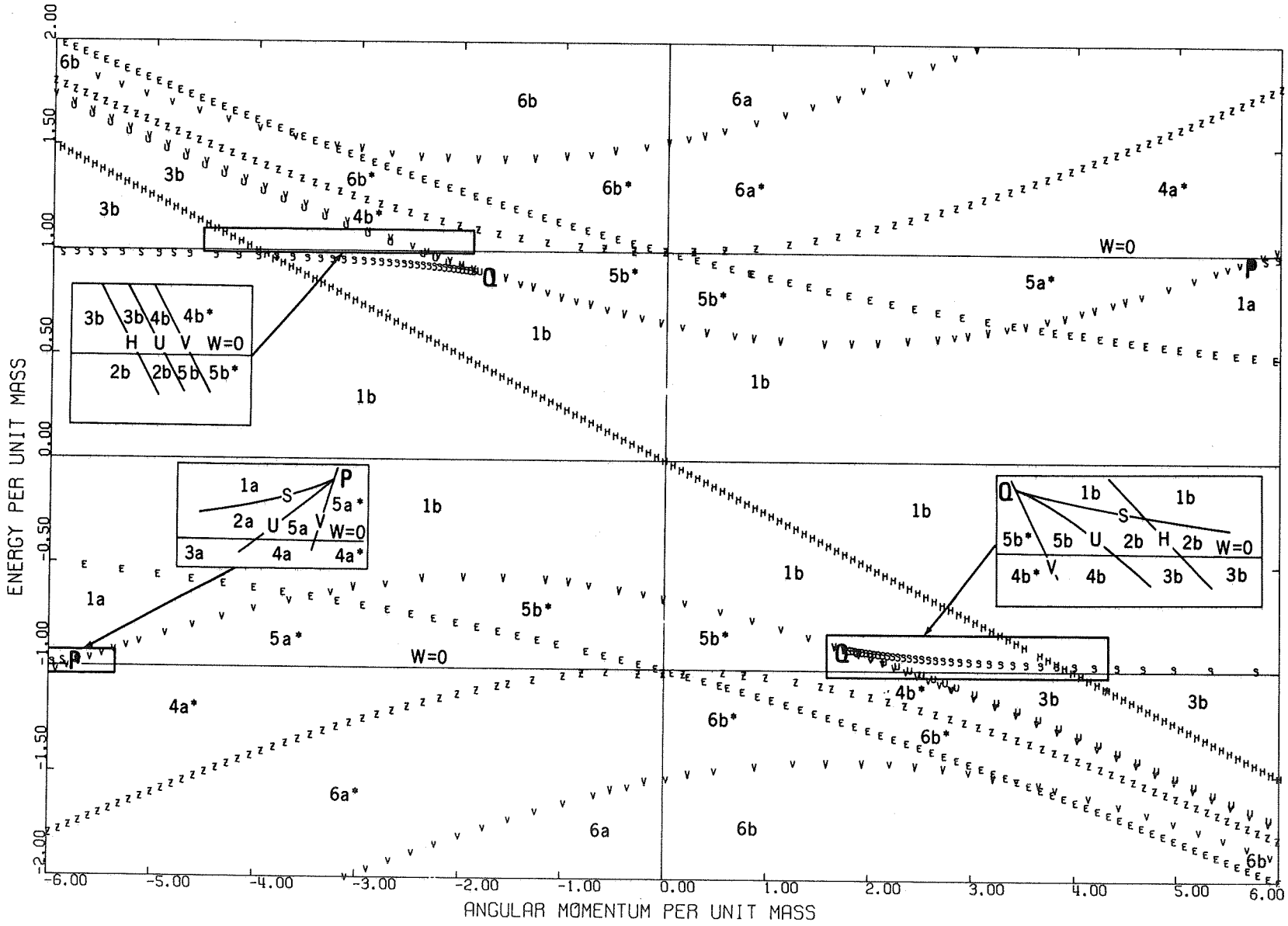

Figure C23—Master diagram for $a = 4.0$, $\beta = 2.0$.

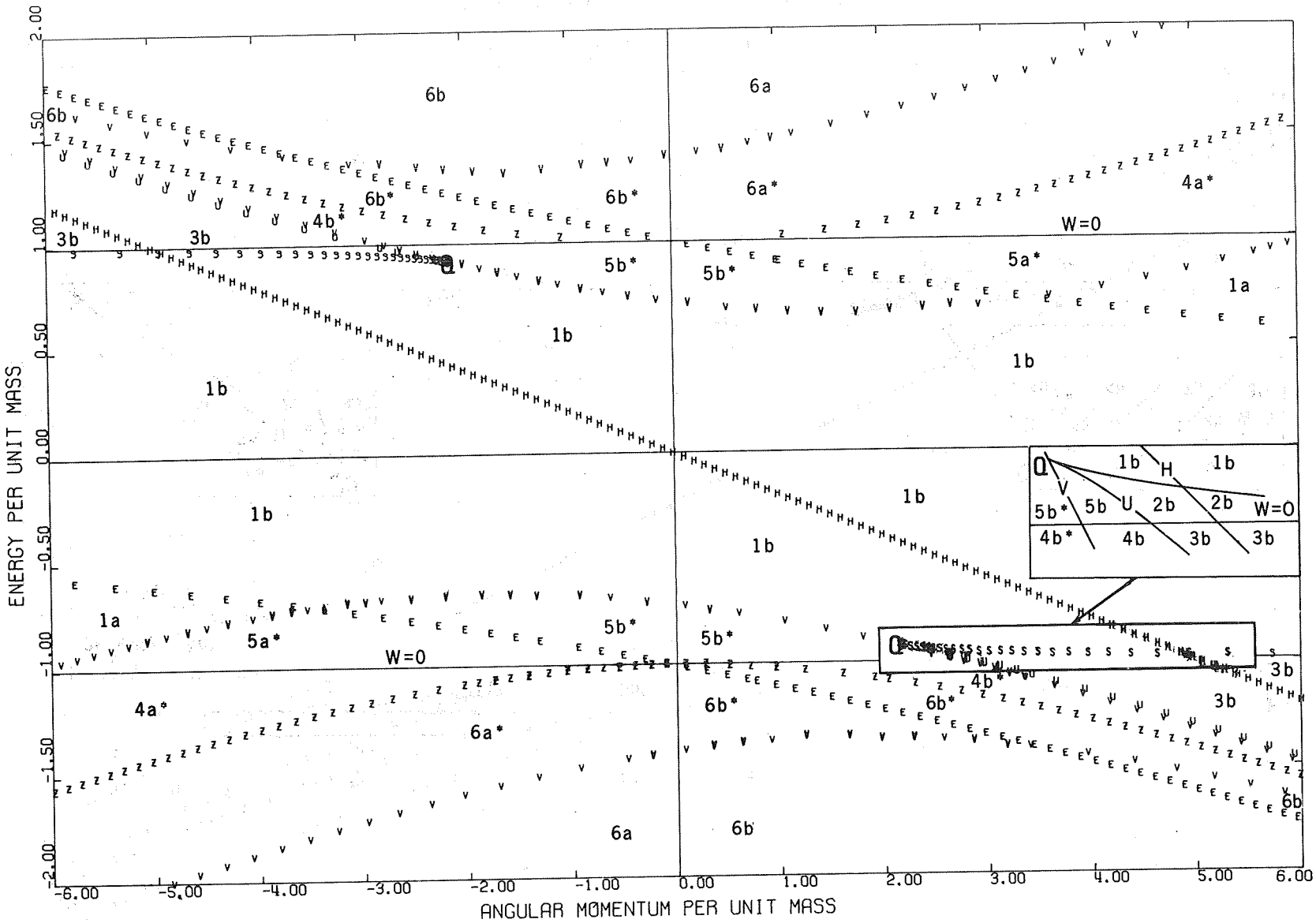

Figure C24—Master diagram for $a = 5.0, \beta = 2.0$.

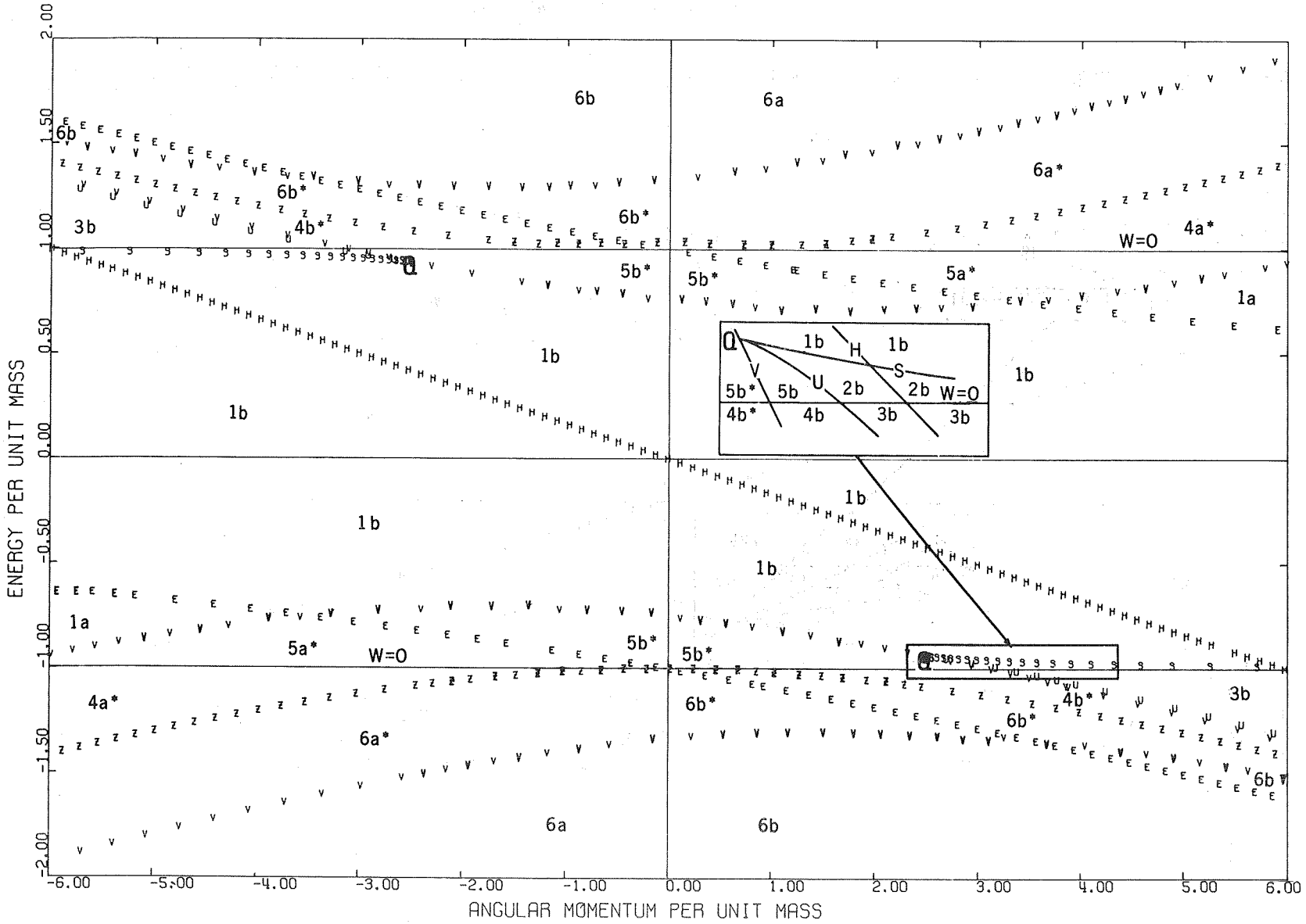

Figure C25—Master diagram for $a = 6.0$, $\beta = 2.0$.

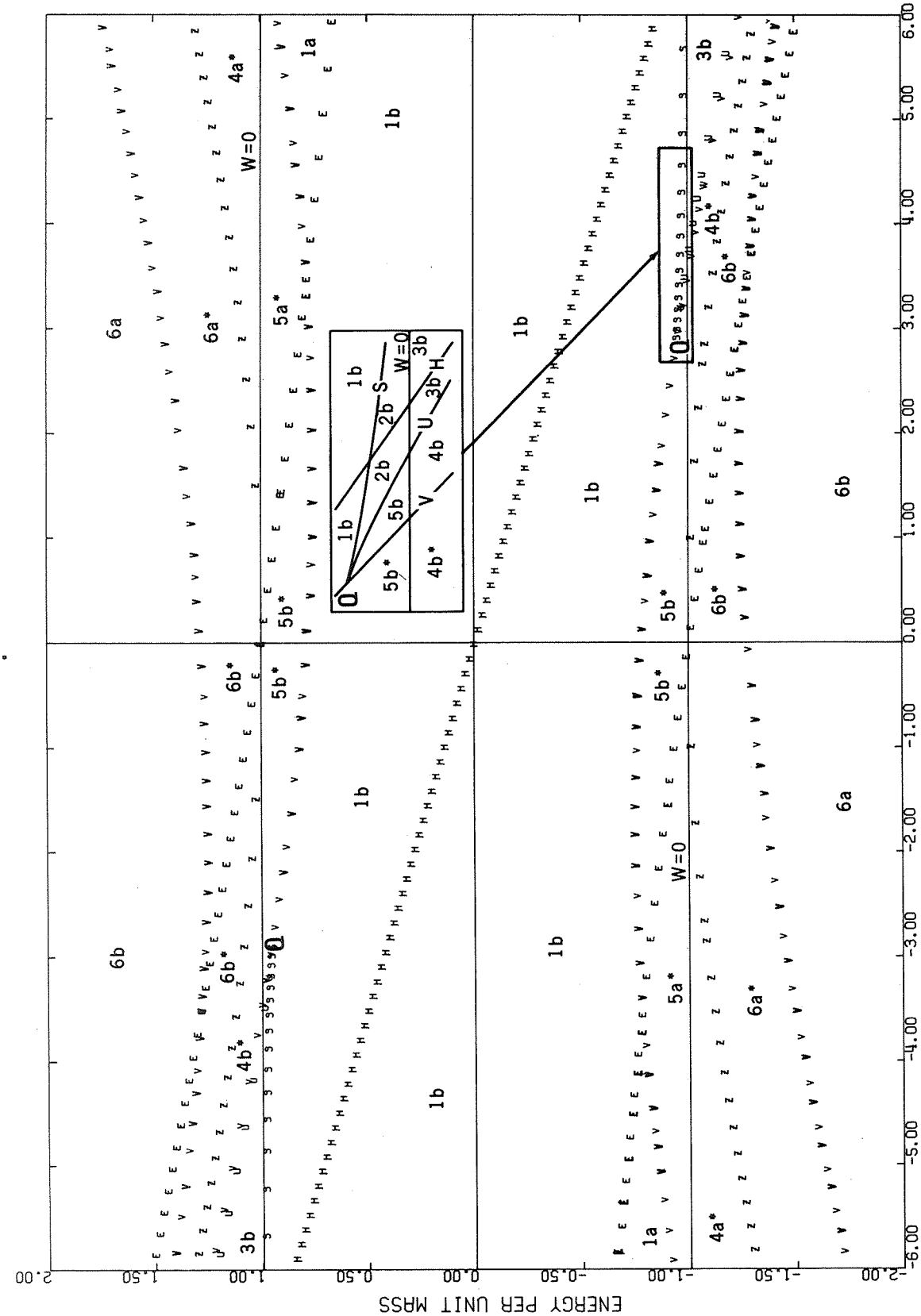

Figure C26—Master diagram for $a = 7.0, \beta = 2.0$.

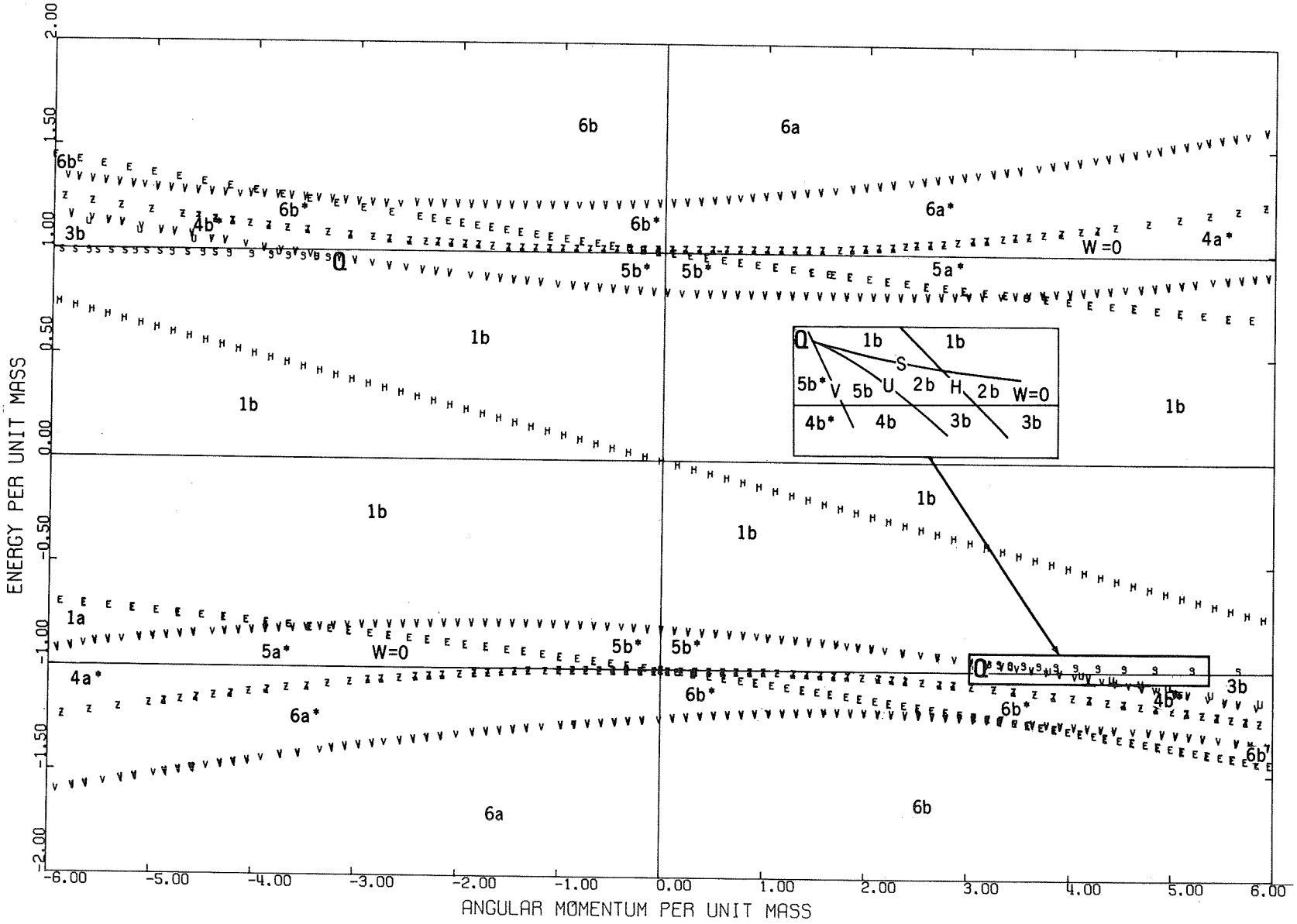

Figure C27—Master diagram for $a = 8.0$, $\beta = 2.0$.

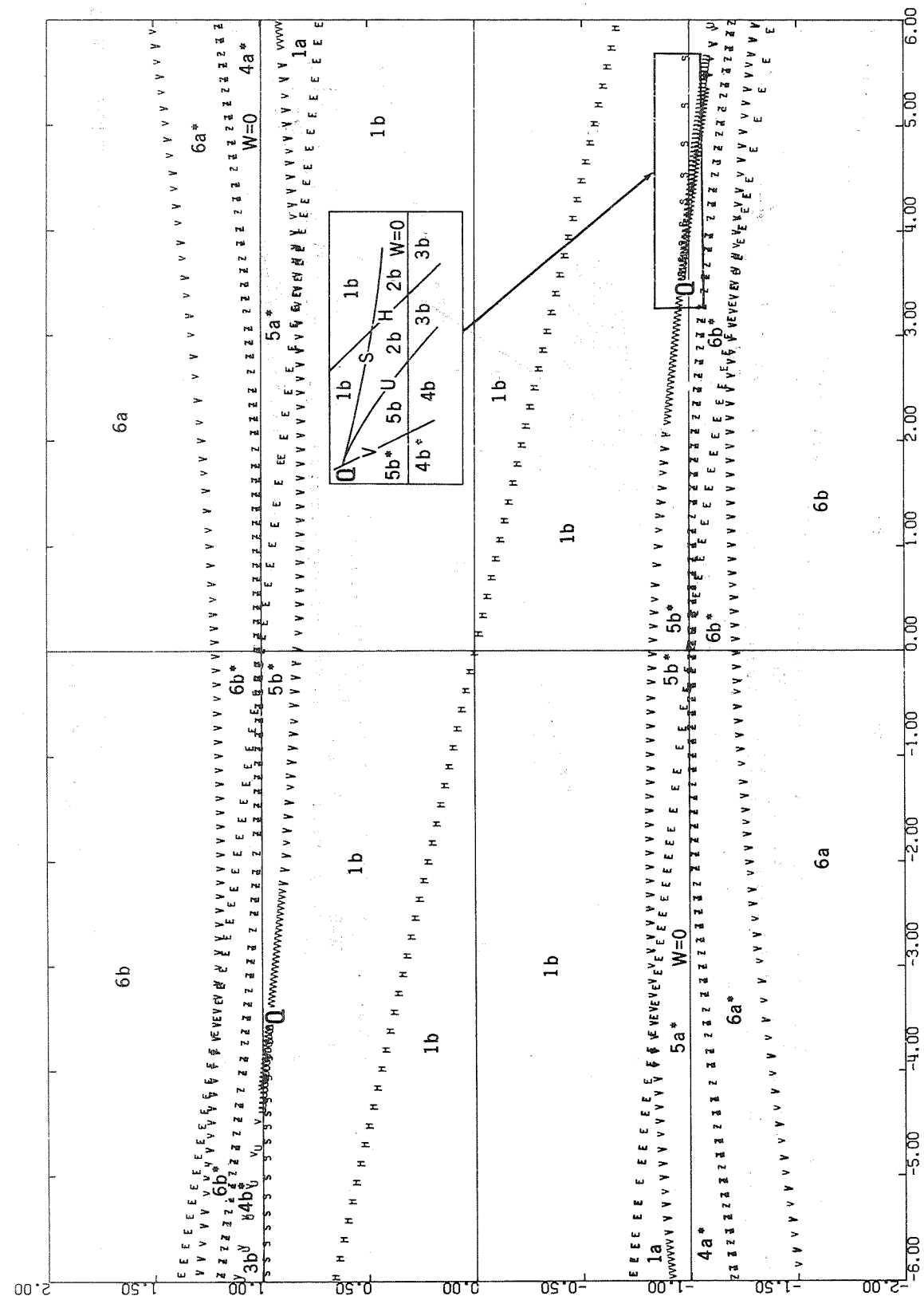

Figure C28—Master diagram for $a = 9.0, \beta = 2.0$.

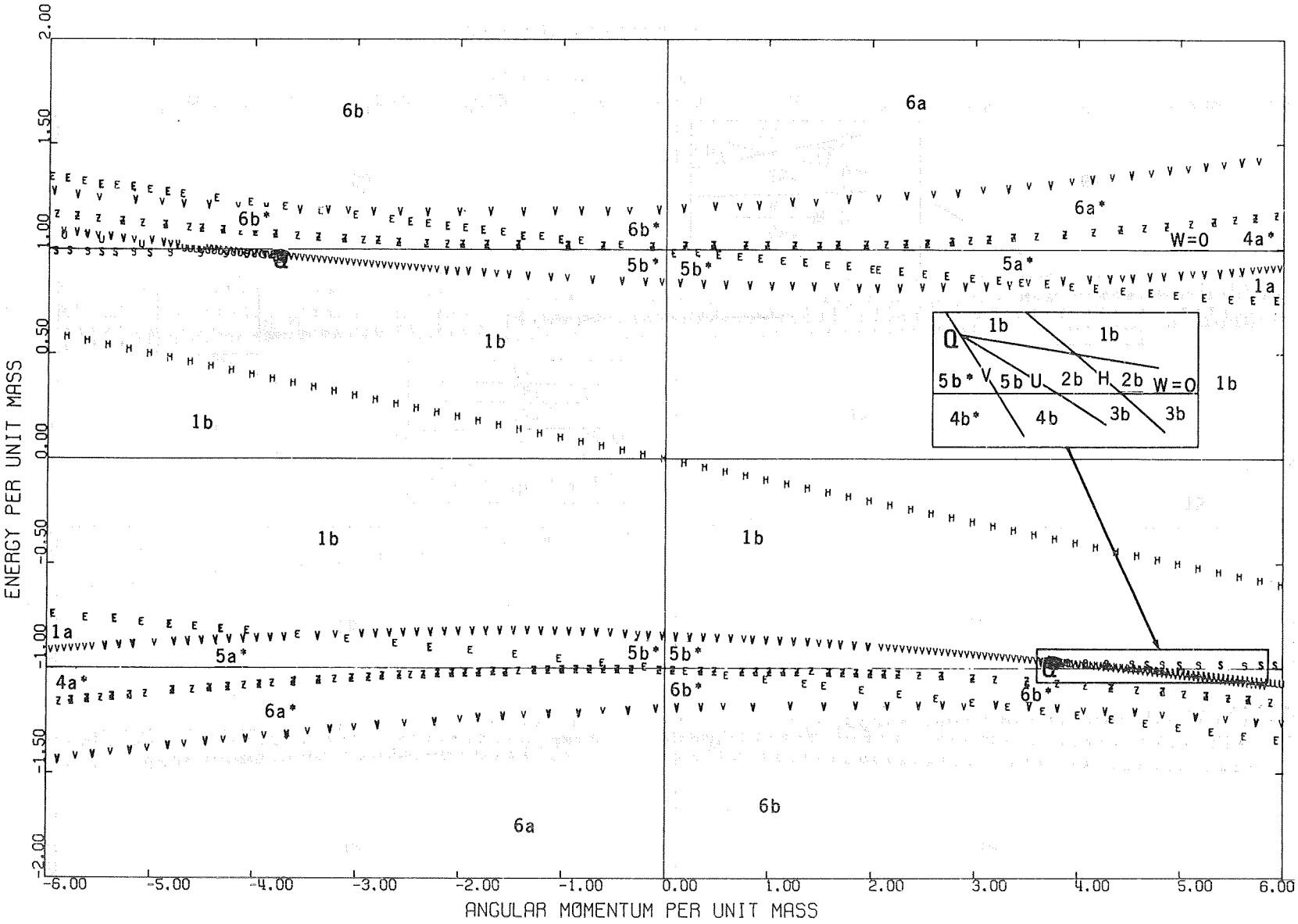

Figure C29—Master diagram for $a = 10.0$, $\beta = 2.0$.

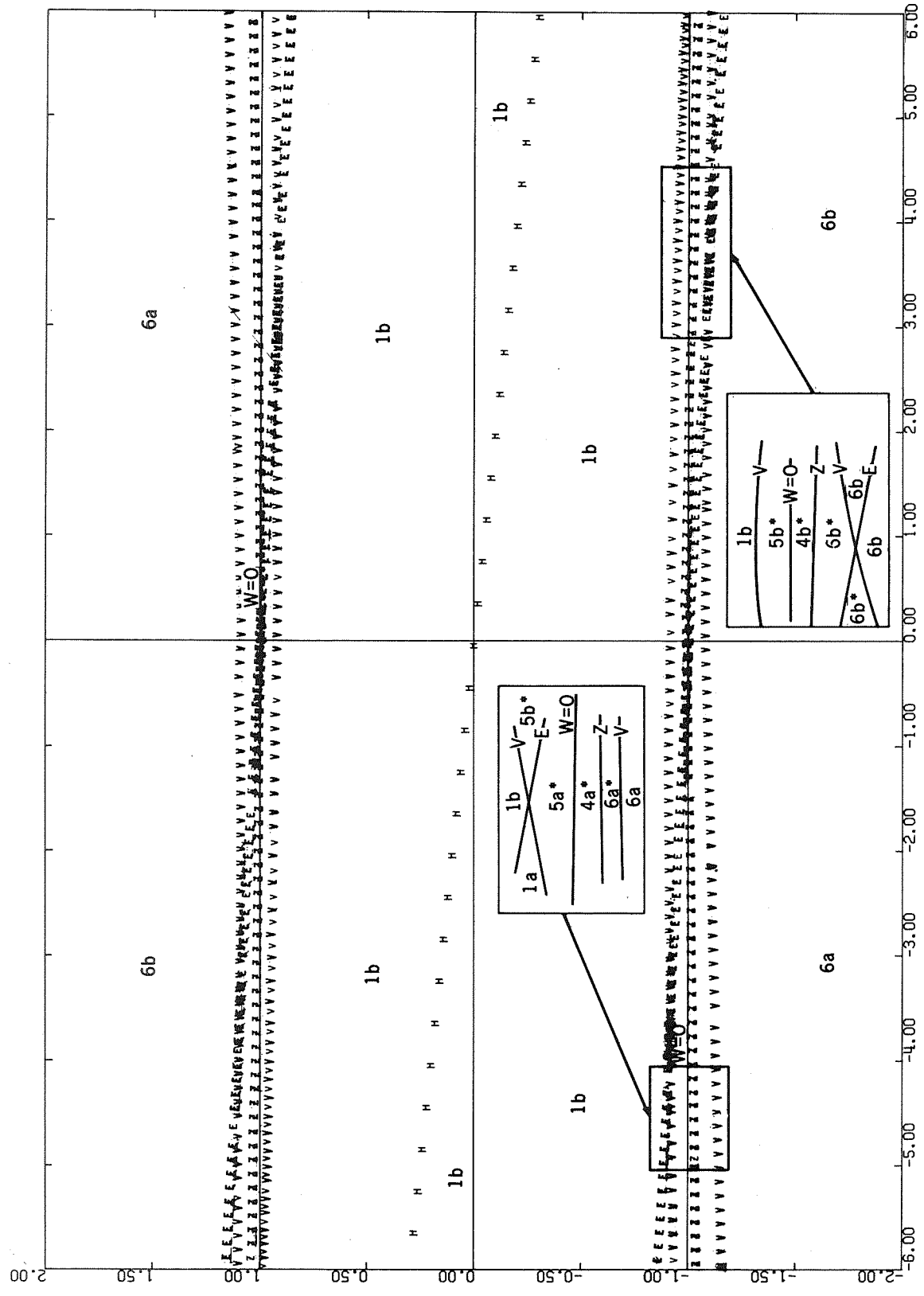

Figure C30—Master diagram for $a = 20.0, \beta = 2.0$.

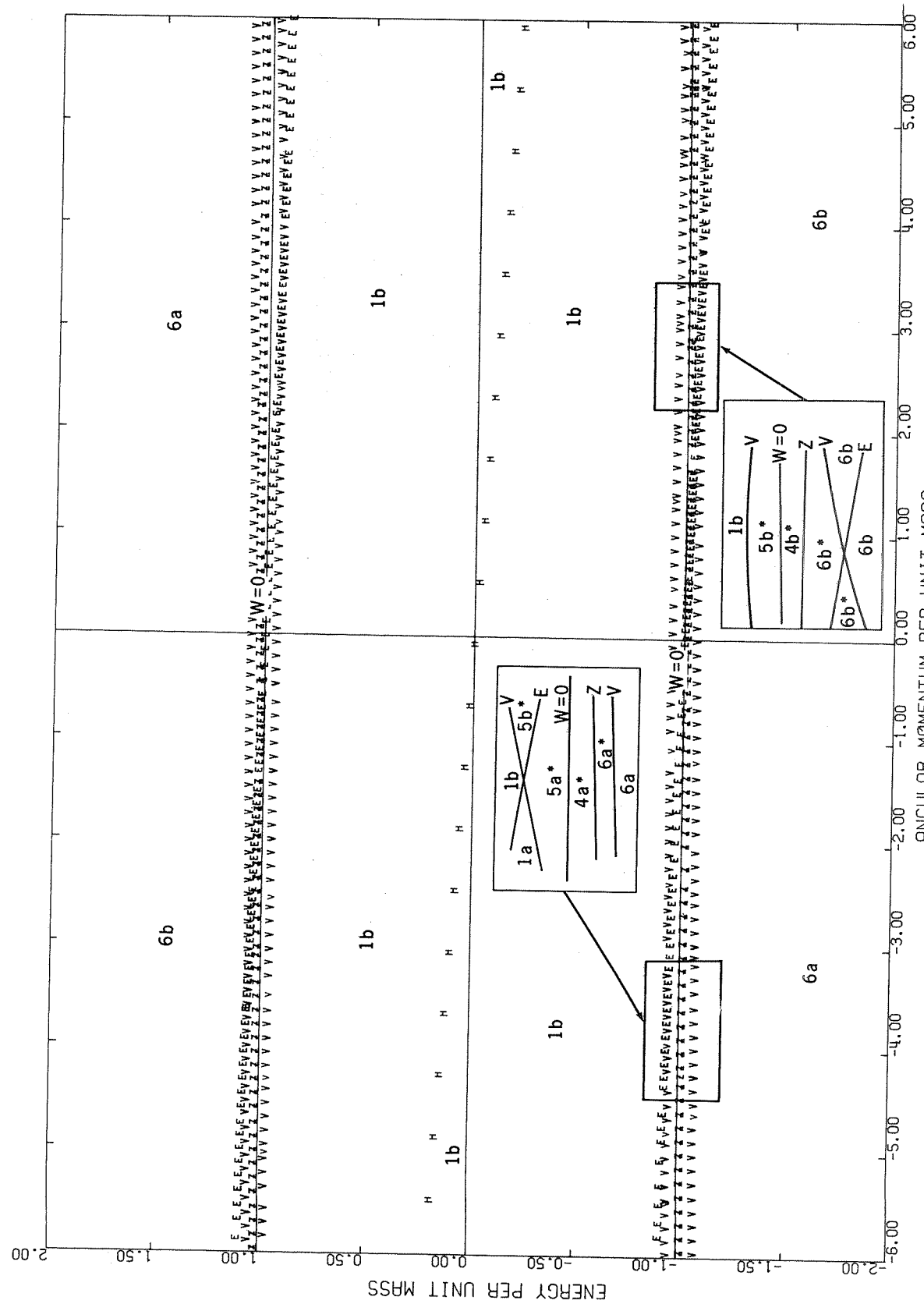

Figure C31—Master diagram for $a = 30.0, \beta = 2.0$.

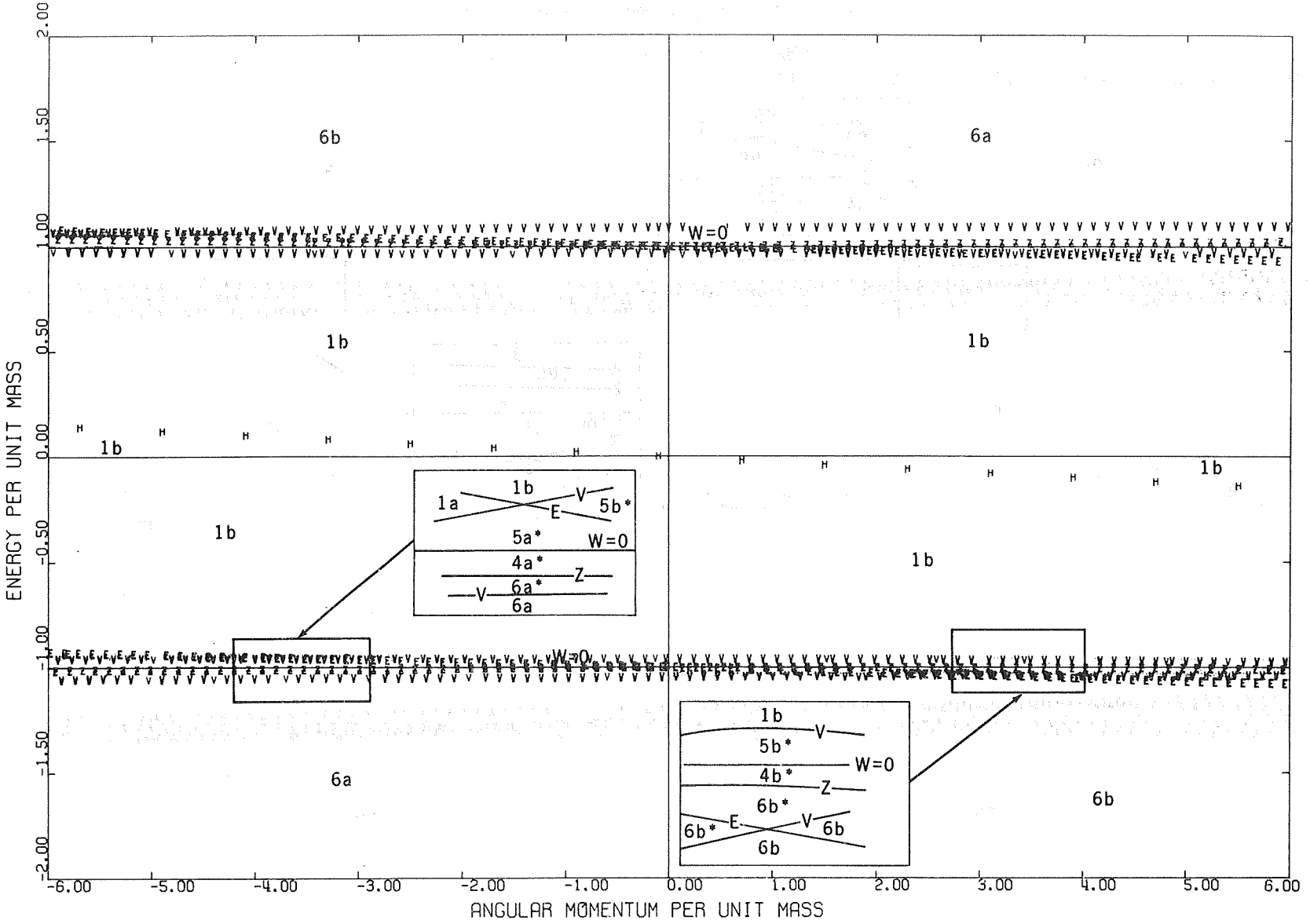

Figure C32—Master diagram for $a = 40.0$, $\beta = 2.0$.

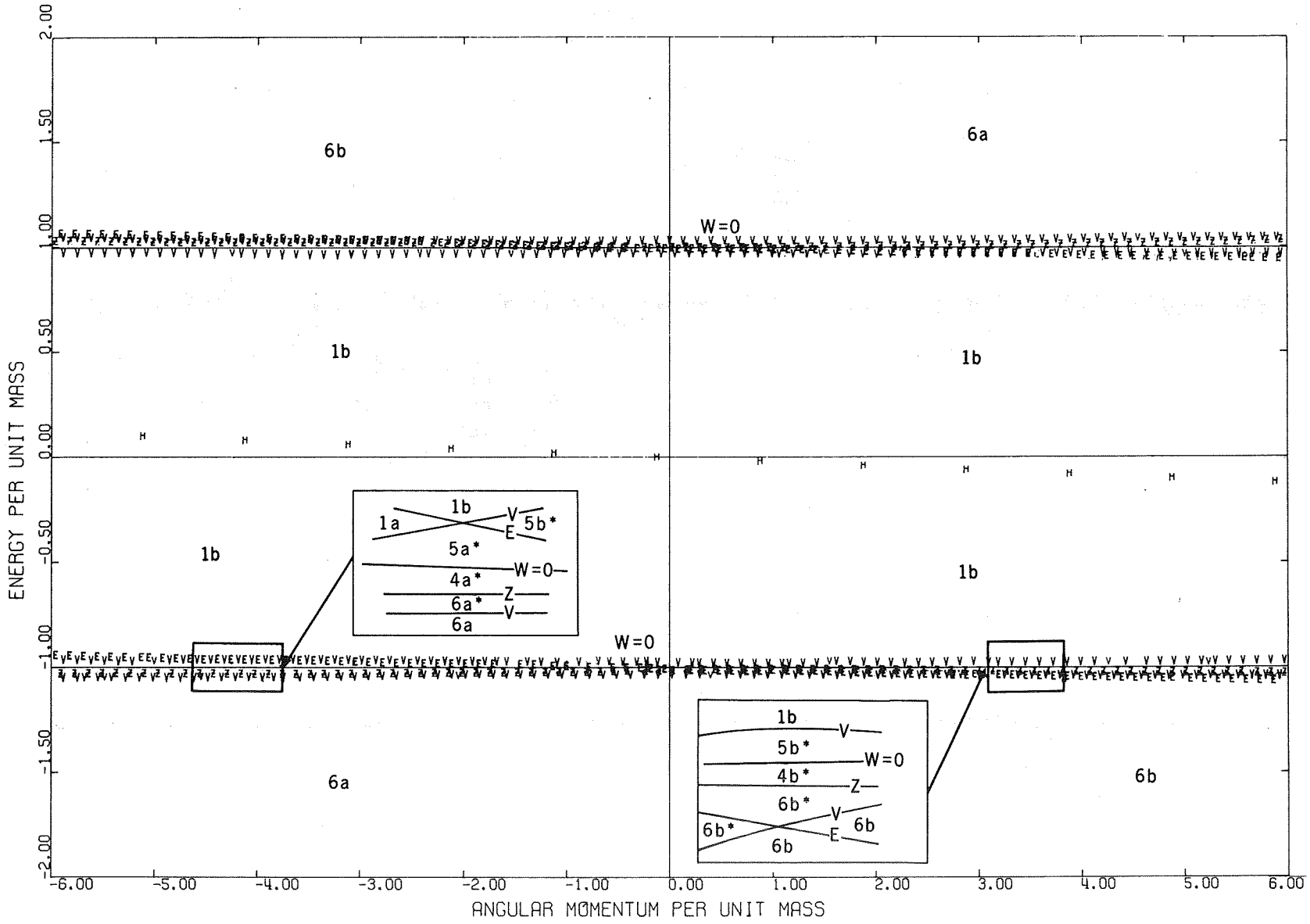

Figure C33—Master diagram for $a = 50.0$, $\beta = 2.0$.

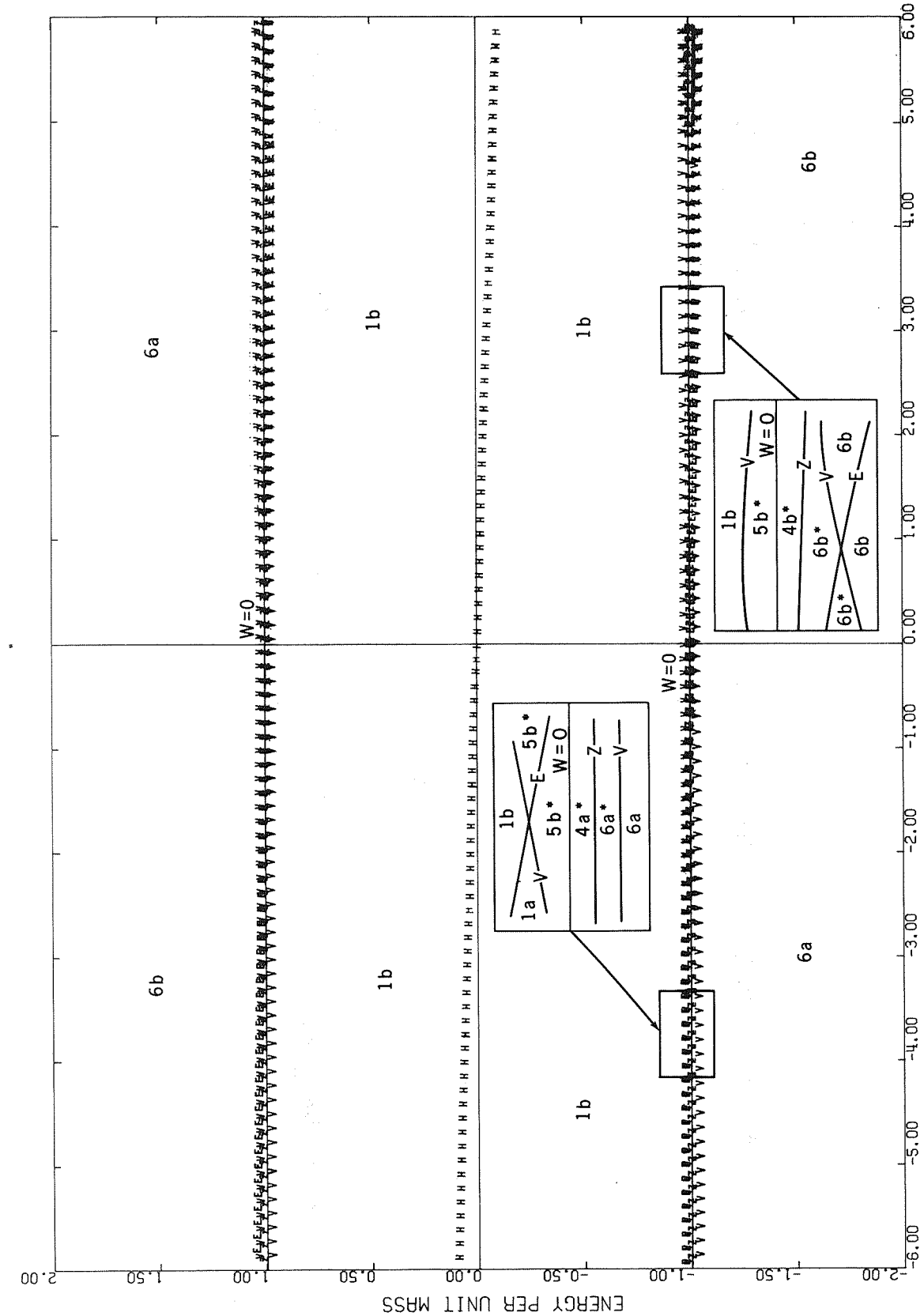

Figure C34—Master diagram for $a = 60.0, \beta = 2.0$.

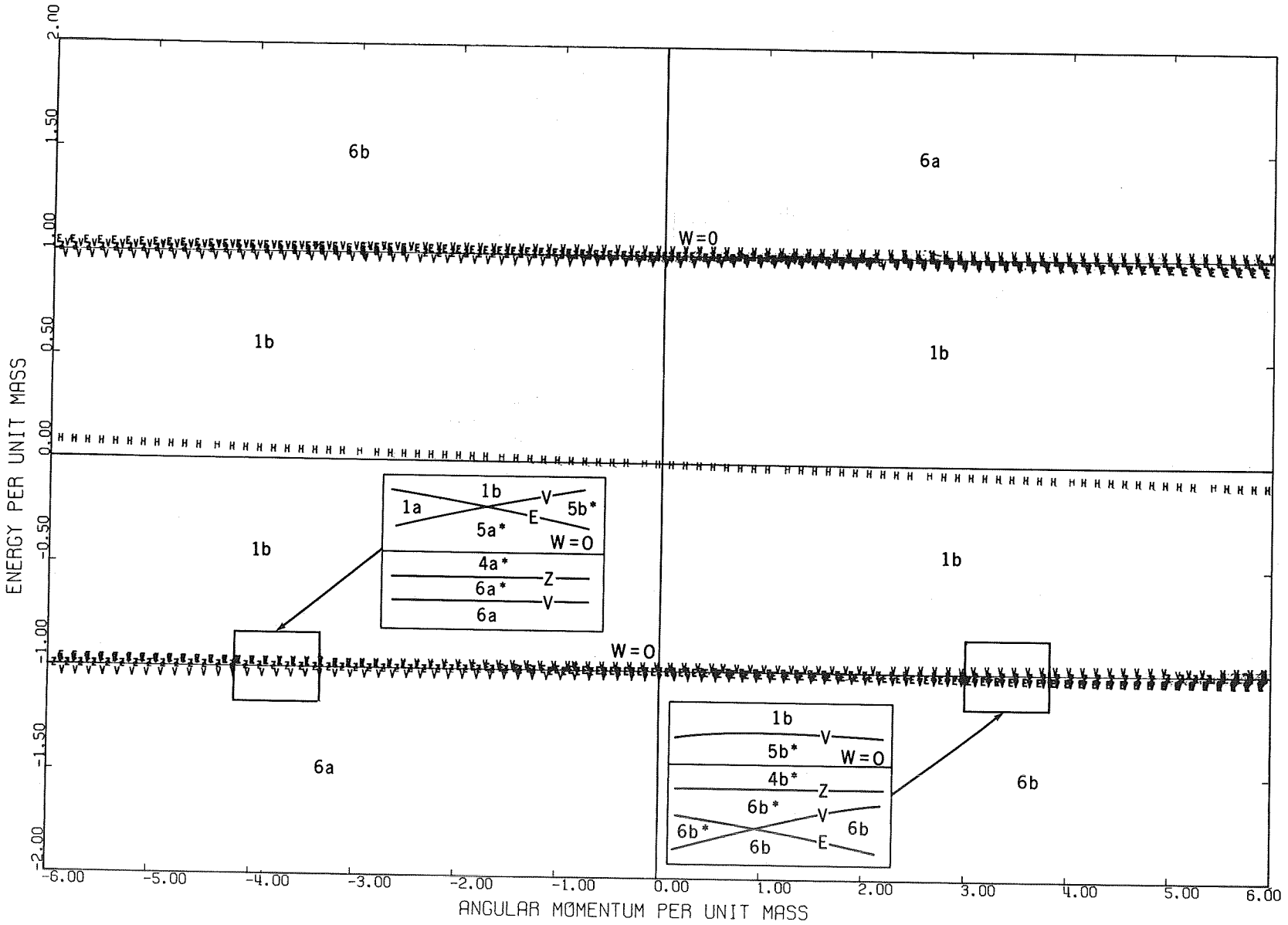

Figure C35—Master diagram for $a = 70.0$, $\beta = 2.0$.

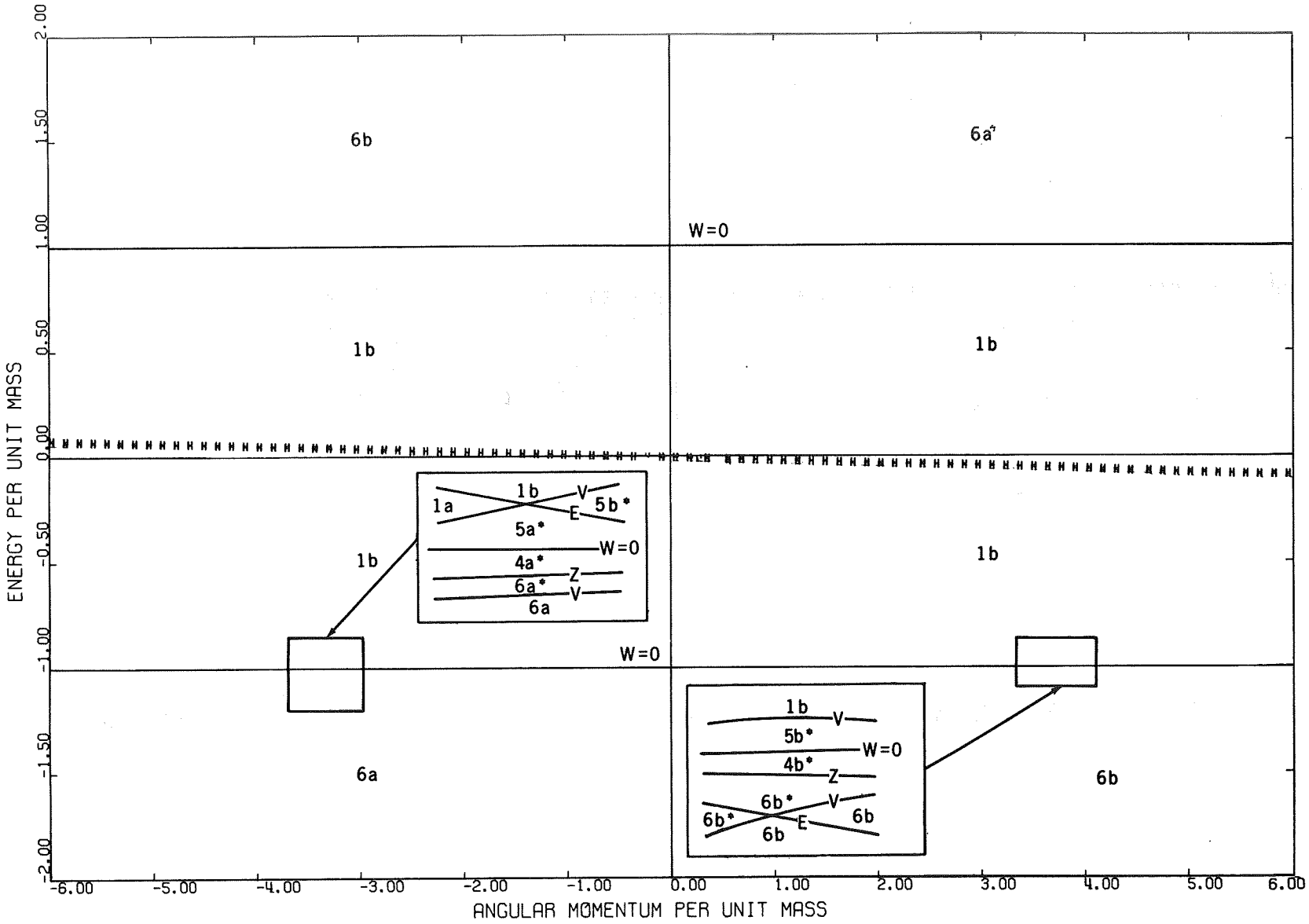

Figure C36—Master diagram for $a = 80.0$, $\beta = 2.0$.

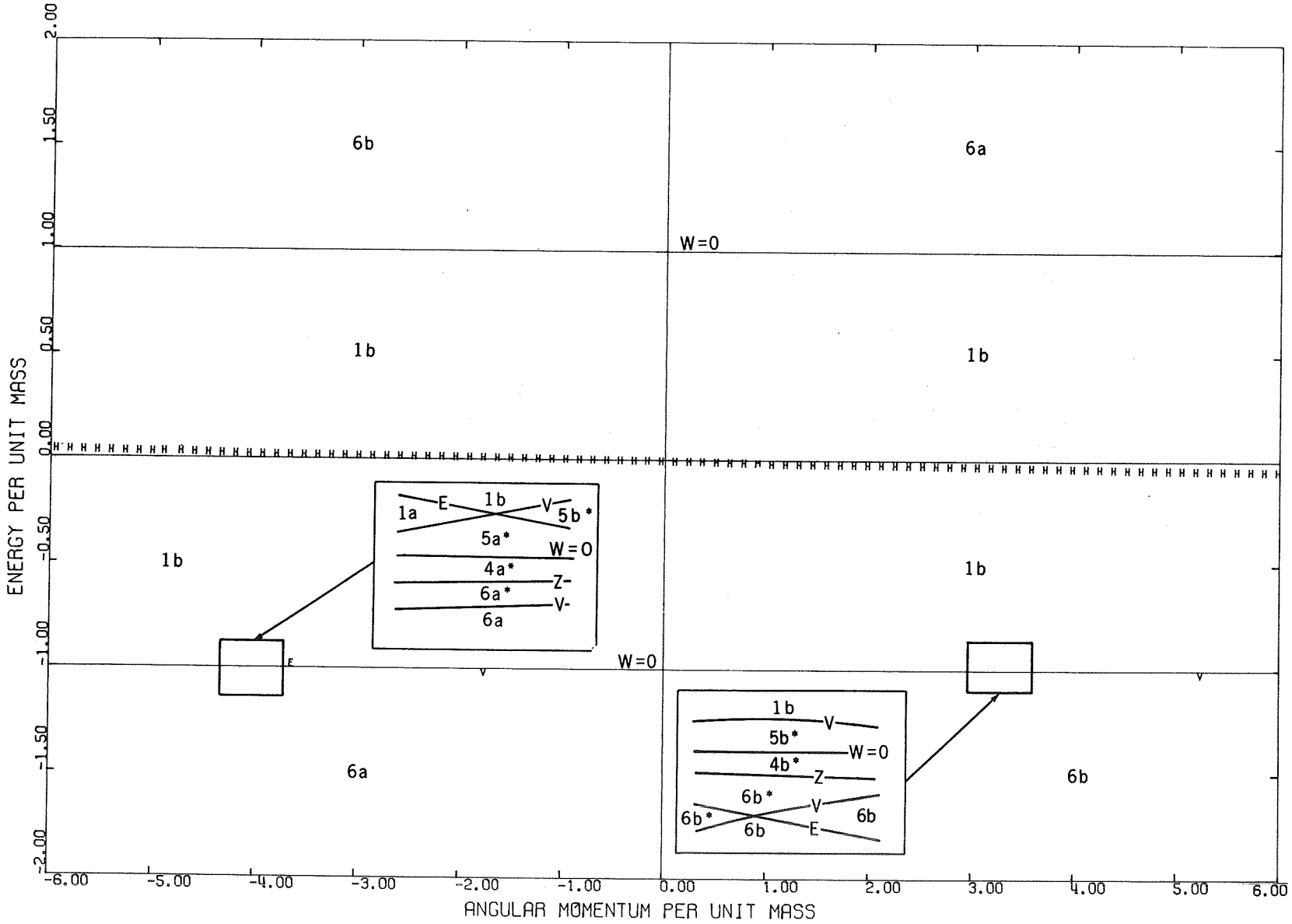

Figure C37—Master diagram for $a = 90.0$, $\beta = 2.0$.

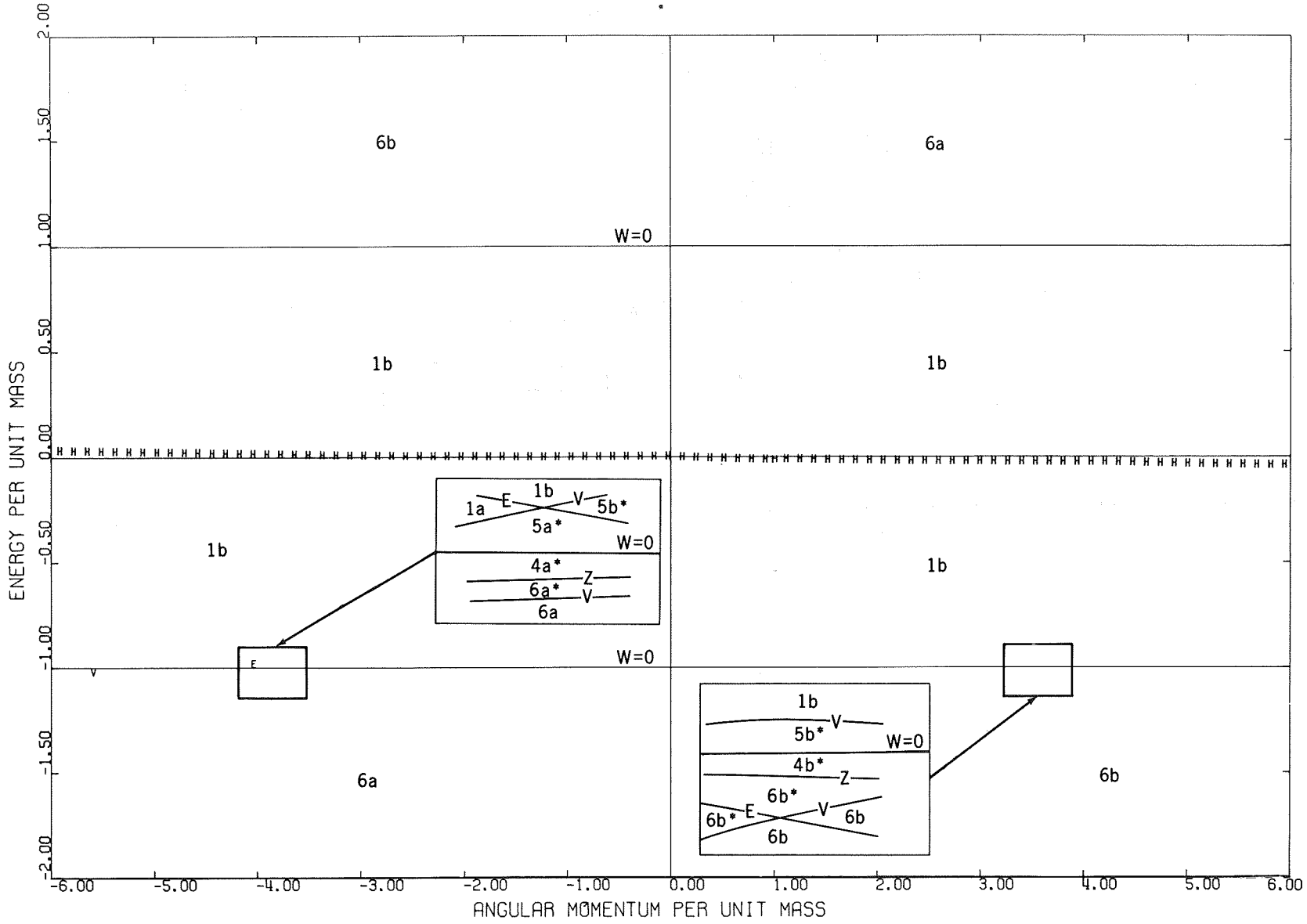

Figure C38—Master diagram for $a = 100.0$, $\beta = 2.0$.

Appendix D

QUALITATIVE SOLUTIONS IN REGIONS OF MASTER DIAGRAMS FOR $0 < a < 1$, $a = 1$, AND $1 < a < \infty$

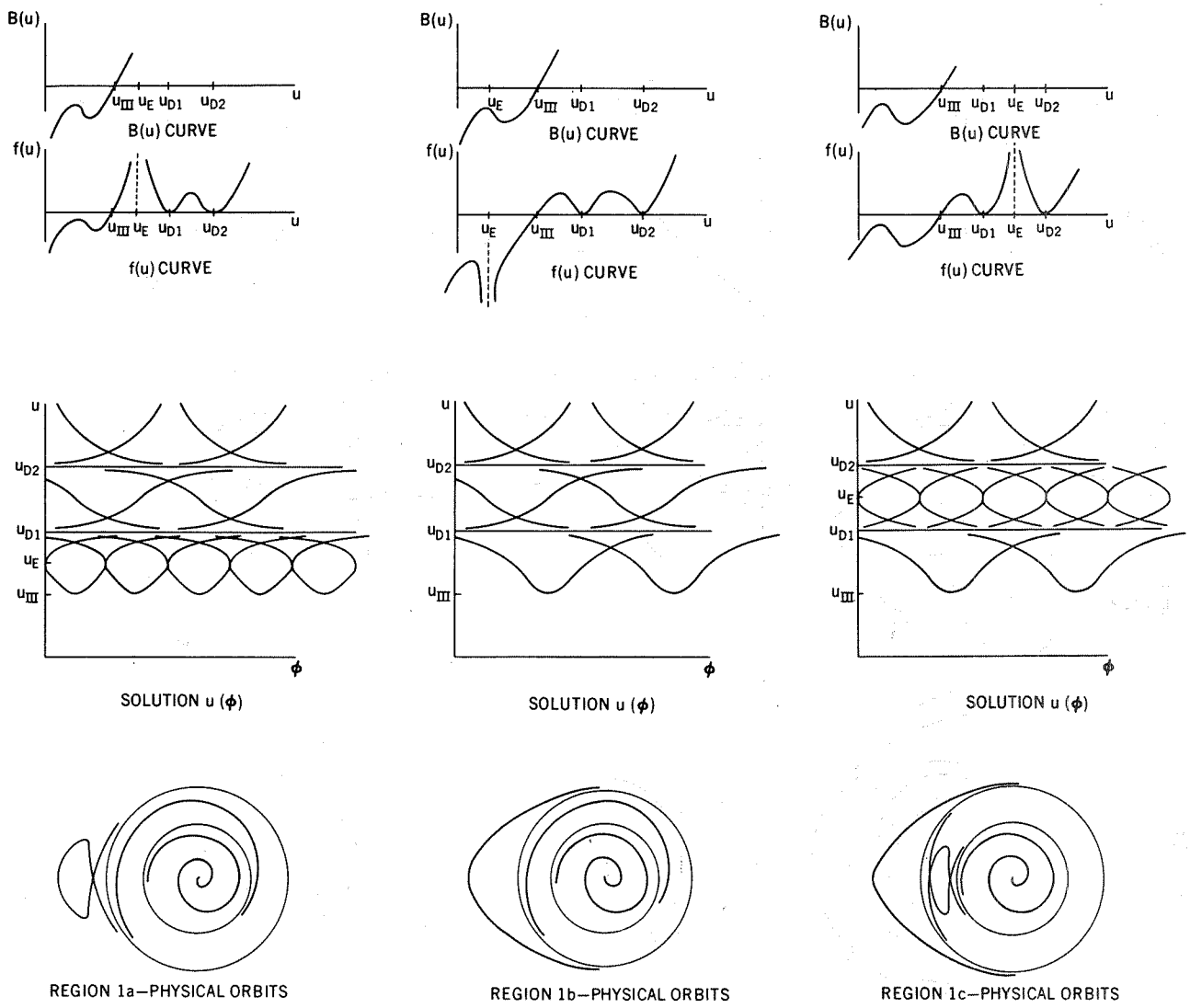

Figure D1—Qualitative solutions in region 1 for $0 < a < 1$.

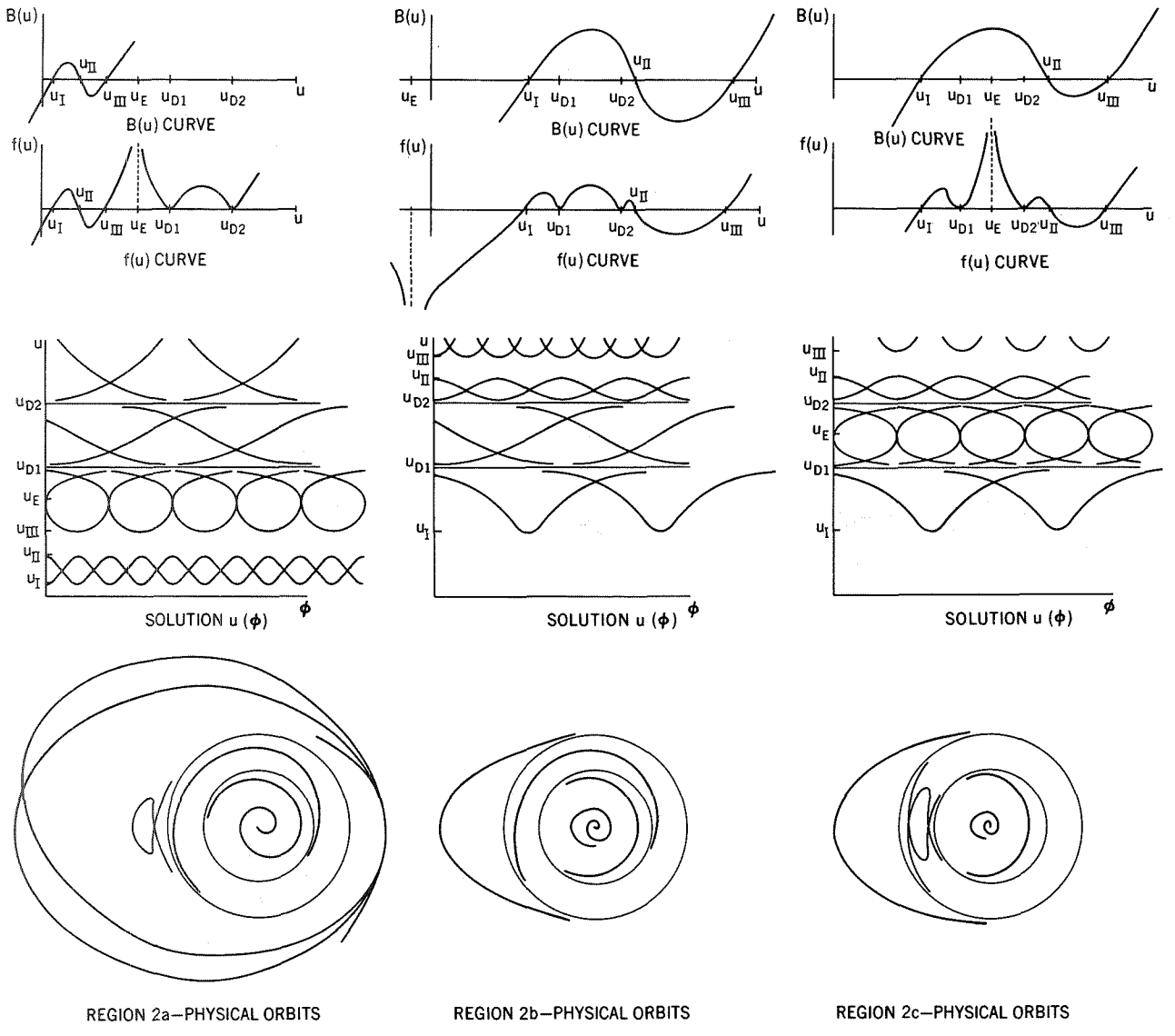

Figure D2—Qualitative solutions in region 2 for $0 < a < 1$.

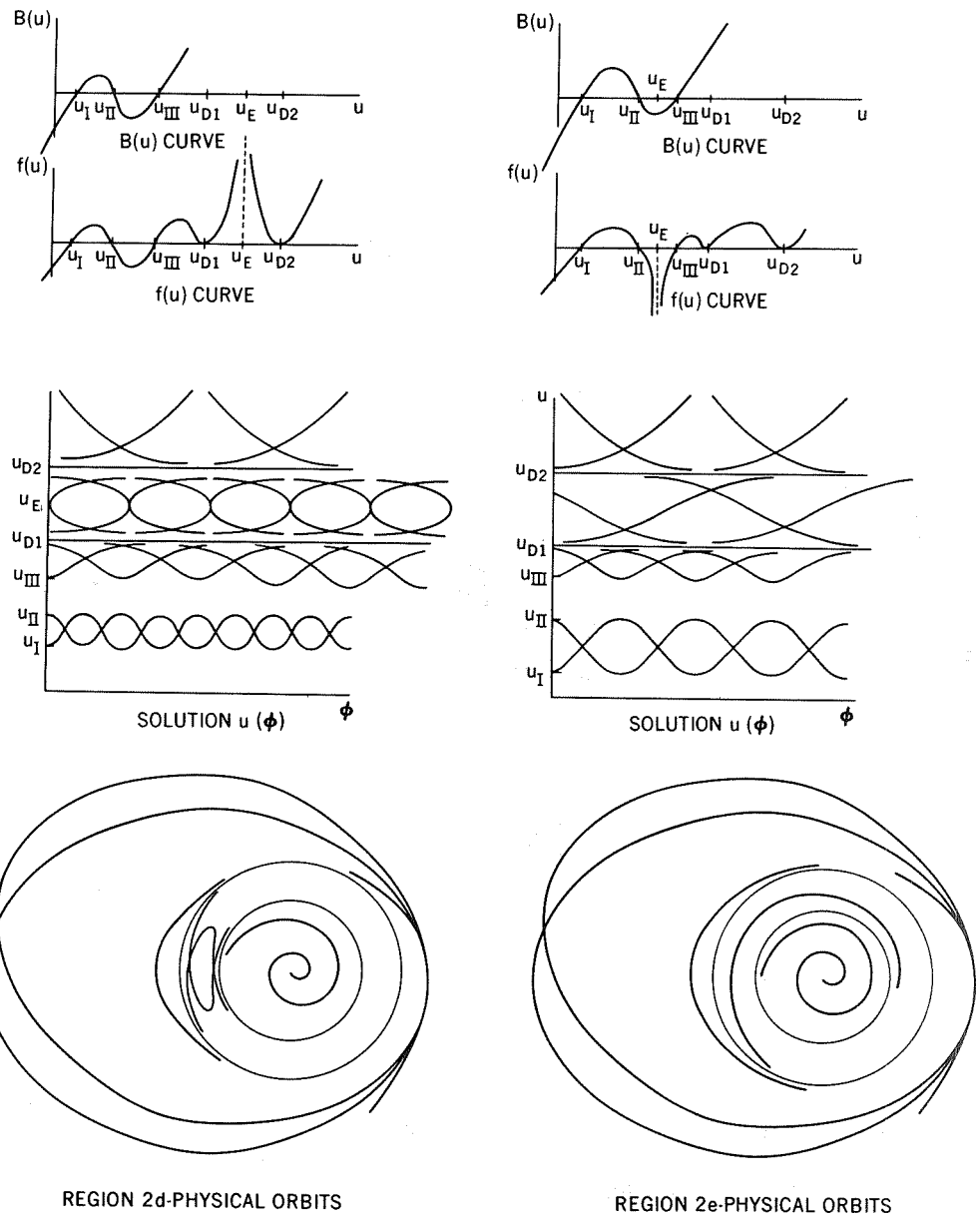

Figure D2 (concluded)—Qualitative solutions in region 2 for $0 < a < 1$.

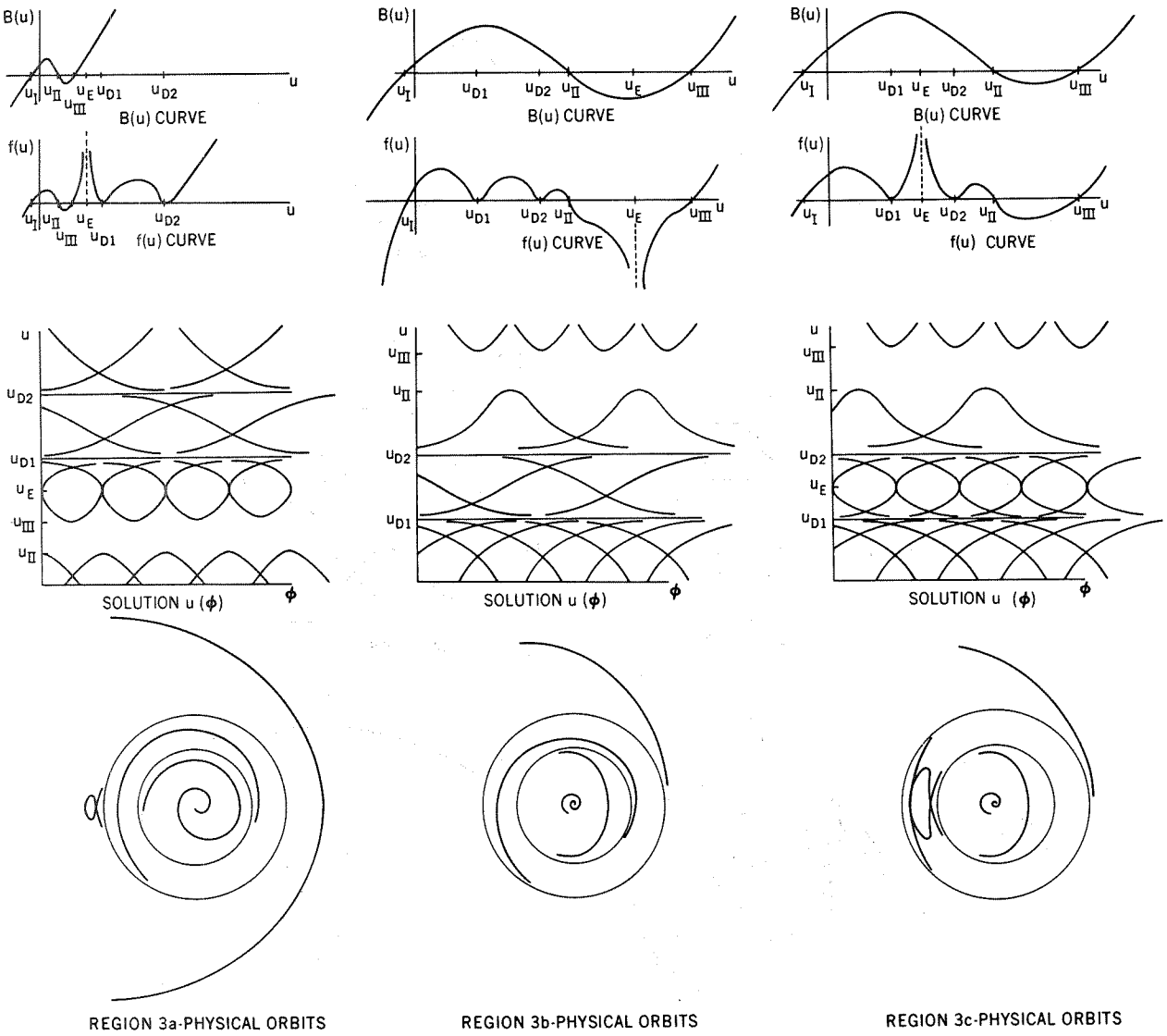

Figure D3--Qualitative solutions in region 3 for $0 < a < 1$.

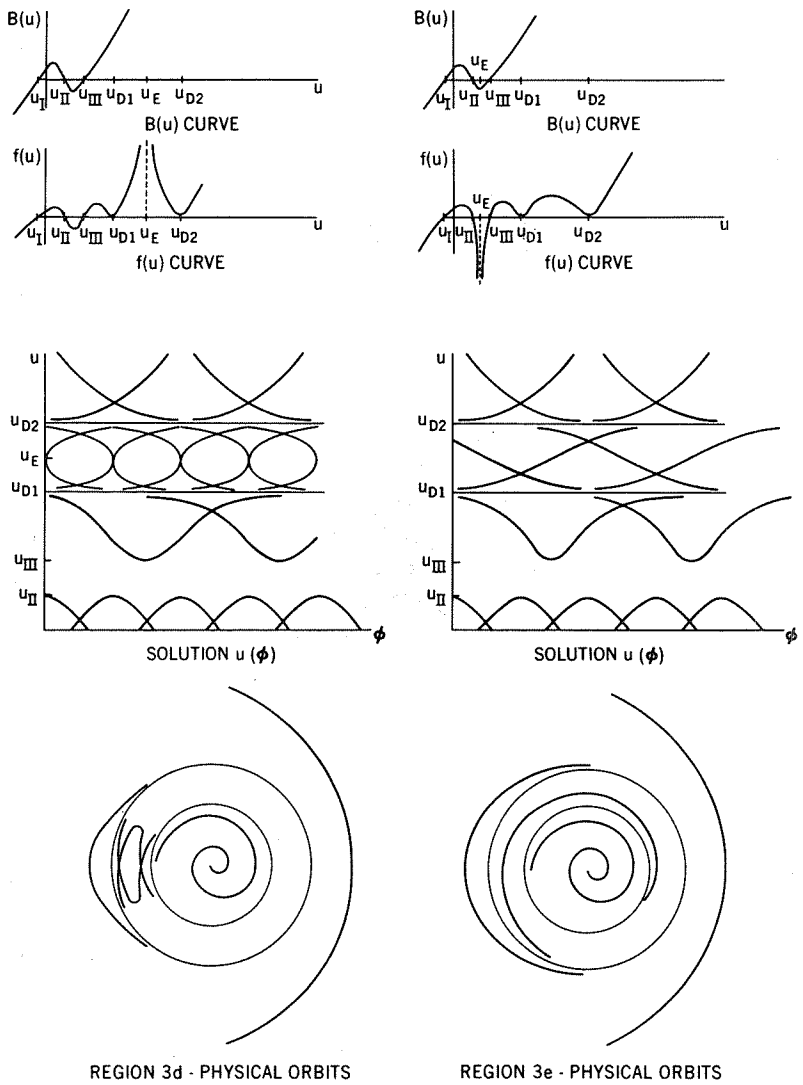

Figure D3 (concluded)—Qualitative solutions in region 3 for $0 < a < 1$.

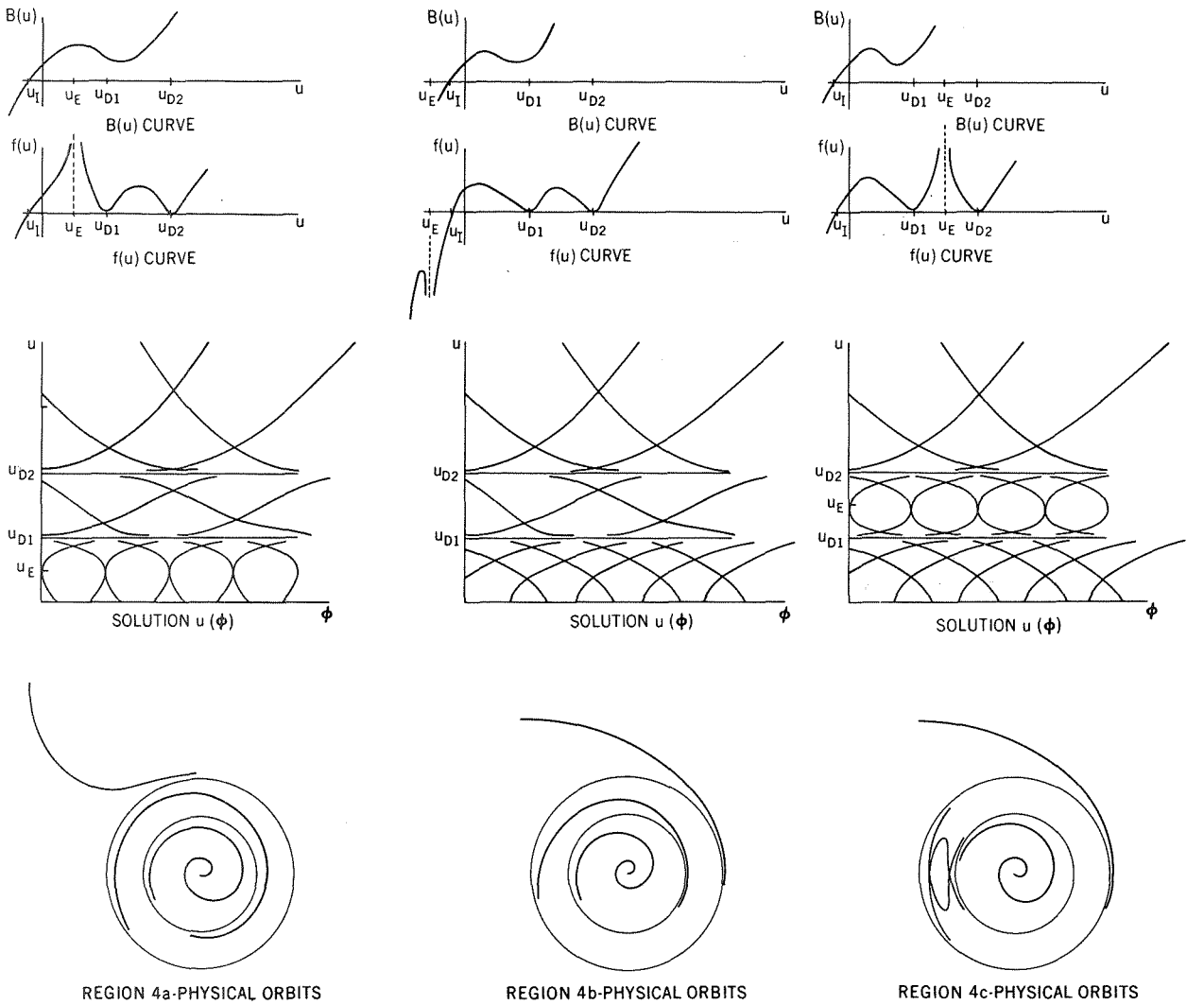

Figure D4—Qualitative solutions in region 4 for $0 < a < 1$.

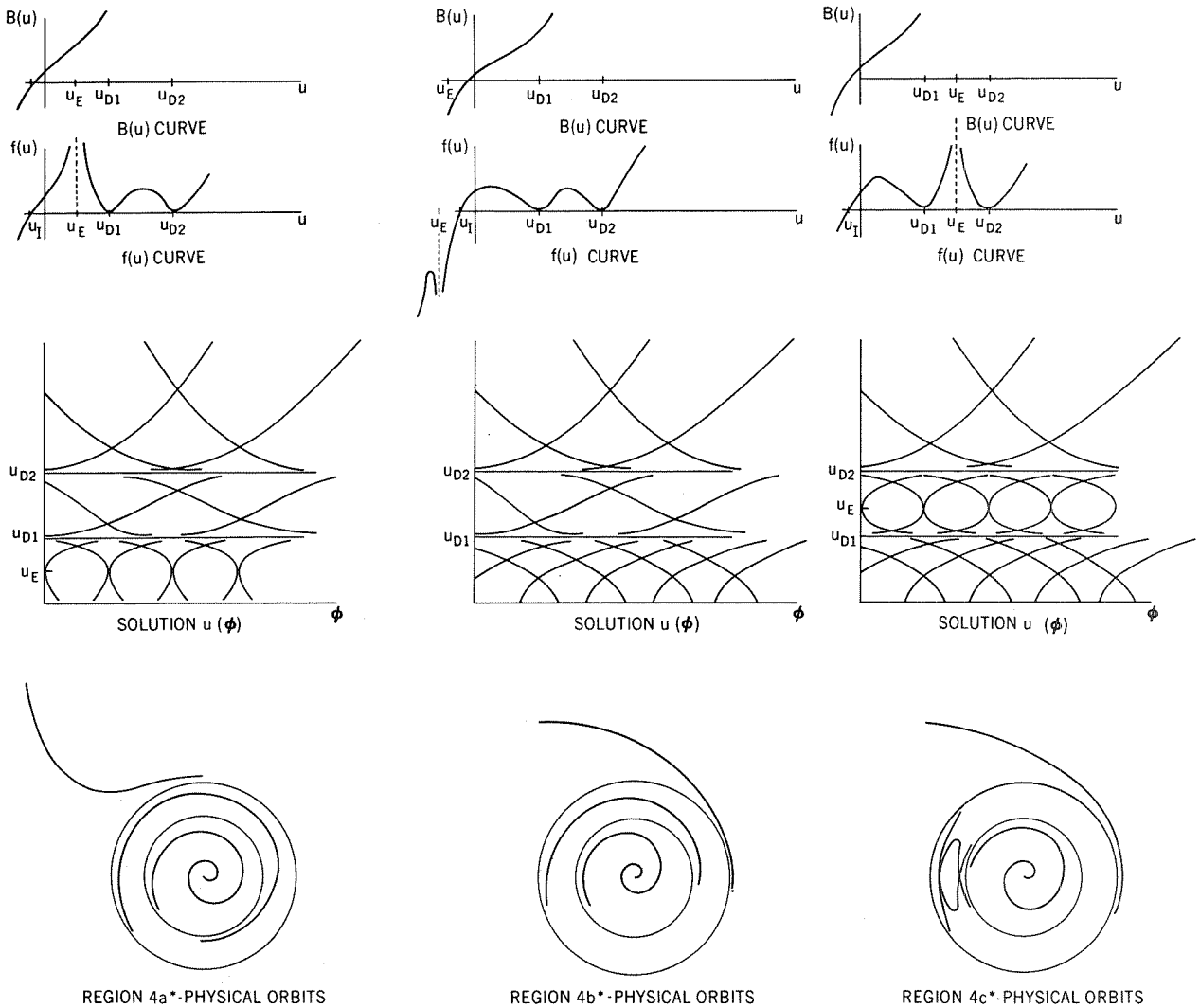

Figure D5—Qualitative solutions in region 4* for $0 < a < 1$.

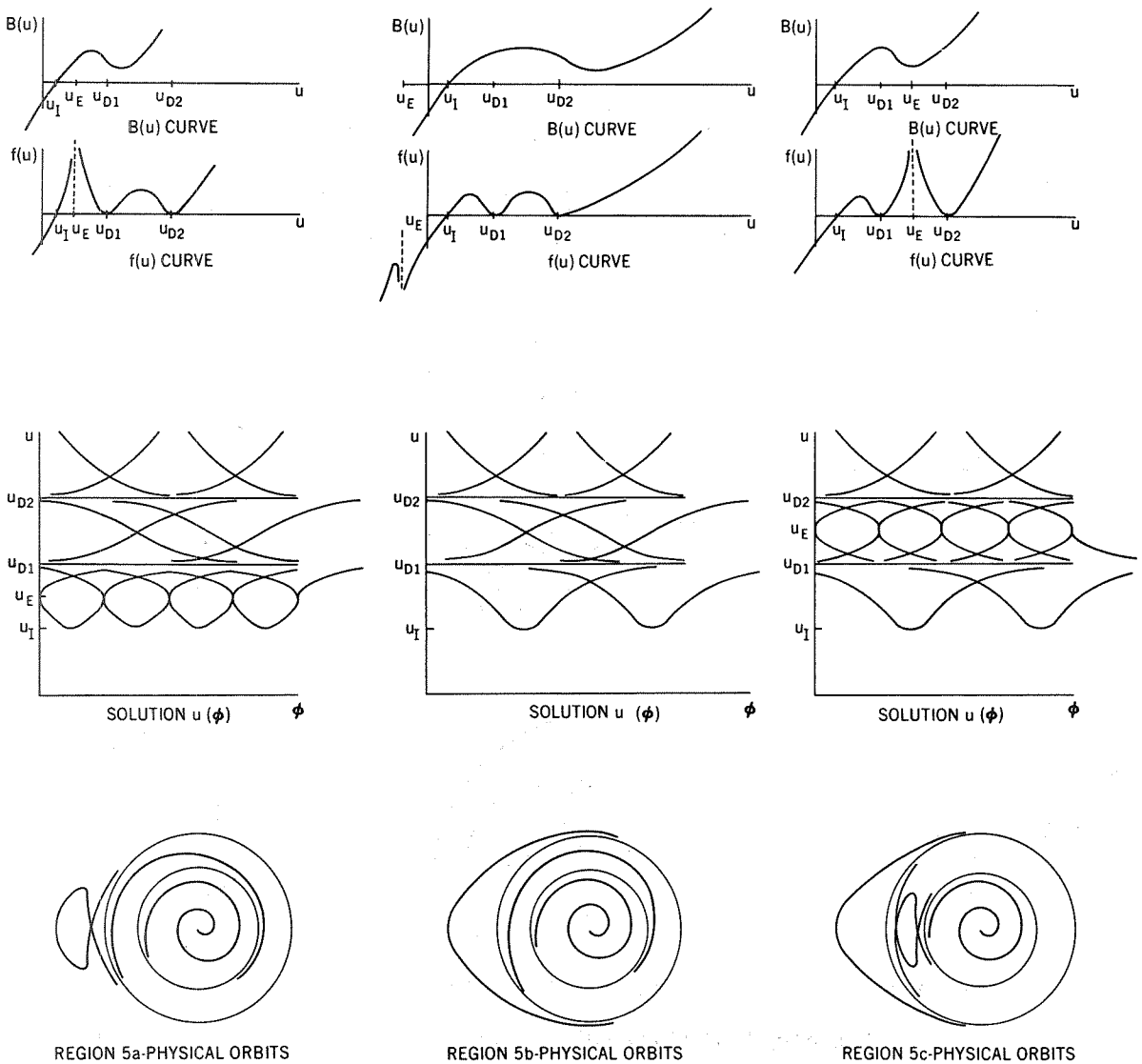

Figure D6—Qualitative solutions in region 5 for $0 < a < 1$.

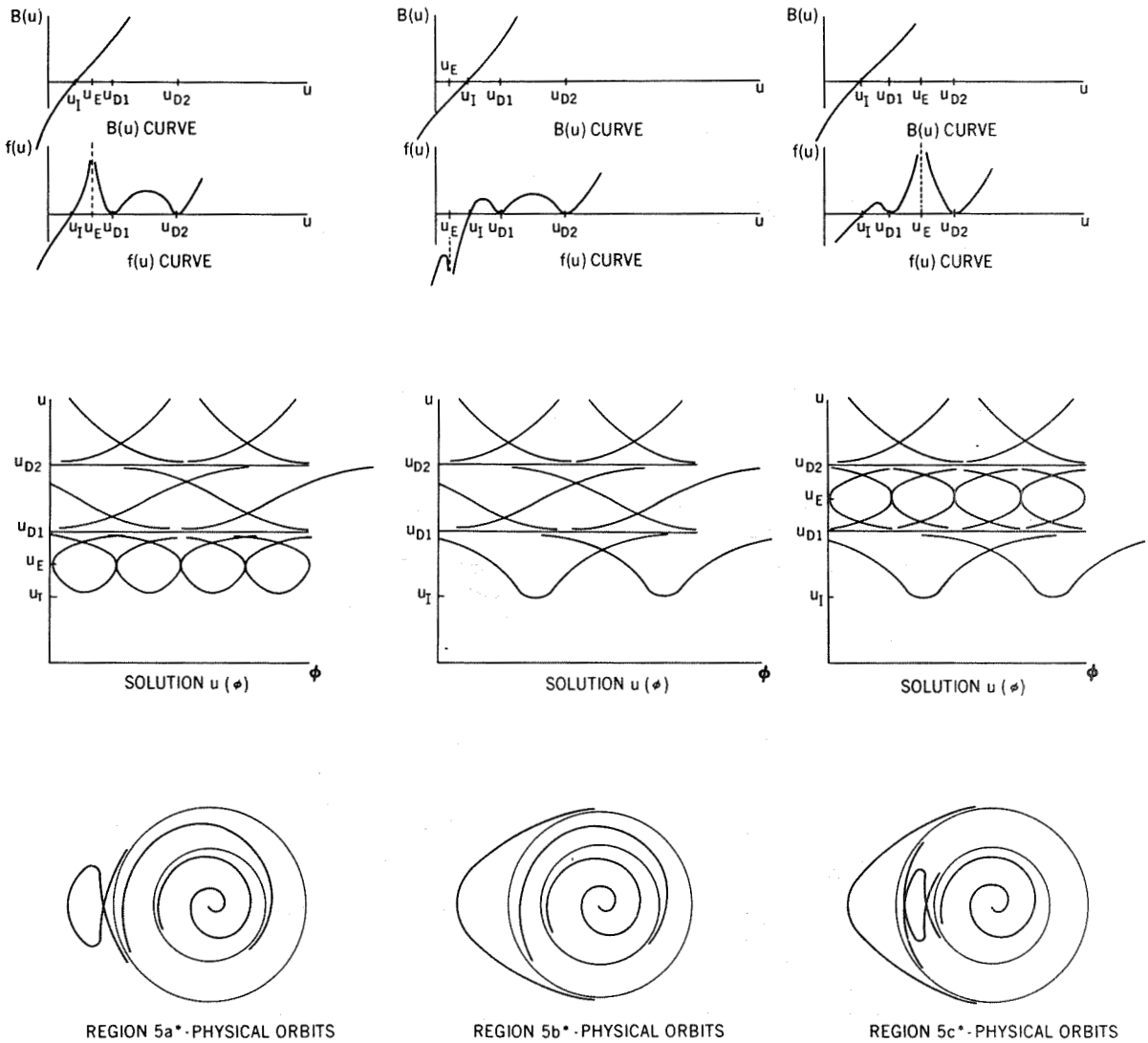

REGION 5a*-PHYSICAL ORBITS

REGION 5b*-PHYSICAL ORBITS

REGION 5c*-PHYSICAL ORBITS

Figure D7—Qualitative solutions in region 5* for $0 < a < 1$.

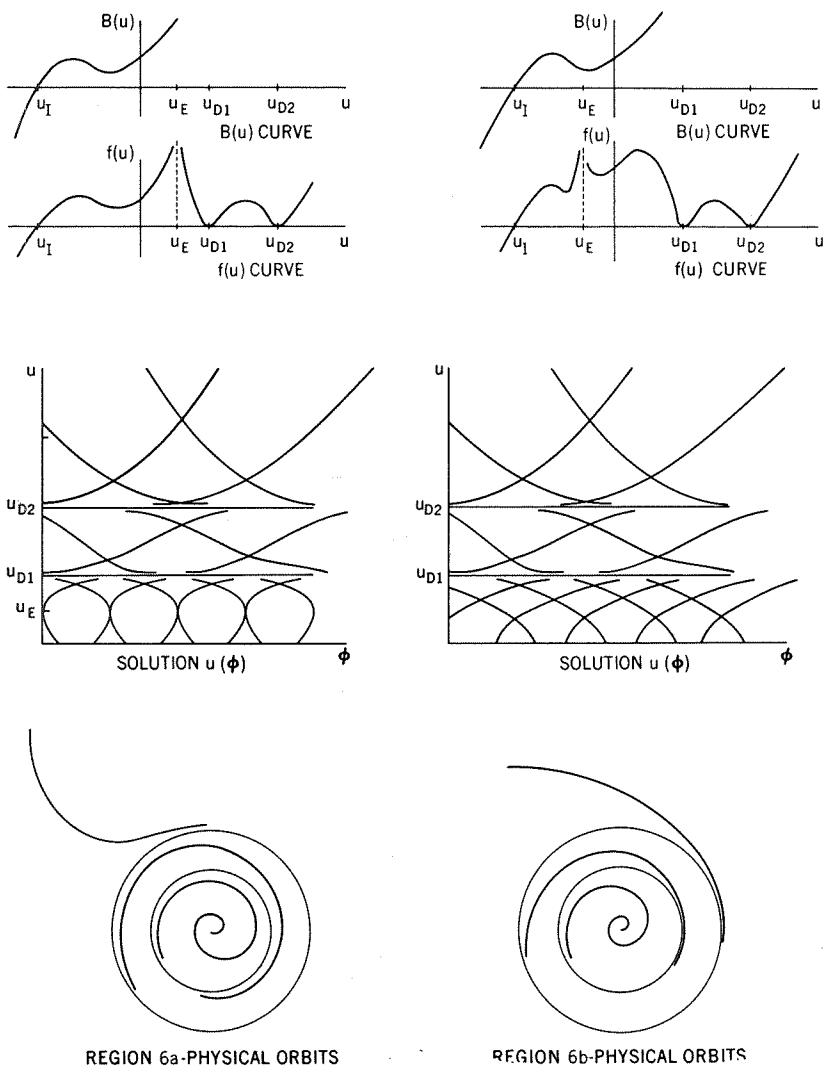

Figure D8—Qualitative solutions in region 6 for $0 < a < 1$.

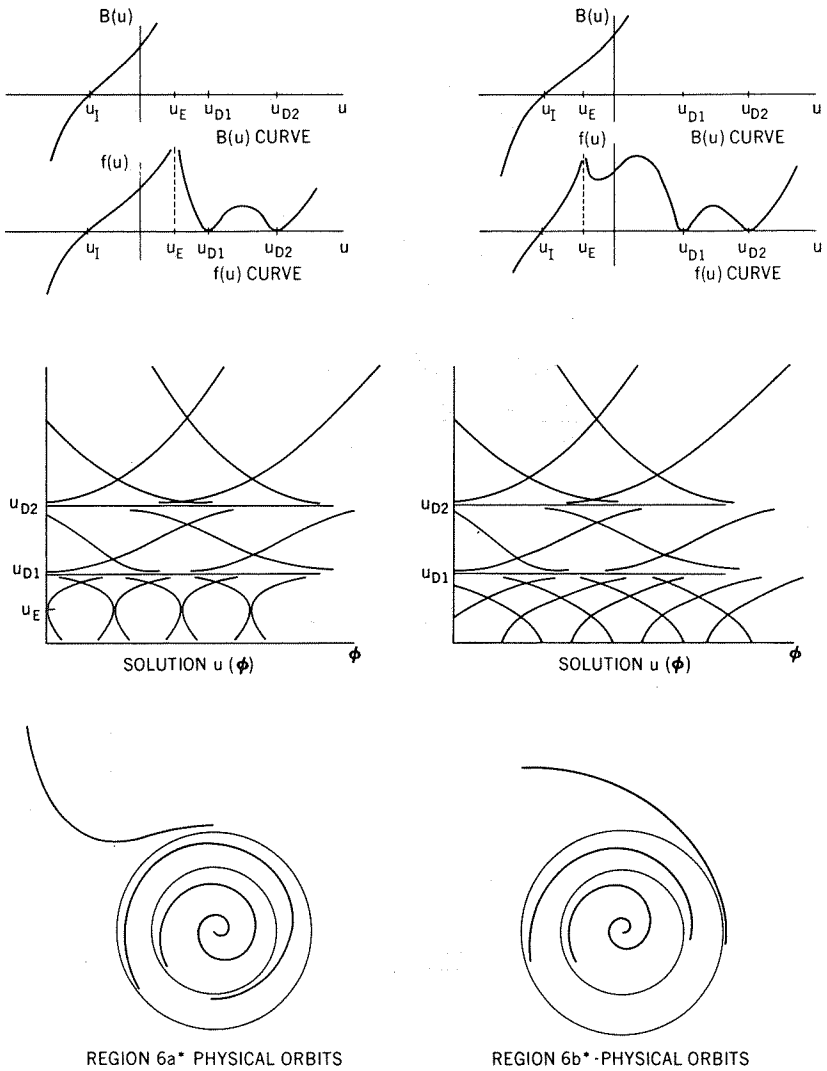

Figure D9—Qualitative solutions in region 6* for $0 < a < 1$.

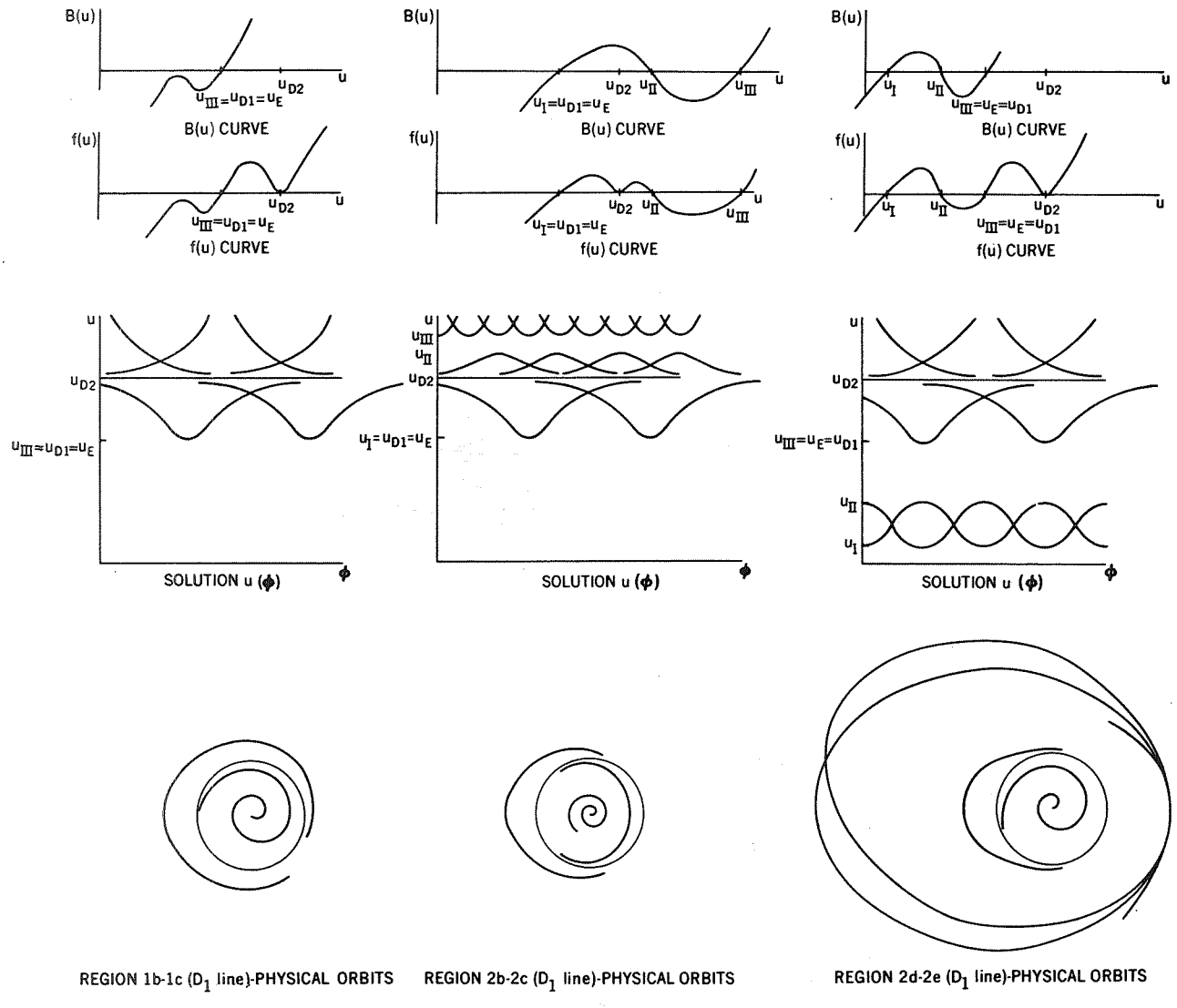

Figure D10—Qualitative solutions on D_1 line for $0 < a < 1$.

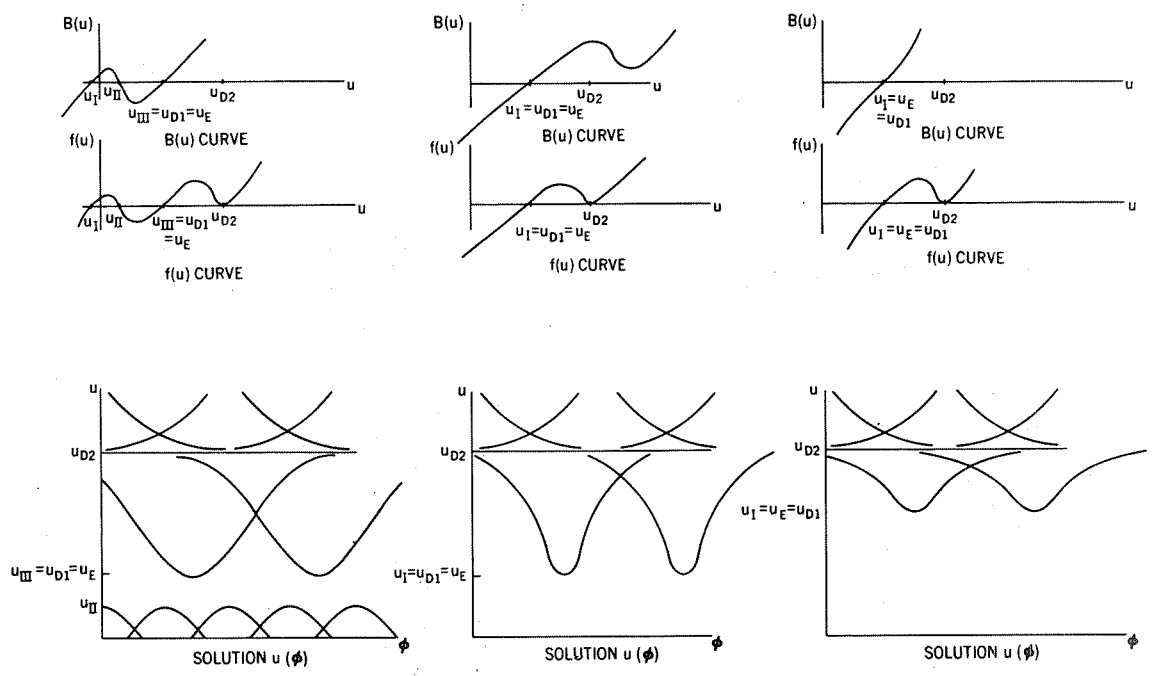

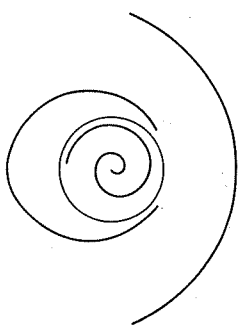

REGION 3d-3e (D_1 line)-PHYSICAL ORBITS

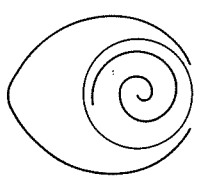

REGION 5b-5c (D_1 line)-PHYSICAL ORBITS

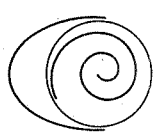

REGION 5b*-5c* (D_1 line)-PHYSICAL ORBITS

Figure D10 (concluded)—Qualitative solutions on D_1 line for $0 < a < 1$.

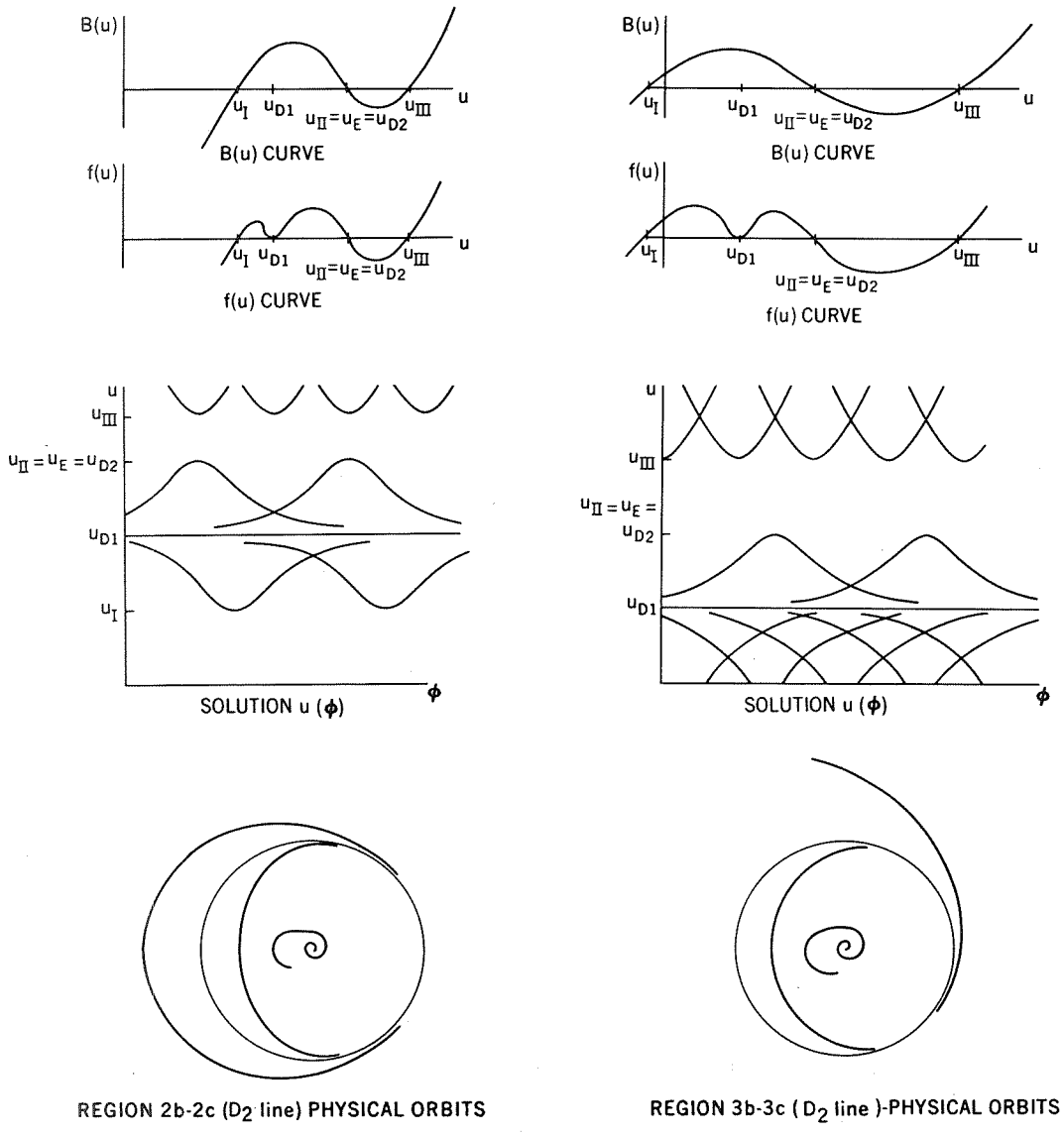

Figure D11—Qualitative solutions on D_2 line for $0 < a < 1$.

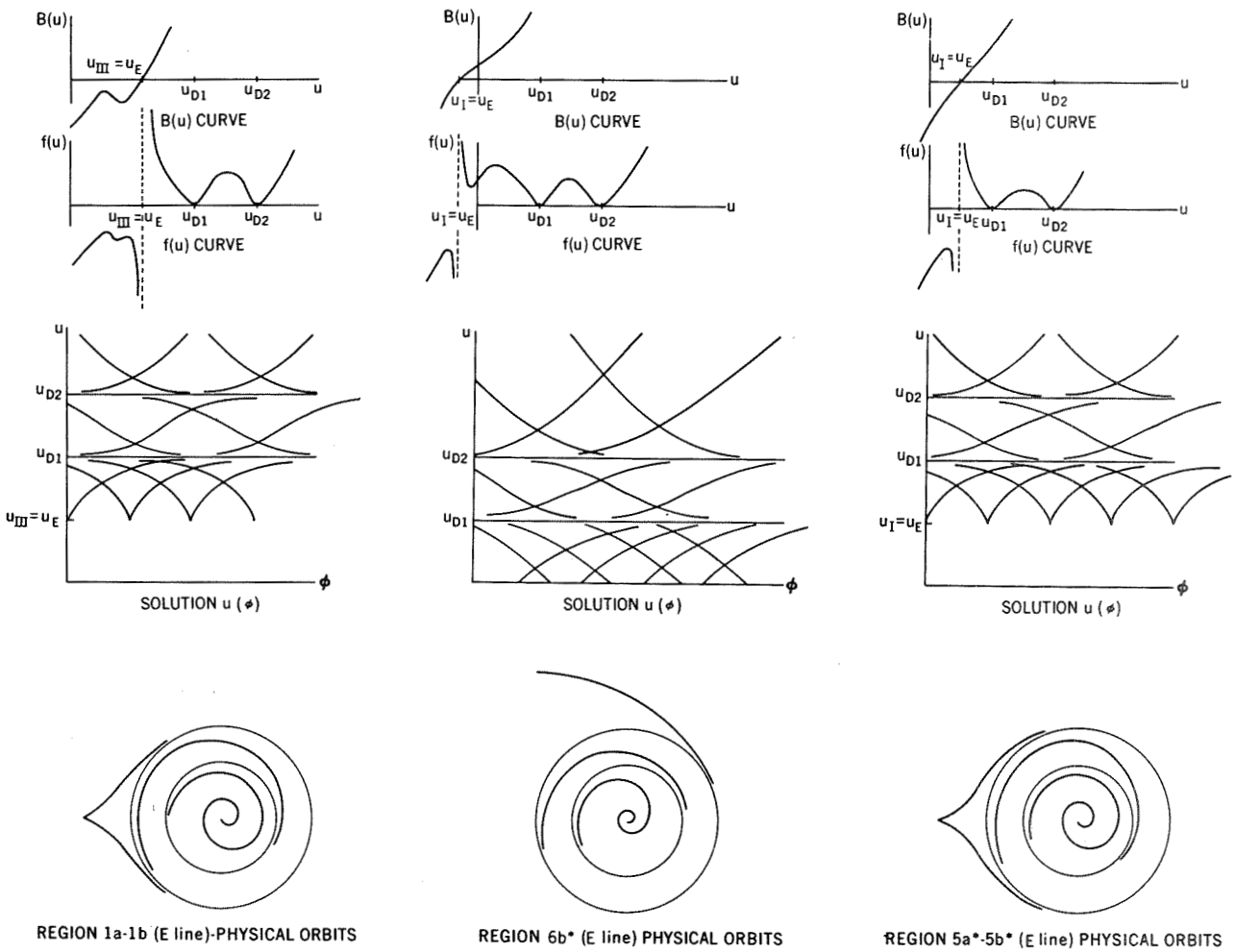

Figure D12—Qualitative solutions on E line for $0 < a < 1$.

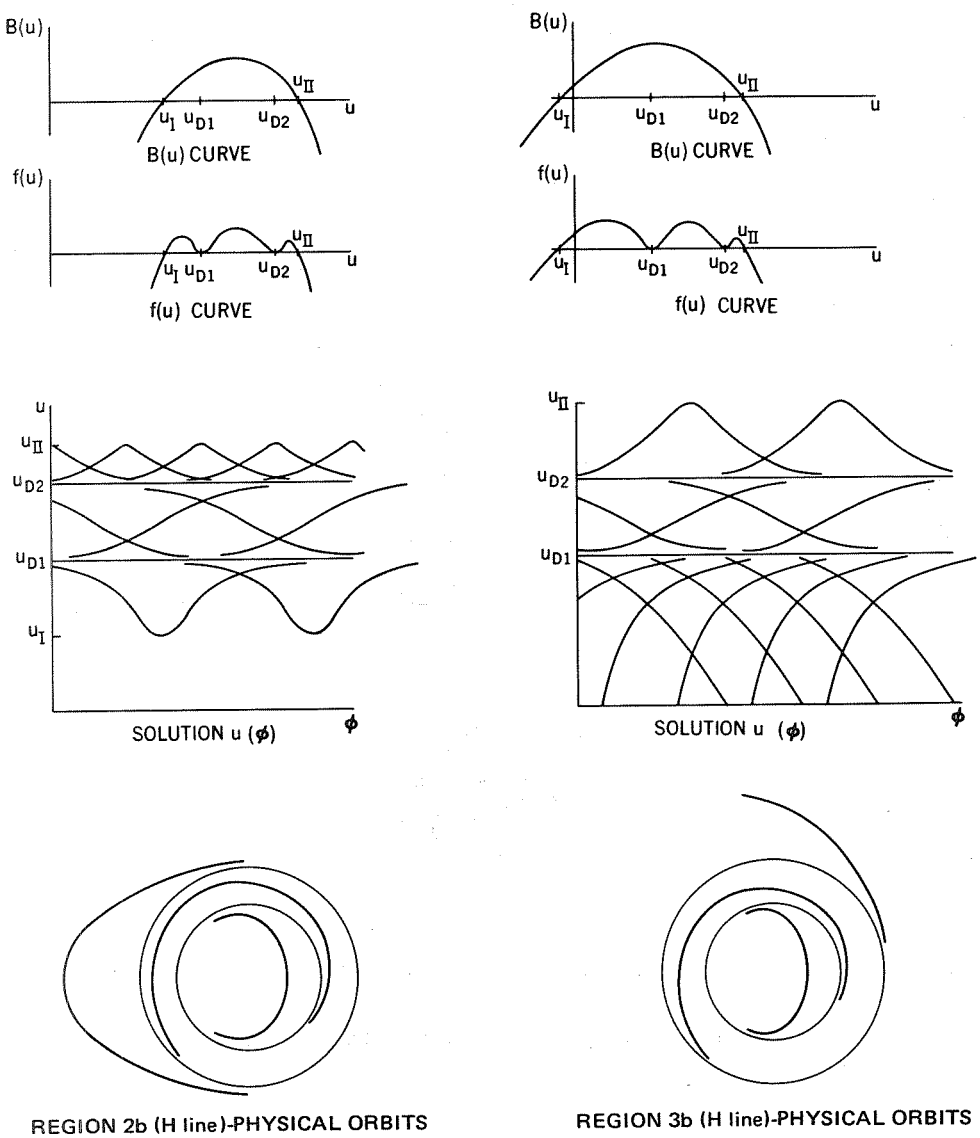

Figure D13—Qualitative solutions on *H* line for $0 < a < 1$.

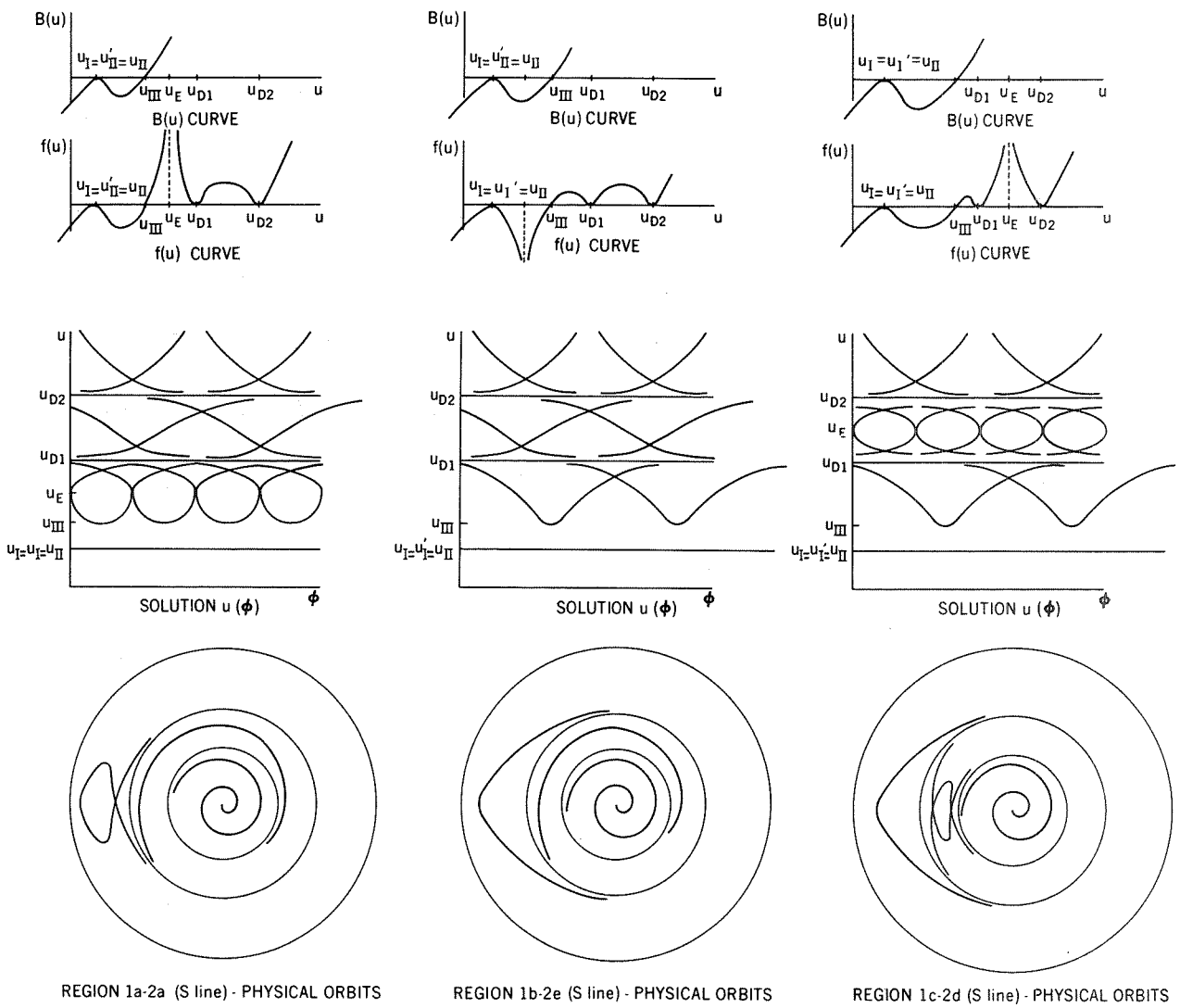

Figure D14—Qualitative solutions on *S* line for $0 < a < 1$.

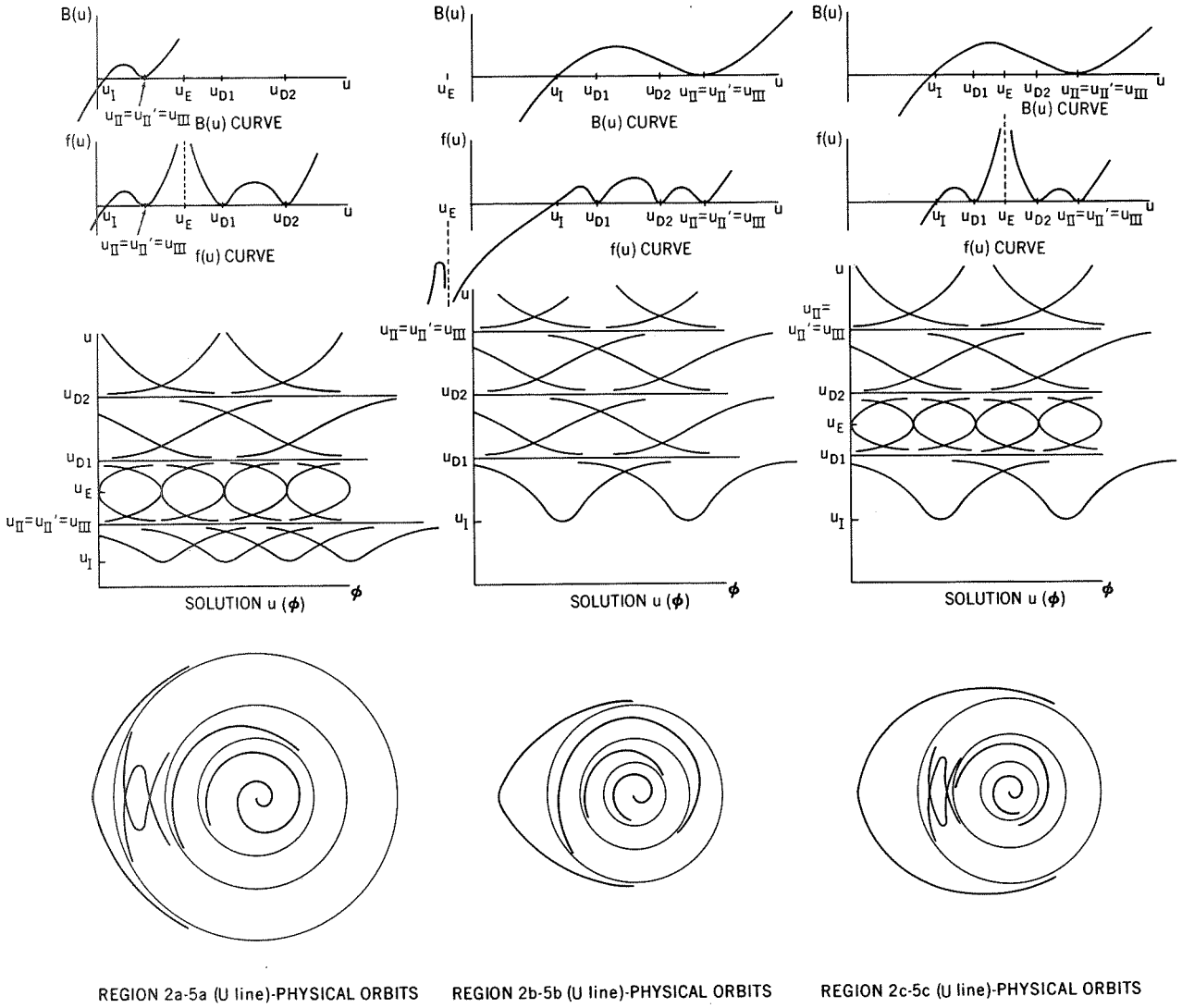

REGION 2a-5a (U line)-PHYSICAL ORBITS

REGION 2b-5b (U line)-PHYSICAL ORBITS

REGION 2c-5c (U line)-PHYSICAL ORBITS

Figure D15—Qualitative solutions on *U* line for $0 < a < 1$.

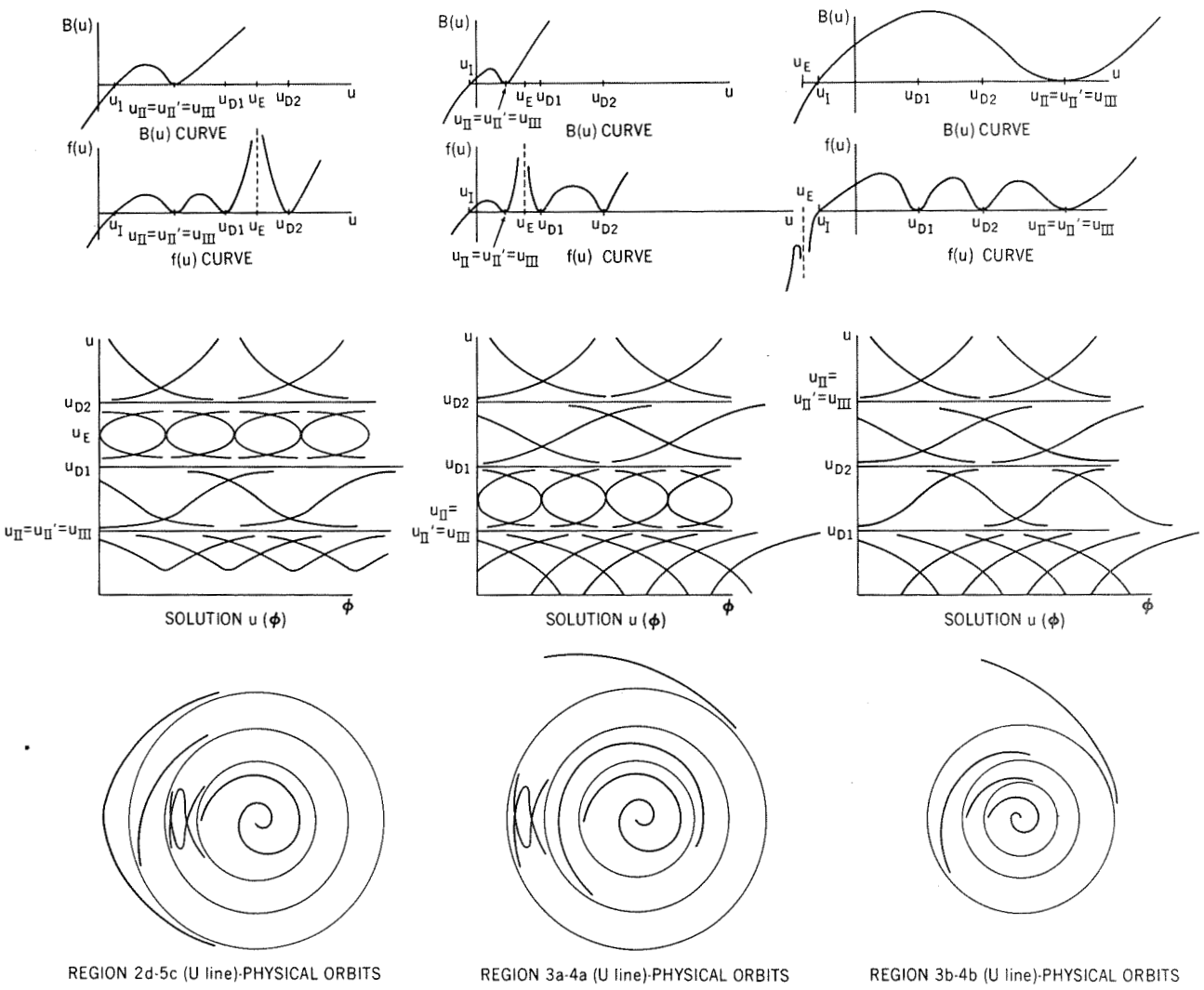

Figure D15 (continued)—Qualitative solutions on U line for $0 < a < 1$.

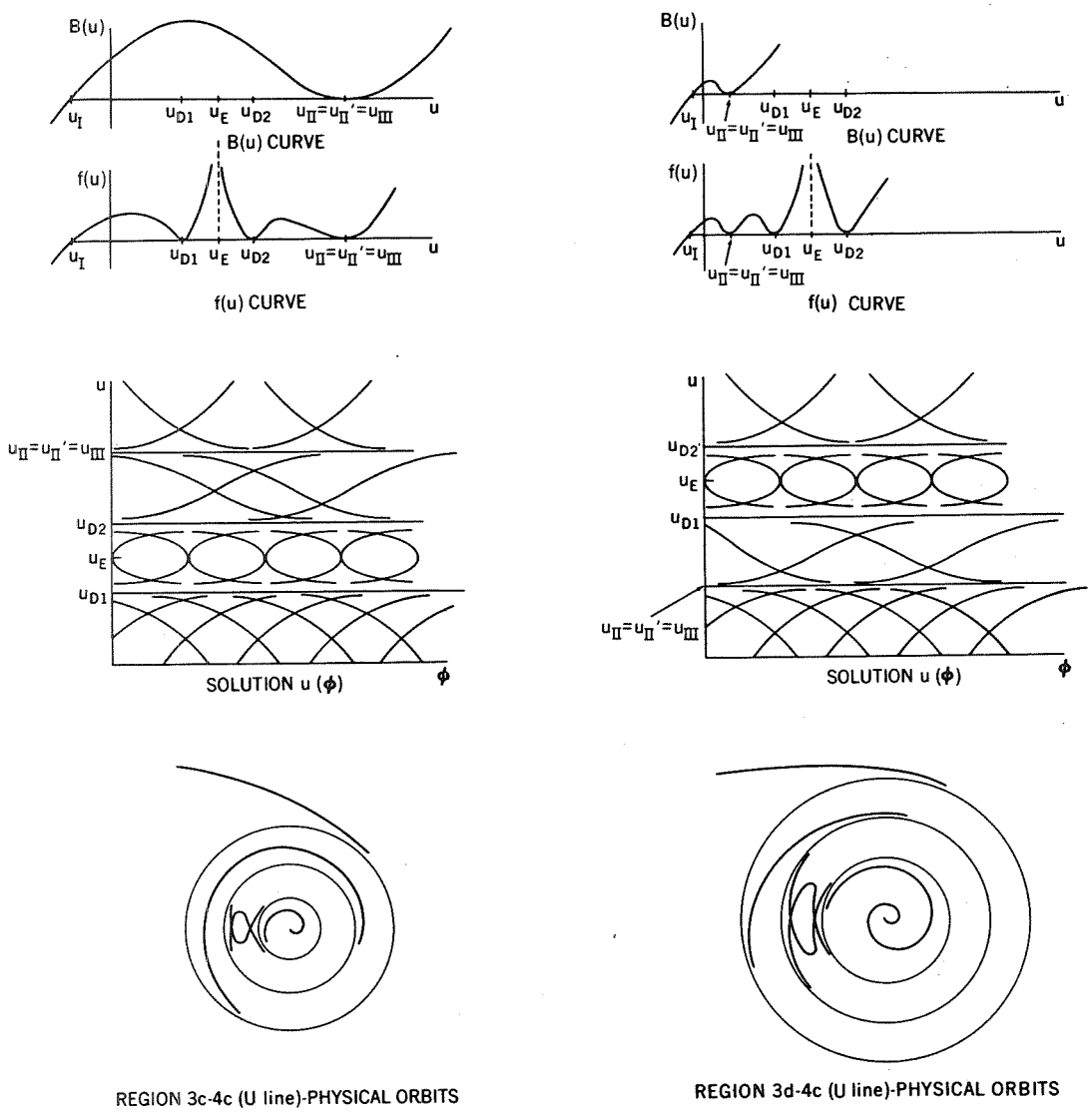

Figure D15 (concluded)—Qualitative solutions on U line for $0 < a < 1$.

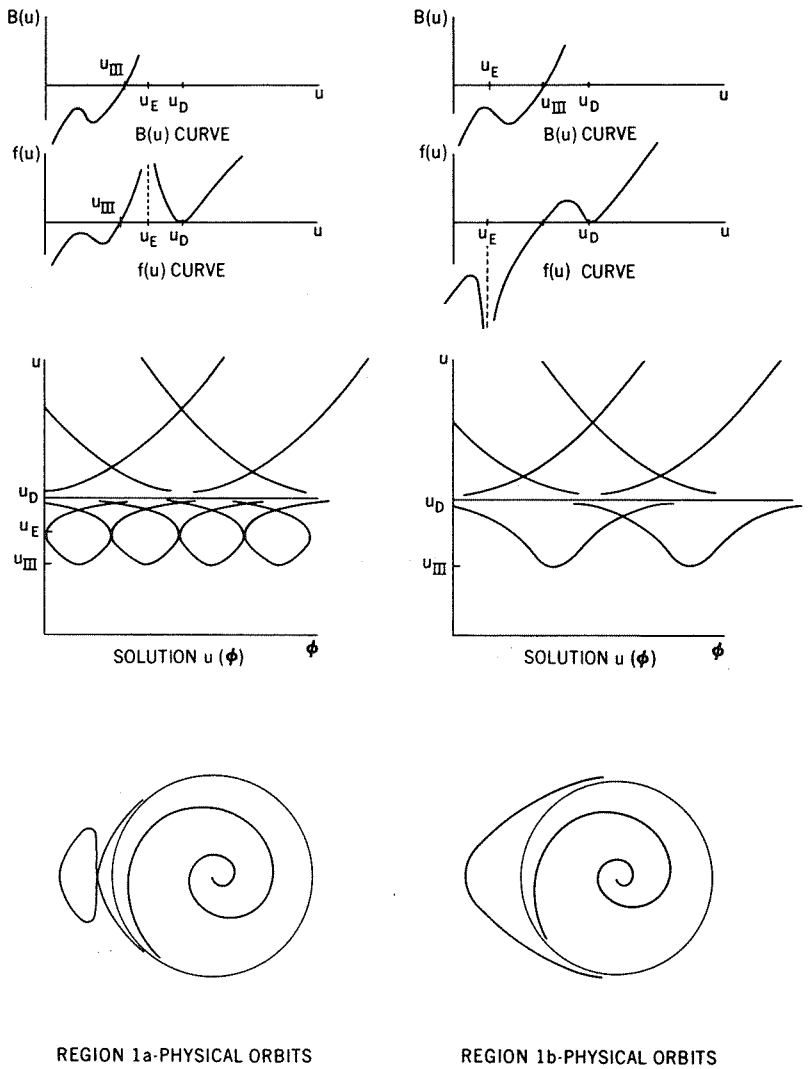

Figure D16—Qualitative solutions in region 1 for $a = 1$.

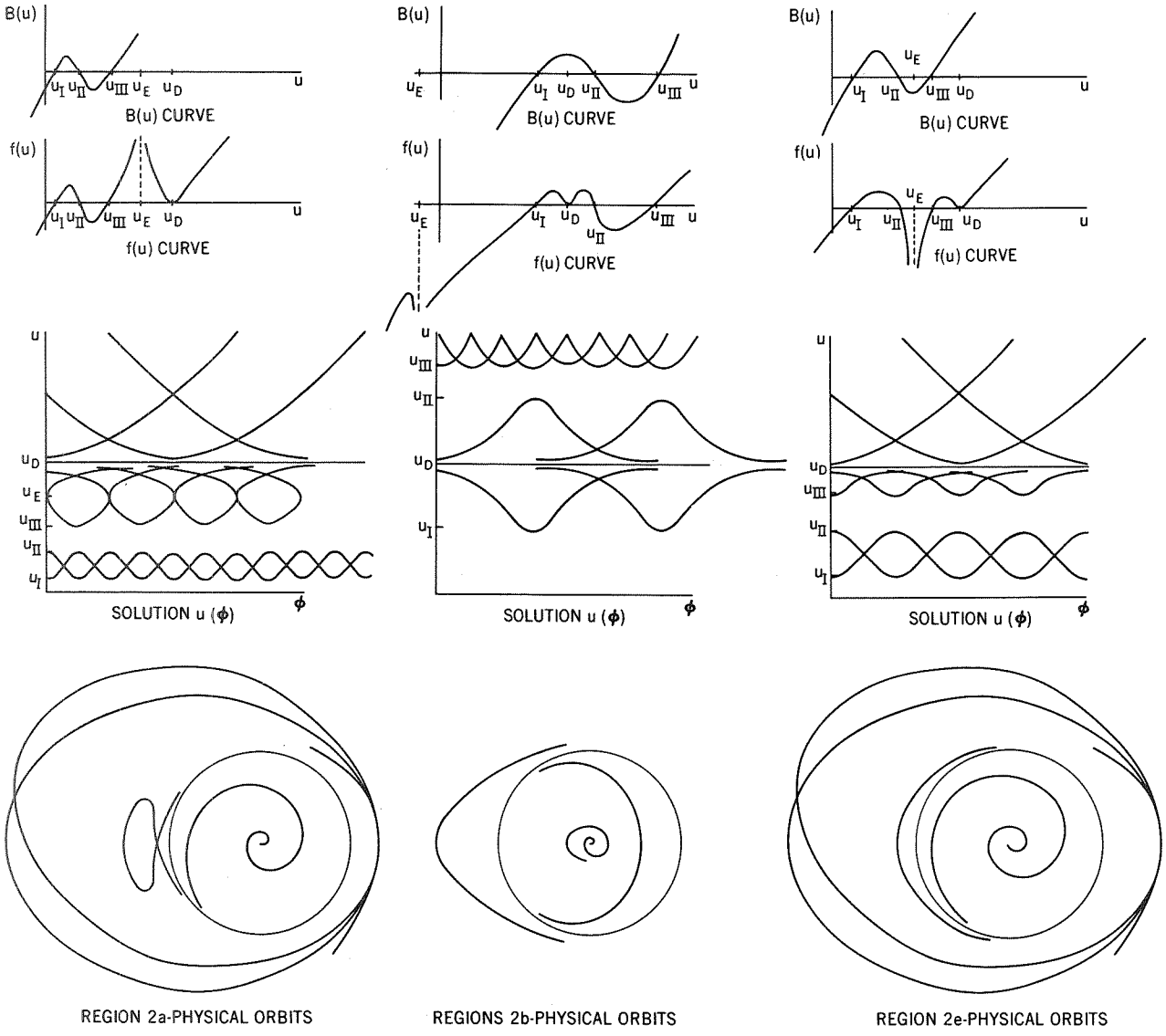

Figure D17—Qualitative solutions in region 2 for $a = 1$.

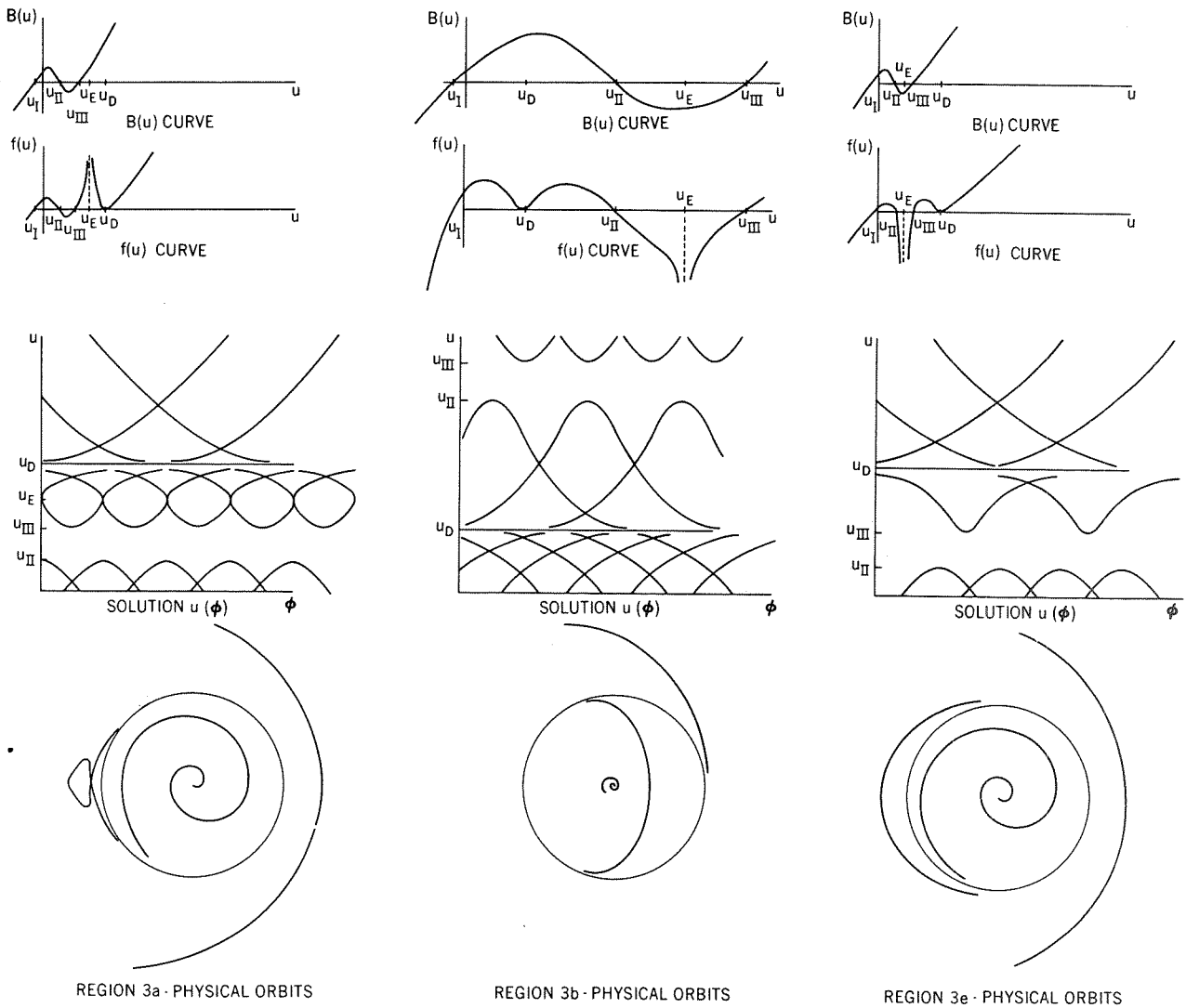

Figure D18—Qualitative solutions in region 3 for $a = 1$.

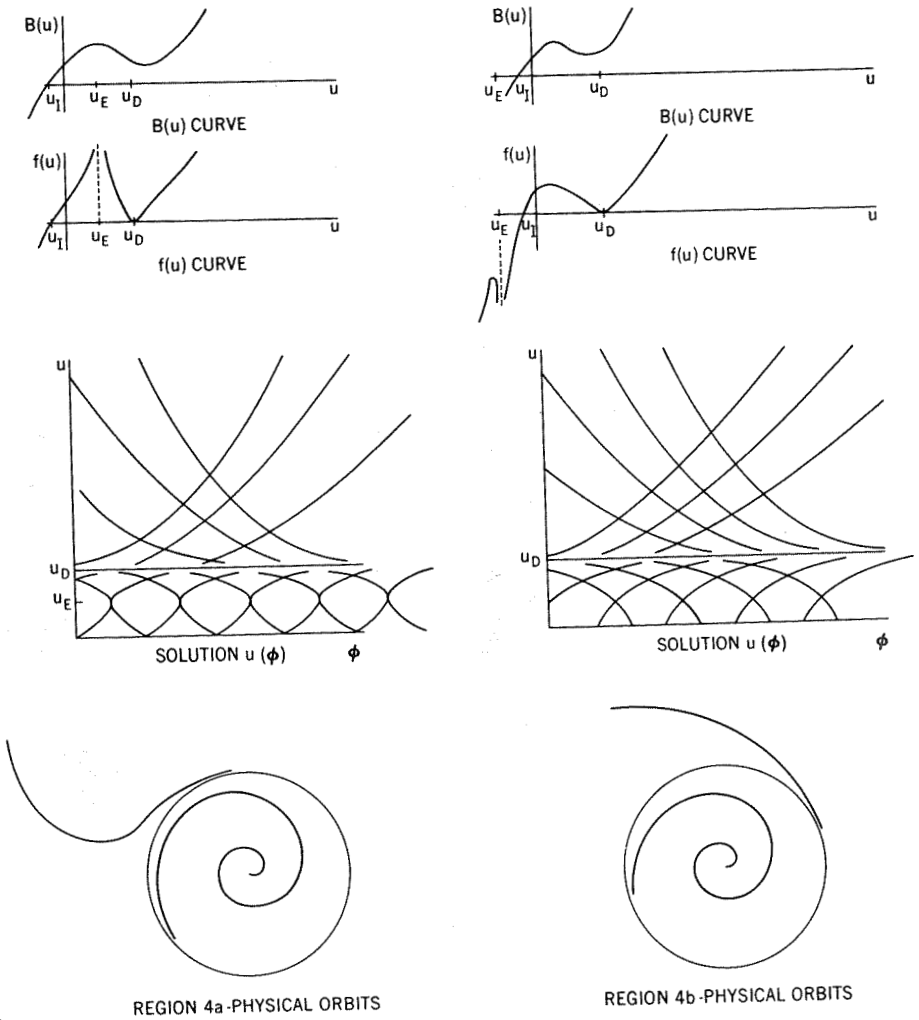

Figure D19—Qualitative solutions in region 4 for $a = 1$.

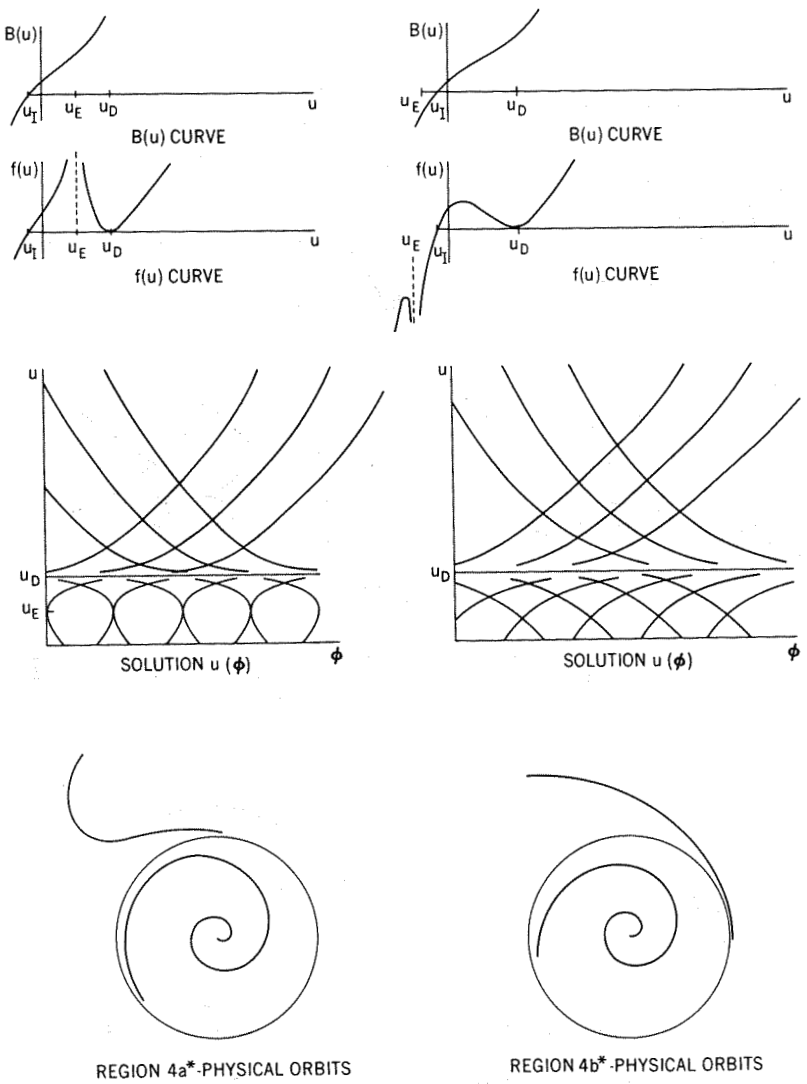

Figure D20—Qualitative solutions in region 4* for $a = 1$.

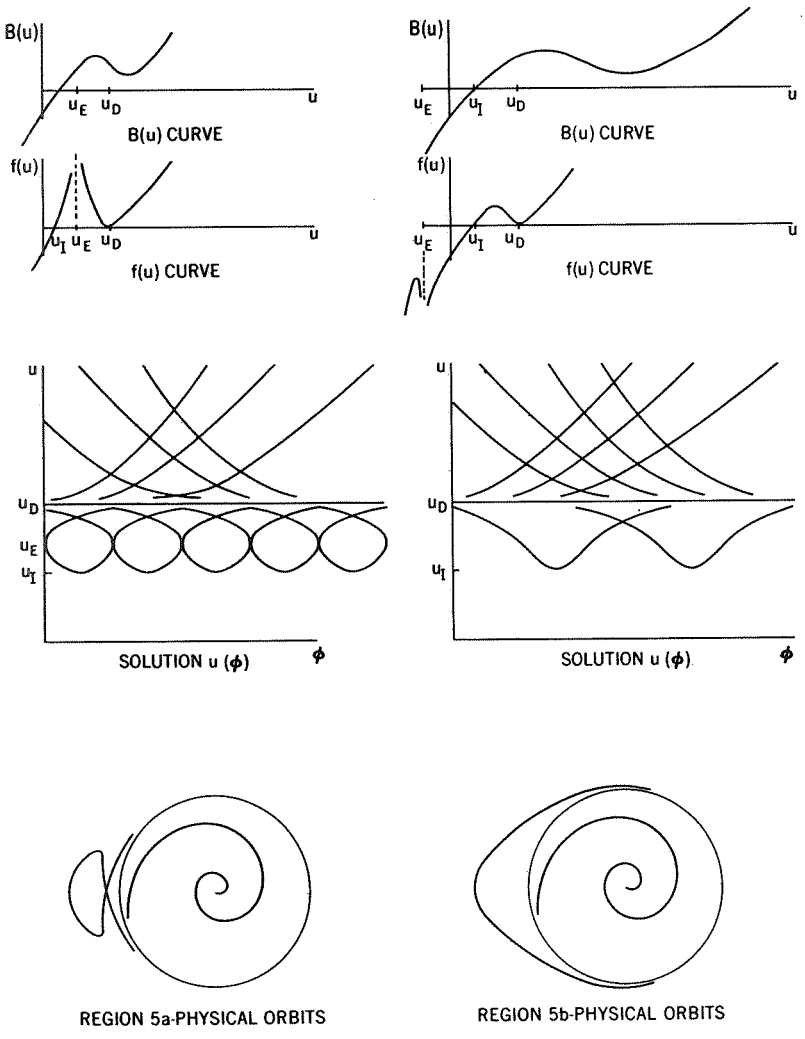

Figure D21—Qualitative solutions in region 5 for $a = 1$.

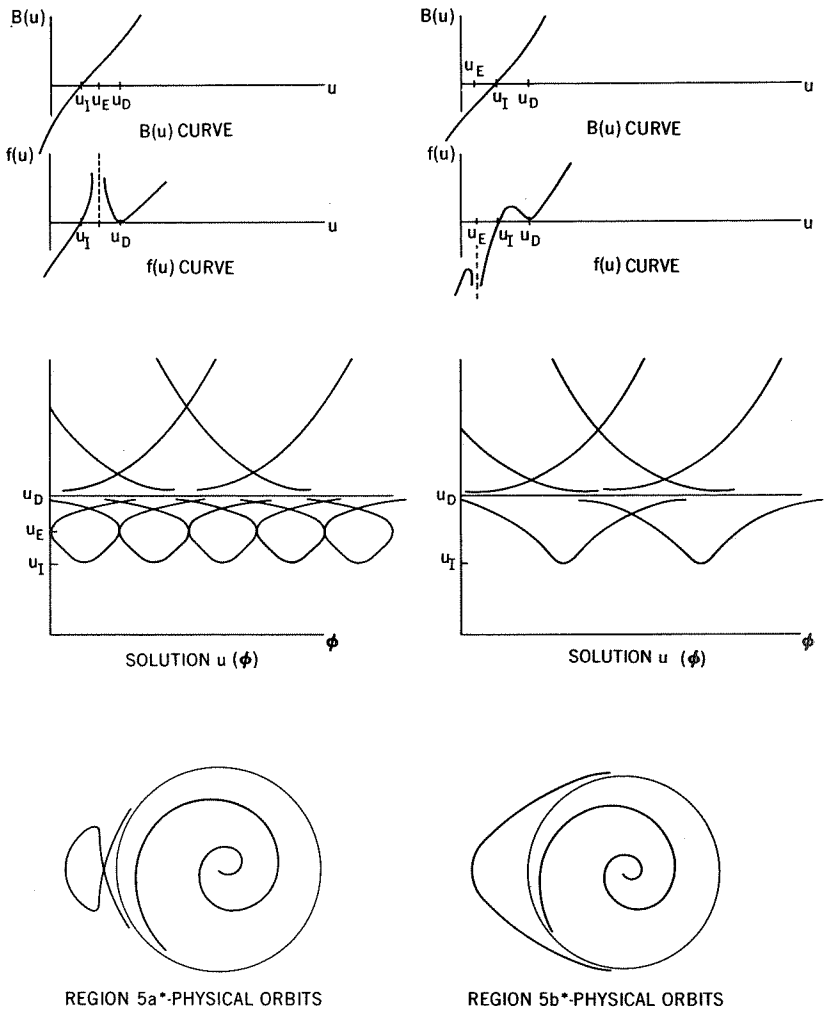

Figure D22—Qualitative solutions in region 5* for $a = 1$.

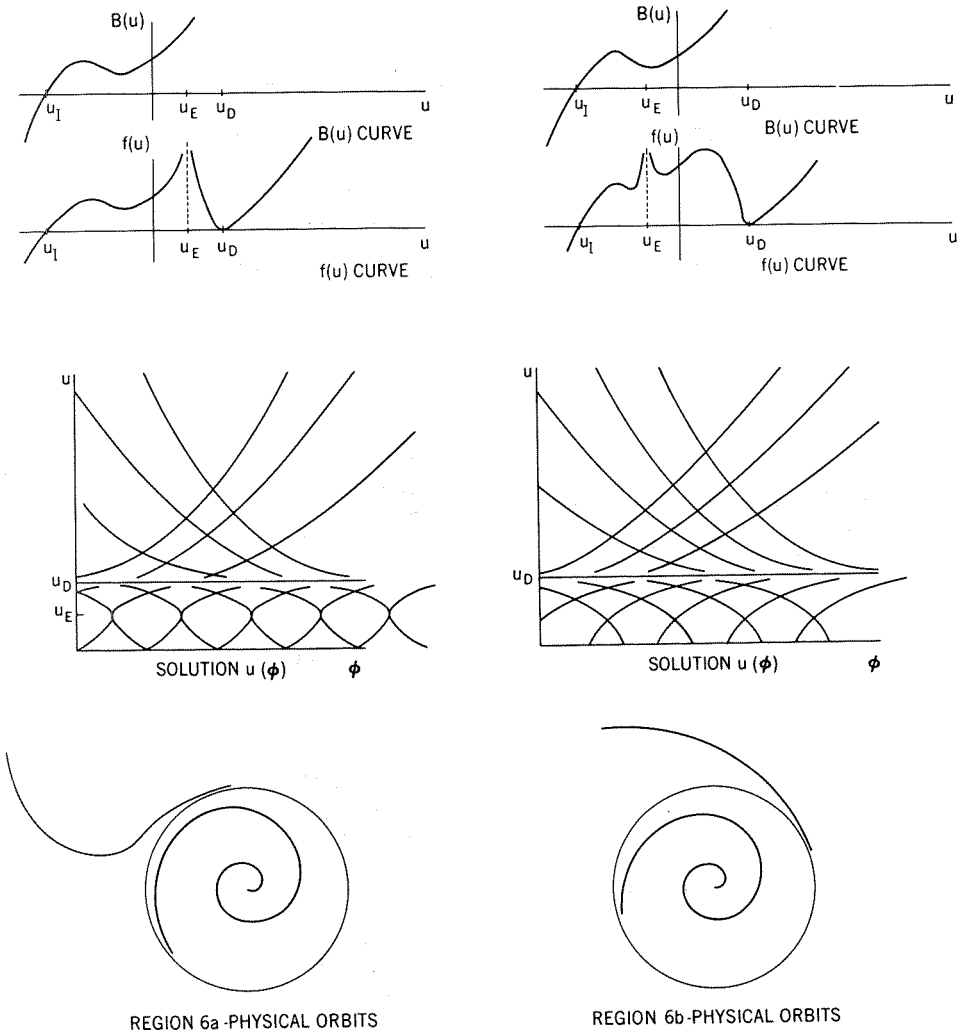

Figure D23—Qualitative solutions in region 6 for $a = 1$.

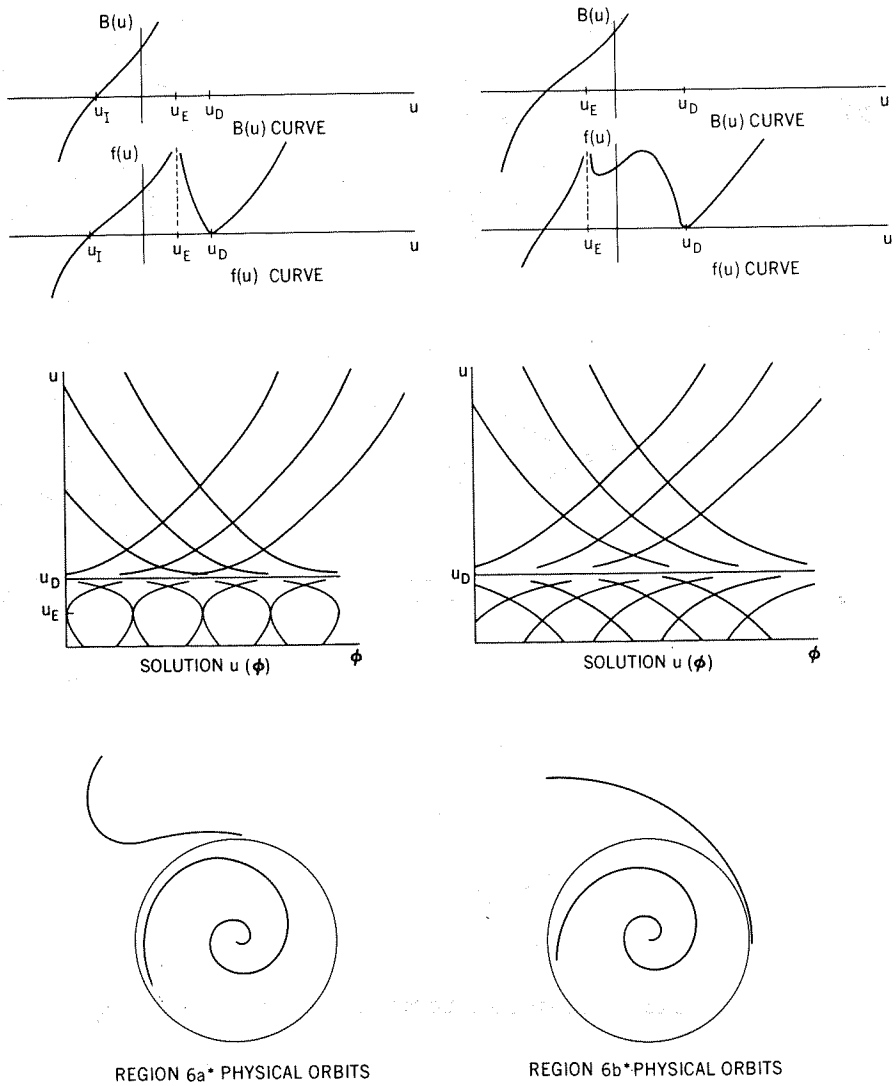

Figure D24—Qualitative solutions in region 6* for $a = 1$.

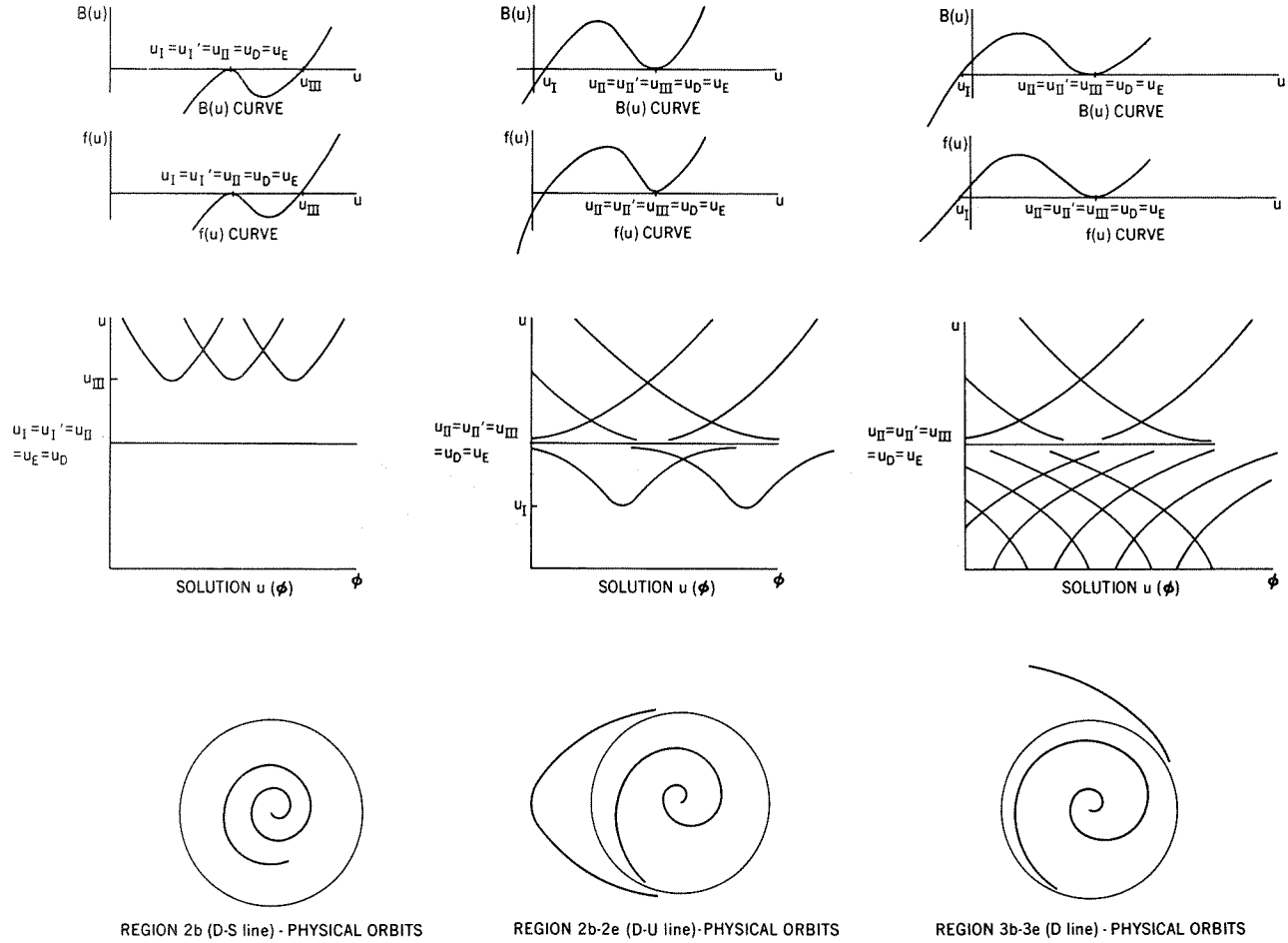

Figure D25—Qualitative solutions on *D* line for $a = 1$.

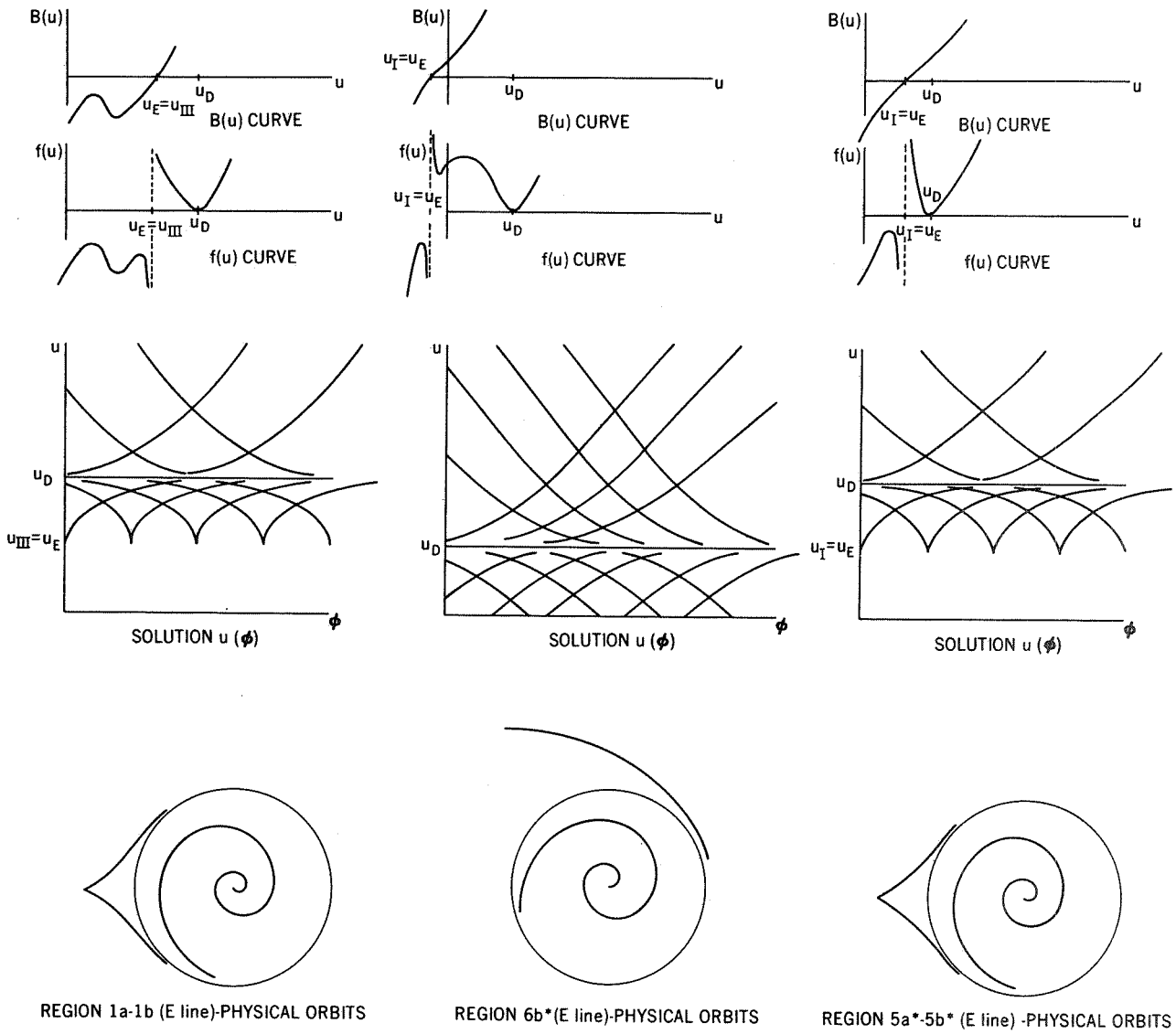

Figure D26—Qualitative solutions on *E* line for *a* = 1.

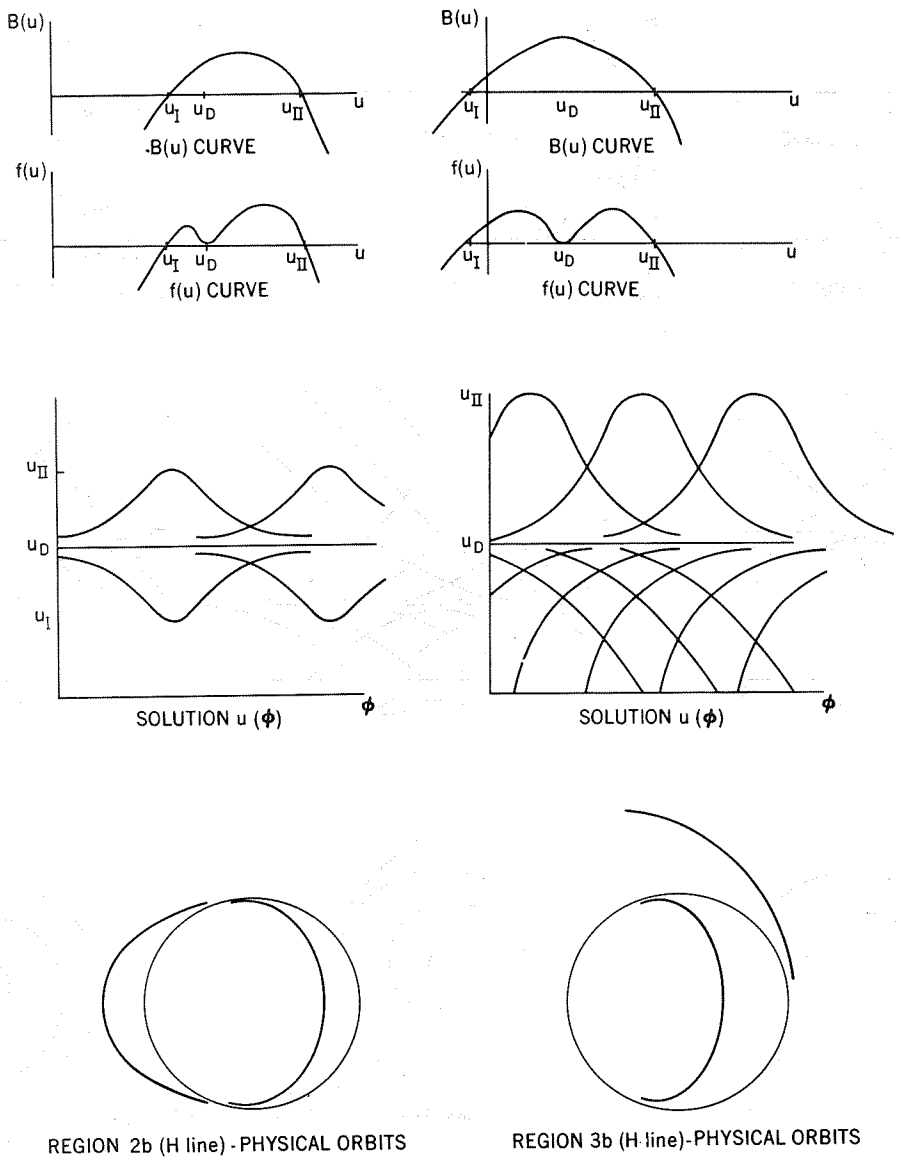

REGION 2b (H line) - PHYSICAL ORBITS

REGION 3b (H line) - PHYSICAL ORBITS

Figure D27—Qualitative solutions on *H* line for $a = 1$.

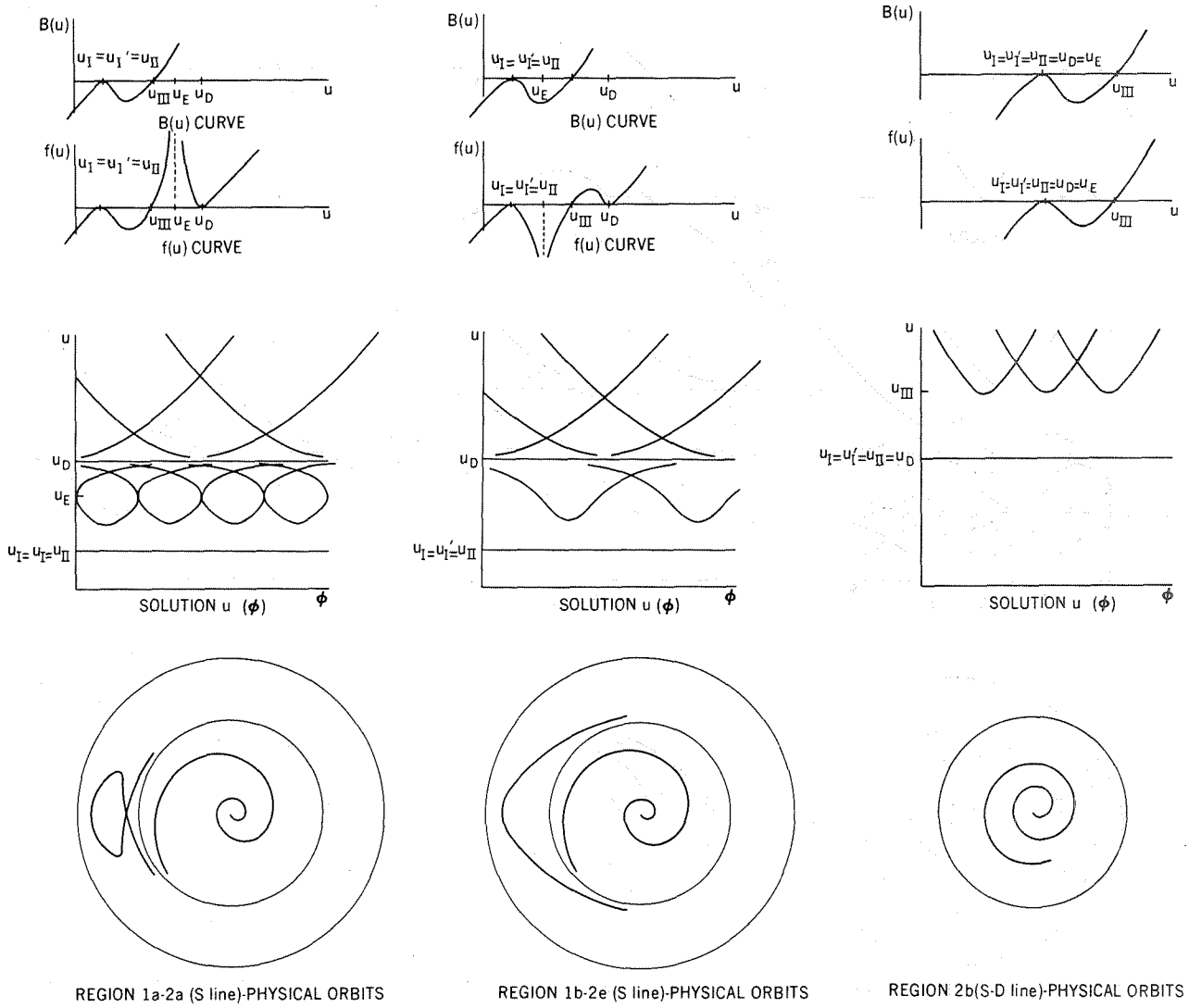

Figure D28—Qualitative solutions on *S* line for $a = 1$.

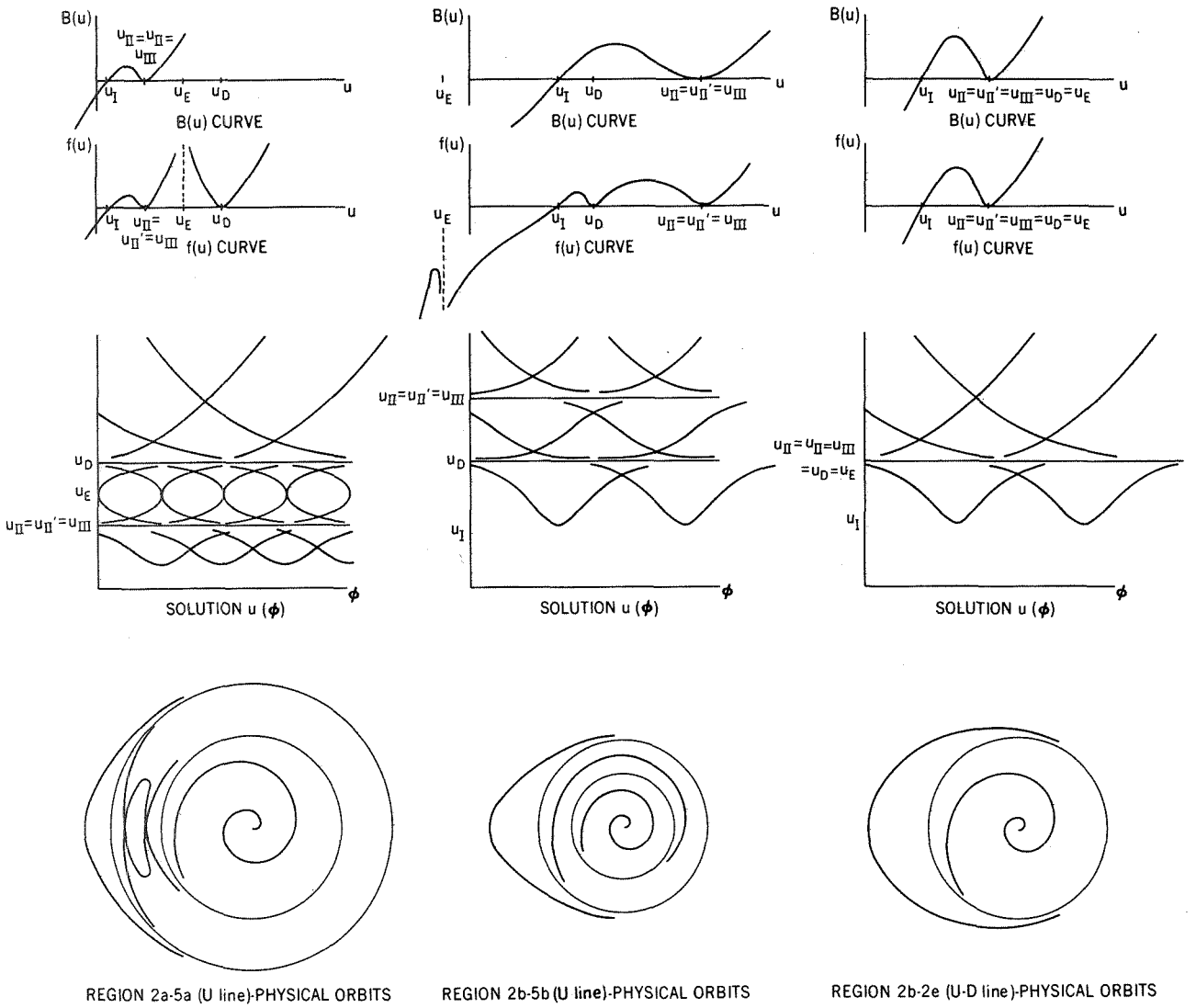

REGION 2a-5a (U line)-PHYSICAL ORBITS

REGION 2b-5b (U line)-PHYSICAL ORBITS

REGION 2b-2e (U-D line)-PHYSICAL ORBITS

Figure D29—Qualitative solutions on *U* line for *a* = 1.

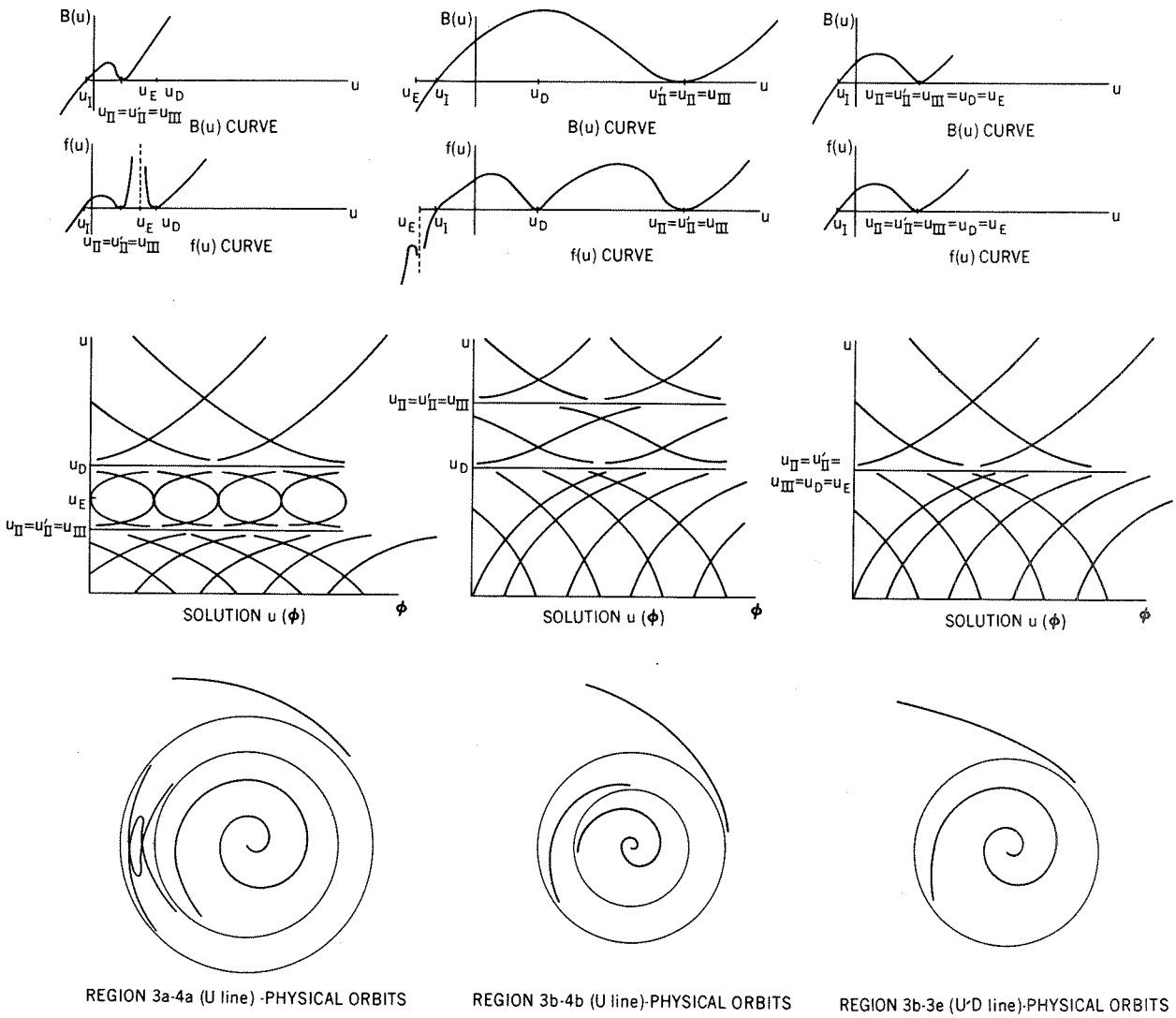

Figure D29 (concluded)—Qualitative solutions on *U* line for $a = 1$.

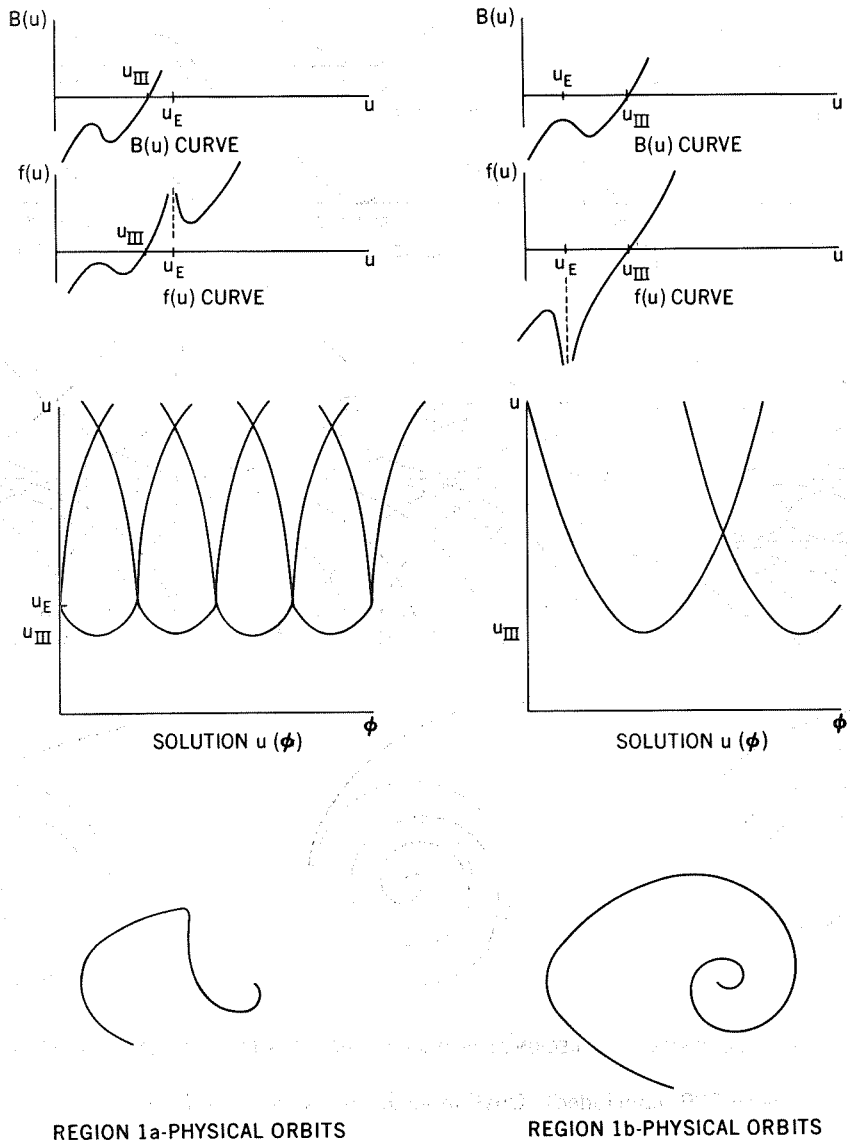

Figure D30—Qualitative solutions in region 1 for $1 < a < \infty$.

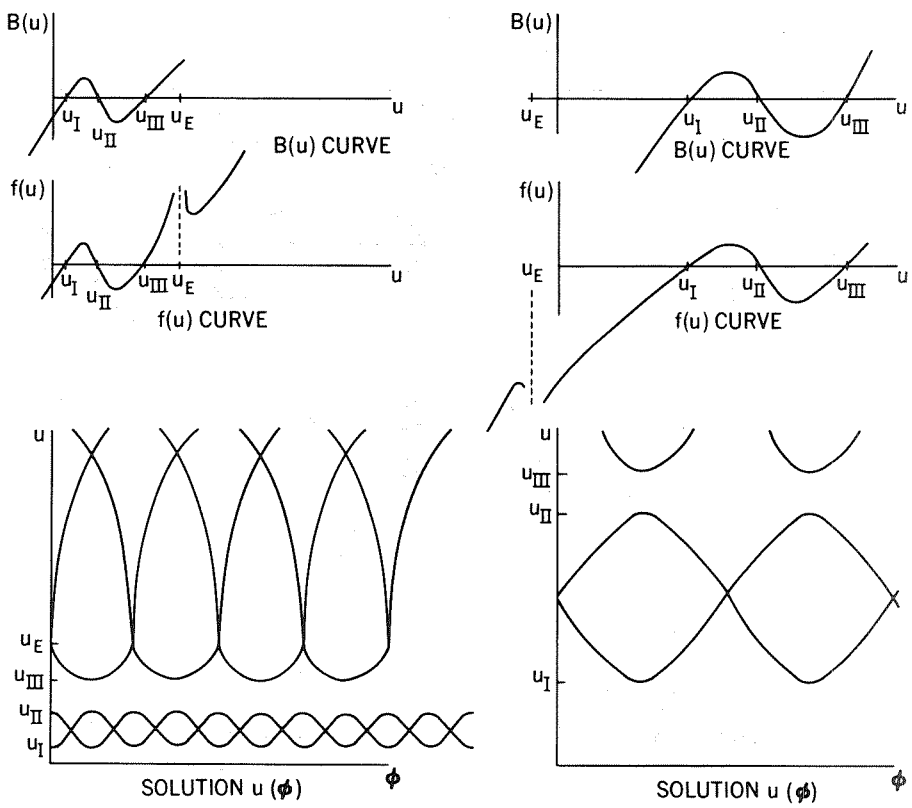

Figure D31—Qualitative solutions in region 2 for $1 < a < \infty$.

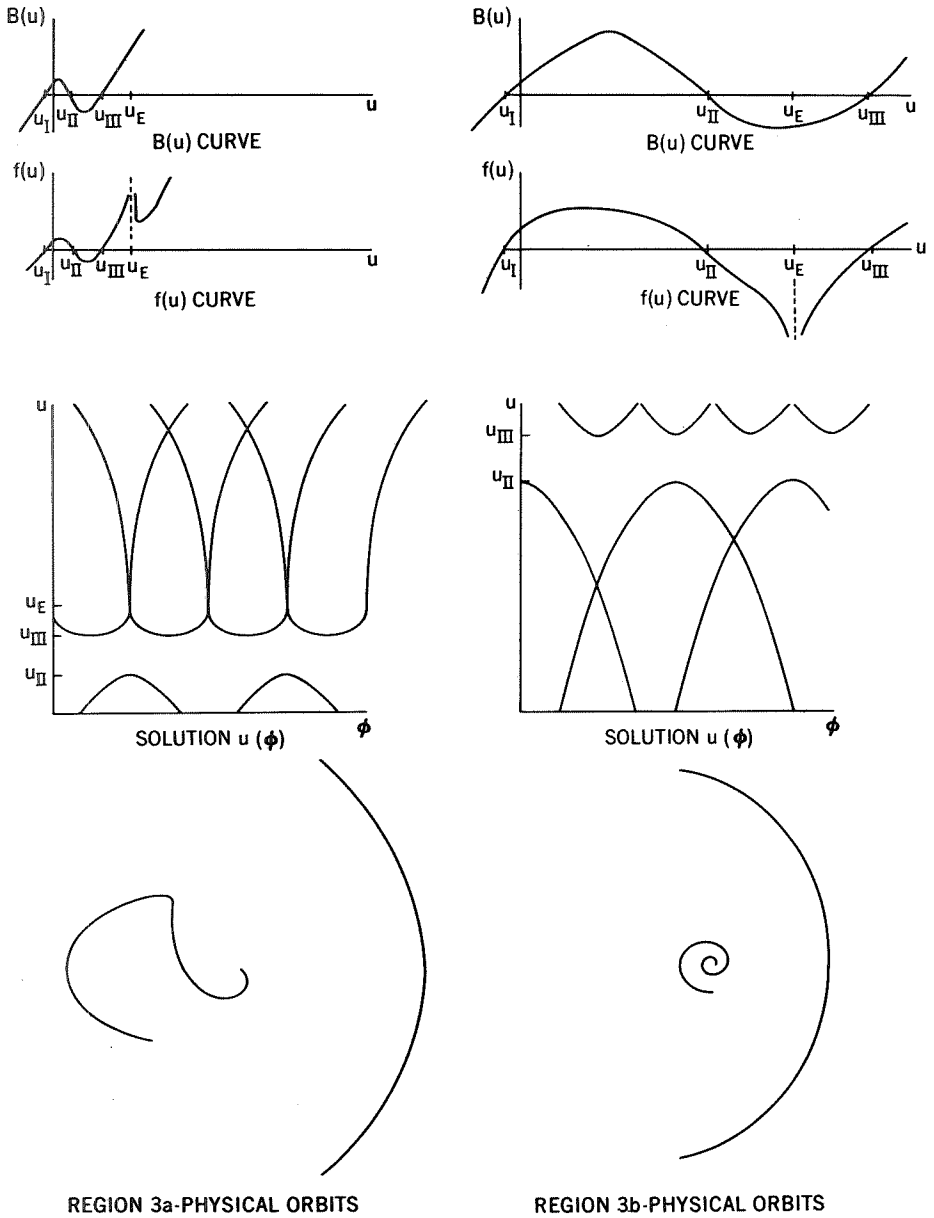

Figure D32—Qualitative solutions in region 3 for $1 < a < \infty$.

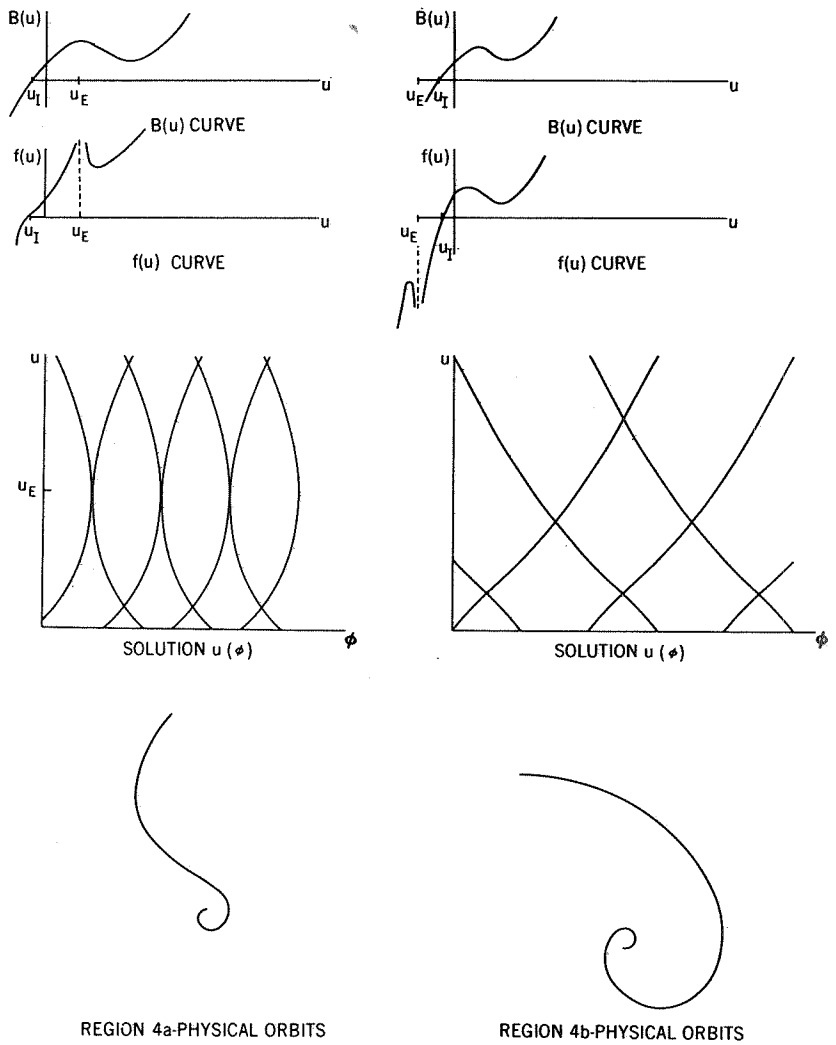

Figure D33—Qualitative solutions in region 4 for $1 < a < \infty$.

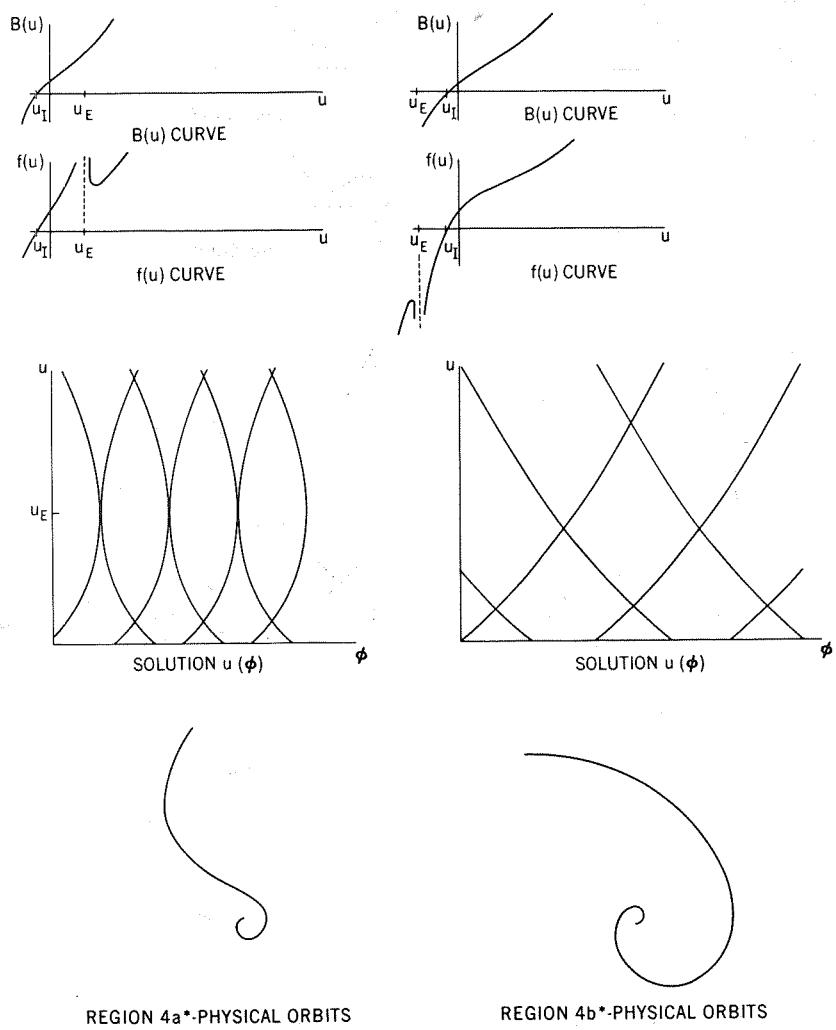

Figure D34—Qualitative solutions in region 4* for $1 < a < \infty$.

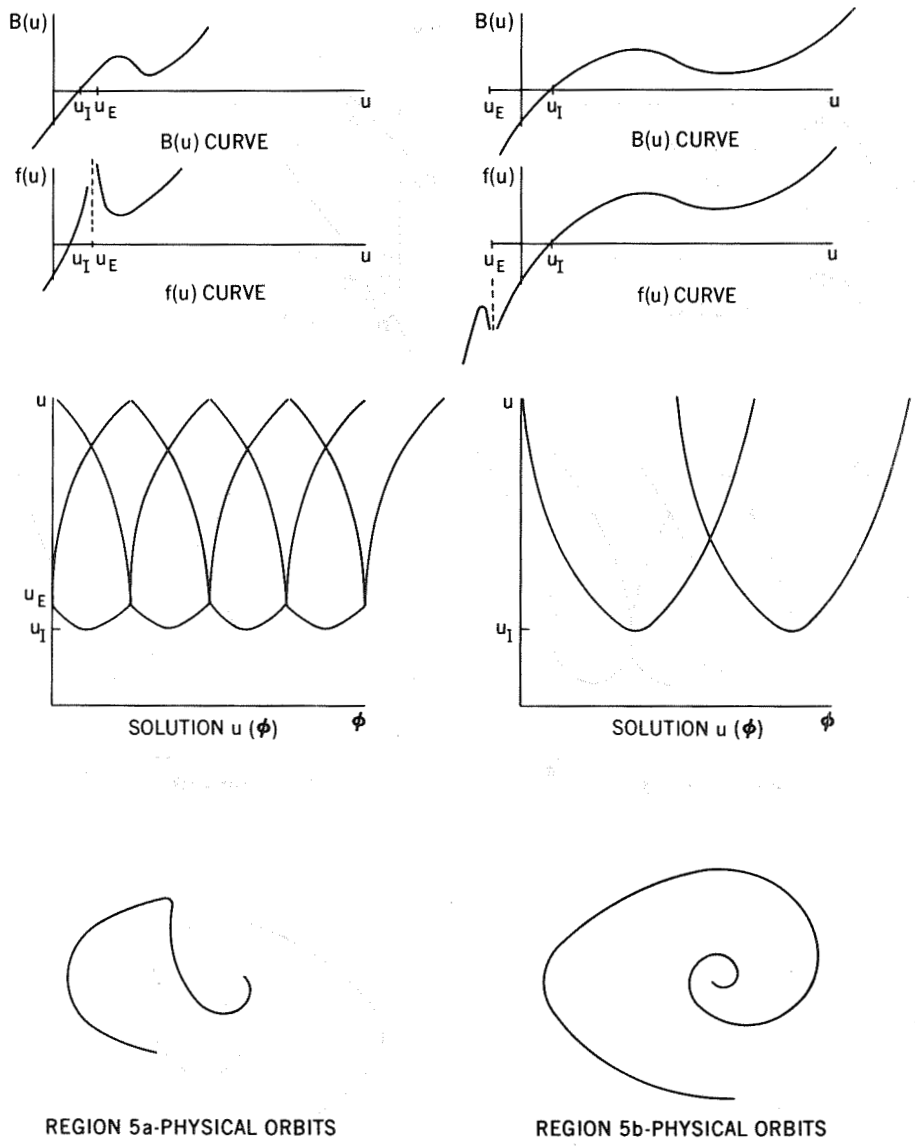

Figure D35—Qualitative solutions in region 5 for $1 < a < \infty$.

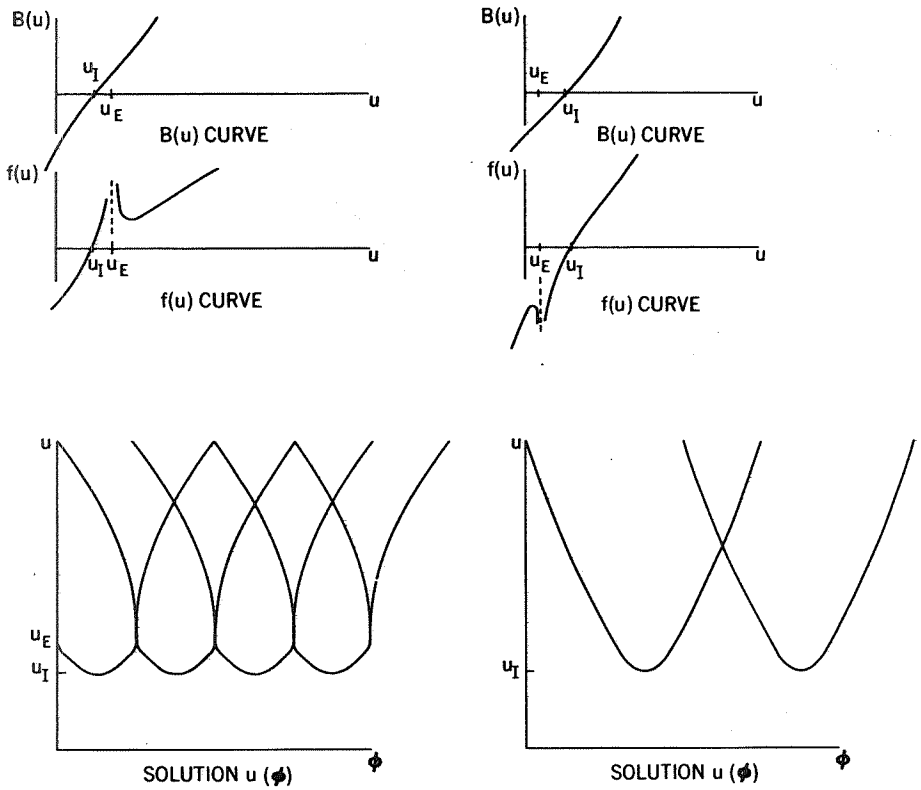

Figure D36—Qualitative solutions in region 5* for $1 < a < \infty$.

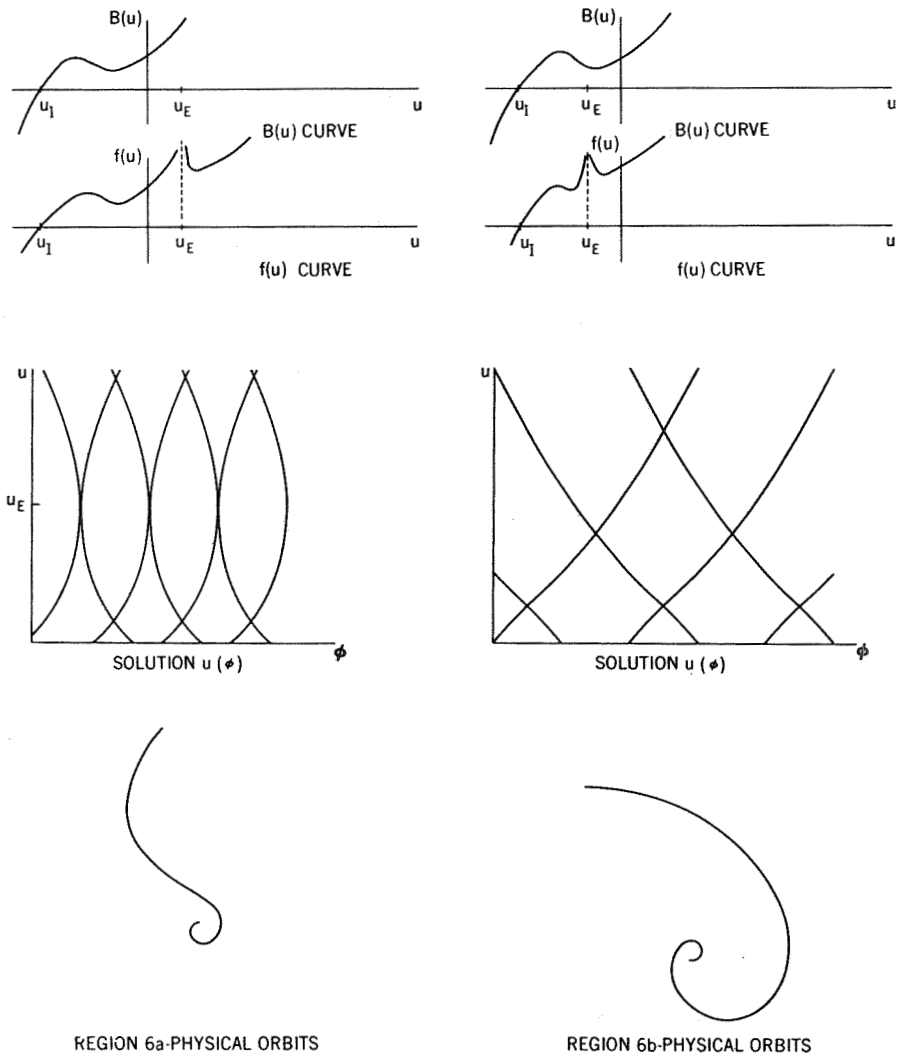

Figure D37—Qualitative solutions in region 6 for $1 < a < \infty$.

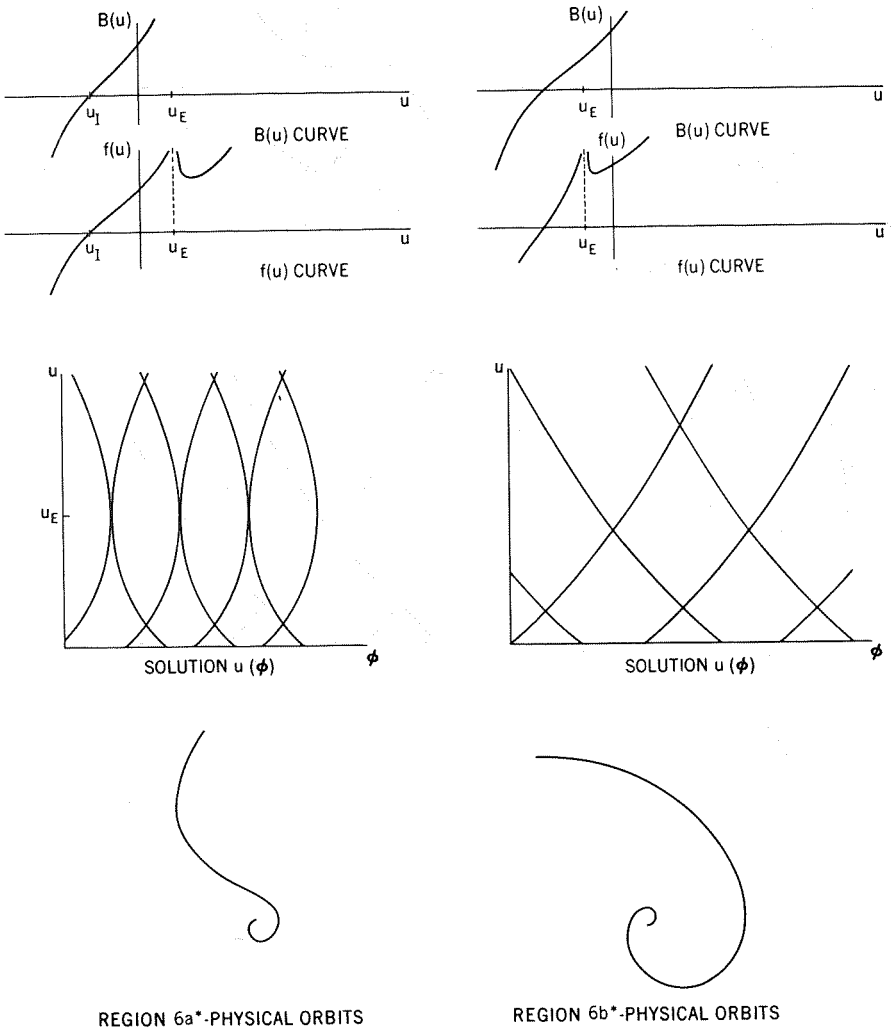

Figure D38—Qualitative solutions in region 6* for $1 < a < \infty$.

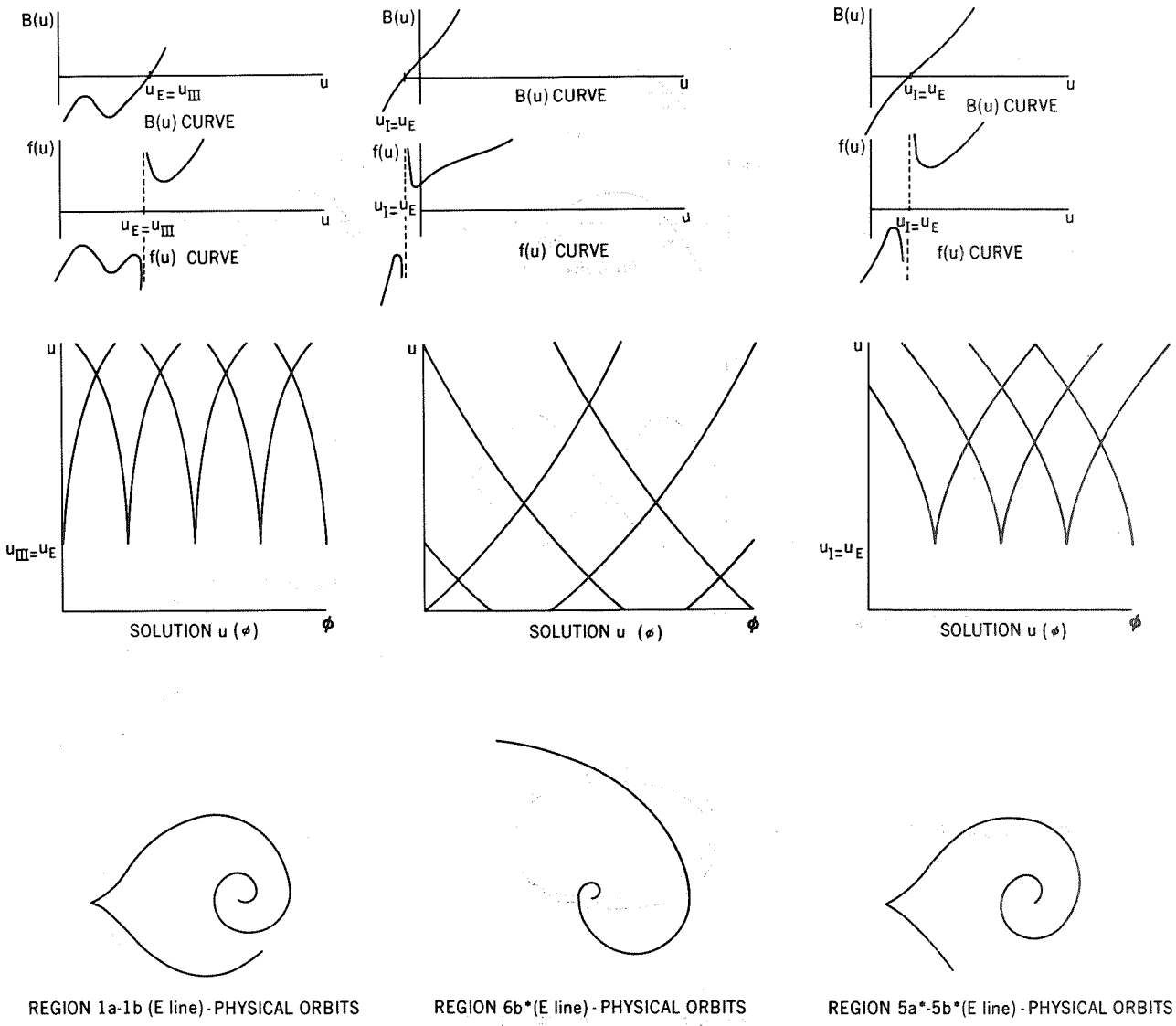

REGION 1a-1b (E line) - PHYSICAL ORBITS

REGION 6b*(E line) - PHYSICAL ORBITS

REGION 5a*-5b*(E line) - PHYSICAL ORBITS

Figure D39—Qualitative solutions on *E* line for $1 < a < \infty$.

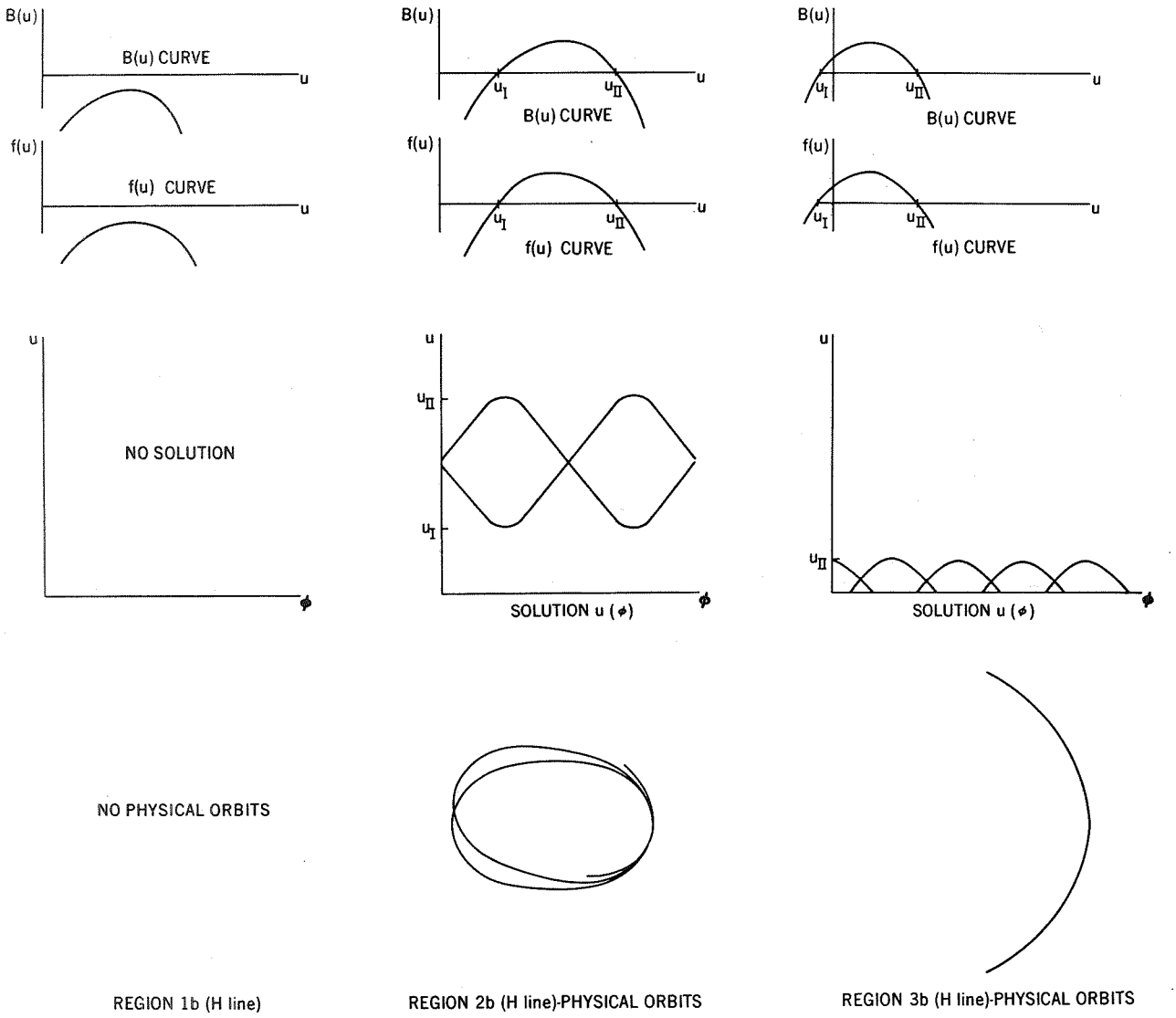

Figure D40—Qualitative solutions on *H* line for $1 < a < \infty$.

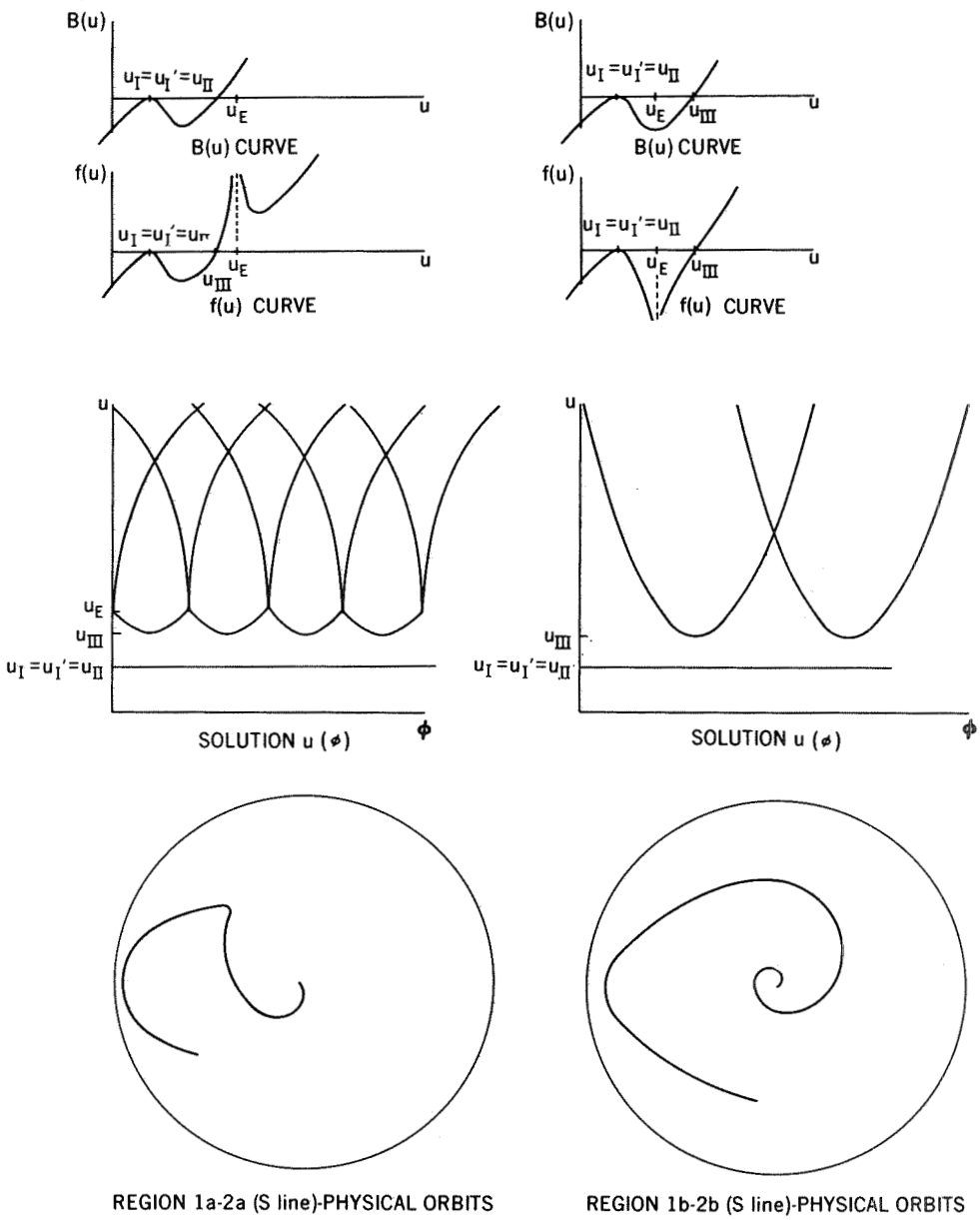

Figure D41—Qualitative solutions on *S* line $1 < a < \infty$.

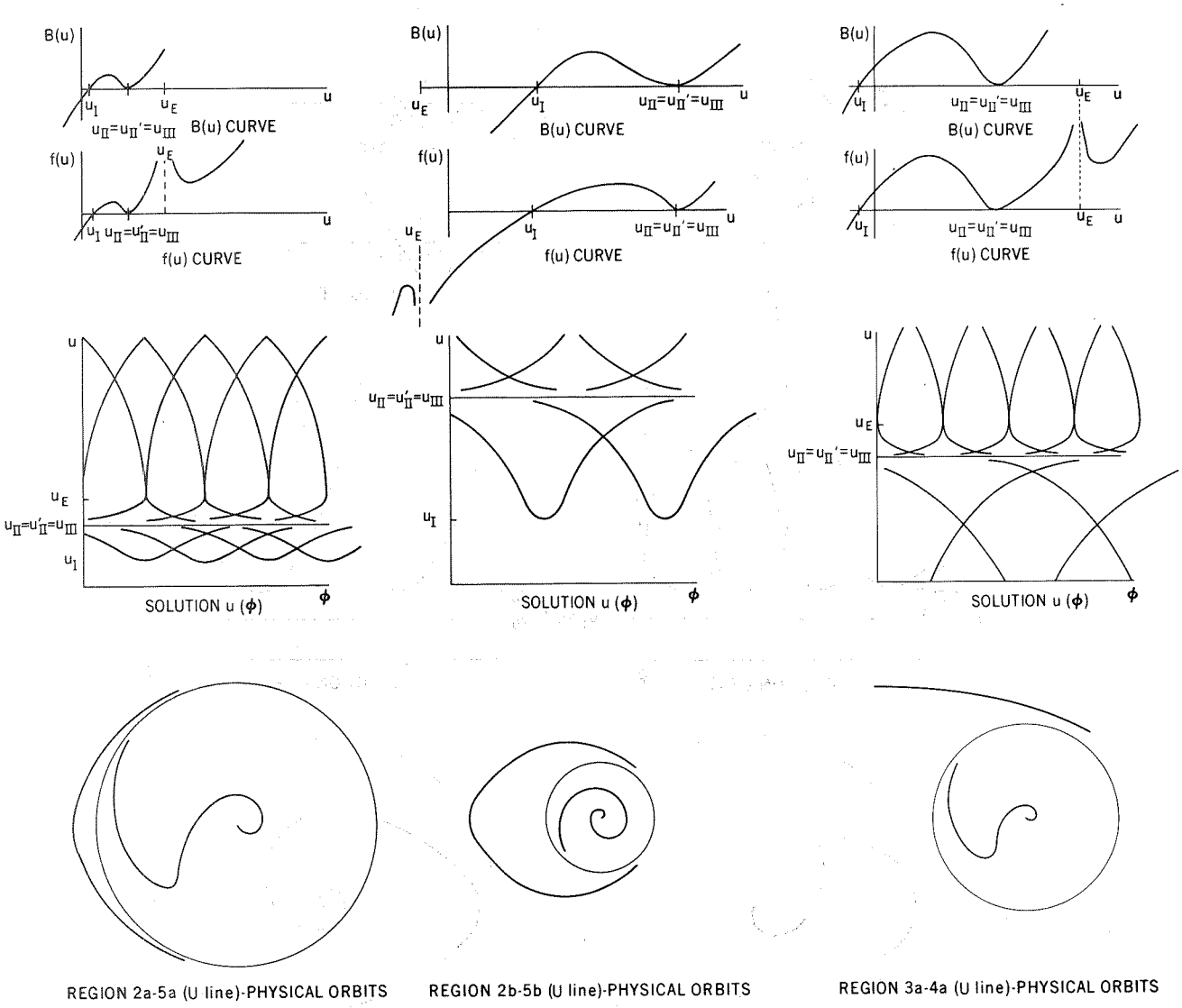

Figure D42—Qualitative solutions on *U* line for $1 < a < \infty$.

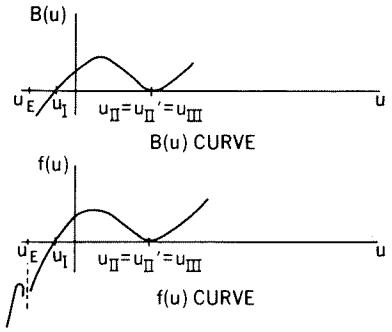

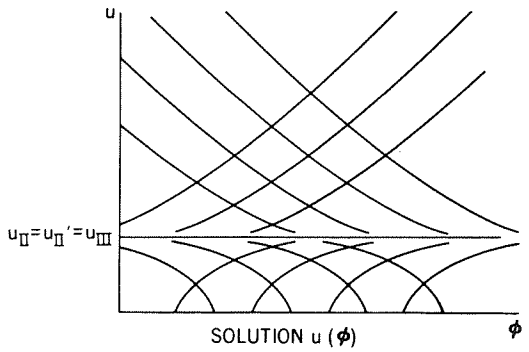

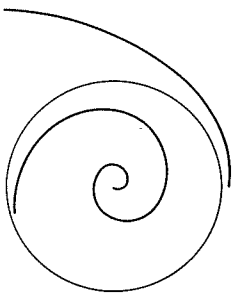

REGION 3b-4b (U line)-PHYSICAL ORBITS

Figure D42 (concluded)—Qualitative solutions on U line for $1 < a < \infty$.

"The aeronautical and space activities of the United States shall be conducted so as to contribute . . . to the expansion of human knowledge of phenomena in the atmosphere and space. The Administration shall provide for the widest practicable and appropriate dissemination of information concerning its activities and the results thereof."

—NATIONAL AERONAUTICS AND SPACE ACT OF 1958

NASA SCIENTIFIC AND TECHNICAL PUBLICATIONS

TECHNICAL REPORTS: Scientific and technical information considered important, complete, and a lasting contribution to existing knowledge.

TECHNICAL NOTES: Information less broad in scope but nevertheless of importance as a contribution to existing knowledge.

TECHNICAL MEMORANDUMS: Information receiving limited distribution because of preliminary data, security classification, or other reasons. Also includes conference proceedings with either limited or unlimited distribution.

CONTRACTOR REPORTS: Scientific and technical information generated under a NASA contract or grant and considered an important contribution to existing knowledge.

TECHNICAL TRANSLATIONS: Information published in a foreign language considered to merit NASA distribution in English.

SPECIAL PUBLICATIONS: Information derived from or of value to NASA activities. Publications include final reports of major projects, monographs, data compilations, handbooks, sourcebooks, and special bibliographies.

TECHNOLOGY UTILIZATION PUBLICATIONS: Information on technology used by NASA that may be of particular interest in commercial and other non-aerospace applications. Publications include Tech Briefs, Technology Utilization Reports and Technology Surveys.

Details on the availability of these publications may be obtained from:

SCIENTIFIC AND TECHNICAL INFORMATION OFFICE

NATIONAL AERONAUTICS AND SPACE ADMINISTRATION

Washington, D.C. 20546